KINETIC STUDIES OF GAS PHASE REACTIONS OF VOLATILE ORGANIC COMPOUNDS (VOCs) RELEVANT IN ATMOSPHERIC CHEMISTRY

By

ASMITA SHARMA

(Enrolment No: CHEM01201404007)

Bhabha Atomic Research Centre, Mumbai

A thesis submitted to the

Board of Studies in Chemical Sciences

In partial fulfillment of requirements

For the Degree of

DOCTOR OF PHILOSOPHY

Of

HOMI BHABHA NATIONAL INSTITUTE

September, 2020

Homi Bhabha National Institute

Recommendations of the Viva Voce Committee

As members of the Viva Voce Committee, we certify that we have read the dissertation prepared by Asmita Sharma entitled "Kinetic studies of gas phase reactions of volatile organic compounds (VOCs) relevant in atmospheric chemistry" and recommend that it may be accepted as fulfilling the thesis requirement for the award of Degree of Doctor of Philosophy.

Chairman – Prof. H. Pal (Ex-BARC)	Signature:	Date: 11-03-21
Guide / Convener – Prof. P. D. Naik (HBNI)	Signature:	Date: 11-03-21
Examiner – Dr. Aloke Das (IISER Pune)	Aloke Das	Date: 11/03/2021
Co-guide – Prof. Awadhesh Kumar (BARC)	Signature: Awadhesh Kumar	Date: 11.03.2021
Member 1 – Prof. R. K. Vatsa (BARC)	Signature:	Date: 11/3/2021
Member 2 – Prof. S. K. Jha (BARC)	Signature: Sanjay Kumar Jha	Date: 11-03-2021

Final approval and acceptance of this thesis is contingent upon the candidate's submission of the final copies of the thesis to HBNI.

I/We hereby certify that I/we have read this thesis prepared under my/our direction and recommend that it may be accepted as fulfilling the thesis requirement.

Date: 11.03.2021 Awadhesh Kumar

Place: Trombay Mumbai

Prof. Awadhesh Kumar
Co-guide

Prof. P. D. Naik
Guide

STATEMENT BY AUTHOR

This dissertation has been submitted in partial fulfillment of requirements for an advanced degree at Homi Bhabha National Institute (HBNI) and is deposited in the Library to be made available to borrowers under rules of the HBNI.

Brief quotations from this dissertation are allowable without special permission, provided that accurate acknowledgement of source is made. Requests for permission for extended quotation from or reproduction of this manuscript in whole or in part may be granted by the Competent Authority of HBNI when in his or her judgment the proposed use of the material is in the interests of scholarship. In all other instances, however, permission must be obtained from the author.

Asmita Sharma

DECLARATION

I, hereby declare that the investigation presented in the thesis has been carried out by me. Whenever contributions of others are involved, every effort is made to indicate this clearly with due reference to the literature and acknowledge of collaborative research and discussions. The work is original and has not been submitted earlier as a whole or in part for a degree / diploma at this or any other Institution / University.

Asmita Sharma

List of Publications arising from the thesis

Journal

1. "Reactions of lactones with tropospheric oxidants: A kinetics and products study". M.P. Walavalkar, A. Sharma, S. Dhanya, P.D. Naik, Atmos. Environ., **2017**,161, 18-26.
2. "Rate coefficients of hydroxyl radical reaction with dimethyl ether over a temperature range of 257–333 K". Monali Kawade, Asmita Sharma, D. Srinivas, Ankur Saha, Hari P. Upadhyaya, Awadhesh Kumar, Prakash D. Naik, Chem. Phys. Lett., **2018**, 706, 558–563.
3. "Rate coefficients of reactions of 1-chlorocyclopentene with tropospheric oxidants at 298 K". Asmita Sharma, Mohini P. Walavalkar, Ankur Saha, Monali Kawade, Awadhesh Kumar, Prakash D. Naik, Atmos. Environ., **2019**, 199, 274–283.
4. "Reactions of tropospheric oxidants- Cl, OH and O_3 with cyclic hydrocarbons with eight carbon atoms at 298 K". Asmita Sharma, Mohini Walavalkar, Awadhesh Kumar, S. Dhanya, Prakash D. Naik. Atmos. Environ., 213, **2019**, 433-443.
5. "Rate coefficients of hydroxyl radical reaction with 1-chlorocyclopentene over a temperature range of 262-335 K". Asmita Sharma, Mohini

Walavalkar, Anmol Virmani, Sumana Sengupta, Awadhesh Kumar, Prakash D. Naik. **(Communicated to Chem. Phys. Lett.)**

Conference/Symposium

1. "Effect of unsaturation on the tropospheric degradation pathways of cyclic hydrocarbons–A comparison of six and eight-membered molecules". A. Sharma, M. P. Walavalkar, H. D. Alwe, S. Dhanya and P. D. Naik, Proc. TSRP, 6 – 9th January 2014, BARC, Mumbai.
2. "Tropospheric oxidation of unsaturated cyclic ethers – contribution towards regeneration of OH radicals". H. D. Alwe, A. Sharma, M. P. Walavalkar, S. Dhanya and P. D. Naik, Proc. TSRP-2014, 6 – 9th January 2014, BARC, Mumbai.
3. "Rate coefficients of reactions of tropospheric oxidants with triple bonded alcohols". M. P. Walavalkar, H. D. Alwe, A. Sharma, S. Dhanya and P. D. Naik, Proc. TSRP, 6 – 9th January 2014, BARC, Mumbai.
4. "Direct observation of OH formation during Cl atom initiated oxidation of hydrocarbons". H. D. Alwe, A. Sharma, M. P. Walavalkar, S. Dhanya,

A. Saha, S. Sengupta and P. D. Naik, Proc. 13th DAE-BRNS Biennial TSRP, January 5 – 9, 2016, BARC, Mumbai.

5. “Rate coefficients of reactions of 1-chlorocyclopentene with tropospheric oxidants”. A. Sharma, M. P. Walavalkar, A. Kumar and P. D. Naik, Proc. TSRP-APSRC 2018, BARC Mumbai.
6. “Kinetic studies of gas phase reactions of cyclic eight membered hydrocarbons”. M. P. Walavalkar, Asmita Sharma, Awadhesh Kumar and P. D. Naik, Proc. TSRP-APSRC 2018, BARC Mumbai.
7. “Assessment of environmental impact of 1-chlorocyclopentene in terms of tropospheric lifetime, global warming and ozone depletion potentials”. A. Sharma, M. P. Walavalkar, A. Kumar and P. D. Naik, Proc. NSE – 20, 13-15th December, 2018, IIT Gandhinagar, Gujarat.
8. “Kinetics of gas phase reaction of hydroxyl radical with 1-chlorocyclopentene over a temperature range of 258-335 using LP-LIF technique”. Anmol Virmani, A. Sharma, M.P. Walavalkar, A. Saha, A. Kumar and P.D. Naik, Proc. NSRP, 6-9th Feb, 2019, Visva-Bharati, Santiniketan.

Asmita Sharma

Dedicated

To

Shri Girish kumar Upadhyaya

ACKNOWLEDGEMENTS

First of all, I would like to express my deep and sincere gratitude to my thesis guide Prof. P. D. Naik and co-guide Prof. Awadhesh Kumar for their guidance, constant encouragement and keen interest. I am also thankful to them for their patience during technical discussions and clarifying my doubts all through these years.

I sincerely thank Dr. S. Dhanya for her support in my research work. I thank the members of the Doctoral Committee, Prof. H. Pal (Chairman), Prof. R. K. Vatsa and Prof. S. K. Jha for their critical review and suggestions during the progress review and pre-synopsis viva-voce.

My sincere thanks to all my lab mates, Mohini Paresh Walavalkar, Monali Kawade, Dr. Sumana Sengupta Dr. Ankur Saha, Anmol Virmani Srinivas, Dr. Hari P. Upadhaya, Hari Prasad Alwe for the scientific discussions and experimental help during the work. I also thank my divisional colleagues for their constant support. I want to thank all my family members, especially my son Ansh and husband Dr. Rajeev Kumar for their support.

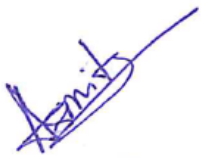

Asmita Sharma

CONTENTS

LIST OF FIGURES

	1.38 ml min^{-1}). The confirmed products by comparison with library are- a and a': 1,5-cyclooctadiene-4-one, b: 5-cyclooctene-1,2-dionecyclooctanone, c': 1,2-epoxy-5-cyclooctene. The product identified by the analysis of the MS fragmentation pattern (inset): 8-chlorocyclooct-5-ene-1-one (14.6 min).	
3.7	Total ion chromatogram of products of the reactions of A: cis-cyclooctene and B: 1,5-cyclooctadiene with O_3 (Column: CPWAX(30 m × 0.25 mm × 0.25 μm)) with temperature programming, 35-2-10-200 and flow of 1 ml min^{-1}). The confirmed products by comparison with library are- a: heptanal, b: 1,2-epoxycyclooctane, c: 9-Oxabicyclo [6.1.0] nonan-4-ol, d: heptanoic acid, e': 4-hepten-1-al, f': 1,2-epoxy-5-cyclooctene, g': 1,5-cyclooctadiene-4-one, h': 1,5-cyclooctadiene diepoxide.	102
4.1	The plots of the fractional decrease in the concentration of 1-chlorocyclopentene against that of a reference compound due to their reaction with Cl atoms. Reference compounds are butane (■), cyclopentene (●) and butane (▲), in N_2; and butene (□) and cyclopentene (○) in the air; total pressure:800 Torr.	129
4.2	The figure shows plots of the fractional decrease in the concentration of 1-chlorocyclopentene versus that of the reference compound due to reaction with OH; the reference compounds used are butane (■) and cyclopentene (●) in N_2, total	132

LIST OF TABLES

	pressure = 800 Torr. The error in the rate coefficients is a combination of the 2σ error of the measurements and the reported error for the reference compound.	
3.3	Relative ratios and rate coefficients of reactions of O_3 with CyO at 298 K with different reference compounds, [CyO] = 100 - 150 ppm, [R] = 50 - 100 ppm. Buffer gas air, Total pressure = 800 Torr. The error in the rate coefficients is a combination of the 2σ error of the measurements and the reported error for the reference compound.	97
3.4	Tropospheric lifetimes (τ) calculated for CyOs with respect to reactions with different tropospheric oxidants. The concentrations used for Cl_{MBL} [15] (under marine boundary layer conditions), OH and O_3[75] are 1.3×10^5, 2×10^6 and 7×10^{11} molecules cm^{-3}, respectively. All the rate coefficients are in the unit of $cm^3molecule^{-1}s^{-1}$. The rate coefficients for CyOs are from the present work. For the calculation of net tropospheric lifetime (τ_{net}) in ambient air, reaction with Cl atom is not considered.	118
4.1	Relative ratios and rate coefficients of the reactions of Cl/OH/O_3 with 1-chlorocyclopentene with different reference molecules, [1-chlorocyclopentene] = 100 - 150 ppm, [R] = 50	130

	– 100 ppm, buffer gas - N_2 and air. Total pressure = 800 Torr for relative rate method (RRM) and 30 Torr for absolute rate method. Numbers in parentheses under the buffer gas column represent the number of times the experiments are repeated.	
4.2	The rate coefficient data for the reaction of the OH radicals with CCP at different temperatures at 30 Torr.	139
4.3	Major products of atmospheric oxidation of 1-chlorocyclopenteneby Cl/OH/O_3, characterized by GC-MS. GC columns used for identification of O_3-initiated products are mentioned in the table. Other experimental conditions are given in the text.	141
4.4	Tropospheric lifetimes calculated for 1-chlorocyclopentene with respect to reactions with different tropospheric oxidants. The concentrations used for $Cl_{Ambient}$, Cl_{MBL} (under marine boundary layer conditions), OH and O_3 are 2.5×10^3, 1.3×10^5, 2×10^6 and 7×10^{11} molecules cm^{-3} [13], respectively.	148
5.1	The rate coefficients of reference molecules used are given in the column Reference. The rate coefficient values determined in the present work are marked in bold. Number of experiments in each case is given in parenthesis.	169
5.2	Rate coefficients and tropospheric lifetimes (τ) calculated for	184

	Cl with DME is taken from Jenkin et al. [151]. The concentrations used for $Cl_{Ambient}$, Cl_{MBL}, OH and O_3 are 1×10^3, 1.3×10^5, 1×10^6 and 7×10^{11} molecules cm^{-3}, respectively (details are given in chapter two)	
7.1	Summary of the rate coefficients of the reaction of molecules with tropospheric oxidants and the tropospheric lifetimes for a quick reference, the details are given in respective chapter.	222

LIST OF REACTION SCHEME

Chapter-7

Summary, Conclusions and Future Work

7.1. Summary

The goal of this thesis is to understand the atmospheric implications of some selected VOCs, which have varied applications and hence released into atmosphere as pollutants. This goal is achieved by investigating the gas phase reaction kinetics of some atmospherically important VOCs with the tropospheric oxidants (OH, Cl and O_3) and identifying the stable products formed for assigning the degradation mechanism. The VOCs are selected from different class of compounds to understand the change in reactivity trends due to structural variations like unsaturation, presence of hetero atom, different functional groups and ring strain. VOCs considered include (a) cyclic hydrocarbons with eight carbon atoms (cyclooctane, cis-cyclooctene and 1,5-cyclooctadiene) to understand any change in the reactivity with unsaturation, and to compare their reactivities with saturated and unsaturated acyclic hydrocarbons, (b) halogenated cyclic hydrocarbon (1-chlorocyclopentene) for comparison of its reactivity with cyclopentene and substituted cyclopentene to understand the effect of substituent Cl on the reactivity, (c) cyclic esters (gamma-valerolactone and alpha-methyl gamma-butyrolactone) to study the effect of the ring O atom on the reactivity, and (d) ethers [dimethylether (straight chain) and epichlorohydrin (cyclic)] to compare the reactivity of cyclic and acyclic ethers and also to investigate the effect of heteroatom (chlorine) on the reactivity. The rate coefficients of reactions of these molecules with Cl, OH, and O_3 at room temperature (298 K) and 1 atm. are determined (k_{Cl}, k_{OH}, and k_{O3}) using relative

rate method. These rate coefficients of a VOC are used to calculate its tropospheric lifetime, which is an essential parameter for assessing its environmental impact. These measured values of the rate coefficients of a VOC with OH, Ozone and Cl are compared to understand relative importance (contribution) of its reactivity or degradation channels with these oxidants, and also with respect to that of analogous molecules in order to understand the reactivity pattern. These oxidants can react with the molecule by abstraction of an H atom and also by addition to the double bond. Hence efforts were made to identify the dominant channel of reaction between addition and abstraction of the oxidants with these pollutants by analyzing the reaction products. Further, the characterization of the reaction products has helped in elucidating the reaction mechanism and thus, in understanding the long term impact of these molecules in the troposphere. In addition, for evaluation of the activation energy (E_a), temperature-dependent rate coefficients for the reactions of dimethyl ether and 1-chlorocyclopentene with the OH radical is also measured using an absolute method of Laser Photolysis-Laser Induced Fluorescence (LP-LIF). The reasonably well-established structure-activity relations (SARs) are also applied in some cases to calculate the rate coefficients to compare with the measured values. The rate coefficients are then used to calculate lifetimes of these VOCs to predict their impact on the atmosphere, for a few studied VOCs, the global warming and ozone depletion potentials are also estimated. In the present work, both relative rate method and absolute method are employed to measure the rate coefficients. The experimental results are supported by theoretical calculations to understand the reaction mechanism.

7.2. Conclusions

The measured rate coefficients for the reaction of the VOCs with the tropospheric oxidants (OH, Cl and O_3), and their calculated tropospheric lifetimes are summarized in Table 7.1. The impact of these VOCs, except ethers, on atmosphere is local, since their tropospheric lifetimes with respect to the oxidants are in hours. However, the tropospheric lifetimes of the ethers investigated are in days, so ethers may have some regional impact on the atmosphere. This is further confirmed by low values of estimated global warming and ozone depletion potential mentioned in the respective chapters. The major degradation pathway of these molecules is mainly their reactions with the OH radicals, except for cyclooctene for which reaction with O_3 is major pathway of degradation. It may be noted that the reactions with Cl atoms are important under the marine boundary layer conditions for all the investigated VOCs.

The product analysis of the reactions of these molecules with OH and Cl suggests that between addition and abstraction reaction mechanisms, the former is the dominant one which is supported by theoretical calculations. The identified stable products and theoretical calculations indicate that the reaction mechanism for both OH and Cl is similar for all the VOCs studied.

The temperature dependence study of rate coefficients for the reaction of the OH radical with dimethyl ether and 1-chlorocyclopentene in the temperature range of 257-335 K indicates that the rate coefficients of dimethyl ether are weakly temperature dependent but that of 1-chlorocyclopentene exhibits negative temperature dependence. This negative activation energy suggests the involvement of a pre-reactive complex in the reaction. The Arrhenius expression for the measured data is given in the respective chapters.

Table 7.1: Summary of the rate coefficients of the reaction of molecules with tropospheric oxidants and the tropospheric lifetimes for a quick reference, the details are given in respective chapter.

Compound	**Rate coefficients (cm^3 $molecule^{-1}$ s^{-1})**		
	k_{Cl} **(τ_{Cl})**	**k_{OH}** **(τ_{OH})**	**k_{03}** **(τ_{O3})**
Cyclooctane	$(4.48 \pm 0.37) \times 10^{-10}$ (231 hrs) $_{\text{Ambient air}}$ (4.8 hrs) $_{\text{MBL}}$	$(1.38 \pm 0.21) \times 10^{-11}$ (9.9 hrs)	
	$\tau_{\text{Total (ambient air)}} = 9.5$ hrs $\tau_{\text{Total(MBL)}} = 3.2$ hrs		
Cycloctene	$(4.68 \pm 0.31) \times 10^{-10}$ (236.4 hrs) $_{\text{Ambient air}}$ (4.6 hrs) $_{\text{MBL}}$	$(5.07 \pm 1.06) \times 10^{-11}$ (2.8 hrs)	$(4.11 \pm 0.76) \times 10^{-16}$ (1.0 hr)
	$\tau_{\text{Total (ambient air)}} = 0.7$ hr $\tau_{\text{Total (MBL)}} = 0.6$ hr		
1,5-cyclooctadiene	$(5.15 \pm 0.74) \times 10^{-10}$ (213.7 hrs) $_{\text{Ambient air}}$ (4.1 hrs) $_{\text{MBL}}$	$(11.11 \pm 1.74) \times 10^{-11}$ (1.3 hrs)	$(1.44 \pm 0.16) \times 10^{-16}$ (2.8 hrs)
	$\tau_{\text{Total (ambient air)}} = 0.9$ hr $\tau_{\text{Total (MBL)}} = 0.7$ hr		

1- Chlorocyclopentene	$(3.51 \pm 1.3) \times 10^{-10}$ (316.6 hrs) $_{\text{Ambient air}}$ (6.1 hrs) $_{\text{MBL}}$	$(5.97 \pm 1.1) \times 10^{-11}$ (2 hrs)	$(1.50 \pm 0.20) \times 10^{-17}$ (26 hrs)
	$\tau_{\text{Total (ambient air)}}$ = 1.8 hrs $\tau_{\text{Total (MBL)}}$=1.4 hrs		
gamma- valerolactone	$(2.26 \pm 0.53) \times 10^{-11}$ (4916 hrs)$_{\text{Ambient air}}$ (94.6 hrs)$_{\text{MBL}}$	$(1.95 \pm 0.58) \times 10^{-12}$ (71.2 hrs)	
	$\tau_{\text{Total (}}$ambient air) =70.2 hrs $\tau_{\text{Total (MBL)}}$= 40.6 hrs		
alpha-methyl gamma- butyrolactone	$(3.42 \pm 0.63) \times 10^{-11}$ (3248 hrs) $_{\text{Ambient air}}$ (62.5 hrs) $_{\text{MBL}}$	$(1.81 \pm 0.43) \times 10^{-12}$ (76.7 hrs)	
	$\tau_{\text{Total (ambient air)}}$ = 76.5 hrs $\tau_{\text{Total (MBL)}}$= 34.4 hrs		
Dimethy ether	1.8×10^{-10} (0.5 day) $_{\text{Ambient air}}$ (64 days) $_{\text{MBL}}$	2.70×10^{-12} (4.3 days)	
	$\tau_{\text{Total (ambient air)}}$ = 4 days $\tau_{\text{Total (MBL)}}$=0.46 day		
Epichlorohydrin	2.59×10^{-12}	2.42×10^{-13}	

	(4469 days) $_{\text{Ambient air}}$ (34 days) $_{\text{MBL}}$	(48 days)	
	$\tau_{\text{Total (ambient air)}}$ = 47 days $\tau_{\text{Total (MBL)}}$=20 days		

7.3. Future scope of work

The rate coefficients reported in this thesis are measured for the first time for most of the VOCs by the relative rate method. Several measurements with more than one reference compounds are carried out to arrive at the rate coefficient. Still, these values can be further verified by an absolute method, such as employing LP-LIF, and a relative rate method using different reference compounds. These additional measurements will provide a better authentic value to the measured rate coefficients, and also help in understanding the temperature dependence of the rate coefficients for the reaction which could not be studied in this thesis work due to the time constraint.

To understand an overall atmospheric impact of the VOCs investigated, further studies are required to characterize even the unidentified stable products and to measure the reactivities of all the products identified, along with studying the reaction under polluted atmospheric condition, i.e., in the presence of NO_x. In the thesis work, a limited number of VOCs are investigated to arrive at structural effect on the reactivity. For a better understanding of these effects, it is desirable to study reactions of more number of VOCs in a particular series. The reactivity of hydrocarbons (oxygenated and halogenated), other than the ones already studied, with different ring size, substituents, or functional groups can be measured to assess the change in the reactivity due to variation

of these parameters. These studies will also help to develop or modify the existing SARs to predict more accurately the reactivity of an unknown VOC. In addition, theoretical calculations are required to support these experimental results and understand in detail the reaction mechanisms.

Although OH is an important tropospheric radical in terms of reactivity and has a greater influence on the atmospheric fate of the trace species, the atmospheric photochemistry generates a variety of other radical species and the most important among them are peroxyl radicals (HO_2 and RO_2) for formation of important tropospheric pollutant, peroxyacetyl nitrate (PAN). Thus, the rate coefficient measurement of trace species with peroxyl radicals is required. However, due to negligible fluorescence of peroxyl radicals, LP-LIF technique is not suitable for their kinetic studies. We need to employ highly sensitive absorption based absolute method, such as Cavity Ring-Down Spectroscopy (CRDS), to measure the rate coefficients of peroxyl radical with trace species. We would like to develop a CRDS technique for the measurement of absolute rate coefficient of peroxyl radicals with trace species.

CRDS is a sensitive absorption based technique, in which the rate of decay of a laser pulse is measured in an optical cavity, formed by two high reflectivity mirrors ($R \geq 0.999$). Two pulsed lasers are employed, one laser is used to photolyze precursor for generation of a desirable radical, and the other laser is used to probe the radicals. The decay time is determined by measuring the time dependence of the light leaking out of the cavity. The intensity of the leaked pulse gradually decays and the decay time is dependent on mirror reflectivity, a path length of the absorbing species and its concentration. From the measurement of the decay time of the laser pulse at various time intervals from

formation of the radical species (photolysis pulse), the concentration-time profile is obtained to determine the reaction rate coefficient. A large number of passes of the pulse between the high-reflectivity mirrors provides an effective path length of even up to a few kilometers if very high reflectivity mirrors are used for the cavity formation. Thus, CRDS is much more sensitive than even a conventional multi-pass system.

Summary

The goal of this thesis is to understand the atmospheric implications of some selected VOCs, which have varied applications and hence released into atmosphere as pollutants. This goal is achieved by investigating the gas phase reaction kinetics of some atmospherically important VOCs with the tropospheric oxidants (OH, Cl and O_3) and identifying the stable products formed for assigning the degradation mechanism. The VOCs are selected from different class of compounds to understand the change in reactivity trends due to structural variations like unsaturation, presence of hetero atom, different functional groups and ring strain. VOCs considered include (a) cyclic hydrocarbons with eight carbon atoms (cyclooctane, cis-cyclooctene and 1,5-cyclooctadiene) to understand any change in the reactivity with unsaturation, and to compare their reactivities with saturated and unsaturated acyclic hydrocarbons, (b) halogenated cyclic hydrocarbon (1-chlorocyclopentene) for comparison of its reactivity with cyclopentene and substituted cyclopentene to understand the effect of substituent Cl on the reactivity, (c) cyclic esters (gamma-valerolactone and alpha-methyl gamma-butyrolactone) to study the effect of the ring O atom on the reactivity, and (d) ethers [dimethylether (straight chain) and epichlorohydrin (cyclic)] to compare the reactivity of cyclic and acyclic ethers and also to investigate the effect of heteroatom (chlorine) on the reactivity. The rate coefficients of reactions of these molecules with Cl, OH, and O_3 at room temperature (298 K) and 1 atm. are determined (k_{Cl}, k_{OH}, and k_{O3}) using relative rate method. These rate coefficients of a VOC are used to calculate its tropospheric lifetime, which is an essential parameter for assessing its environmental impact. These

measured values of the rate coefficients of a VOC with OH, Ozone and Cl are compared to understand relative importance (contribution) of its reactivity or degradation channels with these oxidants, and also with respect to that of analogous molecules in order to understand the reactivity pattern. These oxidants can react with the molecule by abstraction of an H atom and also by addition to the double bond. Hence efforts were made to identify the dominant channel of reaction between addition and abstraction of the oxidants with these pollutants by analyzing the reaction products. Further, the characterization of the reaction products has helped in elucidating the reaction mechanism and thus, in understanding the long term impact of these molecules in the troposphere. In addition, for evaluation of the activation energy (E_a), temperature-dependent rate coefficients for the reactions of dimethyl ether and 1-chlorocyclopentene with the OH radical is also measured using an absolute method of Laser Photolysis-Laser Induced Fluorescence (LP-LIF). The reasonably well-established structure-activity relations (SARs) are also applied in some cases to calculate the rate coefficients to compare with the measured values. The rate coefficients are then used to calculate lifetimes of these VOCs to predict their impact on the atmosphere, for a few studied VOCs, the global warming and ozone depletion potentials are also estimated. In the present work, both relative rate method and absolute method are employed to measure the rate coefficients. The experimental results are supported by theoretical calculations to understand the reaction mechanism.

Chapter-1

Introduction

1.1. Background

Advances in technology and with increasing demand by human being, the burden on atmosphere is increasing due to emission of chemical compounds, particularly volatile organic compounds (VOCs) from various anthropogenic (chemical industries, vehicular exhaust, etc.) and natural sources (wildfires, volcano activity, vegetation, etc.), which may have detrimental effect on the air quality and global climate change. Thus, it is necessary to investigate the impact of any compound on the atmosphere before being used at an industrial level. To understand the environmental impact of organic compounds, both natural and anthropogenic origin, it is required to investigate the reactions and estimate the lifetimes (residence time) of these molecules in the atmosphere. These depend on their nature and reactivity, and are mainly decided by three processes i.e. 1) Photodissociation by sunlight available in the atmosphere, 2) Dissolution in aqueous media and 3) Reaction with oxidative species (Cl, OH, NO_x, O_3, etc) [1]. Depending on the lifetime of a VOC, the impact can be very different from local (aerosol generation, ozone generation in the troposphere) to regional (acid rain, the formation of photochemical smog) to global (global warming, ozone depletion in the stratosphere). For example, chlorofluorocarbons (CFCs) are not reactive in the troposphere and thus have long tropospheric lifetime leading to the global impact on the atmosphere. The trace species can undergo different reactions at different atmospheric conditions. For example,

oxides of nitrogen lead to ozone generation in the troposphere, whereas they are responsible for ozone depletion in the stratosphere.

In modelling the atmospheric changes, like the global climate change and estimation of the tropospheric air quality and the stratospheric ozone depletion, the investigation of the processes that the molecules undergo in the troposphere and stratosphere is required.

In this thesis, an effort has been made to understand the kinetics and the degradation mechanism in the atmosphere of some selected VOCs. We have selected saturated and unsaturated cyclic hydrocarbon and esters, and both cyclic and acyclic ethers for investigating their reactions with tropospheric oxidants, OH radicals, and Cl atoms and O_3. We have used the relative rate method to measure the rate coefficients of reaction of VOCs with tropospheric oxidants (Cl, OH and O_3). In addition, we also employed the absolute method for the reaction of some of the VOCs with OH. We have corroborated experimental results of some of the VOCs with the theoretical calculations to understand the reaction mechanism.

1.1.1. Atmosphere

The earth's atmosphere consists of several layers that differ in parameters such as composition, temperature and pressure. These parameters of the atmosphere vary considerably with height (latitude). The density of atmosphere shows a sharp decrease with increasing latitude (decreases exponentially with altitude). Based on temperature variation, the atmospheric structure is divided into four thermal layers or "spheres" that are separated by transition regions, or "pauses". The atmosphere is divided into four

layers (troposphere, stratosphere, mesosphere and thermosphere) based on the temperature variation in the Earth's atmosphere (given in Fig. 1.1). The troposphere is the region extending from the earth's surface to a height of about 6–10 km, in which most weather changes occur. The troposphere is composed of nitrogen (about 78%), oxygen (about 21%), argon (about 0.9%), carbon dioxide (0.04%) and other gases along with VOCs in trace amounts. To maintain the heat balance of the earth, the atmospheric gases play a significant role, through absorption of IR radiation emitted by the earth surface. The temperature decreases linearly with altitude (negative lapse rate) from average surface temperature of about 298 K, or 25˚C till the top layer of the troposphere, which is known as the tropopause, where the temperature is about –56˚C. The troposphere contains 70% of the mass of the whole atmosphere, including almost all of the water vapour (which forms clouds and rain) and oxidants (O_2), which reacts mainly with trace oxidants (OH, NO_3, O_3, Cl, etc.). Troposphere is a turbulent region of the atmosphere, directly in contact with earth surface, where mixing of various trace species is fast and influences the life on the earth. VOCs and other trace species from the anthropogenic and biogenic origin are directly released into the troposphere. Based on the extent of anthropogenic activities and pollution, the troposphere is further characterised as remote troposphere and polluted/urban troposphere. The lowest part of the troposphere, where the emission of trace species is the maximum, is known as boundary layer/ marine boundary layer (in case of a coastal area). The main interest of the work presented in the thesis is to study the reactions of VOCs taking place mainly in the troposphere.

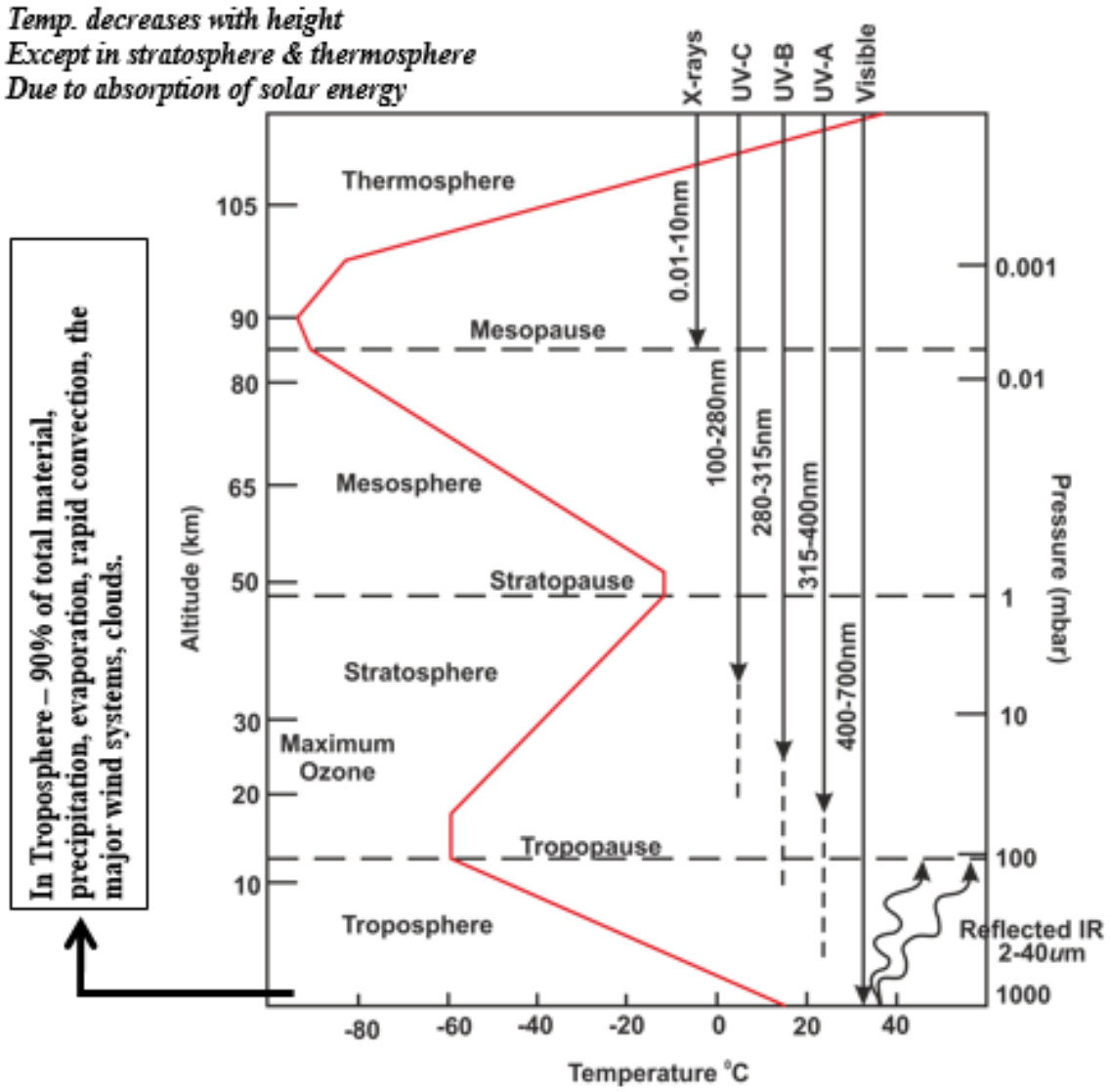

Fig. 1.1. Layers of atmospheric along with temperature profile and available solar radiation. (----- line indicates partial penetration). (Adapted from Seinfeld and Pandis - Atmospheric chemistry and physics) [7].

1.2. Effect of pollutants

Trace species present in the atmosphere due to release from natural and anthropogenic sources, in higher concentration than natural abundance, are known as pollutants. These include VOCs, particulate matter, inorganic oxides (CO_2, SO_2, NO_X),

CH_4, etc. These are further divided as primary pollutants and secondary pollutants, the former are directly emitted into the atmosphere from their sources and the latter are formed in the atmosphere, due to the reactions of the primary pollutants. Depending on nature and reactivity of trace species, its impact on the environment affects directly or indirectly the human being. For example, direct effects of trace species are carcinogenic and mutagenic effects of carbonyl and aromatic compounds [2], respiratory diseases, headache, irritation of eyes [2]. Whereas the indirect effects are global warming, ozone depletion, acid rain and photochemical smog.

1.2.1. Global warming

Every day the earth receives a large amount of energy from the sun (wavelength range available in different part of the earth's atmosphere is shown in Fig. 1.1) and part of it is absorbed by earth (66 %) and the rest (34%) is reflected and scattered back into space. Thus an optimum climatic condition is maintained for supporting life on the earth. The earth absorbs part of the radiation falling on it and gets heated up, the heated earth surface emits radiation in the infrared region (2-40 μm with the maximum at 10 μm). A part of the emitted IR radiation is absorbed by water vapour (4-8 μm) and carbon dioxide (2-15 μm). Due to this reabsorption of outgoing IR radiation, the earth's average surface temperature is maintained around 15˚C, and this absorption of radiation emitted by earth surface by atmospheric gases is known as greenhouse effect (heating of earth's surface). Due to industrialisation, green revolution, deforestation and many other man-made activities, the concentrations of CO_2, nitrous oxide, VOCs (e.g. chlorofluorocarbons) in the atmosphere have increased tremendously. These species contribute to the greenhouse effect by absorbing IR radiation emitted by the earth surface, and therefore the average

Earth's temperature is increasing. This phenomenon of increased earth's average surface temperature is popularly known as global warming and the contribution of a particular trace chemical species in the troposphere to global warming is estimated based on its global warming potential, which is measured relative to CO_2. Thus, global warming potential (GWP) indicates the capacity of a compound to trap heat in the atmosphere with respect to the reference CO_2 molecules.

1.2.2. Acid rain

SO_2 and NO_X (NO, NO_2, NO_3, etc.) are released into the atmosphere from natural as well as anthropogenic sources (volcanic eruption, burning of fossil fuels, vehicular exhaust, etc.). In troposphere, SO_X, NO_X, hydrocarbon, and soot particles undergo heterogeneous reactions in the cloud and produce nitric acid (HNO_3) (Eqn. 1.4) and sulphuric acid (H_2SO_4) (Eqn. 1.5). These oxidation reactions in cloud change the pH value of pure water droplet from neutral (pH 7) to acidic (less than 7), and when this mixture precipitates, it is known as acid rain. It damages sculptural materials and retards the growth of trees.

$$NO + O_3 \rightarrow NO_2 + O_2 \quad (1.1)$$

$$NO_2 + O_3 \rightarrow NO_3 + O_2 \quad (1.2)$$

$$NO_2 + NO_3 \rightarrow N_2O_5 \quad (1.3)$$

$$N_2O_5 + H_2O \rightarrow 2HNO_3 \quad (1.4)$$

$$SO_2 + \frac{1}{2}O_2 \xrightarrow[soot\ particles]{(HC,NOx)} H_2SO_4 \quad (1.5)$$

1.2.3. Ozone depletion

Ozone (O_3) in the stratosphere plays a very important role for sustaining life on the earth by absorbing harmful UV radiation (280-320 nm), as this radiation has high potential to trigger skin cancer, sunburn and cataracts. In the stratosphere, there is an equilibrium between oxygen and ozone concentration, as postulated by Chapman, Eqn. 1.6-1.11.

Chapman mechanism [3,4],

$$O_2 \xrightarrow{h\nu} O + O \qquad (\lambda < 240 \text{ nm}) \tag{1.6}$$

$$O(^3P) + O_2 + M \rightarrow O_3 + M (M = N_2, O_2) \tag{1.7}$$

$$O_3 \xrightarrow{h\nu} O_2 + O(^1D) \qquad (\lambda < 320 \text{ nm}) \tag{1.8}$$

$$O(^1D) + M \rightarrow O(^3P) + M \tag{1.9}$$

$$O + O_3 \rightarrow 2O_2 \tag{1.10}$$

$$\text{Net: } O_3 \rightleftharpoons O_2 + O \tag{1.11}$$

The total amount of ozone in the stratosphere is determined by a balance between photochemical production and recombination. In the stratosphere, the maximum concentration of O_3 is at the height of about 30 km from the earth surface and depends on the location.

Ozone is a very reactive species and can be removed by many free radical catalysts; the important ones are chlorine and bromine atoms. These species take part in the reactions which disturb O_3-O_2 equilibrium leading to depletion of ozone (Eqn. 1.12, 1.13).

Ozone depletion due its reaction with other reactive species (X)

$$X + O_3 \rightarrow XO + O_2 \tag{1.12}$$

$$XO + O \rightarrow X + O_2 \quad (1.13)$$

where X is a free radical catalyst, which can be H, OH, NO, Cl, or Br.

The observed Antarctic region ozone layer depletion is attributed mainly to the emission of chlorofluorocarbons (CFCs) and other halogenated ozone-depleting substances (ODS) into the atmosphere. As these compounds are inert to the tropospheric oxidants, they have a long life in the troposphere and enter into the stratosphere and take part in ozone depletion. The halogenated compounds have high absorption cross-section in the available UV radiation in the stratosphere and undergo photodissociation, producing active atomic catalysts (Cl, Br). In the last thirty years, it is observed that in Antarctica, during the springtime (September-November) the stratospheric O_3 concentration is considerably reduced (below 200 Dobson Units) compared to ozone concentration during other periods. This considerable decrease in ozone concentration in Antarctica during springtime is known as ozone hole and it is attributed to heterogeneous reactions on the polar stratospheric clouds (PSCs). In Antarctica during winter, there is the formation of polar stratospheric clouds (PSCs) where cold air gets trapped, at a temperature below -78˚C. In springtime, active Cl_2 species are released through complex interfacial chemistry and photochemistry in polar stratospheric clouds (Fig. 1.2).

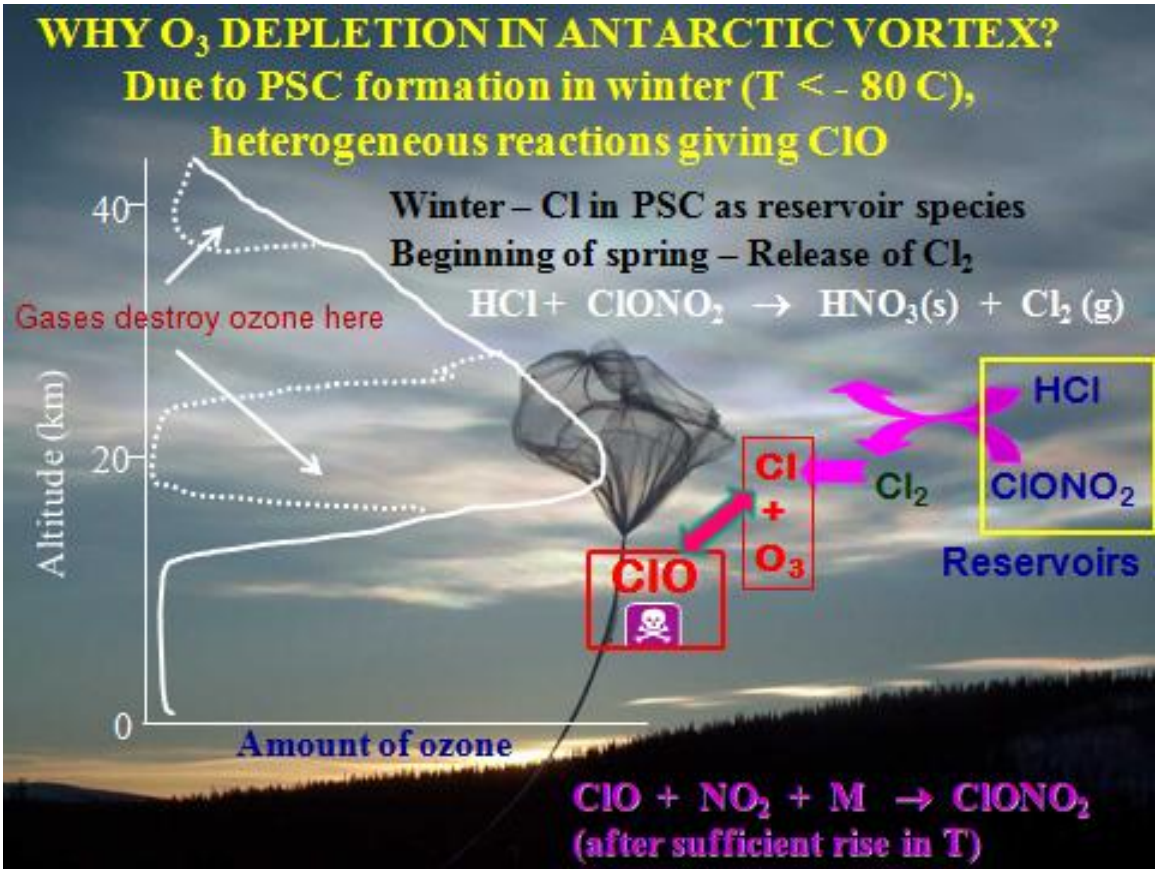

Fig. 1.2. Distribution of ozone over the altitude in the atmosphere and reactions responsible for ozone hole in Antarctica in winter. (Adapted from Seinfeld and Pandis - Atmospheric chemistry and physics) [7].

The Montreal Protocol was adopted in 1987 [5] after the experimental confirmation of ozone hole in the Antarctic region during springtime, and it bans the production and use of CFCs, halons and other ozone-depleting compounds.

1.2.4. Photochemical smog

Trace chemicals species present in the atmosphere participate in photochemical reactions by absorbing solar radiation. Release of trace species (VOCs, NO_X, etc.) into

the atmosphere does not cause any major problem, but their reactions with the reactive substances produced by the photochemical reaction in the atmosphere do cause a serious environmental problem. The reaction product is known as photochemical smog (a mixture of pollutants that are formed when VOCs and nitrogen oxides react in the presence of sunlight), which is oxidising in nature. It is characterized by brown hazy fumes, which cause respiratory problems, eye irritation, extensive damage to plants, etc.. O_3 and PAN (Peroxyacyl nitrate) are products of photochemical smog.

1.2.5. Particulate matter

Particulate matter (PM) is the term for an air suspended complex mixture of all microscopic solid and liquid particles. These particles originate from human activities (Polycyclic aromatic hydrocarbon (PAH), fly ash from plants, smoke from incomplete combustion, fuel combustion (coal, fuel oil, natural gas, wood) and natural processes (pollen, volcanic eruptions, blowing of dust and soil by wind, spraying of salt by seas and oceans). These particles vary greatly in size, composition, and origin, and may be harmful (that depends on nature and size of PM). Size of PM is the most important property that can vary from 0.0002µm to 500µm. Based on the size they can be classified as PM_{10} (coarse and fine particles), $PM_{2.5}$ (fine particles, which are very harmful as they damage lungs) or $PM_{0.1}$ (ultrafine particles). PM reduces visibility and quality of air in the atmosphere. It absorbs and reflects incident solar radiation, and thus reduces the solar flux.

1.3. The fate of trace species (VOCs) in the atmosphere

The type of environmental problem a trace species will impose depends on the lifetime of species in the atmosphere. The life of trace species depends on the rates of

different degradation processes the trace species undergoes in the atmosphere. The major degradation processes for trace species are photodissociation, deposition and reactions with oxidative species [6]. If the lifetime of the species is in seconds/days/years, it will cause local /regional (acid rain)/ global (ozone depletion, global warming) effect, as depicted in the Fig. 1.3.

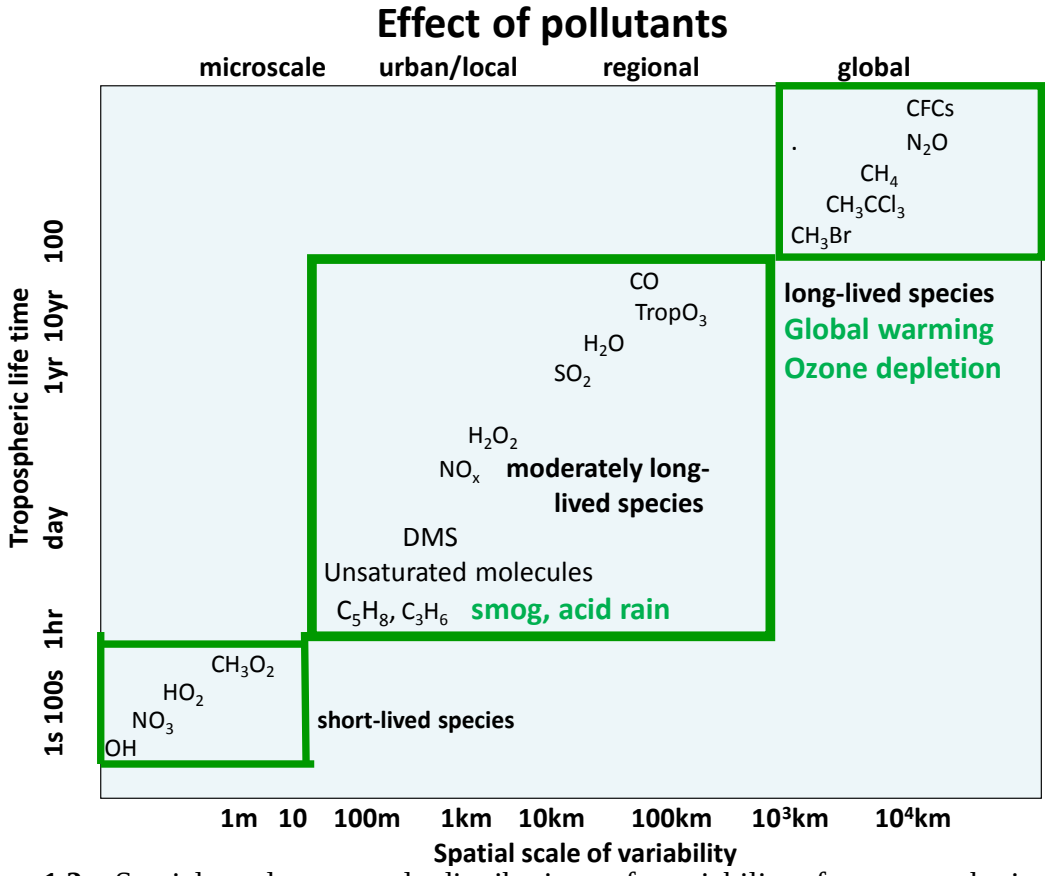

Fig. 1.3. Spatial and temporal distribution of variability for atmospheric trace constituents. (Adapted from Seinfeld and Pandis - Atmospheric chemistry and physics) [7].

1.3.1. Photodissociation

When a molecule absorbs solar radiation present in the atmosphere of energy higher than its dissociation energy, it gets excited to a higher energy state and dissociates,

if the potential energy is favourable. This process is known as photodissociation, and the rate of this process depends on the absorption cross-section spectrum of the molecule, the intensity of solar radiation available at wavelengths less than the dissociation threshold wavelength of the molecule, and quantum yields of dissociation process at the above wavelength region.

Rate= J (rate coefficient) n (concentration)

$$\boldsymbol{J(s^{-1}) = \int_{\lambda} F(\lambda)\sigma(\lambda)\Phi(\lambda)d\lambda} \qquad (1.14)$$

J = rate coefficient of photodissociation, F(λ) = spectral actinic flux, σ(λ) = absorption cross section and Φ(λ) = photodissociation quantum yield at wavelength λ.

Most of the VOCs are not degraded in the troposphere by this process, due to very low absorption cross-section of the molecules in the available wavelength region and unfavourable available wavelength region for dissociation process, but this is the main degradation channel for VOCs if migrated into the stratosphere.

1.3.2. Dissolution in the aqueous phase

Most of the VOCs are hydrophobic in nature and hence, have very low solubility in water. The partition of a VOC from air to atmospheric water such as an ocean, rain, dew, and ice is governed by mass transfer of the VOC from air to water through an air-water interface. Once dissolved in water, it is mainly deposited at earth's surface, and this process is known as a wet deposition.

The rate of dissolution of the VOC in the aqueous phase is decided by Henry's law constant K_H, which depends on the nature of gas, temperature, humidity and various other conditions. The mass of a gas that dissolves in a given amount of liquid at a given

temperature is directly proportional to the partial pressure of the gas above the liquid. Concentration of gas in aqueous phase [M] is given by the relation,

$$[M] = K_H \times p \quad (1.15)$$

where p is the partial pressure of the gas in equilibrium, and K_H is Henry's law constant. If the trace species emitted into the atmosphere is semi-volatile in nature and has high solubility in the aqueous phase, the removal by dissolution in atmospheric water droplets is one of the major pathways from the troposphere. In addition to wet deposition, VOCs are also removed by dry deposition. Unlike in wet deposition, where these are first dissolved in atmospheric water droplets, in dry deposition VOCs are transported to the ground level and absorbed/adsorbed onto water surfaces, vegetation, plants and soil surface.

1.3.3. Reaction with oxidative species

The earth's atmosphere is oxidizing in nature due to presence of reactive species like O_xH (OH and HO_2, the former is the most important species), O_3, NO_x (NO_3, NO_2, NO) and Cl atoms (important species in polluted and coastal regions). Among these, OH and O_3 are daytime oxidants and NO_3 is night time oxidant. Chemical species emitted into the atmosphere are mainly degraded in the troposphere by reacting with these oxidants, as reaction with the oxidizing species is the most important degradation pathway for most of the trace chemical species present in the troposphere [8]. The rate of this degradation process for a chemical species M is given by

$$(dM/dT)_{ox} = \sum_i k_i[X_i]\,[M] \quad (1.16)$$

where, k_i is the rate coefficient for the reaction of M with oxidizing species '*i*' and X_i is the concentration of the oxidising species in the troposphere. The rate of the degradation process depends on the nature of chemical species M, temperature and location of emission of M.

1.3.3.1. Formation of hydroxyl radical in the troposphere

Most of the trace chemical species emitted into the atmosphere are degraded in the troposphere by reaction with OH radicals, which is known as a detergent or a scavenger of the troposphere. The OH radical is produced in troposphere by the reaction of water vapour with O (^{1}D), and the latter is produced by photolysis of O_3.

$$O_3 \xrightarrow{h\nu} O_2 + O(^1D) \qquad (\lambda \leq 330 \text{ nm}) \qquad (1.8)$$

$$O(^1D) + M \rightarrow O(^3P) + M \qquad (1.9)$$

$$O(^3P) + O_2 + M \rightarrow O_3 + M \qquad (1.7)$$

$$O(^1D) + H_2O \rightarrow 2\,OH \qquad (1.17)$$

The formation of OH radicals is controlled by UV radiation present in the troposphere, O_3 and water vapour concentrations and also on mixing ratio of the region. So, even though the production of the O(^{1}D) (Reaction 1.8) is less, it is compensated by higher mixing ratio of H_2O and produces ~ 0.2 OH radicals per O (^{1}D) atom formed in the air of 50% relative humidity at 298 K and atmospheric pressure.

In the troposphere, the OH radical is also generated by photolysis of HONO and H_2O_2, the former being formed by the reaction of NO_2 with water on surfaces at night.

$$HONO \xrightarrow{h\nu} OH + NO \qquad (\lambda \leq 400 \text{ nm}) \qquad (1.18)$$

$$H_2O_2 \xrightarrow{h\nu} 2OH \qquad (\lambda \leq 370 \text{ nm}) \qquad (1.19)$$

HO_2 is formed by oxidation of VOCs in the troposphere. In polluted regions, where NO_x and O_3 are in high concentrations, HO_2 reacts with NO/O_3 and produces OH radicals.

$$HO_2 + NO \rightarrow OH + NO_2 \quad (1.20)$$

$$HO_2 + O_3 \rightarrow OH + 2O_2 \quad (1.21)$$

$$OH + O_3 \rightarrow HO_2 + O_2 \quad (1.22)$$

All the above processes for the OH radical generation take place in the presence of light, which is available during the daytime. During night time, OH is produced by the reaction of O_3 with alkenes (Reactions 1.23 and 1.24). The O_3 + alkene reaction initially forms an ozonide, which breaks up to form a carbonyl and a "Criegee" intermediate, which on further dissociation forms the OH radical [9].

$$CH_3CH = CHCH_3 + O_3 \rightarrow CH_3CHO + CH_3CHOO^{\bullet} \quad (1.23)$$

$$CH_3CHOO^{\bullet} \rightarrow {}^{\bullet}CH_2CHO + OH \quad (1.24)$$

The tropospheric OH radical concentrations were estimated by modelling calculation to be 10^6 species cm^{-3} by accounting the penetration of UV radiation in the wavelength region 300-320 nm.

The peak daytime concentration of the OH radical was measured spectroscopically in the northern hemisphere to be in the range of (2-10) × 10^6 molecules cm^{-3} [10]. The OH radical concentration was also estimated by measuring the concentration of methyl chloroform (1,1,1-trichloroethane). Methyl chloroform is a molecule of only anthropogenic origin with its loss from the atmosphere depends mainly on reaction with the OH radicals. Thus, comparing the total emissions of methyl

chloroform with its measured concentrations, the diurnally, seasonally and annually-averaged 24-h OH radical concentration was evaluated to be 1×10^6 molecules cm^{-3} [11]. Although OH is the most important oxidant in the troposphere, other oxidants, such as NO_3 and O_3, also affect the lifetimes of both anthropogenic and natural species in the troposphere.

1.3.3.2. Sources of O_3 in atmosphere

Ozone is very important for sustaining life on the earth as it absorbs harmful UV radiation in the stratosphere, UV radiations have a detrimental effect on human health, like it can cause skin cancer etc.. Ozone in the troposphere is considered a greenhouse gas (i.e. absorbs and emits radiation) and may contribute to global warming, but it is also an important oxidant in troposphere responsible for the degradation of pollutants (especially unsaturated hydrocarbon). The concentration of O_3 is 20-30 parts per billion by volume (ppbv), but in polluted areas, it can reach up to 100 ppbv. Tropospheric ozone is mainly formed by photolysis of NO_2 in air. The concentration of O_3 depends upon the concentration of NO_x, CO, and VOCs (precursors of NO_2). In the troposphere, ozone is formed via a sequence of reactions starting from the formation of peroxy radicals, which occurs when the above precursors react in the atmosphere in the presence of sunlight. The peroxy radicals thus formed react with NO to produce NO_2, which on photolysis (NO_2 absorbs radiation < 400 nm) produces ground-state atomic oxygen. Ozone is formed on subsequent reaction of an oxygen atom with molecular oxygen. The sequence of reactions for the generation of O_3 from NO_2 is given below.

$$NO_2 \xrightarrow{hv} NO + O(^3P) \quad (\lambda \leq 400 \text{ nm}) \qquad (1.25)$$

$$O(^3P) + O_2 + M \rightarrow O_3 \quad (1.7)$$

$$NO + O_3 \rightarrow NO_2 + O_2 \quad (1.1)$$

These reactions (1.25, 1.7, 1.1) represent 'no net change' cycle of NO_x since rapid interconversion of NO and NO_2 (in the absence of competing reactions) maintain steady-state concentrations with no net production or destruction of O_3. However, photochemical oxidation of CO and VOCs (RH) by the OH radical produces hydroperoxy (HO_2) and alkyl peroxy (RO_2) radicals as intermediates in the troposphere which can also convert NO to NO_2.

$$\bullet OH + CO \rightarrow \bullet HOCO \quad (1.26)$$

$$\bullet HOCO + O_2 \rightarrow HO_2\bullet + CO_2 \quad (1.27)$$

$$\bullet OH + RH \rightarrow R^{\bullet} + H_2O \quad (1.28)$$

$$R\bullet + O_2 \rightarrow RO_2 \quad (1.29)$$

$$HO_2 + NO \rightarrow OH + NO_2 \quad (1.20)$$

$$RO_2 + NO \rightarrow RO + NO_2 \quad (1.30)$$

These reactions result in net production of ozone upon photolysis of NO_2 as O_3 is not consumed for the conversion of NO to NO_2. Thus, the photostationary state of O_3 gets perturbed. The average concentration of O_3 in the troposphere is 7×10^{11} molecules cm^{-3} [12].

1.3.3.3. Sources of Cl atom in troposphere

Degradation of VOCs by reaction with Cl is not a significant channel in the ambient condition, due to a low concentration of Cl atom (10^3 atoms cm^{-3} [14]). However, in the remote marine boundary layer, the peak concentration of Cl atoms during

sunrise is reported to be 1.3×10^5 atoms cm^{-3} [13,14]. Under the above condition, the degradation of some VOCs, such as hydrocarbons, by reactions with Cl atoms is as significant as reaction with OH radicals, and in some favourable cases can be more effective than the latter [15].

The presence of the Cl atom in the troposphere is attributed to both natural (volcanic eruption, the heterogeneous reaction of sea salt in the coastal area) and anthropogenic (coal combustion, incineration and industries) sources. Tons of Cl atom precursors (in the form of Cl_2 and HCl) are released from industries and coal combustion, and these precursors undergo degradation to produce Cl atom.

$$Cl_2 \xrightarrow{h\nu} 2Cl^{\cdot} \quad (1.31)$$

$$HCl + OH^{\cdot} \rightarrow Cl^{\cdot} + H_2O \quad (1.32)$$

In the polluted and coastal region, the following reactions are responsible for the generation of Cl atoms [16].

$$HCl + OH^{\cdot} \rightarrow Cl^{\cdot} + H_2O \quad (1.32)$$

$$\dot{C}l + O_3 \rightarrow ClO + O_2 \quad (1.33)$$

$$ClO + HO_2 \rightarrow HOCl(g) + O_2 \quad (1.34)$$

$$HOCl(g) \rightarrow HOCl(aq) \quad (1.35)$$

$$HOCl(aq) + Cl^-(aq) + H^+(aq) \rightarrow Cl_2(aq) + H_2O \quad (1.36)$$

The species, Cl_2 and HOCl are accumulated at night time and undergo photodissociation after sunrise, releasing Cl atoms and are responsible for a high concentration of Cl atom in the morning. In addition to these, the marine region

precursors, such as Cl_2, ClNO, or $ClNO_2$, are also formed by heterogeneous reactions of sea salts aerosols and N_2O_5, or other oxidants (OH and O_3) [17].

$$HCl(g) + N_2O_5(g) \rightarrow HNO_3(l) + ClNO_2(g) \quad (1.37)$$

$$NaCl(s) + N_2O_5(g) \rightarrow NaNO_3(s) + ClNO_2(g) \quad (1.38)$$

$$NaCl(s) + O_3(g) \rightarrow Cl_2(g) + Products \quad (1.39)$$

The species, Cl_2 and $ClNO_{x\ (x=1,\ 2)}$ undergo photolysis after sunrise, producing Cl atom through reactions 1.31 and 1.40, respectively.

$$ClNO_x \xrightarrow{hv} Cl + NO_x \quad (1.40)$$

1.3.4. Tropospheric lifetime

Tropospheric lifetime (or residence time) of a molecule is defined as the average time that the molecule remains in the troposphere and estimated from the ratio of its mass or concentration (M) to the rate at which it is depleted, dM/dt.

$$\boldsymbol{\tau} = \frac{\mathbf{M}}{\mathbf{dM}/\mathbf{dt}} \quad (1.41)$$

As mentioned above, removal processes of a species from the atmosphere includes photodissociation, precipitation in aqueous phase and reaction with tropospheric oxidants, which is described by the following equation for a lifetime, τ.

$$\tau = \left[\int_{\lambda} \boldsymbol{F(\lambda)\sigma(\lambda)\Phi(\lambda)d\lambda} + \boldsymbol{k_{deposition}} + \sum_{\mathbf{i}} \mathbf{k_i[X_i]}\right]^{-1} \quad (1.42)$$

But for most of the trace species, it has been observed that the reaction with the tropospheric oxidants is the most important degradation channel among the three processes, and the tropospheric lifetime with respect to oxidants is calculated as follows.

$$\boldsymbol{\tau} = [\mathbf{M}]\left[\sum_i \mathbf{k_i}[\mathbf{X_i}]\,[\mathbf{M}]\right]^{-1} \quad (1.43)$$

$$\tau = \left[\sum_i \mathbf{k_i}[\mathbf{X_i}]\right]^{-1} \quad (1.44)$$

where k_i is the rate coefficient for the reaction of M with oxidant species *'i'*, and 'X_i' is the average concentration of oxidant species '*i*' in the troposphere.

Depending upon the value of τ, a species is characterized either as short-lived (up to 1 hour), moderately lived (up to 1 year) or long-lived (up to 100 years). The tropospheric lifetimes decide the nature of impact a species imposes on atmosphere, varying from local (for short and moderately lived species) to global (for long-lived species).

Identifying the most significant reaction among reactions of species with various oxidants (OH, Cl, O_3) is also important in understanding the important pathway of degradation of the species. This can be done by comparing the individual tropospheric lifetimes, τ_i, considering the reaction of VOC with specific species X_i alone, as given below.

$$\tau_i = 1/k_i\,[X_i] \quad (1.45)$$

In terms of the individual oxidant specific tropospheric lifetimes, the overall tropospheric lifetime (τ) is

$$\tau = \left[\sum_i (\tau_i)^{-1}\right]^{-1} \quad (1.46)$$

Thus as mentioned earlier, the harmful effects of a chemical species depend on the tropospheric residence time, which in turn depends on the rate coefficients of the reactions of the chemical species with tropospheric oxidants, especially in the case of organic molecules having low solubility in water coupled with very low photodissociation cross-section in the visible range of the solar spectrum. This emphasizes the need to study the kinetics of reactions of organic molecules with different oxidizing species in the troposphere. Thus there is a significant effort to determine the rate coefficients of reactions of the VOCs with the tropospheric oxidants.

1.4. Methods and techniques for kinetics study

Kinetics of a reaction can be studied by measuring the time-dependent concentration of a reactant or a product at a particular temperature. The concentration can be measured in real-time by directly probing the species of interest, or by some other indirect methods. Thus, in general, two methods, namely, the absolute and the relative rate methods, are adopted to study the rate coefficient of a reaction.

1.4.1. Absolute method

In this method, the concentration of a reactant or a product is measured directly as a function of reaction time by probing the species. In this type of experiments, for bimolecular second-order reaction, the kinetic measurements are carried out under pseudo-first order condition, i.e., by maintaining the concentration of one of the reactants very low compared to another reactant.

For a bimolecular reaction,

$$A + X \rightarrow Product \qquad (1.47)$$

$$\frac{-d[A]}{dt} = \frac{-d[X]}{dt} = k[A][X] = k'[X] \quad (1.48)$$

under the condition, [A] >> [X].

In the thesis work, kinetic studies of the reaction of a reactant, A, with an oxidant species, X, which is generated in situ from its precursor, are studied in the presence of an excess of the reactant A. Under the above condition, depletion of [X] is measured to obtain the pseudo-first order rate coefficients, k'. By obtaining the pseudo-first order rate coefficients at different concentrations of A, the bimolecular rate coefficient (k) of reaction (1.47) is determined. Different techniques can be used for generating or introducing X in the system and also to follow its concentration.

In our laboratory at Radiation & Photochemistry Division, Bhabha Atomic Research Centre, Laser Photolysis-Laser Induced Fluorescence (LP-LIF) and Fast flow-Discharge Systems (FF-DS) were developed and employed for kinetic measurement. However, only LP-LIF is employed in this thesis work. Short descriptions of these two techniques are given below.

1.4.1.1. Laser Photolysis-Laser Induced Fluorescence (LP-LIF)

The LP-LIF technique is a pump-probe technique where a short pulse laser (pump laser) is used for in situ generations of one of the reactant species from its precursor. The concentration of the species is probed as a function of reaction time by selectively exciting the species by another short-pulse laser (a probe laser) at various delay time from the pump laser pulse and measuring the fluorescence intensity. Under the controlled experimental conditions with the lifetime of the excited state being much shorter than the collisional deactivation, the integrated intensity of the fluorescence (I_{LIF}) is proportional

to the concentration of species X, the Einstein absorption coefficient (B_{12}), laser intensity (I_{laser}) and ϕ (quantum yield of formation of X), as given below.

$$I_{LIF} \propto \phi I_{Laser} B_{12} [X] \quad (1.49)$$

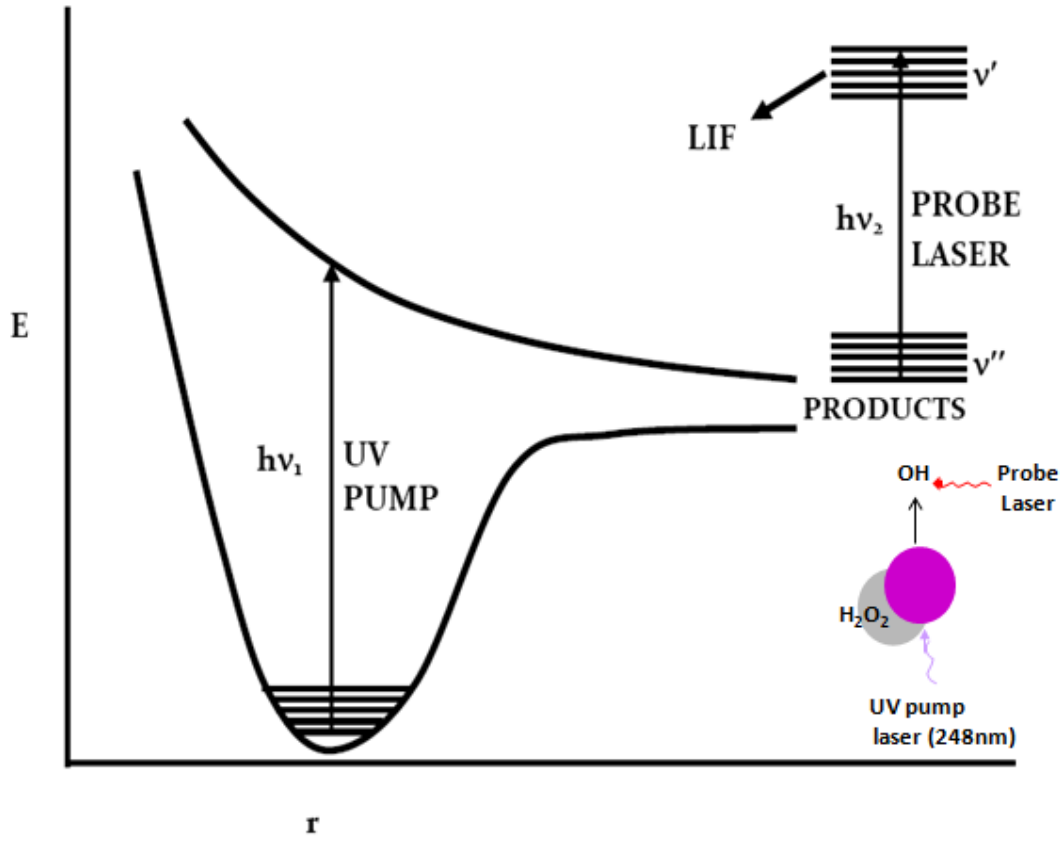

Fig. 1.4. Schematic of LIF technique for measurement of species concentration [OH].

The fluorescence spectra are generally red-shifted with respect to the absorption spectra in most of the cases. Since the measurement of the shifted emission will have less interference from the scattered photons, this feature makes fluorescence measurement an advantageous method for detection of suitable species. Fluorescence is collected at the right angle to the excitation source, to minimize the contribution of the scattered light to the measured fluorescence signal. These two features improve the signal-to-noise ratio of

the technique. However, all the species are not amenable to LIF detection. To apply the LIF technique, certain criteria should be fulfilled. The most important criterion is that the species must fluoresce. Moreover, the band systems must be well characterized spectroscopically, and these should be accessible with available tunable lasers.

In the present thesis, the bimolecular rate coefficient for the reaction of VOCs with OH is measured using LP-LIF technique. Here, the measurements of rates of OH decay in absence & presence of a known excess concentration of VOC (maintaining pseudo-first order condition with [VOC]>>[OH]) are carried out. The hydroxyl radicals are generated in situ by photolysis of H_2O_2 at 248 nm using KrF excimer laser, and its concentrations are monitored by collecting the resulting fluorescence after exciting the $P_1(2)$ line in the (0,0) band of the ($A^2\Sigma$, $v'=0$) ← ($X^2\Pi$, $v''=0$) transition at 308 nm using tunable dye laser. Here, the total fluorescence intensity is proportional to the concentration of the OH radicals. The temporal profile of OH concentration is followed by varying the time delay between the pump and the probe laser pulses from 10 μs to 10 ms, in steps of a few microseconds with the help of a delay generator, to measure the pseudo-first order rate coefficient.

At a particular (constant) temperature, the pseudo-first order rate coefficient values obtained at various VOC concentrations are plotted against the concentration of the VOC, the slope of the plot gives the value of the bimolecular rate coefficient of species (VOC) with the OH radical. Further details of this technique are discussed in Chapter 2 of this thesis.

1.4.1.2. Fast Flow-Discharge Systems (FF-DS)

The flow tube technique is one of the oldest techniques employed for the measurement of kinetic data of the reaction of importance to combustion and atmospheric chemistry. Braun and Lenzi [18] were the first to develop the flow tube technique for kinetic experiments by suitably adapting the discharge tube studies of Wood and Bonhoeff [19]. The flow tube technique was revised extensively along with its instrumentation in the 1960s. In combustion and atmospheric reaction, one of the reactants is either a radical or an atomic species, and in most of the discharge flow tube systems, this species is generated in-situ by electrodeless microwave discharge from its precursor. In flow tube experimental setup, flow velocity (v) is related to reaction time by $t = z/v$, where z is the reaction zone length. The reaction time is varied by varying z, at constant v, for this purpose either the reactants are mixed at a varied distance from the detection zone or by inserting one of the reactants at various distance from the detection zone, employing an injection tube for injection. The latter method is adopted in most of the experimental setup. For studying fast reactions by this method, a steady linear flow velocity of several meters per second is required which can be achieved by employing high-speed pumps. The detection techniques like, mass spectrometry, chemiluminescence and fluorescence are employed for concentration measurement of one of the reactants or products. A schematic of the fast discharge flow setup, developed in our laboratories [20] to measure the rate co-efficient of O (^{3}P) atoms with various VOCs, is shown in Fig. 1.5**.**

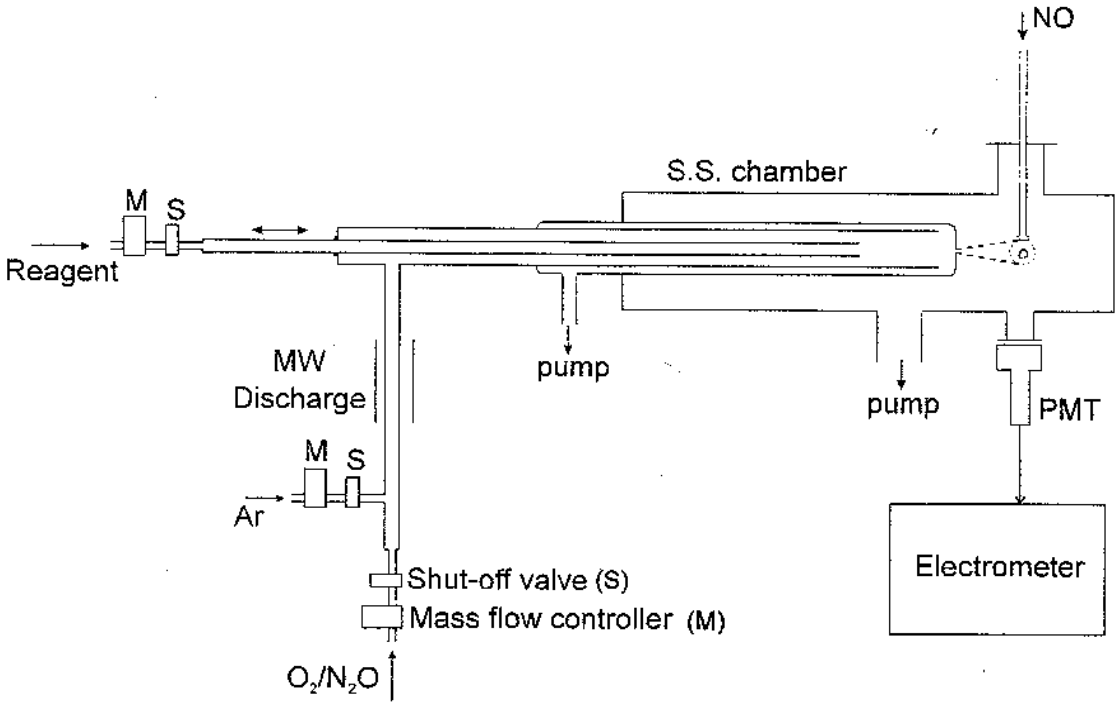

Fig. 1.5. A schematic of fast discharge flow setup [20].

In this setup, the reaction is arrested at the end of the flow tube by effusing out a small portion of the gas mixture into another chamber and concentration of oxygen atom is measured by titrating with NO gas, at various reaction zone lengths.

1.4.2. Relative rate method

The relative rate method is based on competition kinetics. In this technique, the reactant (sample) species, reference species, the precursor of reactive species and buffer gas are mixed in a vessel, and the reactive species are generated in-situ. The relative depletion in the reactant and the reference species concentration is monitored to obtain the rate coefficients of the sample species with reactive species, from the known rate coefficient of reference species with reactive species. The relative rate method relies on the fact that the reference compound and the sample compound do not react with each

other, and both these compounds are removed solely by reactions with the reactive species.

Considering the reaction of the reactive oxidizing species, X, with a sample, S, and reference, R,

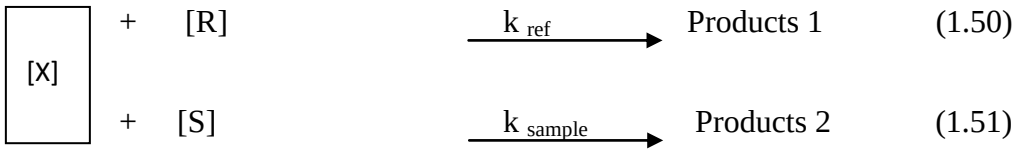

The relative rate equation is expressed as,

$$\log\left(\frac{[S]_{t=0}}{[S]_t}\right) = \frac{k_{sample}}{k_{ref}} \log\left(\frac{[R]_{t=0}}{[R]_t}\right) \quad (1.52)$$

Here $[R]_t$ and $[S]_t$ are the concentrations of the reference compound and the sample, respectively, at time t, and $[R]_{t=0}$ and $[S]_{t=0}$ are their initial concentrations.

A plot of $\log\left(\frac{[S]_{t=0}}{[S]_t}\right)$ against $\log\left(\frac{[R]_{t=0}}{[R]_t}\right)$ represents a straight line with slope equal to $\frac{k_{sample}}{k_{ref}}$. Thus, by measuring the concentrations of the reference compound and the sample at different times, the rate coefficient of the sample with the oxidant species, X, can be calculated from the slope, by inserting the known rate coefficient of reference with oxidant species, X. In the thesis work, the Gas Chromatography (GC) technique is employed to measure the relative concentration of the reference compound and the sample compound, in the reaction vessel by generating oxidant species in-situ from its precursor by photolysis technique. The details of the experimental setup employed are given in the experimental Chapter 2.

1.5. Degradation mechanism of VOCs in troposphere

In addition to the lifetime of a VOC with respect to tropospheric oxidants, the impact of a VOC on the environment also depends on the products formed during these reactions. The products of these reactions are mostly oxidized products. The typical reaction mechanism is shown in Scheme 1.1.

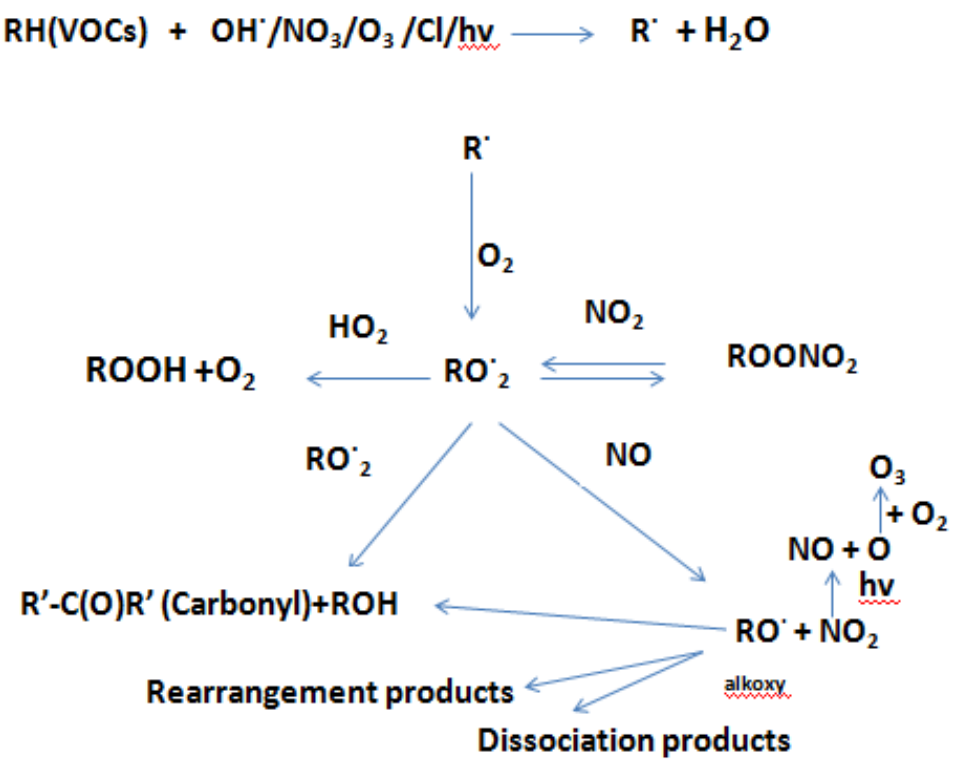

Scheme 1.1: Typical mechanism for degradation of VOCs by tropospheric oxidants.

The VOCs (primary pollutants or secondary products of primary pollutants) react with tropospheric oxidants (OH radicals, NO_3 radicals, Cl atoms, and O_3) or undergo photodissociation to form radicals. Depending on the nature of a VOC, the reaction mechanism occurring in the troposphere may involve the formation of an alkyl or substituted alkyl radical (as shown in Scheme 1.1), which further reacts with oxygen and generates a peroxy radical. These peroxy radicals react mutually or react with NO_x and

form an alkoxy radical. The saturated hydrocarbons mostly degrade in the troposphere by reactions which involve H-atom abstraction by OH radicals, Cl atom and NO_3 radical, while for unsaturated hydrocarbons, the dominant reaction channel involves an initial addition of OH/Cl/NO_3/O_3 to the carbon atom of a C=C bond. Alcohol and ketone/aldehydes are the major products of these reactions. Smog chamber studies have shown that unsaturated hydrocarbon reactions with OH and O_3 lead to secondary organic aerosol generation [21]. In some cases, the primary pollutants are not that harmful but their reaction products are harmful to the environment. Hence, in order to understand the total impact of a VOC on the environment, it is necessary to analyze the products formed on its reactions with tropospheric oxidants. The analyses of the stable products formed during the reactions of these VOCs with tropospheric oxidants have been carried out by Gas Chromatography (GC) and Gas Chromatograph-Mass Spectrometry (GC-MS) techniques.

1.6. Theoretical calculations

It is important to compare the experimental results with theoretical predictions to get a real insight into a chemical reaction. The theoretical studies are required to either support a reaction mechanism, proposed based on the measured reaction coefficients and identified stable products, or propose a new mechanism, based on nature of the transition state involved and energetics of the reaction. The work carried out in this thesis is mostly supported by *ab initio* molecular electronic structure theories. Gaussian 03 and 09 [22] programs are employed to investigate structures and energetics of different radical and molecular channels. Theoretical calculations, using *ab initio* Molecular Orbital Theory and Density Functional Theory (DFT), are performed to investigate the potential energy

surface (PES) of the reaction of a VOC with either Cl or OH. The geometries of the ground electronic states of the VOC, the transition-state (TS) structures, and the reaction products are optimized at the HF/6-311+G(d,p), B3LYP/6-311++G(d) or B3LYP/6-311++G(d,p) level of theory. The harmonic vibrational frequencies and the force constant are calculated to ensure the stationary points on the PESs to be true saddle points, and also for zero-point energy correction. All calculated TS structures have only one imaginary frequency and one negative eigenvalue of the force constant matrix. The single point energies for various optimized geometries are calculated at the QCISD(T)/6-311++G(d,p) or G3 level of theory. Some specific details of the theoretical methods employed for different system are discussed in the corresponding chapters of this thesis. Some of the keywords for the methods, which are used in this work, are listed in Table 1.1. The basis sets represent the molecular orbitals within a molecule. It is understood as forcing each electron to a particular region of space. Table 1.2 lists the commonly used basis functions with their basic criteria and field of usefulness. Larger basis sets impose lesser constraints on electrons, and more accurately approximate exact molecular orbital. Thus, one can systematically increase the size of the basis set until the results converge to within some desired limits of accuracy.

Table 1.1: Commonly used methods in Gaussian calculation.

Keyword	Methods
HF	Hartree-Fock Self-Consistent Field
MP2	2nd Order Møller-Plesset Perturbation Theory
QCISD	Quadratic Configuration Interaction (Singles and Doubles)
CIS	Configuration Interaction (Singles)
MP3	3nd Order Møller-Plesset Perturbation Theory
MP4	4nd Order Møller-Plesset Perturbation Theory
QCISD(T)	Quadratic CI (Singles, Doubles and Triples)

Table 1.2: Commonly used basis functions and their description.

Basis set	**Description**	**No. of basis functions**	
		heavy atom#	**hydrogen**
STO-3G	Minimal basis set: Used for more qualitative results for big systems	5	1
3-21G	2 sets of functions in the valance region: Used when 6-31G is too expensive	9	2
6-31G(d)	Adds polarization functions to	15	2

	heavy atoms: Used for most jobs up to medium size systems		
6-31G(d,p)	Adds polarization functions to hydrogen as well: Used when hydrogen atoms are the site of interest	15	5
6-31+G(d)	Adds diffuse functions: Most important for systems with lone pairs, anions, excited states	19	2
6-31+G(d,p)	Adds p functions to hydrogen as well: Used when diffuse functions are needed over 6-31G(d,p)	19	5
6-311+G(d,p)	Adds extra valance functions (3 sizes of s and p functions) to 6-31+G(d,p)	22	6
6-311+G(2d,2p)	Puts 2d (diffuse functions) on heavy atoms and 2p functions on hydrogens.	27	9
6-311++G(2df,2pd)	Puts 2d and 1f functions (and	34	14

	diffuse functions) on heavy atoms and 2p and 1d functions on hydrogens		
6-311++G(3df,3pd)	Puts 3d and 1f functions (and diffuse functions) on heavy atoms and 3p and 1d functions on hydrogens	39	18

[#] Lithium through Neon.

Most of the VOCs contain H atom bonded to carbon atom and hence reaction proceeds mostly via abstraction of H atom with atomic and radical species.These H atoms can be in different chemical environment, and thus can have different reactivity, which is difficult to find out experimentally. Theoretical calculations can predict, both qualitatively and quantitatively, the relative reactivity of different types of H atoms in a VOC. Similarly, presence of an unsaturation centre in a VOC can lead to an addition reaction of OH or Cl. Thus, an addition reaction to an unsymmetrical C=C bond can have a preferential attack on either carbon centre of the double bond. Again, theoretical calculations can predict the relative reactivity of these two centres.

1.7. Scope of the present work

In this thesis, an effort has been made to understand the kinetics and the degradation mechanism in the troposphere of some selected class of VOCs. The selected VOCs are (a) saturated and unsaturated cyclic hydrocarbon (containing eight carbon atoms) to understand any change in reactivity with unsaturation and to compare its

reactivity with saturated and unsaturated acyclic hydrocarbon, (b) unsaturated cyclic halogenated hydrocarbon (1-cholorocyclopentene) for comparison of its reactivity with cyclopentene and substituted cyclopentene to understand the effect of substituent Cl on the reactivity, (c) esters (gamma-valerolactone, GVL and alpha-methyl gamma-butyrolactone, AMGBL) to study the effect of the ring O atom on the reactivity, (d) ethers (dimethyl ether and epichlorohydrin) to compare the reactivity of cyclic and acyclic ethers and also to investigate the effect of the heteroatom (chlorine) on the reactivity. These VOCs are anthropogenic pollutants, released from industries, where they are used in the synthesis of important drugs and, combustion of fossil fuels or they are present in the atmosphere due to oxidation of other pollutants. The reactions of these pollutants play a major role in the tropospheric chemistry. The rate coefficients of reactions of these molecules with Cl, OH, and O_3 at room temperature (298 K) are determined (k_{Cl}, k_{OH}, and k_{O3}) using relative rate method using Gas Chromatography (GC) coupled with Flame Ionization Detector (FID) technique, which is essential for assessing their impact on environment. These measured values of the rate coefficients with OH, O_3 and Cl are compared to understand the relative importance of their reactivities or to identify the most important degradation channels among these oxidants, and also these values are compared with that of analogous molecules in order to understand the reactivity pattern. In addition, for evaluation of the activation energy (E_a), the temperature-dependent rate coefficients for the reaction of some VOCs with the OH radical are also measured using an absolute method of Laser Photolysis-Laser Induced fluorescence (LP-LIF) technique. The reasonably well-established structure-activity relations (SARs) are also applied in some cases to calculate rate coefficients for a comparison with the measured values. The

rate coefficients are then used to calculate lifetimes of these VOCs to predict their impact on the atmosphere, which are also used (for certain VOCs studied) to estimate their global warming and ozone depletion potentials.

In order to understand the total impact of VOCs, their major degradation products are identified using GC and GC-MS techniques. Experimental results are corroborated with theoretical calculations to understand the reaction mechanism.

Chapter-2

Experimental Methods

2.1. General introduction (OVERVIEW)

The chapter deals with the experimental techniques and methodology adopted in the estimation of the tropospheric lifetime of some important class of compounds (saturated and unsaturated cyclic hydrocarbon and esters, and both cyclic and acyclic ethers (VOCs)) due to its reaction with tropospheric oxidants (OH, Cl, and O_3). The chapter also deals with the characterization of stable products of the reactions. The studies are used for understanding the major degradation pathways of the VOCs, including the relative importance of OH, Cl, and O_3 in degradation processes of a VOC, and their polluting nature, both of which are based on the tropospheric lifetime of a VOC with respect to the oxidants. The stable product analysis of the reactions of VOCs with oxidants is used in elucidating the degradation mechanisms of the VOCs. For calculating the tropospheric lifetime of VOCs, the rate coefficients for the reaction of the VOCs with the tropospheric oxidants are measured by relative rate method. An absolute method is also employed for the reaction of OH with some VOCs, and in such measurements, the temperature-dependent rate coefficients are measured and their expression obtained for the reaction. Both the absolute and relative rate methods used for the rate coefficients measurements are well tested and established in our laboratory. The LP-LIF method was standardized for the measurement of absolute rate coefficient by studying the reaction of $CF_3CH_2OCH_2CF_3$ (Bis-2,2,2 trifluoroethyl ether) with OH [23]. Similarly, for standardizing the relative rate method, the rate coefficients for the reactions of cyclic

unsaturated hydrocarbons with tropospheric oxidants ($OH/Cl/O_3$) were measured using GC [14,25-29]. In this chapter, the details of procedures adopted for sample preparation, methods and techniques employed, including theoretical calculations are discussed. Since all the experimental work in this thesis is carried out in the gas-phase, vacuum systems are also discussed briefly.

2.2. Experimental techniques employed for rate coefficient measurements

Two different techniques, as mentioned above, are adopted for measuring the rate coefficients of the VOCs with tropospheric oxidants. The relative rate methodology, using gas chromatography for quantitative analysis of reactants, and the absolute methodology, employing laser photolysis-laser induced fluorescence (LP-LIF) for concentration measurement, are discussed at reasonable length in this chapter.

2.2.1. Relative rate method

The relative rate method of measuring the rate coefficients for the reaction of VOCs with oxidants is a well-established methodology, and it is being used extensively [14,25-29]. The methodology is based on competitive kinetics. Here, the fractional decrease in concentrations of a sample (a VOC for which the rate is to be measured) and a reference compound (a VOC for which the rate coefficient is well established and reported) is measured, by allowing both the chemical species to react simultaneously with the oxidant of interest in the reaction chamber. From the above measurement, the rate coefficient for the reaction of the sample with the oxidant is calculated considering the known value of the rate coefficient of the reference with the oxidant.

In the condition of simultaneous reactions of the oxidizing species (X) with reference (R) and sample (S), and assuming that sample and reference are removed solely by reaction with oxidizing species only.

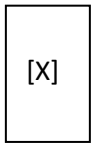

$$+ \quad [R]_{reference} \xrightarrow{k_{ref}} \text{Products} \qquad (2.1)$$

$$+ \quad [S]_{sample} \xrightarrow{k_{sample}} \text{Products} \qquad (2.2)$$

The rate of decrease in reference (R) concentration due to reaction with the oxidizing species (X) can be expressed as

$$\frac{d[R]}{dt} = -k_{ref}\,[X]\,[R] \qquad (2.3)$$

Similarly, the rate of decrease of sample (S) concentration is expressed by the Eqn. as

$$\frac{d[S]}{dt} = -k_{sample}\,[X]\,[S] \qquad (2.4)$$

On rearranging the expressions (2.3) & (2.4) and further integrating, we get

$$\frac{d[R]}{[R]} = -k_{ref}\,[X]\,dt \quad \Rightarrow \quad \int_{[R]t=0}^{[R]t} d(\ln[R]) = -k_{ref}\,[X] \int_{t=0}^{t} dt \qquad (2.5)$$

$$\frac{d[S]}{[S]} = -k_{sample}\,[X]\,dt \quad \Rightarrow \quad \int_{[S]t=0}^{[S]t} d(\ln[S]) = -k_{sample}\,[X] \int_{t=0}^{t} dt \qquad (2.6)$$

As the reactions (2.1) and (2.2) are carried out in the same reaction cell, the concentration of 'X', at any time 't', [X], is the same in the Eqn. (2.5) and (2.6) and hence, on dividing the expressions (2.6) by (2.5), we get,

$$\int_{[S]t=0}^{[S]t} d(\ln [S]) = \frac{k_{sample}}{k_{ref}} \int_{[R]t=0}^{[R]t} d(\ln[R]) \qquad (2.7)$$

$$\Rightarrow \quad \ln\left(\frac{[S]t}{[S]t=0}\right) = \frac{k_{sample}}{k_{ref}} \ln\left(\frac{[R]t}{[R]t=0}\right) \qquad (2.8)$$

Here, $[R]_t$ and $[S]_t$ are concentrations of reference compound and sample, respectively, at time t, and $[R]_{t=0}$ and $[S]_{t=0}$ are the corresponding initial concentrations. The above expression can be rearranged as follows.

$$\log\left(\frac{[S]t=0}{[S]t}\right) = \frac{k_{sample}}{k_{ref}} \log\left(\frac{[R]t=0}{[R]t}\right) \quad (2.9)$$

The Eqn. (2.9) is the expression for the relative rate equation which relates the fractional loss of sample and reference with the rate coefficients k_{sample} and k_{ref}.

Thus, by plotting the fractional loss of sample, S, versus the corresponding fractional loss in reference, R, with X at various interaction time of R and S, a straight line is generated with the slope equal to $\frac{k_{sample}}{k_{ref}}$. From this slope value, the rate coefficient of the sample (k_{sample}) is calculated from the known rate coefficient value of the reference (k_{ref}). The relative method described above has associated advantages as it does not require the absolute concentration of the sample (reagent) and the fast time-resolved techniques, and hence any conventional technique of detection can be employed. For an absolute method of the rate coefficient measurements, costly and advanced time-resolved techniques are required. In the work reported in this thesis, employing the relative rate method for rate coefficients determination, the concentrations of a reference, as well as sample compounds in the reaction vessel, are measured by the Gas Chromatography (GC) technique. The details of the experimental methodology adopted for the measurement of rate coefficient of VOC with the oxidant species are explained below.

2.2.1.1. Experimental set up and procedural details of relative rate method

In all the experiments, the reactants, buffer gas and precursor of the oxidant species are taken in the gaseous form and the desired initial concentrations are maintained

by taking the measured partial pressures of individual species. The vacuum manifold (shown in Fig. 2.1) is employed for this purpose. Vacuum manifold is a closed cylindrical glass tube, having outlets that can be connected to the sample bulbs, reaction vessel, vacuum pump and gauge (capacitance manometer) for measuring pressure. Each outlet has a vacuum stop cock for controlling the flow of gas. The outlet of the vacuum manifold, which is connected to a vacuum pump is passed through a trap immersed in liquid nitrogen container to condense chemical species, except the buffer gas, and thus preventing the pump (pump oil) from contamination by chemical species. All the experiments are carried out in a 3 L volume reaction vessel of cylindrical shape. The reaction vessel, as shown in Fig. 2.1, is made of either Pyrex or Quartz glass depending on wavelength to be used for photolysis of precursor to form the oxidant. The lamps used are either from Sankyo Denki or Rayonet at 254 nm or 350 nm, respectively.

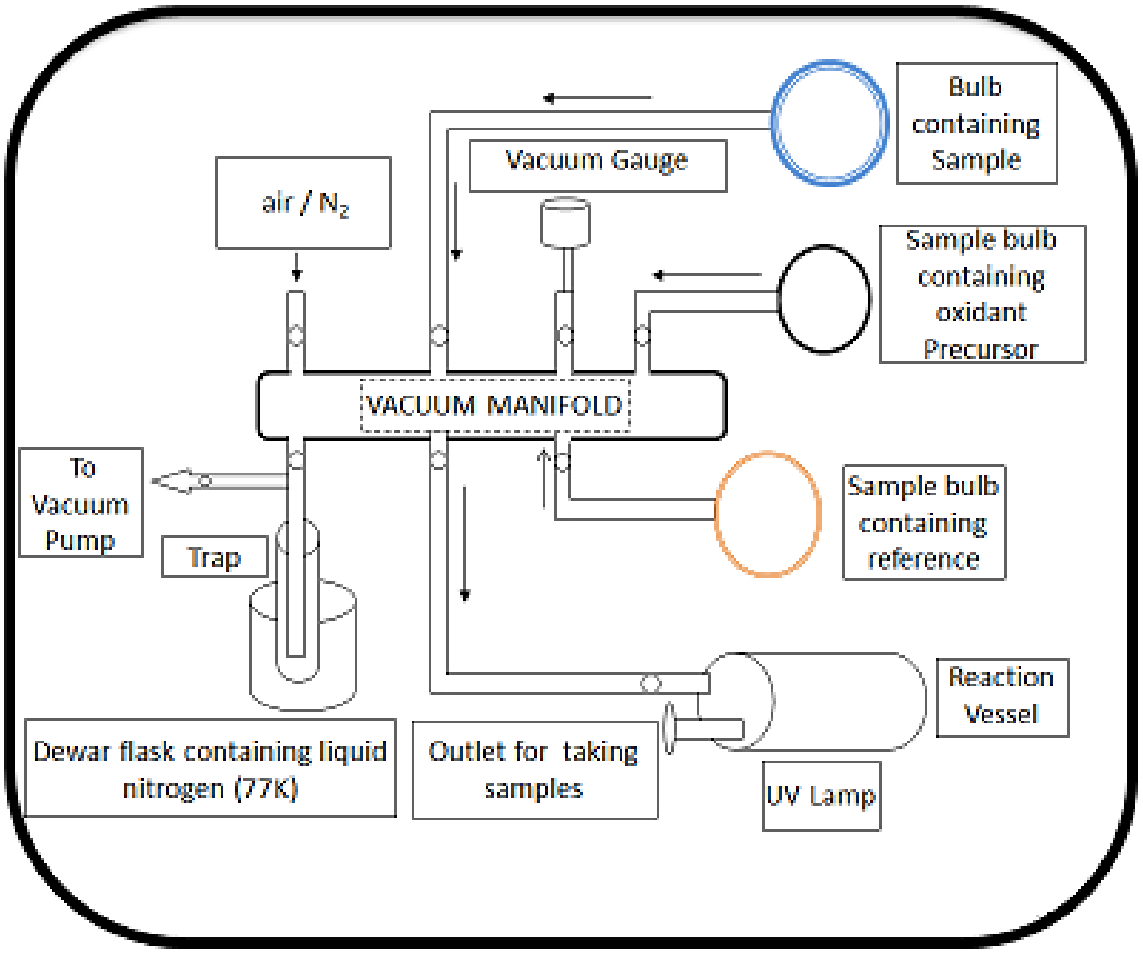

Fig. 2.1. Experimental set up employed for relative rate coefficient measurements.

The reaction vessel consists of a sealed silicon rubber septum port for drawing out samples for the GC/GCMS analysis. Before sample filling and also in the subsequent filling of chemical species in the reaction vessel, the reaction vessel and manifold are pumped by a vacuum pump to a pressure at least three orders lower than the partial pressure of any chemical species in the reaction vessel. Thus, it is ensured that the impurities from the external sources are negligible compared to the concentration of the chemical species in the reaction vessel.

Materials

Nitrogen gas (purity >99.9%, INOX Air Products Ltd., Mumbai, India) and ultrapure air (Zero grade, Chemtron Science Laboratories, Mumbai, India) are used as buffer gases. High purity oxygen (>99.9%, Alchemie Gases & Chemicals Pvt. Ltd., Mumbai, India) is used to generate ozone/oxygen mixture. Cyclooctane (>99%), cis-cyclooctene (>95%), 1,5-cyclooctadiene (>99%), 1-chlorocyclopentene (97%), gamma-valerolactone (99%), alpha-methyl gamma-butyrolactone (98%), dimethyl ether (≥99.9%) and epichlorohydrin (97%) are procured from Sigma Aldrich. Among the reference molecules, ethane (>99%), propane (>99%), butane (>99%), cis-butene (>99%) and 1-butene (>99%) are from Matheson, n-pentane (>97%), n-hexane (>97%), 1,4-cyclohexadiene (>99%), cyclohexane (>97%), cyclopentene (>96%) and 1,2-dichloroethane (99.5%) as well as tetrahydrofuran (>97%) used as OH scavenger, are from Sigma Aldrich. Samples of the compounds were stored in evacuated glass vessels and subjected to freeze-pump-thaw cycles before use.

2.2.1.2. Sample preparation

Before the reaction kinetics experiment, all the requisite gaseous samples are prepared in the sample bulbs of volume 5 or 10 L in a buffer gas, and these include a reactant compound, a reference compound and a precursor compound for an oxidation species. For preparing the gaseous samples of reagents from their liquid form, a liquid sample is taken in a small diameter cylindrical cell having a Teflon stopcock and a connector for coupling with the vacuum manifold. The liquid sample is subjected to many freeze-pump-thaw cycles to remove trapped air and high volatile impurity, if any, before taking its vapour for preparing the gaseous sample.

The sample bulb containing a reactant/ reference/ precursor at a desired partial pressure, is prepared by taking the sample first and subsequently adding the buffer gas to make the total pressure of ~800 Torr. These prepared sample bulbs are stored for several hours to allow thorough mixing before being used for preparing the reaction mixture in the reaction vessel for kinetic experiments. All the sample bulbs are covered by a black cloth to avoid unwanted photolysis of chemical species by any external light source. Similarly, the reaction vessel is prevented from the external light source during the experiment, except during the photolysis for kinetic measurement.

The reaction mixture, consisting of a sample, reference compound and precursor to an oxidant (O_2-O_3 mixture in case of ozone reaction), is prepared in the reaction vessel, using the vacuum manifold, and the total pressure is maintained at 800 ± 3 Torr, by adding nitrogen. The pressure is measured by a capacitance manometer (Pfeiffer Vacuum) mounted on the vacuum manifold. The reaction mixture is kept for an hour or longer to allow thorough mixing before starting the actual experiment. Experiments were also conducted in ultrapure air to see the influence of O_2 on the measured rate coefficient and also to carry out the kinetic and stable product analysis under the condition nearly similar to the atmospheric conditions.

2.2.1.3. Generation of oxidative species

In all the experiments, the oxidant species are generated by photolysis of their precursor molecules, in a gas mixture containing the sample, reference, buffer gas and the precursor molecules for the oxidant species. The precursor should fulfill the criteria that it doesn't react with the sample and the reference in the dark condition, and similarly the

co-fragment of the oxidant molecule also should not react with the sample and reference species. The photolysis wavelength employed for the generation of oxidative species in kinetics experiments is selected such that the absorption cross-section of the sample and the reference molecules, at the employed wavelength, is zero or very negligible. The precursor molecule is selected such that it fulfills the above two criteria. Depending on the photolysis wavelength of the precursor, either Pyrex or Quartz reactor is employed for the kinetic studies. In the thesis work, the oxidative species (OH, Cl, and O_3) are generated by photolysis of suitable precursor compounds, and details of their generation are given below.

OH radical generation

In the kinetic studies of saturated hydrocarbons with OH radicals, O_3 and water mixture is used for generation of the OH radical. The above mixture is filled in the reaction vessel, along with other reactants and buffer gas, and is exposed to 254 nm lamp to generate O (^{1}D) atom by photolysis of O_3. The OH radical is produced by very fast (diffusion control) reaction of O (^{1}D) atom with H_2O, which is represented in the equations below,

$$O_3 \xrightarrow{h\nu\ (254\ nm)} O(^1\mathrm{D}) + O_2 \qquad (2.10)$$

$$O(^1\mathrm{D}) + H_2O \rightarrow 2OH \qquad (2.11)$$

For the reactions of unsaturated hydrocarbons with OH radicals, H_2O_2, instead of O_3, and water mixture is used as a precursor to the OH radical, as unsaturated hydrocarbons react with O_3 molecule even under dark condition [30,31]. The commercially available H_2O_2 (70% in water) is concentrated by evaporation of water by

slow pumping using the vacuum manifold. The concentrated H_2O_2 (> 95% mole fraction) sample was analyzed by titration with $KMNO_4$, and used as a precursor of the OH radicals.

$$H_2O_2 \xrightarrow{hv\ (254\ nm)} 2\ OH\cdot \qquad (2.12)$$

The quantum yield for this reaction is reported to be about 2, with almost no generation of H and HO_2 [32].

Cl atoms generation

Cl atoms can be generated by photolysis of a suitable precursor, such as oxalyl chloride $(COCl)_2$, trichloroacetyl chloride (CCl_3COCl) or chlorine gas (Cl_2) [33,34].

$$Cl_2 \xrightarrow{hv\ (350\ nm)} 2Cl\cdot \qquad (2.13)$$

$$CCl_3COCl \xrightarrow{hv\ (254\ nm)} Cl\cdot + Fragment \qquad (2.14)$$

$$(COCl)_2 \xrightarrow{hv\ (254\ nm)} 2Cl\cdot + 2CO \qquad (2.15)$$

Before selecting the precursor for kinetic studies for Cl atom generation, it is ensured that the counter photo fragment does not interfere with the measurements. For this purpose, the kinetics measurement of similar nature and the well-studied compound is performed with the selected precursor. It is further confirmed by measuring the rate coefficient (k) values with another suitable precursor for Cl radicals.

Preparation of ozone

For studying the kinetics of reactions of unsaturated hydrocarbons with O_3, O_3 is generated by corona-discharge method as O_3-O_2 mixture (<2% O_3) using an ozone generator (shown in Fig. 2.2).

Fig. 2.2. Picture of ozone generator used to generate O_3, for studying the kinetics of reactions of unsaturated hydrocarbons with O_3.

Ozone is generated using ozone generator which works on the principle of corona-discharge method, wherein O_3 is produced by electric discharge of oxygen molecules. Two oxygen radicals are formed after rupture of the oxygen molecule by corona-discharge. Subsequently, these two oxygen radicals can generate O_3 after combining with oxygen molecule. The inlet of ozone generator is connected to high purity oxygen cylinder via pressure regulator and the outlet of ozone generator is connected to one of

the inlets of vacuum manifold system and eventually to a pre-evacuated glass bulb, which is also connected to another inlet of the vacuum manifold. Initially only oxygen is allowed to flow through the system to set the required flow rate of oxygen into ozone generator. Once the required flow of oxygen is achieved, the electrical supply of generator for corona-discharge is initiated. Through another inlet of vacuum manifold, the gas is allowed to bubble through a potassium iodide solution, prepared in a beaker, to check for ozone formation. The generation of ozone is confirmed by change in color of potassium iodide solution from colorless to yellow upon reaction with ozone. Then this oxygen-ozone mixture is filled in a pre-evacuated Pyrex glass bulb. The concentration of O_3 in O_3-O_2 mixture is checked by a UV-Vis spectrophotometer. This mixture (generally <2% of O_3) is added to the reaction mixture intermittently through a syringe.

2.2.1.4. Selection of reference compound

In the kinetics studies of a VOC with an oxidant using a relative rate method, a reference molecule is selected, whose rate coefficient with the oxidant is well-established and very close to that of the sample. In addition, it is ensured that the retention times of the sample and reference in the selected GC column are well separated. This is taken care by adjusting the column temperature and flow rate of the carrier gas. It is also ensured that the products, which are formed in the reaction mixture, also do not interfere with the retention times of the reactants. This is verified by carrying out separate experiments (before and after photolysis, consuming about 90% of the reactants) in a mixture containing sample, reference, and buffer gas in the presence of the precursor. In the work carried out in this thesis, ethane, propane, butane, cis-butene, 1-butene, n-pentane, n-

hexane, 1,4-cyclohexadiene, cyclohexane, cyclopentene and 1,2-dichloroethane are taken as the reference molecules.

The experimental set-up for determination of rate coefficients using relative rate method is shown in Fig. 2.1.

2.2.1.5. Technique used for concentration measurement of reactants

Gas chromatography

Chromatography is a technique used to separate, identify and quantify the components in a mixture. The separation is based on the rates at which the components in the mixture are partitioned or distributed between the two phases (stationary phase and mobile phase) and carried through a stationary phase by the mobile phase.

In Gas Chromatography, a column acts as the stationary phase that contains a liquid adsorbed on a finely divided inert solid support, while a carrier gas (hydrogen, helium, nitrogen, air, etc.) acts as the mobile phase. The sample containing different components is injected into the injection port, and these components are then carried by a desired flow of the mobile phase through the temperature-controlled stationary phase. Different components of the sample get partitioned between the mobile phase and the stationary phase. Depending on the difference in affinity towards the stationary phase and the mobile phase, and on boiling point, different components of the sample move at different rates through the column and get eluted from the column at different times from their injection into the column. This time is characteristic (unique) for a particular compound, and depends on the type of column, temperature and the flow rate of the mobile phase. The retention time (t_R) is defined as the time taken by a compound to reach the detector after injecting the sample into the column. In the present experiment, two

different types of GC instruments, Shimadzu GC-2014 and Shimadzu GC-2010 equipped with flame ionization detector (FID, used for the analysis of hydrocarbons) and thermal conductivity detector (TCD, also known as universal detector), are used.

A computer system is interfaced with the Gas Chromatograph to interpret the output signal in the form of peaks at different retention times. The area of a particular peak is proportional to the concentration of the eluted compound in the sample. Since the rate coefficient determination using the relative rate method requires only the ratio of the concentrations at a fixed time to its initial concentration, the preparation of the calibration curve of the peak area employing the standard samples is not required, and hence not performed in these studies.

In the present work of the rate coefficient measurements, GC in conjunction with FID is used for detection as this detector permits sensitive detection of organic hydrocarbon compounds in the gas mixture that are sampled during the present studies. The sampling is carried out by manual injections. Depending on properties of the reactants in a gas mixture, like polarity and boiling point, either stainless steel packed columns or capillary columns are used for the separation.

2.2.1.6. Determination of relative rate ratios

The room temperature rate coefficients for the reactions of some selected compounds (presented in this thesis) with tropospheric oxidants (OH, Cl and O_3) are measured by the relative rate method after satisfying all the criteria required for this method. Prior to the measurement of the rate coefficients, the stability of the reaction mixture with respect to the wall losses and dark reactions is checked for about 8 hours, which is more than the total time of any relative rate measurement experiment performed

in the thesis work. The wavelength for photolysis of the precursor to generate oxidant molecules is selected such that at the selected wavelength the reactants don't have absorption, and hence do not undergo dissociation. The absence of photolysis of the reactants is further confirmed by irradiating a mixture of reactants and the buffer gas for a very long time (greater than 10 times of the maximum irradiation time in the rate coefficient measurement studies), and measuring the concentration of the reactants before and after the irradiation. In all such experiments, carried out as a part of the reaction kinetic studies, no decrease in the concentration of the reactants on irradiation at the selected wavelength was observed.

All the experiments are performed in a 3 L Pyrex/Quartz reaction cell and at 298 ± 3 K. The reactants and the precursor to an oxidant molecule are filled in the reaction cell from their pre-prepared mixture in the buffer gas, and additional buffer gas is filled from the buffer gas cylinder to make the total pressure in the cell to 800 Torr. The above-filled reaction mixture in the cell is allowed to get equilibrated for more than one hour for uniform distribution of reactants and precursor molecule in the buffer gas. The uniform distribution of reactant is checked by withdrawing the reactant from the reaction cell at an interval of 5 minutes after an equilibration time of 30 minutes, and the constant value of the reactant concentration within the error bar of the measurements confirms the attainment of uniform distribution after 30 minutes. For all the concentration measurement in the kinetic studies, 1 ml of the mixture is withdrawn using a gas-tight syringe (either SGE-500F-GT or Hamilton-500) from the sealed port of the cell, and immediately injected manually into GC for concentration measurements. The reaction mixture is irradiated for a very short time (30 secs to 1 minute), which depends on the

intensity of the light source, the absorption cross-section of the precursor and the quantum yield for the generation of oxidation species at the irradiation wavelength. The oxidation species generated from photolysis of the precursor molecule in each irradiation step reacts with sample and reference simultaneously, and thus decrease concentrations of the reactants in the reaction mixture. The irradiated reaction mixture is allowed to get equilibrated, and the concentrations of the sample and the reference molecules are followed by Gas Chromatography (GC) technique in conjunction with Flame Ionization Detection (FID). The fractional decrease in concentrations of the sample and the reference is plotted according to the relative rate equation (Eqn. 2.9), as shown in Fig. 2.3. A linear plot with approximately zero intercept ensures that the decrease in the concentration of the reactants is exclusively due to their reaction with oxidation species, and any interference from the secondary reactions is negligible. From the slope of this plot, the rate coefficient of the sample with the oxidant molecule is measured relative to that of the reference with the oxidant species. The experiments are repeated number of times to obtain a reproducible and reliable value of the above slope, which is used for calculating the rate coefficient of the sample with the oxidant molecule by taking the reported value of the rate coefficient of the reference with the oxidant molecule. The kinetic measurements for all the reported studies are carried out with more than one reference compound to minimize the error in the reported value of the reference compound as well as to rule out any error in the measurement due to any unforeseen interferences.

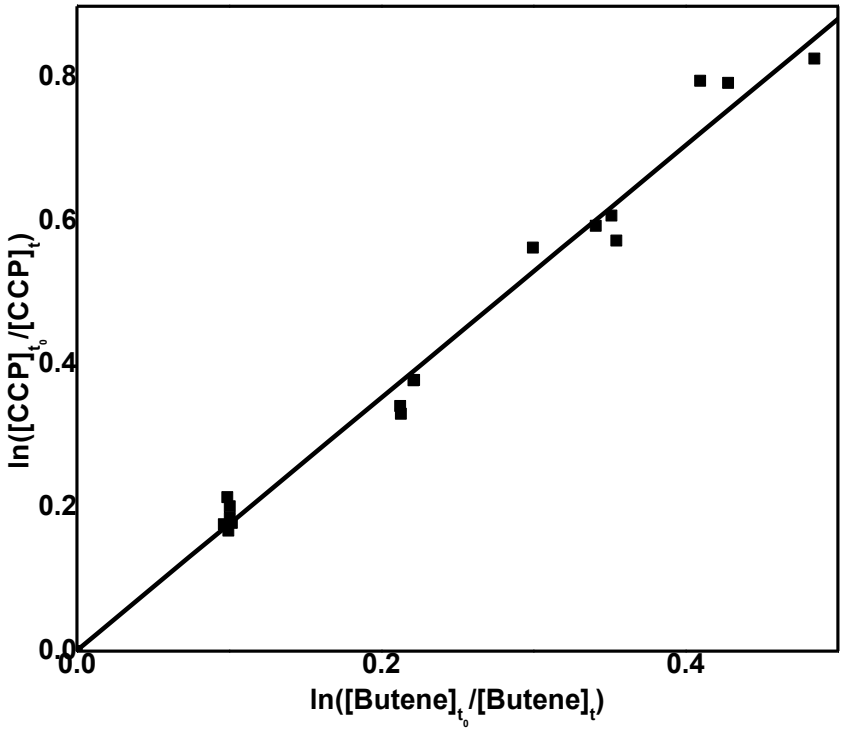

Fig. 2.3. A typical plot of the fractional decrease in concentrations of the sample and the reference due to their reaction with the oxidant molecules (the fractional decrease in concentration of 1-chlorocyclopentene (CCP) plotted against that of a butene in their reaction with OH radical, at 800 Torr of N_2).

2.2.1.7. Error analysis

The kinetic measurements involve the determination of the concentration of the unreacted sample and reference at various reaction times (after each reaction step). For this purpose, the sample is withdrawn and injected into the chromatograph for concentration determination. As an uncertainty is always associated with any measurement due to random and systematic errors, the measurements of kinetic

parameters are also associated with various kinds of errors. These errors should be accounted for to get reliable data. The uncertainties in the relative rate experiments are calculated using appropriate methods, as explained below.

(i) The error in the individual value of the slope is 2 times the standard deviation (σ), i.e. 2σ of the least-squares fitting of the data.

(ii) Error on the average value of the slopes is determined using the error propagation method using the following Eqn.

$$\left(\frac{\Delta y}{y}\right)^2 = \left(\frac{\Delta a}{a}\right)^2 + \left(\frac{\Delta b}{b}\right)^2 + \cdots \qquad (2.16)$$

where, $\frac{\Delta y}{y}$ is the relative error on the average slope and $\frac{\Delta a}{a}$, $\frac{\Delta b}{b}$, …. are the relative errors on the individual slope.

The error arising due to continuous sampling of the reaction mixture is very small, <2%, and hence not added to the total error. The rate coefficient is calculated as

k_s= average slope × k_R

and final error, Δk_S, in the value of k_S is calculated by combining the errors in the relative rate ratios with the errors reported for the respective reference rate coefficients using the statistical error propagation equation,

$$\Delta k_s = k_s \sqrt{\left(\frac{\Delta y}{y}\right)^2 + \left(\frac{\Delta k_R}{k_R}\right)^2} \qquad (2.17)$$

where, Δk_s = error in the calculated rate coefficient, k_S = calculated rate coefficient, Δy = error in slope and y= average slope, Δk_R = error in the reference rate coefficient and k_R = rate coefficient of the reference molecule. The experiments are repeated with different reference molecules to take care of any error in a specific case.

In case of the reaction of unsaturated hydrocarbons with O_3, OH is also generated [35], which will react with the reactants (sample as well as the reference molecule) and interfere with the relative rate measurement. Hence, to evade this, a suitable compound with high reaction rate coefficient (like cyclohexane, tetrahydropyran) with OH with sufficiently high concentration is also filled in the reaction chamber to scavenge OH. This adopted methodology in the kinetic measurement introduces an additional error in the measured rate coefficient.

2.2.2. Absolute method

In kinetics studies, the rate of reaction is measured by monitoring the change in concentration of a reactant with time. To minimise the effect of secondary reaction and side reaction, the concentration of the reactant in the reaction mixture should be maintained as low as possible. The OH radical reactions with a VOC are fast, and hence to monitor the kinetics of the reaction even at the low concentrations of reactants require the detector system with microsecond time resolution. Hence, the method of detection to be used should be properly selected which is sensitive to the small change in the concentration of the compound and having time resolution appropriate for kinetic studies. In our kinetic studies, the reaction of OH radicals with a VOC is carried out under the pseudo-first order condition ([A] >>> [OH]), where A is the VOC for the kinetic studies, employing fast time-resolved laser photolysis-laser induced fluorescence (LP-LIF) technique.

$$A + OH \rightarrow Product \tag{2.18}$$

$$\frac{-d[A]}{dt} = \frac{-d[OH]}{dt} = k[A][OH] \tag{2.19}$$

For kinetic studies, the OH radical is generated in situ by laser photolysis (LP) and its concentration, in terms of LIF intensity, is measured at various time interval during its decay, in presence of the reactant A. The details of this technique are discussed below.

2.2.2.1. Laser Photolysis-Laser Induced Fluorescence (LP-LIF) technique

The schematic of laser photolysis-laser induced fluorescence (LP-LIF) set-up used in the work presented in this thesis is shown in Fig. 2.4.

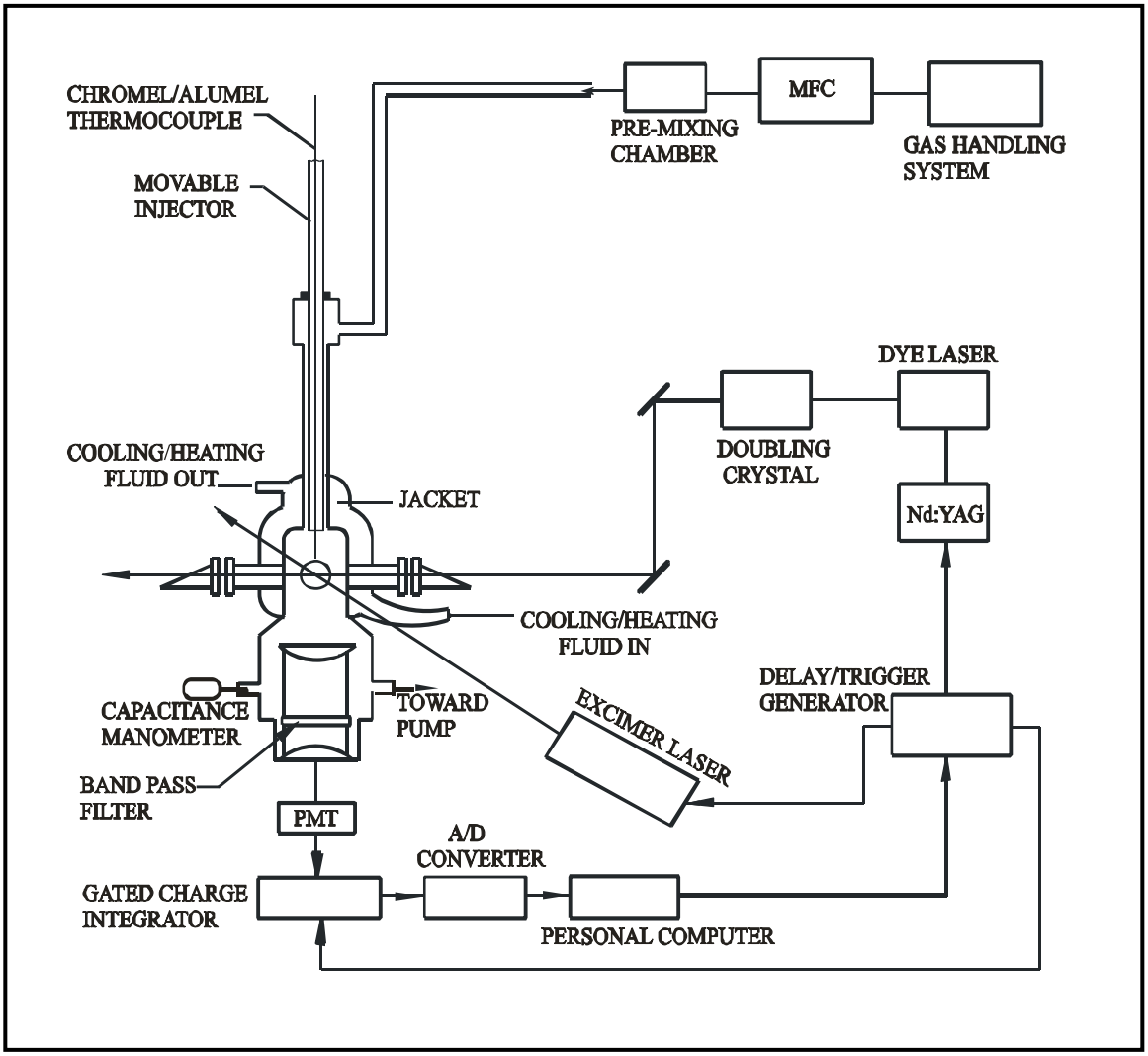

Fig. 2.4. Schematic diagram of the LP-LIF experimental set-up used.

Description of reaction cell

A double-walled reaction cell made of Pyrex glass, Fig. 2.4, is used for performing the reaction kinetic studies under a slow flow condition. The cell is equipped with three ports for introducing the reaction mixture, to connect a pressure transducer for measuring the total pressure in the cell and for pumping the cell by a vacuum pump. The reaction cell has two crossed arms at the right angle, fitted with MgF_2 and quartz windows at the Brewster angle, for entry and exit of the pump and the probe laser beams with minimum scattering, and intersection of these beams at the centre of the reaction cell. The required concentration of the reactant in the reaction cell is maintained by mixing the known flow of the sample (the known concentration of a reactant in buffer gas), OH radical precursor in buffer gas and buffer gas in a premix chamber and then introducing it into the reaction cell. The detector is attached to the arm at the bottom of the cell to collect the fluorescence from the intersection volume of the photolysis and the probe lasers. The fluorescence is collected by a lens (focal length 50 mm and diameter 38 mm), and detected by a photomultiplier tube (PMT, Hamamatsu, model R 928P). To cut-off the scattering from the photolysis laser, a band-pass filter (λ_{centre} = 310 nm, FWHM = ±10 nm, Transmission at 310 nm = 10%) is placed between the collecting lens and the PMT. The laser intensities of both the pump and the probe lasers are monitored to normalize the fluorescence intensities during the analysis. The probe laser frequency is calibrated to an accuracy of ± 0.3 cm^{-1} using an optogalvanic cell (Fe-Ne). The spectral resolution of the probe laser is found to be 0.06 cm^{-1}. The measured fluorescence signal was gated by a boxcar integrator (SRS250, gate width 100 ns) for integration and averaging. The average signal of 30 laser shots is fed to an interface (SRS245) for A/D conversion, for a good S/N ratio. The flow velocity in the reaction is adjusted such that

each laser shot sees the fresh reaction mixture. For studying the gas-phase reactions of VOCs with OH at different temperatures, the temperature of the reaction cell is varied by circulating ethylene glycol-water mixture from a thermostated bath, through the outer jacket of the cell. The temperature and the pressure inside the cell are continuously monitored and kept constant during the experiments.

A brief description of the flow system, sample preparation, lasers, boxcar integrator and delay generator employed in the experiments is given below.

Flow system

The absolute measurement of the rate coefficient for the reaction of the OH radical with a sample is carried out in the reaction cell under flow condition. Linear flow velocity in the reaction cell needs to be maintained such that each new laser photolysis pulse sees the fresh reaction mixture, and thus the required linear flow velocity in the reaction cell depends on the repetition rate of the photolysis laser. In our LP-LIF setup for kinetic measurement, both photolysis and probe lasers employed are working at 20 Hz, with a beam size of 3 mm. To eliminate the secondary reaction in the intersection region of the reaction cell due to products from the preceding pulse, a flow velocity of 12 cm/sec is maintained using a throttle valve between the reaction cell and the pumping system. This flow velocity ensures that the mixture region seen by the preceding pulse flows away from the interaction region, and thus each new pulse sees the fresh reaction mixture devoid of any products formed in the preceding pulse.

2.2.2.2. Sample preparation

The compound for which the bimolecular rate coefficient is to be determined is prepared in a buffer gas in the Pyrex glass bulb of 10 L volume. Before this, the liquid

sample is subjected to a number of freeze-pump-thaw cycles to remove trapped air and high volatile impurity present, if any, by connecting it to the vacuum manifold. First, the glass bulb is connected to the vacuum manifold, evacuated and then passivated with sample vapour. To prepare the sample in the bulb, the glass bulb is again evacuated and filled with the required pressure of the sample vapour and the total pressure in the bulb is made to about 800 Torr by adding high purity N_2 gas from the gas cylinder connected to vacuum manifold, using a capacitance manometer. Before using the prepared sample for kinetics studies, it is kept aside for at least 3 to 4 hrs for complete uniform distribution of the compound in the buffer gas matrix. This is checked by analyzing the gas mixture by an FTIR absorption spectrometer at various time intervals from its preparation time. Besides, the concentration of the sample in the bulb is measured by an FTIR absorption spectrometer before and after the kinetic experimental studies.

2.2.2.3. Photolysis laser for formation of OH radical

In the kinetic studies, the OH radicals are generated in situ in the reaction mixture by photolysis of H_2O_2, using 248 nm wavelength KrF excimer laser, operating at 20 Hz. The fluence of ≤ 2 mJ cm^{-2} is used for all the kinetic experiments by using filters and also by changing the high voltage of the KrF laser system.

$$H_2O_2 \xrightarrow{hv\ (248\ nm)} 2\ OH\cdot \qquad (2.12a)$$

The specifications of KrF (248 nm) excimer laser employed as photolysis laser are given in Table 2.1.

Table 2.1: Specifications of KrF (248 nm) excimer laser employed.

S.No.	Feature	Optimum value

1	Energy per pulse	380 mJ (max)
2	Pulse Energy Stability	$\leq \pm 2\%$
3	Pulse Width	≤ 30 ns
4	Temporal jitter	$\leq \pm 5$ ns
5	Repetition rate	50 Hz (max)
6	Beam divergence	3 x 1 $mrad^2$
7	Trigger	Internal and external (TTL)

2.2.2.4. Probe laser for LIF detection of OH radical: Nd:YAG laser pumped dye laser

In our kinetic studies, the reaction of OH radicals with a VOC is carried out under the pseudo-first order condition ([A]>>> [OH]), where A is the VOC for the kinetic studies. The OH radical is generated in-situ by photolysis of H_2O_2 molecules, and its concentration as a function of time is monitored by decay in its LIF intensity for obtaining the pseudo-first order rate coefficient with the reactant A. For this purpose, the OH radicals need to be pumped to an emissive electronically excited state from its ground state, and the total fluorescence emitted by the excited OH radicals is to be monitored. The total fluorescence intensity is proportional to the concentration of the ground state OH radicals at the time of excitation, and depends on the intensity of the excitation source (probe laser). As shown in Fig. 2.5, the excitation spectra of OH lie in the region of 308 nm. The ro-vibronic lines in the spectra are due to the ($A^2\Sigma$, $v'=0$) $\leftarrow$ ($X^2\Pi$, $v''=0$) transition. The nomenclature of a ro-vibronic line is based on the transition involved. The ground electronic state of OH is $^2\Pi$, which has two spin-orbit states $^2\Pi_{1/2}$ and $^2\Pi_{3/2}$, the latter being the lower in energy. The transitions originating from the $^2\Pi_{1/2}$ and $^2\Pi_{3/2}$ spin-

orbit states are designated as 2 and 1, respectively. The number in the parenthesis refers to the rotational quantum number, N″. Thus, $P_1(2)$ and $Q_1(2)$ lines originate from the $^2\Pi_{3/2}$ spin-orbit state and N″=2 involving transitions ΔJ = ΔN=-1 (P-branch) and ΔJ = ΔN=0 (Q-branch), respectively. Similarly, $R_2(1)$ lines originate from $^2\Pi_{1/2}$ spin-orbit state and N″=1 with ΔJ = ΔN=1 (R-branch).

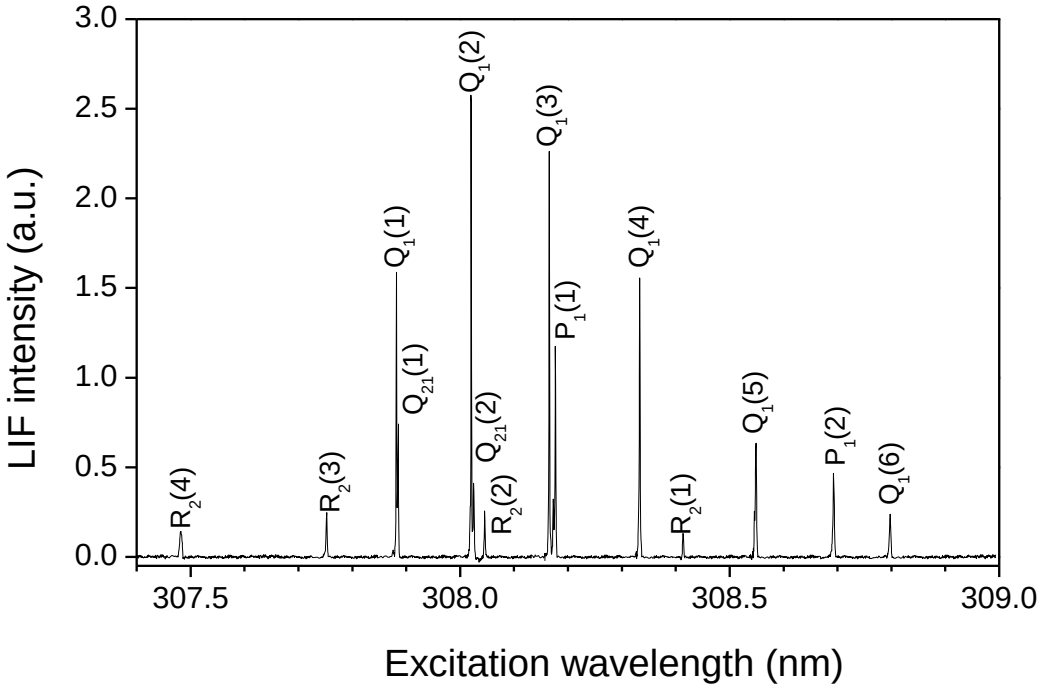

Fig. 2.5. Partial excitation spectrum of the ($A^2\Sigma$, v′=0) ← ($X^2\Pi$, v″=0) transition of the OH radical.

The excitation source, probe laser beam, in the region of 308 nm is generated by second harmonics of Nd:YAG (532 nm) pumped Dye laser with DCM special dye and doubling the fundamental dye laser output in KDP crystal. The detailed description of the probe laser system is given below.

As mentioned above, Nd:YAG laser is employed as a pump laser to pump the dye laser. Nd:YAG stands for Neodymium: Yttrium Aluminium Garnet, the trivalent Nd^{3+} is incorporated in the $Y_3Al_5O_{12}$ lattice. In the work, commercial seeded- Nd:YAG laser system from Quantel (Model: YG980), having KDP crystals for doubling and tripling of the fundamental output at 1064 to generate 532 and 352 nm laser beams, is used. In this laser system, flash lamps are used for the optical pumping of the Nd:YAG crystal. The characteristics of Quantel Nd:YAG laser pumped dye laser are given in Table 2.2.

Table 2.2: Specifications of seeded Nd:YAG pumped dye laser employed in kinetic studies.

Laser	Features	Specified value
Pump Laser: Second harmonic of seeded Nd:YAG laser (532 nm)	Energy	1400 mJ at 1064 nm ≤ 500 mJ at 532 nm
	Pulse width	≤ 8 ns
	Line width	0.003 cm^{-1}
	Rep. rate	20 Hz
Dye laser	Temporal jitter	≤ 2 ns
	Wavelength range	216-850 nm
	Beam divergence	≤ 0.5 mrad
	Line width	≤ 0.06 cm^{-1}
	Fundamental output energy	10-25% of pump energy
	Doubling energy	10-15% of fundamental output
	Mixing after doubling	15-20% of Doubling output

To pump the dye laser the second harmonic output (532 nm) of the Nd:YAG laser is obtained by passing the fundamental Nd:YAG laser beam through KDP crystal at a phased matched angle.

In the present work of measurement of the bimolecular rate coefficient for the reaction of OH with a VOC, the tunable Dye laser (Quantel), with frequency doubling and mixing modules (TDL90), is used as a probe laser in LP-LIF technique. This dye laser is operated with DCM special dye and pumped by the second harmonic of Nd:YAG laser at 532 nm. This dye provides the fundamental wavelength tuning range of 600-640 nm. By using a KDP crystal, the fundamental dye laser output is frequency-doubled to obtain the dye laser output in the range of 300-320 nm, which is used for probing the OH radical. In all the experiment OH is probed by exciting the $P_1(2)$ line of the $(A^2\Sigma, v'=0) \leftarrow (X^2\Pi, v''=0)$ transition at 308 nm, and collecting the resulting total fluorescence through a lens. The pulse width of the laser is 8 ns, and the energy used for all kinetic measurement is < 20 μJ/pulse. The low energy is used in kinetic experiments to keep the LIF intensity proportional to the excitation intensity, and the normalized LIF intensity with excitation intensity to be proportional to the concentration of the OH radicals.

2.2.2.5. LIF technique

In case of an absolute method of measurement of the bimolecular rate coefficient of the OH radicals with a VOC, Laser-Induced Fluorescence (LIF) is used for monitoring the decay of the OH radical concentration in presence of the reactants. LIF is an advanced excitation spectrum–based detection technique. Here, the excitation spectra of species (to be detected) are studied for its identification. As the OH excitation spectra are well

studied and reported, this technique can be used for the OH radical identification and concentration measurement.

Upon absorption of a photon of appropriate wavelength, the OH radical in its ground state is pumped to an excited electronic state, much lower than its dissociation level. The OH radicals in the excited state can decay to a lower electronic state, or the ground state of the same multiplicity, by a phenomenon known as fluorescence. This involves the emission of light with a wavelength slightly red-shifted (in most of the cases) with respect to absorption light. This feature makes fluorescence measurement an advantageous method for detection of suitable species since the interference from the scattered photons from the excitation source can be minimized. To further minimize the contribution of the scattered light, fluorescence is collected at the right angle to the excitation source.

In the present case to record the excitation spectra of the OH radical (formed after photolysis of H_2O_2), the second harmonic of the tunable dye laser pumped by Nd:YAG laser is used. Here, the wavelength of the excitation source (dye laser) is tuned in steps, and at each step, the total fluorescence is collected, as shown in Fig. 2.6.

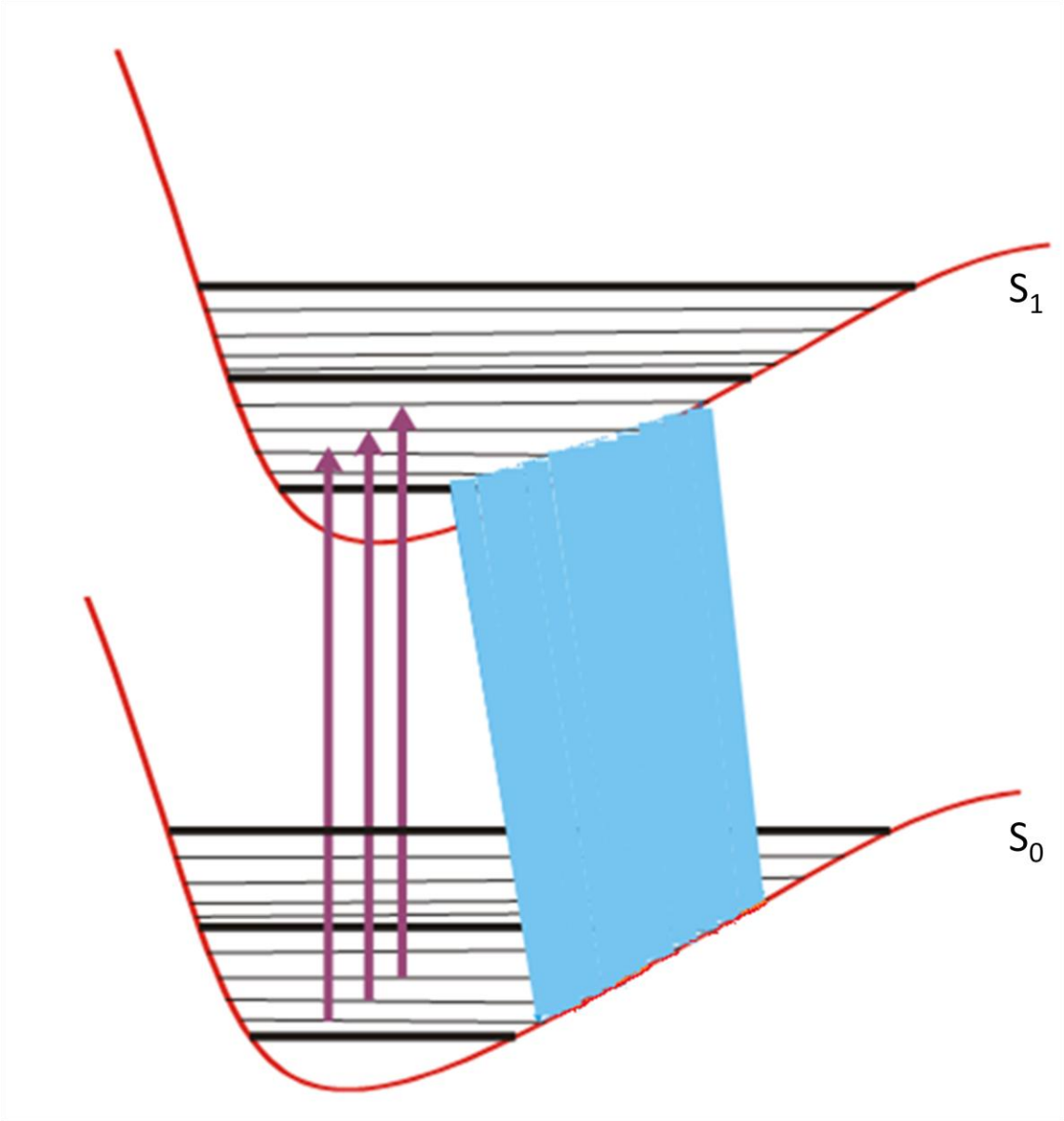

Fig. 2.6. The excitation spectrum is measured by tuning the wavelength of the excitation source in steps and collecting the total fluorescence at each step.

The excitation spectra of the OH radical, shown in Fig. 2.5, consist of several well-resolved rotational lines of the ($A^2\Sigma$, $v'=0$) ← ($X^2\Pi$, $v''=0$) system at ~308 nm. Any rotational line of this vibronic band (0, 0) can be employed for probing the OH radical, and the resulting fluorescence can be detected. In the present work, it is probed by

exciting the $P_1(2)$ line in the (0, 0) band as this spectral line is well resolved from the other OH spectral lines.

2.2.2.6. Boxcar integrator

In all the kinetic experiments, a boxcar integrator is used to integrate the PMT signal generated due to LIF impinging on it. For this purpose, the PMT signal is fed to the signal input of the boxcar integrator, and it is gated with predefined width at a predefined delay time (adjusted using a delay generator) to minimize the noise in the integrator signal output. In all the kinetic experiments, the boxcar integrator is used in the static mode, that is the gate position is fixed relative to the trigger input. The sensitivity of the instrument is set such that the signal output is not saturated at the highest value of the signal amplitude. The signal is averaged for 30 samples to increase the S/N ratio, and the average output is fed to PC via the A/D conversion module. Some important specifications of the Boxcar used in the present studies are given in Table 2.3.

Table 2.3: Specifications of the Boxcar

S. No.	Feature	Properties	Specifications
1	Trigger	Internal trigger External trigger	0.5 Hz to 20 kHz 1 MΩ input impedance. Trigger threshold 0.5 to 2 V
2	Delay	Delay range	1 ns to 10 ms
3	Gate	Gate Width	1 ns to 15 μs
4	Averaging	Type Number of samples	Exponential moving average Max. 10,000

2.2.2.7. Delay generator

The time synchronization of all the equipment in an experiment, such as photolysis laser, probe laser, oscilloscope and boxcar integrator, is carried out using a delay generator. In our experiment, the delay generator (triggered internally) acts as a MASTER and controls all other equipment by generating appropriate external trigger pulses. The temporal profile of OH concentration is followed by varying the time delay between the pump and the probe laser pulses from 10 μs to 10 ms, in steps of a few microseconds. This experiment is carried out with the help of the delay generator, which is controlled by a PC through GPIB interface with data acquisition and control program. The important specifications of the delay generator used in LP-LIF experimental are given in Table 2.4.

Table 2.4: Specifications of delay generator used in LP-LIF experiments.

S. No.	Feature	Parameters	Specifications
1	Delays	Channels Range	Four independent delay outputs: A, B, C and D 0 to 999.999,999,999,995 s
2	Frequency	Repetition rate	0.001 Hz to 1.000 MHz
3	Inputs	External trigger	Impedance: 1 MΩ or 50 Ω Threshold : ± 2.56 Vdc
4	Outputs	Channels Load Risetime	T0, A, B, C, D, AB, -AB, CD and –CD 50 Ω or high impedance 3 ns

		Type	TTL, ECL, NIM, VAR
5	Interface	Computer interface	IEEE 488 Standard GPIB

2.2.2.8. Measurement of bimolecular rate coefficient

As mentioned earlier in this chapter, the LP-LIF technique is used under the pseudo-first order condition to measure the bimolecular rate coefficient for the reaction of OH with VOCs in the temperature range 262-335 K in a flowing condition to minimize the interference from the reaction products in the measured rate coefficient. The OH decay is measured both in the absence and the presence of a known excess concentration of the VOC (sample). The required partial pressure of the sample (VOC), the precursor to OH (H_2O_2) and the buffer gas in the reaction cell is maintained by introducing the prepared sample in N_2 (known concentration), the saturated H_2O_2 vapour in N_2 (by the slow and continuous bubbling of N_2 gas) and N_2/air buffer gas. Each component of the gas mixture is introduced into the reaction cell through separate calibrated mass flow controllers (MFCs) via a premixed chamber. These MFCs are calibrated for N_2 flow by well-known d*P*/d*t* method, for this the rate of change of pressure in a large volume bulb (10 L) filled with N_2 is measured. A constant flow of 7 SCCM of N_2 gas is bubbled through concentrated H_2O_2 solution in all the experiments, and subsequently, it is passed through a trap prior to the premix chamber to arrest any H_2O_2/H_2O droplets from entering the reaction cell. The prepared sample, H_2O_2 seeded in N_2 and the buffer gas N_2 are mixed in the premix chamber, and then allowed to flow into the reaction cell. The total pressure in the reaction cell is maintained constant (~ 30 Torr) by keeping the sum of the flow of the sample in N_2, the buffer gas N_2 and H_2O_2 seeded in N_2 constant. The Teflon tubing

and glass joints are used to reduce the catalytic dissociation of H_2O_2. The flow velocity of the experimental mixture is kept enough (~12 cm/sec) to make sure that a fresh gas mixture is seen by each photolysis laser pulse (20 Hz). In the cell, the H_2O_2 concentration is kept constant by maintaining a fixed flow of N_2 through H_2O_2 bubbler. In the initial blank experiment, only H_2O_2 seeded in N_2, and N_2 buffer are allowed to flow through the reaction cell. The hydroxyl radicals are generated by photolysis of H_2O_2 in the reaction cell, at 248 nm, using a KrF excimer laser (20 Hz) with a laser beam diameter of 0.3 cm and the fluence in the range of 0.2-2 mJ cm^{-2}. The probe laser is a dye laser (Quantel TDL90) working on DCM special dye (Lambdachrome, LC 6501, 590-640 nm, λ_{max} = 625nm) with a frequency doubling and mixing module. The total fluorescence intensity, which is proportional to the concentration of OH radicals, is measured by exciting the P_1 (2) line of the (0, 0) band of the ($A^2\Sigma^+ \leftarrow X^2\Pi$) transition of the OH radicals at 308 nm using dye laser. The fluorescence from the excited OH, after passing through a bandpass filter (λ_{centre} = 310 nm, FWHM = ±10 nm, T = 10%), is collected by a lens from the intersection volume of the pump and probe lasers, and detected by a photomultiplier tube (PMT; Hamamatsu, model R928P), which is kept orthogonal to both the laser beams. The decay kinetics of OH radicals is measured, in the pump-probe experiment. The temporal profile of the OH concentration is followed by varying the pump and probe time delay from 10 μs to 10 ms, in steps of a few microseconds using a delay generator. The PMT signal at each step (the set time delay between the photolysis and probe pulse) is fed to the boxcar integrator and gate of the boxcar with the width of 100 ns is kept in the region, with the help of oscilloscope, such that the contribution of the scattered signal of the photolysis laser pulse in the captured signal by boxcar is the minimum. A PC is used to

control the scan of the dye laser via an RS232 interface, and to collect data through a GPIB interface, using a control and data acquisition program.

The integrated LIF signal is averaged for 30 laser pulses before feeding into the A/D conversion module. The digitized signal is fed to the PC, along with the output of the delay generator. Both the pump and the probe laser intensities are monitored by photodiodes, and the outputs of the photodiodes are fed to the boxcar and the gate integrated average values of 30 laser pulses are transferred to PC via A/D module for normalizing the averaged LIF signal intensity. The LIF intensity normalized by photolysis and probe laser intensity at each pump-probe delay time is plotted against the pump-probe delay time to obtain the decay of LIF signal, which is equivalent to the decay of the OH radical concentration.

Similar experiments are carried out to measure the decay kinetics of the OH radicals in the presence of the sample (VOC), by introducing the prepared sample in the reaction cell along with the buffer gas and the precursor seeded in N_2 gas. Now, the flow rate of the buffer gas is reduced by the same value as the flow rate of the prepared sample to maintain the total pressure in the reaction cell constant. In all the experiments, the partial pressure of H_2O_2 in the reaction cell is maintained to keep the number density of the H_2O_2 molecule $\sim 1\times10^{14}$ molecules cm^{-3}. At the typical photolysis laser fluence (~ 2 mJ cm^{-2}) used in the kinetic experiment, the OH number density generated in the intersection region is in the range of 10^{10}–10^{11} molecules cm^{-3}. The concentration of the sample in the reaction cell is kept > 10^{15} molecules cm^{-3} to maintain the pseudo-first order condition in the reaction cell, [sample]>> [OH]. Under the above condition, the OH

radical concentration follows the first-order decay kinetics. Following its generation by reaction (2.12a), the OH radicals undergo the reactions as shown by reactions 2.20 to 2.22, in the reaction cell in the intersection region.

$$OH + H_2O_2 \text{ (undissociated)} \rightarrow HO_2 + H_2O \qquad (k_2) \qquad (2.20)$$

$$OH \rightarrow \text{diffusion out of the detection zone} \qquad (k_3) \qquad (2.21)$$

$$OH + \text{sample} \rightarrow \text{Products} + H_2O \qquad (k_4) \qquad (2.22)$$

where k_2, k_3, and k_4 are the rate coefficients.

The concentration of OH radicals generated by a photolysis laser pulse in the intersection volume at the time, t=0, decays due to their diffusion from the intersection volume, as well as their reactions with undissociated H_2O_2 and sample molecules. Therefore, the time-dependent decay of the OH radicals can be written as:

$$-d[OH]/dt = [OH] (k_2[H_2O_2] + k_3 + k_4 [\text{sample}]) \qquad (2.23)$$

Since total pressure and $[H_2O_2]$ in the reaction cell are kept constant, the diffusion rate of the OH radicals and decay due to reaction with H_2O_2 remain constant throughout the experiment. The concentration of the OH radicals at any time, $[OH]_t$, is given by the Eqn. 2.24,

$$[OH]_t = [OH]_0 \exp [- (k' + k_4 [\text{sample}]) t] \qquad (2.24)$$

where $k' = k_2[H_2O_2] + k_3$, and it is the rate coefficient for the loss of the OH radicals due to diffusion, reaction with undissociated H_2O_2 and all other depletion processes of the OH radicals, except for that with the sample. As the experiments are performed under the pseudo-first order condition with [sample] in excess, there will be an insignificant change in its concentration, and thus considered as a constant in the intersection volume. Under these conditions, $[OH]_t$ is expressed by the pseudo-first order kinetics equation (2.25),

$$[OH]_t = [OH]_0 \exp[-k_I t] \quad (2.25)$$

where, $k_I = k' + k_4[\text{sample}]$, and it is the pseudo-first order rate coefficient.

The pseudo-first order rate coefficient (k_I) for the decay of the OH radical has the value of the bimolecular rate coefficient k_4 embedded in it. The value of k_I can be determined by monitoring the decay of the OH radical concentration in real-time as shown in Fig. 2.7, and calculated from the plot of ln(Signal) versus decay time (delay between pump and probe laser pulses) as shown in Fig. 2.8. The slope of this plot is the pseudo-first order rate coefficient at a constant excess concentration of the sample.

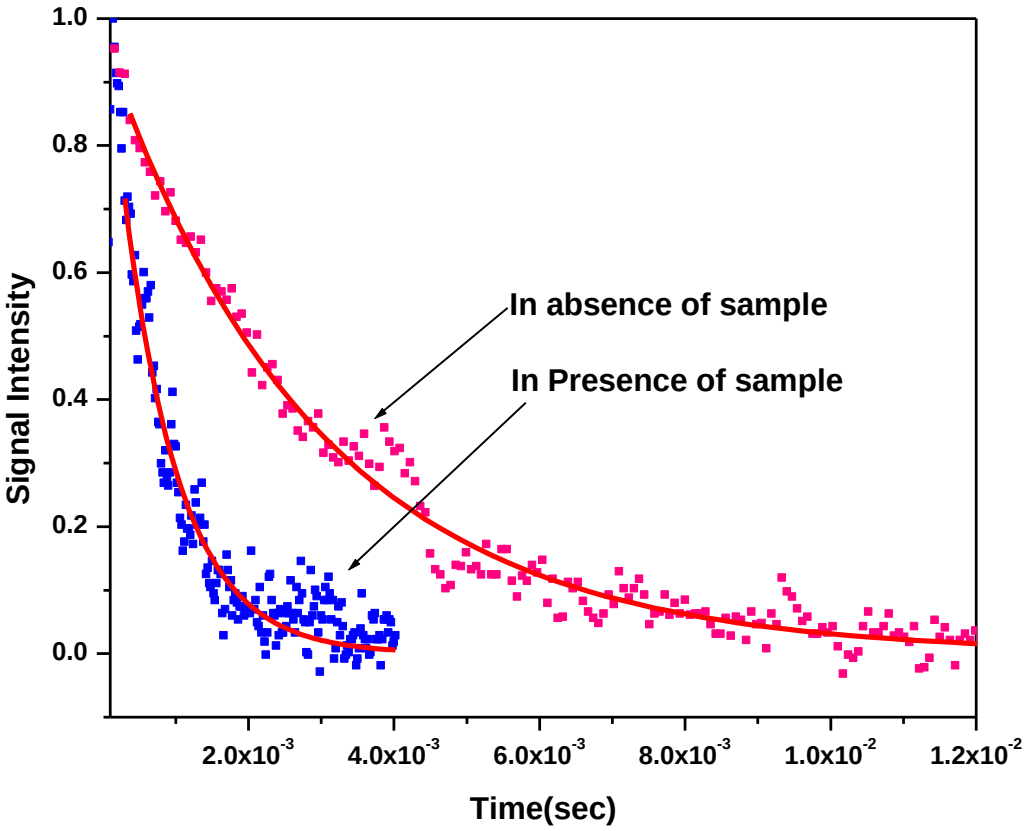

Fig. 2.7. Decay profile of the OH radical obtained by varying the time delay between pump and probe laser. The signal (LIF) intensity is proportional to [OH].

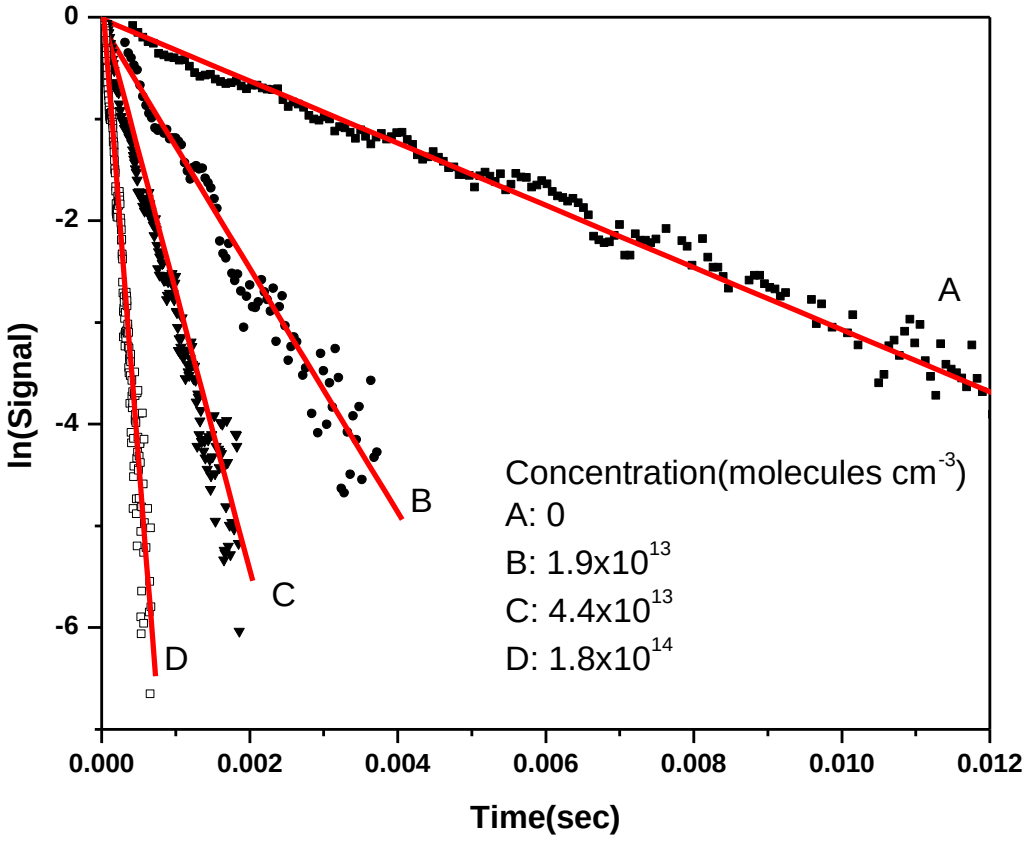

Fig. 2.8. The measured OH radical decay profiles at 298 K, with increasing concentration of 1-chlorocyclopentene for various curves: A = 0; B = 1.9×10^{13}; C = 4.4×10^{13} and D = 1.8×10^{14} molecules cm^{-3}.

The pseudo-first order rate coefficient values, measured at a particular constant temperature are plotted against number densities of the sample (sample concentration) to obtain the bimolecular rate coefficient at that temperature. A typical such plot is shown in Fig. 2.9. As mentioned earlier, this method is well tested and established in our laboratory for the absolute measurement of the rate coefficient for the reaction of the OH radical

with a VOC. Therefore, we have discussed this method using the data measured in the thesis.

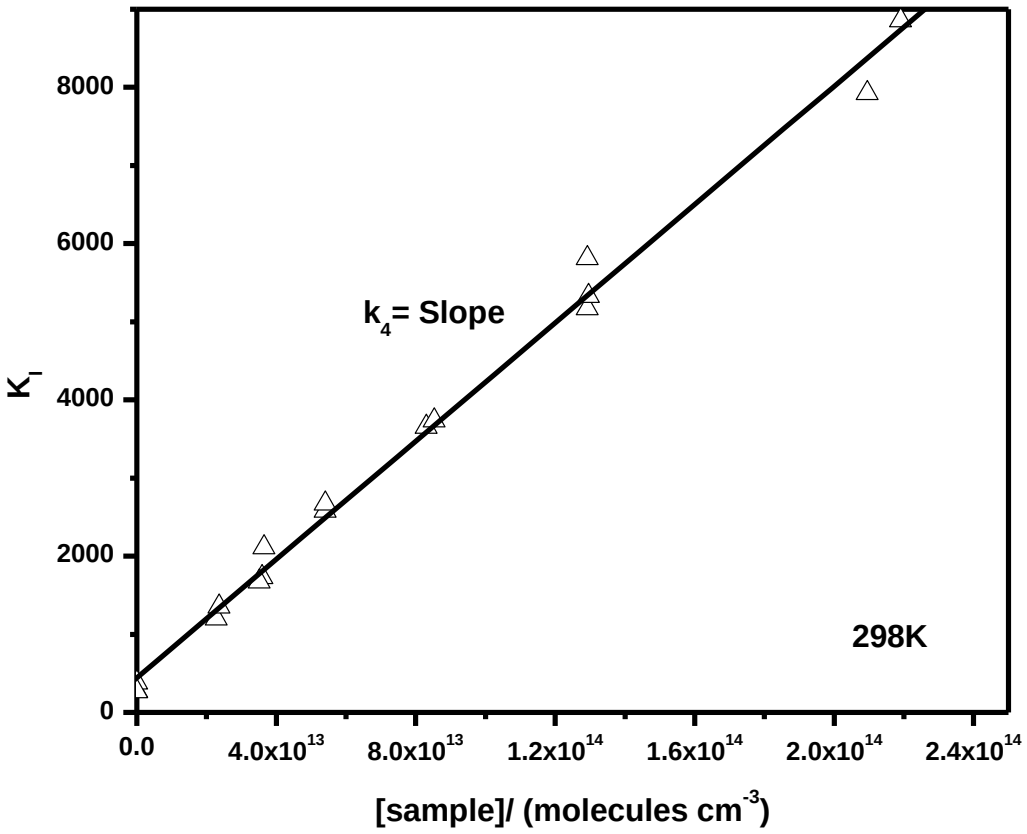

Fig. 2.9. Variation of the k_I with concentration (number density) of the sample with slope corresponding to the bimolecular rate coefficient, k_4.

At a particular constant temperature and pressure, the experiments are repeated for at least 3-4 times to get reliable results. The number density of the sample in the reaction volume (intersection volume) is calculated from the known concentration of the sample in the sample bulb prepared for the experiments, the ratio of the flow rate of prepared sample to the total flow rate used in the experiment and the total pressure in the cell

during the experiments. It is re-confirmed by analysis of outlet of the reaction cell by FTIR spectrometer.

The bimolecular rate coefficients are measured at different temperatures in the range of 262 to 335 K. The temperature of the reaction volume (intersection volume) in the reaction cell is varied by circulating water-ethylene glycol (1:1 mixture) from a thermostatic bath through the outer jacket of the double-walled Pyrex glass cell. The temperature at the intersection volume is measured using a Chromel-Alumel thermocouple mounted on a linear feed through.

The natural log of the values of bimolecular rate coefficients (k_4) determined at various temperatures (ln k_4) are plotted against 1/temperature (T) to calculate activation energy (E_a) and pre-exponential factor A of the Arrhenius equation (Eqn. 2.26), for the reaction as shown in Fig. 2.10.

$$lnk = lnA - \frac{E_a}{RT} \qquad (2.26)$$

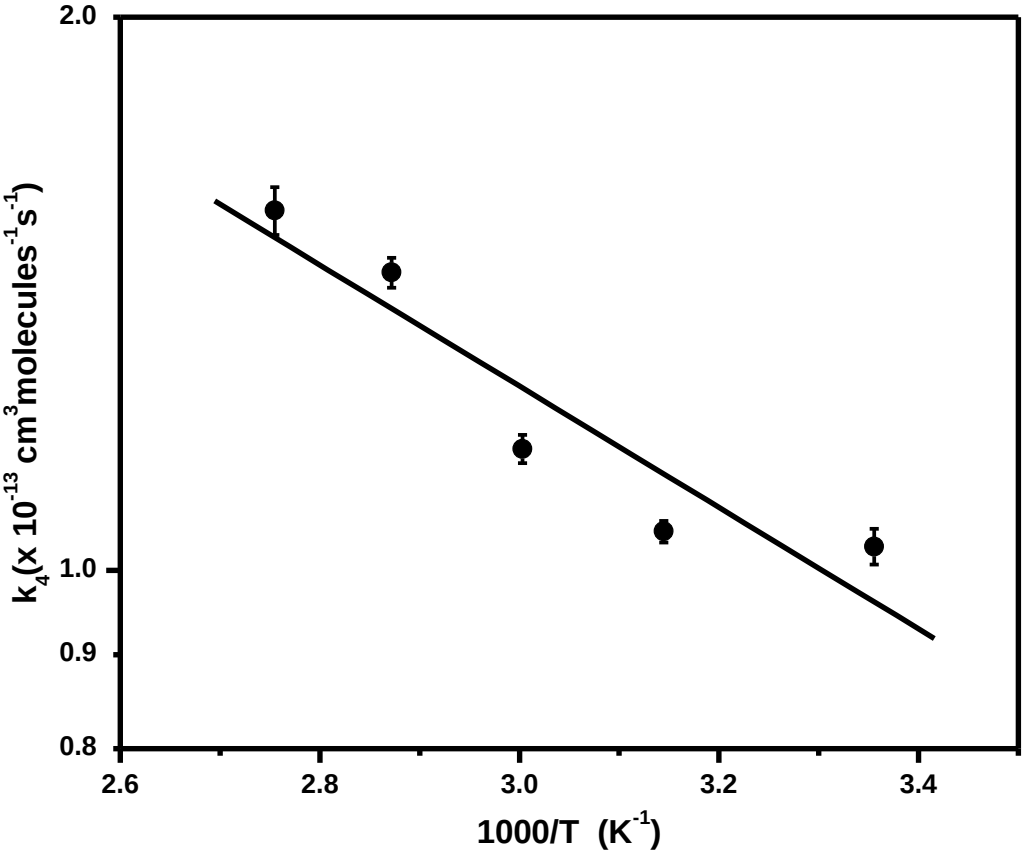

Fig. 2.10. Arrhenius plot of the average value of rate coefficient k_4 (T) of the reaction of sample molecule with OH radicals.

FTIR spectrometer

The exact concentration of the sample for kinetic studies is measured before and after the kinetic experiments by FTIR absorption spectrophotometer (Bruker IFS 66s/V FTIR), using a calibration curve prepared with known concentrations of the sample. A Pyrex cell of path length 28 cm fitted with KBr windows is used for IR absorption studies and concentration determination. The IR absorption spectra of a sample in the range of 500-2500 cm^{-1} are measured with a spectral resolution of 0.1 cm^{-1}, employing a liquid-

nitrogen-cooled wide range MCT detector. A known pressure of the sample is taken in the cell and the total pressure is made up to 760 Torr with N_2 as a buffer gas. IR absorption spectrum of 1-chlorocyclopentene is shown in Fig. 2.11. Absorption spectra of 1-chlorocyclopentene are recorded at various pressures of 1-chlorocyclopentene, in the linear absorption region. The plot of absorbance versus the sample concentration is shown in Fig. 2.12.

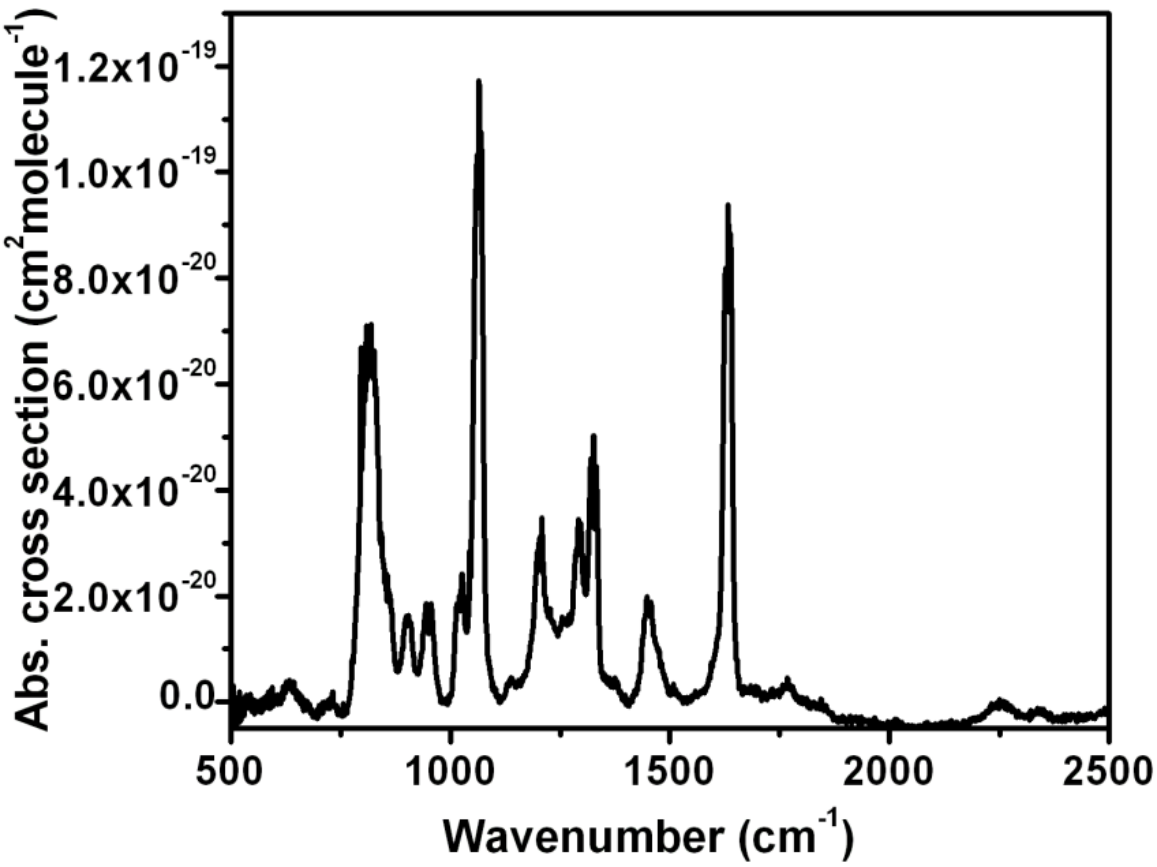

Fig. 2.11. The absorption spectra for 0.5 Torr of 1-chlorocyclopentene with a total pressure of 760 Torr with the addition of nitrogen, in the wavenumber range of 500-2500 cm^{-1} at 298 K.

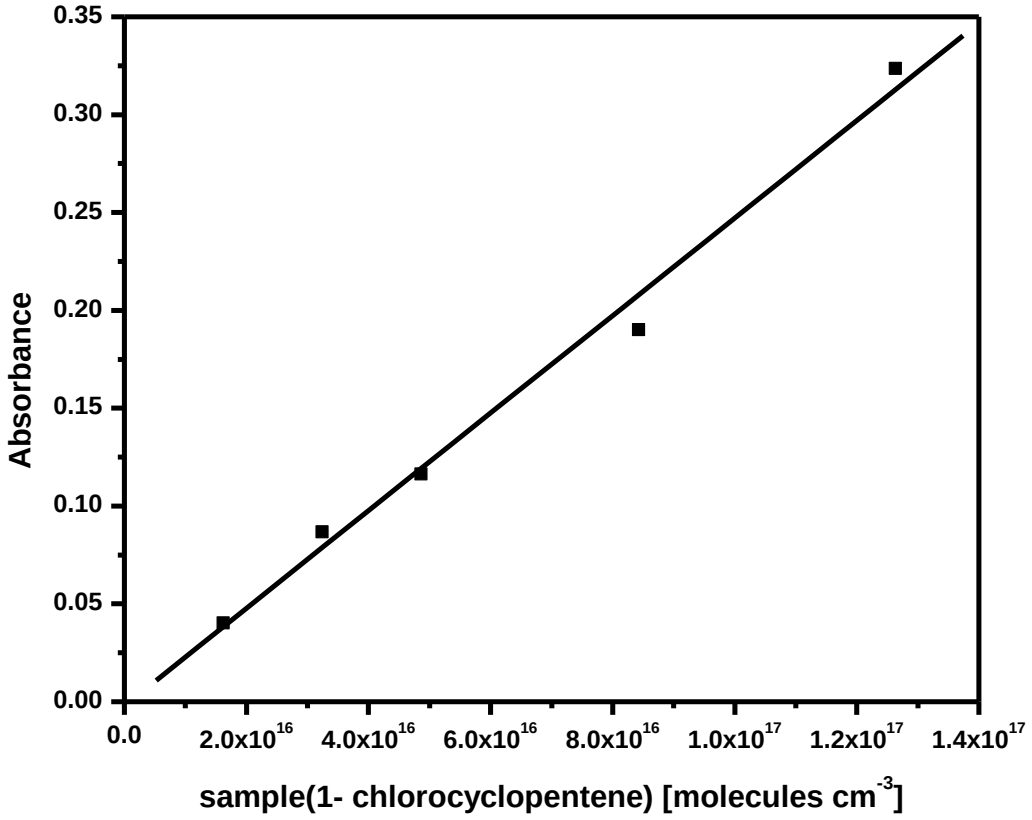

Fig. 2.12. Plot of integrated absorbance at the peak wavenumber of 808.3 cm^{-1} versus 1-chlorocyclopentene concentration, at a total pressure of 760 Torr by adding N_2 gas.

Calculation of IR absorption cross section of sample

The absorption spectra of the sample measured by FTIR spectrometer are converted into absorption cross-sections on Y-axis, employing the relation (Eqn. 2.27),

$$\sigma(\nu) = \frac{ln\,(10)\times A_{CCP}(\nu)}{[CCP]\times l} \qquad (2.27)$$

where σ (ν) is the absorption cross-section in units of cm^2 $molecule^{-1}$ at wavenumber ν; $A_{CCP}(\nu)$ is the absorbance of 1-chlorocyclopentene (sample) at wavenumber ν, [CCP] is the concentration of 1-chlorocyclopentene in molecules cm^{-3}, and l is the optical path

length (28 cm). These absorption cross-section data are used to calculate the radiative efficiency of the sample used for the calculation of global warming potential. This will be discussed later in this chapter.

2.3. Stable product analysis

In order to assess the effect of the stable products, formed in the studied reactions of the VOCs with oxidant species, on the environment, these products are analyzed. The products are characterized by a Gas Chromatograph and Gas Chromatograph coupled with a Mass Spectrometer techniques, using suitable columns (both packed and capillary column) like HT8 (30 m × 0.25 mm × 0.25 μm) and CP WAX 52CB (30 m × 0.25 mm × 0.25 μm) columns, independently. The observed spectral features of the products obtained by GC-MS are compared with the reported mass spectra in the library for identification. The details of GC-MS are given below.

Gas Chromatography-Mass Spectrometry

Gas Chromatography-Mass Spectrometry (GC-MS) is a hyphenated analytical instrumental technique. In this technique, a Gas Chromatograph (GC) is used for the separation of the components of a mixture, and a Mass Spectrometer (MS) detects the separated components. The components of a mixture, separated in GC column enter the MS chamber, where they get ionized and the ions are detected which yield an ion chromatogram. The smaller ions formed due to fragmentation of the molecule after ionization have characteristic relative abundances that provide a 'fingerprint' for the molecular structure. All the ions formed are analysed by the mass analyser. In this work, GC-MS (GCMS-QP2010 model, Shimadzu Make) equipped with electron impact source

for ionisation (the energy of an electron is 70 eV) and a quadrupole mass analyser, which separates the fragments (ions) according to their m/z values, is used. Each chemical compound generates typical mass spectra of the generated fragments. The characteristics of the mass spectra are used to identify the compound by comparing the observed mass spectra with the reported one in the library. Alternatively, the compound is identified by studying its fragmentation pattern. The typical ion chromatograms for the products of Cl initiated oxidation of 1-chlorocyclopentene are given in Fig. 2.13.

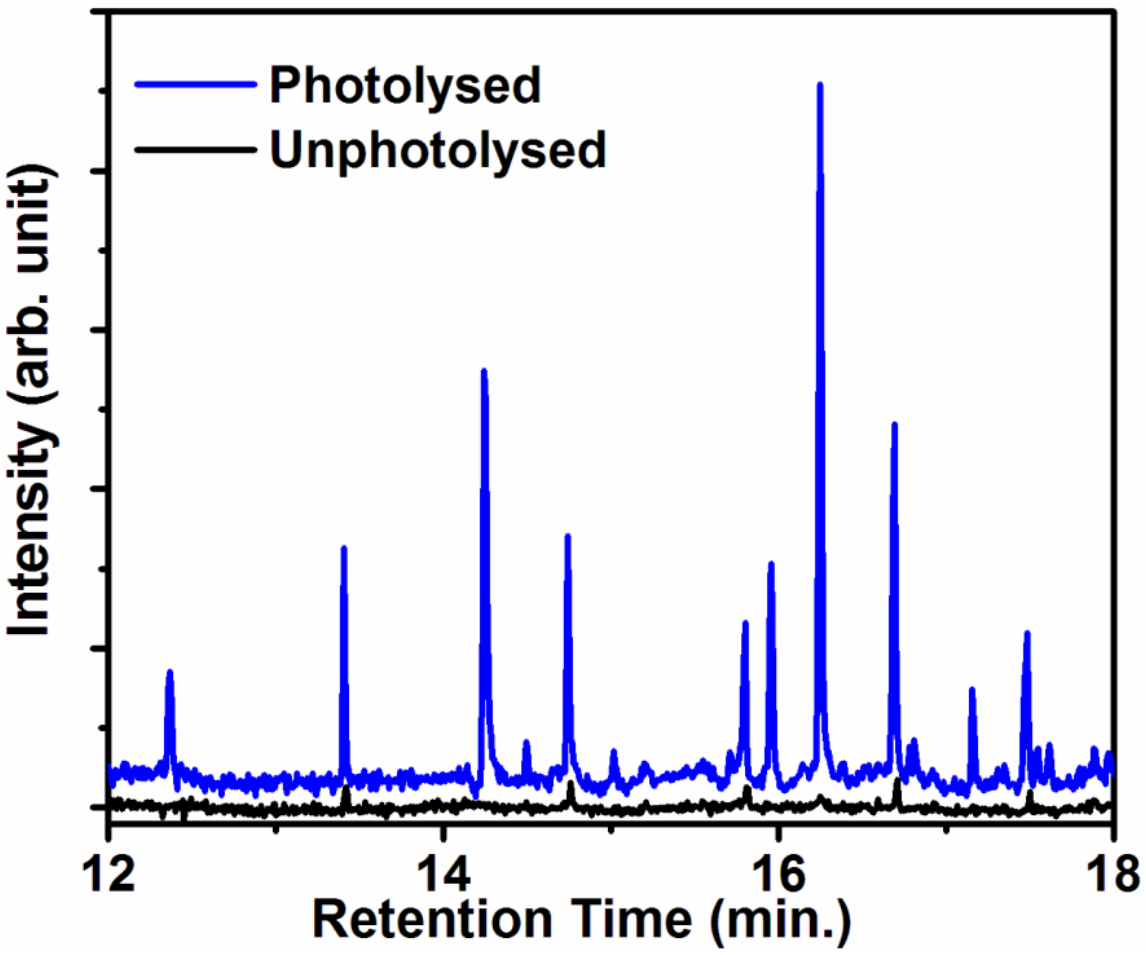

Fig. 2.13. Total ion chromatogram for the products of Cl initiated oxidation of 1-chlorocyclopentene.

In the thesis, only the important spectra of the products are provided. We have not given all the spectra of the products just to avoid increasing the number of pages.

2.4. Global warming potential (GWP) calculation

As explained in the earlier section of this chapter, using FTIR spectrometer, the IR absorption spectra of a sample are measured, which are then converted into absorption cross- sections using relation (Eqn. 2.27). From these values of absorption cross-sections, the integrated absorption cross-sections at 1 cm^{-1} band interval are calculated and assigned to the centre of each band. Thus, all the absorption spectra obtained at various pressures of a compound, maintaining the total pressure of ~760 Torr, are converted into absorption cross-section spectra, and the mean value of integrated cross-section at $1cm^{-1}$ band interval is obtained in a wavelength range of 400-2500 cm^{-1}. These values are employed for the radiative efficiency calculation, using a modified Pinnock curve [36] incorporating the Oslo Line-By-Line model, the latter takes into account atmospheres representing the tropics and extra-tropics. The estimated radiative efficiency and the global lifetime of the sample are used to estimate global warming potential of the sample, and this can be carried out in two ways.

1) The GWP value for a sample can be estimated with respect to CO_2 using the expression given by Hodnebrog et al. (Eqn. 2.28) [100].

$$(GWP)_x(TH) = \frac{\int_0^{TH} a_x[x(t)dt]}{\int_0^{TH} a_r[r(t)dt]} \qquad (2.28)$$

where, a_x = radiative forcing of a unit mass of x added to current atmospheric composition.

Radiative forcing is the amount of energy per unit area per unit time absorbed by unit mass of greenhouse gas that would otherwise be lost to space. The parameter x(t) = atmospheric decay function of x (in a time horizon TH that depends on the lifetime of the species), and a_r and [r(t)] are the corresponding quantities for the reference gas (i.e. CO_2).

The halocarbon global warming potential (HGWP) of a sample (presently 1-chlorocyclopentene (CCP) is considered as a sample) relative to CFC-11($CFCl_3$) is calculated using a semi-empirical equation (2.29) [37,38].

$$HGWP_{CCP} = \frac{\tau_{CCP}}{\tau_{CFCl_3}} \times \frac{M_{CFCl_3}}{M_{CCP}} \times \frac{RE_{CCP}}{RE_{CFCl_3}} \frac{\left(1\text{-}\exp^{-t/\tau_{CCP}}\right)}{\left(1\text{-}\exp^{-t/\tau_{CFCl_3}}\right)} \qquad (2.29)$$

where τ_x, M_x, RE_x (x=CCP or $CFCl_3$) and t denote the global atmospheric lifetimes, the molecular weight, radiative efficiency and time horizon, respectively. Using the HGWP value, the global warming potential (GWP) of a sample, relative to CO_2, can be estimated by multiplying this HGWP value with the GWP value of $CFCl_3$. The GWP values of $CFCl_3$ on a time horizon of 20 and 100 years as 6730 and 4750, respectively [39].

2.5. Ozone depletion potential calculation

If the sample has a chlorine atom, it can possibly contribute to the stratospheric ozone depletion. The ozone depletion potential (ODP) of a sample (here also, 1-chlorocyclopentene, CCP, is considered as the sample) can also be estimated, using a semi-empirical equation (2.30) [38],

$$ODP_{CCP} = \frac{\tau_{CCP}}{\tau_{CFCl_3}} \times \frac{M_{CFCl_3}}{M_{CCP}} \times \frac{n}{3} \qquad (2.30)$$

where, τ_x and M_x, have the usual meaning as in Eqn. (2.29), n is the number of chlorine atoms in CCP (that is 1), and the number 3 refers to the three chlorine atoms in $CFCl_3$. Using the value of τ_{CFCl3} as 45 years [39], the ODP value of the sample can be calculated.

Chapter-3

Tropospheric Oxidation of Cyclic Hydrocarbons with Eight Carbon Atoms

3.1. Introduction

Most of the volatile organic compounds (VOCs) are continuously emitted to the earth's troposphere from biogenic and anthropogenic sources. Among them, cyclic and acyclic alkanes and alkenes are important classes of VOCs released into the troposphere from various sources, such as automobile exhausts, gasoline vaporization, forest fire, rubber abrasion, etc. [40-43]. Many such hydrocarbons may also be released from industry, where they are already in use as solvents, precursors etc. Recently, their catalytic oxidation by molecular oxygen has been proposed to produce selective functionalized precursors [44], which are likely to increase their industrial importance. Thus, they are significant constituents of ambient air, comprising 10% of the non-methane organic compounds observed in urban areas [45]. The kinetics and products of the reactions of many VOCs with major tropospheric oxidants, namely OH and ozone, have been studied extensively to understand their total impact on local pollution. In the tropospheric degradation of some VOCs such as hydrocarbons, Cl atoms are as important as OH radicals due to the large ratio of the rate coefficients of reaction with Cl atoms to that with OH radicals. Cl atom reaction is even more effective for the degradation of some VOCs than OH, in the conditions of the marine boundary layer and in the polluted urban atmosphere [16]. The atmospheric oxidation of these hydrocarbons leads to the gas

phase as well as particulate products. The oxidative photochemistry of the unsaturated hydrocarbons initiates the processes that ultimately lead to ozone generation and photochemical smog. The importance of each of the tropospheric oxidant in the oxidative degradation of these hydrocarbons varies depending on the rate coefficients of their reactions, the conditions in the local atmosphere, etc. In this context we had investigated the reactions of Cl atoms with cyclic alkenes (C5 – C7), acyclic 1-alkenes (C6 – C9) [14,46]. In this, the major interest was an assessment of the importance of the reaction of Cl in the degradation of these alkenes, and gaining understanding on the variation of the rate coefficients with structure, unsaturation and substitution. It is observed that the rate coefficients of the reactions with Cl atoms do not increase much with increasing unsaturation. Although the addition is the most prominent reaction of Cl and OH with unsaturated molecules, a definite possibility of abstraction of H atom exists even for reactions of the OH radicals [25,47-49], especially in large unsaturated cyclic hydrocarbons such as cyclooctene. The major products in our studies, mentioned above, indicated a significant contribution of H atom abstraction in the case of the reaction of Cl, the maximum abstraction being from the carbon atom away from unsaturation. In the present study, we have extended our investigations to the reactions of tropospheric oxidants with eight-membered cyclic hydrocarbons (CyOs), cyclooctane, cis-cyclooctene and 1,5-cyclooctadiene, to understand the effect of unsaturation on the rate coefficients and occurrence of H atom abstraction in these cyclic molecules. These measured rate coefficients can be compared to that in 1-alkenes for the reactions of both Cl atom and OH radical. In addition to these, the reactions with ozone also have been studied to obtain

the rate coefficients, so as to compare the relative importance of these three oxidants in the degradation of CyOs.

There are many studies on the reactions of OH with cyclooctane [50-53], and the rate coefficient is almost established. There are some studies on the reactions of cyclooctene with OH and O_3, where the rate coefficients, as well as the major products, are reported [31,47,54]. Investigations on the kinetics of 1,5-cyclooctadiene are very limited [31]. As discussed above, the rate coefficients for some of the reactions of these CyOs with tropospheric oxidants are already reported, but that for the reaction of cyclooctene with Cl and 1,5- cyclooctadiene with OH are measured for the first time. Most of the earlier studies on the products were carried out in the presence of NOx. In the present case, the gas phase products are investigated under NOx free conditions, and compared with our earlier results with other hydrocarbons.

3.2. Experimental

The rate coefficients at room temperature (298 ± 2 K) are determined using a relative rate method, where the rate of decrease in the concentration of the CyOs, namely cyclooctane, cis-cyclooctene and 1,5-cyclooctadiene, due to their reactions with the atmospheric oxidants (X), is compared to that of a reference molecule (R), with known rate coefficient.

$$CyO + X \rightarrow \text{products} \quad (3.1)$$

$$R + X \rightarrow \text{products} \quad (3.2)$$

Assuming that CyO and R react only with the reactant X, the fractional loss of CyO and R is related by the standard expression,

$$\ln\left[\frac{[CyO]_{t_0}}{[CyO]_t}\right] = \left[\frac{k_X^{CyO}}{k_X^R}\right] \ln\left[\frac{[R]_{t_0}}{[R]_t}\right] \qquad (3.3)$$

where, $[CyO]_{t_0}$, $[\mathrm{CyO}]_t$, $[R]_{t_0}$ and $[R]_t$ are the respective concentrations at time 0 and t, and k_X^{CyO} and k_X^R are the rate coefficients for reactions (3.1) and (3.2), respectively. Thus, the plot of logarithms of the ratios of fractional changes in the concentrations of both CyO and R at various specific times gives a straight line with zero intercepts and slope of k_X^{CyO} / k_X^R, and the rate coefficient k_X^{CyO} *i*s calculated using the known value of k_X^R.

The details of the experimental setup and procedure for determining the rate coefficient of the reaction of Cl atom, OH and O_3 are described in Chapter 2: Experimental methods. Briefly, in situ photolysis of CCl_3COCl and H_2O_2/ O_3-H_2O mixture at 254 nm is used to generate Cl atoms and OH radicals, respectively. Monochromatic UV lamps from Rayonett are used for photolysis. Ozone, generated as O_3/O_2 mixture (< 2%) using an ozonizer, is injected at intervals and allowed to react with CyO and R. In the experiments to determine the rate coefficients of reactions with ozone, high concentration of tetrahydrofuran (THF, 2400 ppm) is used as an OH radical scavenger, which is a secondary product of the reaction of these organics with ozone. All the three compounds have boiling points in the same range, and hence the pressure of the sample could be kept in the same range. The reaction mixture, consisting of CyO (50-100 ppm), reference molecule (50-100 ppm), the source molecule for OH/Cl generation (H_2O_2/CCl_3COCl), and buffer gas (N_2 / air), are taken in a Quartz reactor. The total

pressure is maintained at 800 ± 3 Torr. After photolysis for a fixed time or after the addition of ozone, the depletion of CyO and R is followed, using a Gas Chromatograph (Shimadzu GC-2014) with a flame ionization detector (FID). Either SE-30 (10%, 2 m × 3 mm) stainless steel columns or AB1MS (30m × 0.25 mm × 0.25 μm) fused silica capillary columns are employed for the separation. The selection of suitable reference molecule R is based on the similarity of the rate coefficients (the ratio of the rate coefficients not exceeding 2.5) and the least interference during the Gas Chromatography analysis, either from the molecule or from the products of their reactions with the oxidants.

Products of the reactions are separated and analyzed by Gas Chromatograph coupled with a Mass Spectrometer and FID (GC-MS-QP2010, Shimadzu). Capillary columns, namely CPWAX (30 m × 0.25 mm × 0.25 μm) and BPX50 (30 m × 0.25 mm × 0.25 μm) under different conditions of flow and temperature programming are used for the separation. All the reactions are carried out with air as a buffer gas, and the depletion of the parent molecule is limited to 50-80%. In the case of the reaction of ozone, the OH radicals are known to be generated leading to OH initiated oxidation, and thus complicating the product distribution. In general, an OH scavenger is added to the reaction mixture in the required concentration to suppress the effects of OH generation. However, the addition of an OH scavenger, and the products formed from its reaction with OH, can mask or overlap with the products of interest. Therefore, the use of a scavenger was avoided in the product analysis studies in the present work, mainly to eliminate possible interference of the scavenger and its products with the products

detection method. Comparison with the present study on the products of reactions of OH with these CyOs helps in identifying the products of ozone reaction only from the combined product distribution.

In addition to the identification of products, quantitative analysis of CO_2 formed during the reaction of O_3 with 1,5-cyclooctadiene is carried out by Gas Chromatograph coupled with a methanizer and FID (GC-MS-QP2014, Shimadzu) using Porapak Q packed column (stainless. steel. tube (5'x ¼")) at 40^oC and 25 ml/min flow rate of N_2 carrier gas.

Nitrogen gas (purity > 99.9%, INOX Air Products Ltd. Mumbai, India) and ultrapure air (Zero grade, Chemtron Science Laboratories Mumbai, India) are used as buffer gases. High purity oxygen (> 99.9%, Alchemie Gases & Chemicals Pvt. Ltd., Mumbai, India) is used to generate ozone/oxygen mixture. Cyclooctane (>99%), cis-cyclooctene (>95%), and 1,5-cyclooctadiene (>99%) are procured from Sigma Aldrich. Among the reference molecules, cis-butene and 1-butene are from Matheson, n-pentane (>97%), n-hexane (>97%), 1,4-cyclohexadiene (>99%), cyclohexane(>97%) and cyclopetene (>96%) as well as tetrahydrofuran (>97%) used as OH scavenger, are all from Sigma Aldrich. Samples of the compounds are stored in evacuated glass vessels and subjected to freeze-pump-thaw cycles prior to use.

3.3. Results

3.3.1. Determination of rate coefficients

Before conducting the experiment to determine the rate coefficients of the reactions of these CyOs employing the relative rate method, the stability of the reaction mixtures to wall losses and dark reactions are examined in each case. The stability is

found to be satisfactory for about 7 – 8 hours, which is more than the total duration of the experiment. Direct photolysis of CyOs is expected to be negligible based on their UV-Vis absorption spectra, and it is further confirmed experimentally. The reactions with each sample and the reference compounds are carried out individually to ensure that the products of the reactions do not interfere with the concentration measurement of CyO and the reference molecules by GC.

The typical logarithmic plots of the relative decrease in the concentration of CyO and references, due to their reactions with Cl atoms, are shown in Fig. 3.1.

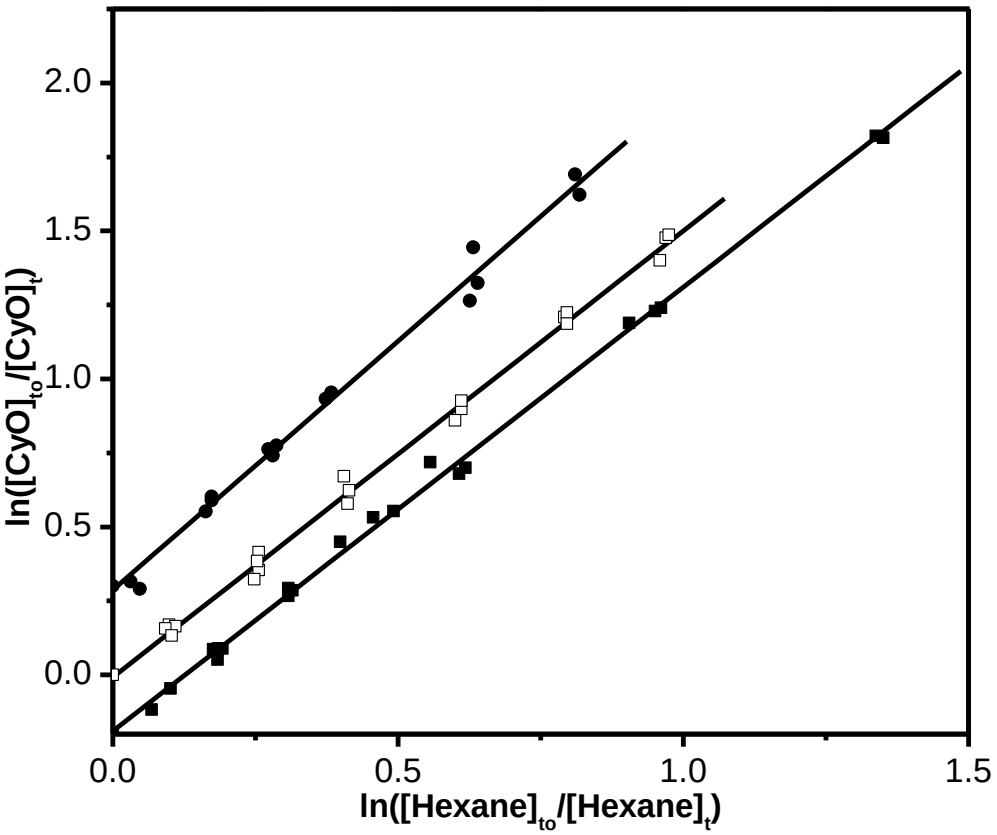

Fig. 3.1. Typical plots of the fractional decrease in the concentration of CyO, relative to

n-hexane, due to the reaction with Cl atoms at 298 ± 2 K, (□) cyclooctane, (■) cis-cyclooctene, shifted in the Y-axis by - 0.2, and (●) 1,5-cyclooctadiene, shifted in the Y-axis by + 0.3 for clarity.

The slopes observed with different reference compounds and the measured rate coefficients are presented in Table 3.1. The average values of the slopes from a number of experiments (given in parentheses) are given for each set of experiments with a reference compound, along with the statistical error. The error in the rate coefficients is a combination of the 2σ error of the slopes and the reported error of k_R, calculated using the statistical error propagation equation. The weighted averages of the rate coefficients obtained with different reference compounds are also included in the Table 3.1 with the calculated errors. In the case of the reaction of the Cl atom with cyclooctane, the experiments are conducted in N_2 as well as air with n-hexane and 1-butene as the reference compounds, and the changes in the slope values in the presence of air (O_2) are found to be negligibly small.

Table 3.1: Relative ratios and rate coefficients of reactions of Cl with CyO at 298 K with different reference compounds, [CyO] = 100 - 150 ppm, [R] = 50 – 100 ppm. Buffer gas - N_2 and air, Total pressure = 800 Torr. The error in the rate coefficients is a combination of the 2σ error of the measurements and the reported error for the reference compound. The number in the parenthesis after the reference compound name represents the number of experiments.

Sample	Reference	Average	Rate	Literature

	compound, $k_{\mathrm{Cl}}^{R} \times 10^{10}$ ($cm^3 molecule^{-1} s^{-1}$)	**slope**	**coefficient** $k_{\mathrm{Cl}}^{CyO} \times 10^{10}$ ($cm^3 molecule^{-1} s^{-1}$)	$k_{Cl} \times 10^{10}$ ($cm^3 molecule^{-1} s^{-1}$)
Cyclooctane	n-hexane (4 in N_2, 3 in air) 3.15 ± 0.40 [27,46][a]	1.47 ± 0.04 (N_2) 1.41 ± 0.20 (Air)	4.63 ± 0.20 4.44 ± 0.84	2.63 ± 0.54 [55] 4.57 ± 0.15 [56]
	1-butene (4 in N_2, 3 in air) 3.21 ± 0.41 [27,46][a]	1.47 ± 0.11 (N_2) 1.48 ± 0.20 (Air)	4.70 ± 0.68 4.74 ± 0.61	
	n-pentane (3) in N_2 2.62 ± 0.34 [27,46][a]	1.52 ± 0.31	3.98 ± 0.96	
		Average (N_2)	**4.48 ± 0.37**	
Cyclooctene	1-butene (4) in N_2	1.47 ± 0.06	4.70 ± 0.62	
	n-pentane (3) in N_2	1.87 ± 0.16	4.60 ± 0.45	
	n-hexane (5) in	1.50 ± 0.15	4.72 ± 0.51	

	N_2			
		Average	**4.68 ± 0.31**	
1,5-Cyclooctadiene	n-pentane (3) in N_2	1.99 ± 0.07	5.04 ± 0.49	6.90 ± 1.33 [13]
	n-hexane (5) in N_2	1.66 ± 0.30	5.21 ± 1.15	
		Average	**5.15 ± 0.74**	

[a]These are values from Ref. [57], corrected using the latest IUPAC rate coefficients [58] for the respective reference molecules [27,46].

Results of similar experiments for the reaction of OH and O_3 are given in Fig. 3.2 and 3.3, and Tables 3.2 and 3.3, respectively. Oxygen is always present in these cases. The rate coefficients of the reference compounds used are listed either in the Table or below the Table as a footnote. Previously reported rate coefficients, if any, are also listed in the Tables for comparison. Our measured values of the rate coefficients of reactions of OH and ozone are found to be matching well with those reported earlier.

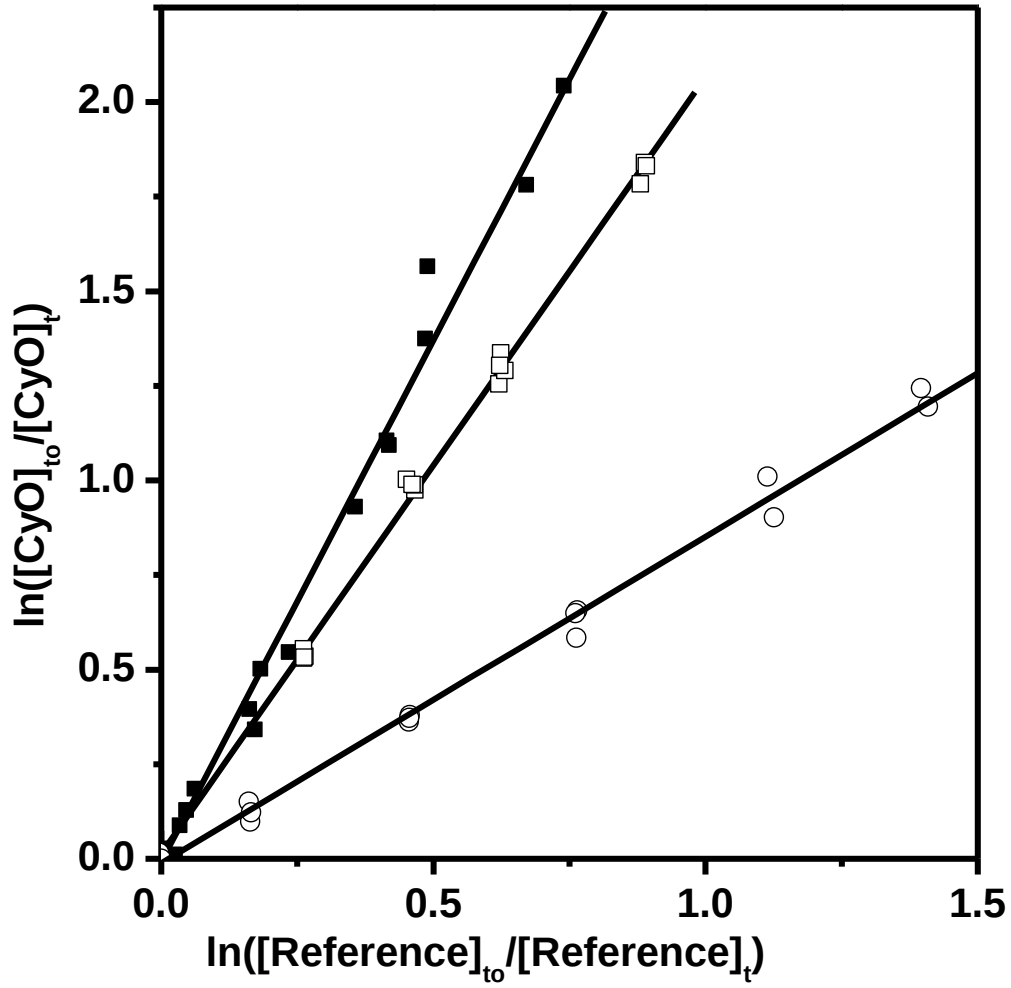

Fig. 3.2. Typical plots of the fractional decrease in the concentration of CyO, relative to different reference molecules due to the reaction with OH, at 298 ± 2 K, (■) cyclooctane with n-hexane, (o) cis-cyclooctene and (□) 1,5-cyclooctadiene with cis-butene as reference molecule.

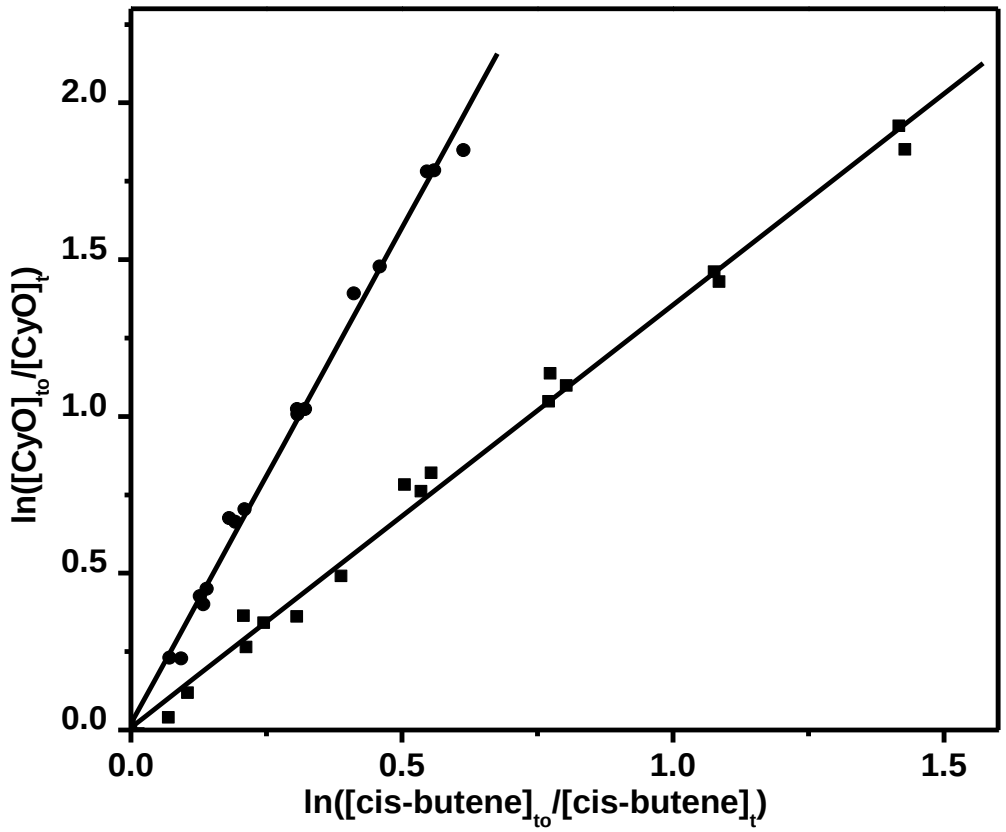

Fig. 3.3. Typical plots of the fractional decrease in the concentration of CyO, relative to cis-butene, due to the reaction with O_3 at 298 ± 2 K, (•) cis-cyclooctene and, (■) 1,5-cyclooctadiene.

Table 3.2: Relative ratios and rate coefficients of reactions of OH with CyO at 298 K with different reference compounds, [CyO] = 100 - 150 ppm, [R] = 50 – 100 ppm. Buffer gas N_2, Total pressure = 800 Torr. The error in the rate coefficients is a combination of the 2σ error of the measurements and the reported error for the reference compound. The number in the parenthesis after the reference compound name represents the number of experiments.

Sample	**Reference compound** $k_{OH}^{R} \times 10^{11}$ ($cm^3 molecule^{-1} s^{-1}$)	**Average slope**	**Rate coefficient** $k_{OH}^{CyO} \times 10^{11}$ ($cm^3 molecule^{-1} s^{-1}$)	**Literature** $k_{OH}^{CyO} \times 10^{11}$ ($cm^3 molecule^{-1} s^{-1}$)
Cyclooctane	n – hexane(5) 0.52 ± 0.10 [8]	2.67 ± 0.31	1.39 ± 0.30	(1.34 ± 0.04) [50] 1.41 [51] 1.35 ± 0.04 [52] (1.42 ± 0.27) [53]
	Cyclohexane(4) 0.69 ± 0.14 [8]	1.96 ± 0.13	1.37 ± 0.29	
		Average	**1.38 ± 0.21**	
Cis-Cyclooctene	Cis-butene (5) 5.60 ± 1.29 [58]	0.90 ± 0.13	5.04 ± 1.37	5.16 ± 0.15 [47]
	Cyclopentene (5) 6.71 ± 1.34 [8]	0.76 ± 0.19	5.10 ± 1.63	
		Average	**5.07 ± 1.06**	
1,5-Cycloocta-diene	Cis-butene (6)	2.01 ± 0.26	11.26 ± 2.97	
	1,4-cyclohexa-diene (5) 9.95 ± 0.39 [8]	1.10 ± 0.13	10.95 ± 1.37	
		Average	**11.11 ± 1.74**	

Table 3.3: Relative ratios and rate coefficients of reactions of O_3 with CyO at 298 K with different reference compounds, [CyO] = 100 - 150 ppm, [R] = 50 - 100 ppm. Buffer gas air, Total pressure = 800 Torr. The error in the rate coefficients is a combination of the 2σ error of the measurements and the reported error for the reference compound. The number in the parenthesis after the reference compound name represents the number of experiments.

Sample	**Reference compound** $k_{O3}^{R} \times 10^{16}$ ($cm^3 molecule^{-1} s^{-1}$)	**Average slope**	**Rate coefficient** $k_{O3}^{CyO} \times 10^{16}$ ($cm^3 molecule^{-1} s^{-1}$)	**Literature** $k_{O3}^{CyO} \times 10^{16}$ ($cm^3 molecule^{-1} s^{-1}$)
Cyclooctene	Cis-butene (5) 1.3 ± 0.2 [58]	3.16 ± 0.32	4.10 ± 0.8	3.86 ± 0.23 [31] 3.74 ± 0.11 [54] 4.51 ± 0.66 [59]
1,5-Cyclooctadiene	Cis-butene(4)	1.30 ± 0.12	1.69 ± 0.30	1.52 ± 0.10 [31]
	1,4-cyclohexadiene (4) 0.46 ± 0.02 [31]	2.58 ± 0.23	1.19 ± 0.12	
		Average	**1.44 ± 0.16**	

3.3.2. Products

The ion chromatograms of the gaseous products of the reactions of OH and Cl with cyclooctane, cis-cyclooctene and 1,5-cyclooctadiene are shown in Fig. 3.4, 3.5 and 3.6, respectively, and that of the reaction of ozone with cis-cyclooctene and 1,5-cyclooctadiene are shown in Fig. 3.7. The use of ozone-water mixture as a source of the OH radical is responsible for a higher percentage of the reaction of cyclooctane, and a higher yield of products in the reaction with OH as compared to that with Cl atom. Most of the major gaseous products are identified by comparing with the reported mass spectra (MS). In some cases, where the spectra are not available in the literature for a comparison, the products are identified by interpreting the fragmentation pattern. Mass spectra of these products are shown as insets in the respective figures.

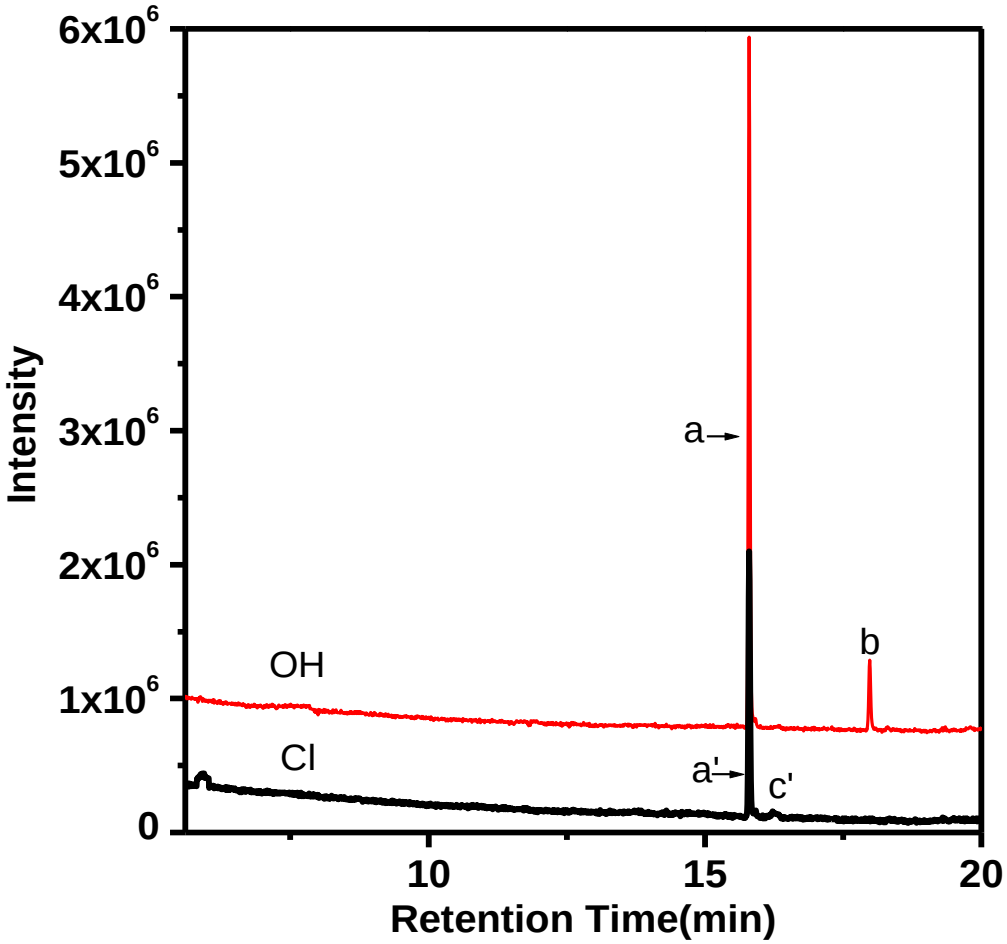

Fig. 3.4. Total ion chromatogram of products of the reactions of cyclooctane with OH and Cl. Column: CPWAX (30 m × 0.25 mm × 0.25 μm) with temperature programming, 32-5-10-200 and flow of 0.96 ml min^{-1}. a and a': cyclooctanone, b: cyclooctanol, c': 4-cycloocten-1-one, d: cyclooctene.

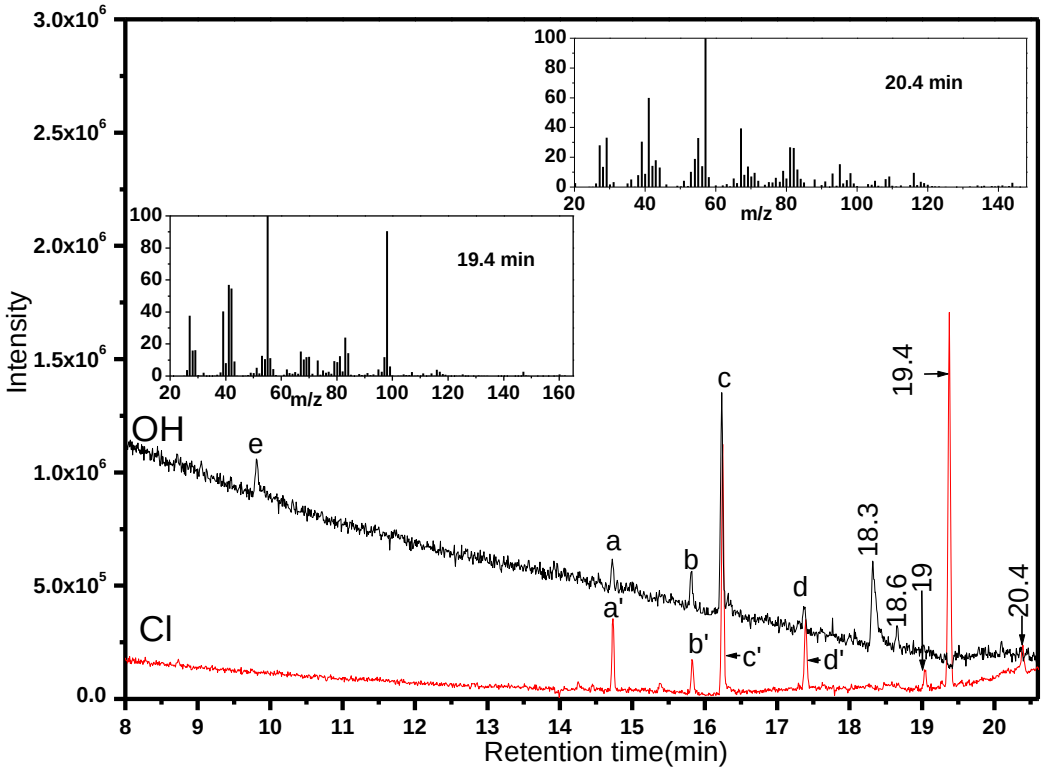

Fig. 3.5. Total ion chromatogram of products of the reactions of cis-cyclooctene with OH and Cl. Column: CPWAX (30 m × 0.25 mm × 0.25 μm) with temperature programming, 32-5-10-200 and flow of 0.96 ml min^{-1}. The confirmed products by comparison with the library are, - a and a': epoxycyclooctane, b and b': cyclooctanone, c and c': 4-cyclooctenone-1-one, d and d': 2-cyclooctene-1-one, and e: heptanal. The products identified by the analysis of the MS fragmentation pattern (insets): 2-chlorocyclooctan-1-one (19.4 min) and 2-chlorocyclooctan-1-ol (20.4 min).

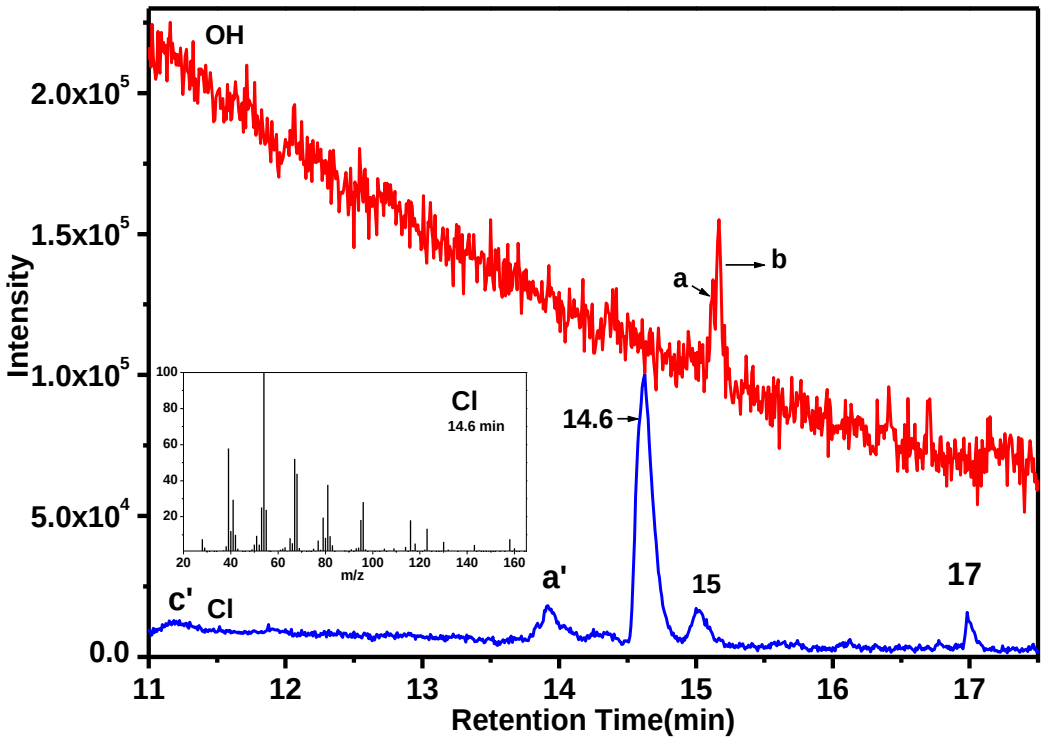

Fig. 3.6. Total ion chromatogram of products of the reactions of 1,5-cyclooctadiene with OH (Column: CPWAX (30 m × 0.25 mm × 0.25 μm)) with temperature programming, 35-2-10-200 and flow of 1 ml min^{-1}) and Cl (Column: BPX50 (30 m × 0.25 mm × 0.25 μm)) with temperature programming, 40-5-10d-150 and flow of 1.38 ml min^{-1}). The confirmed products by comparison with library are- a and a': 1,5-cyclooctadiene-4-one, b: 5-cyclooctene-1,2-dionecyclooctanone, c': 1,2-epoxy-5-cyclooctene. The product identified by the analysis of the MS fragmentation pattern (inset): 8-chlorocyclooct-5-ene-1-one (14.6 min).

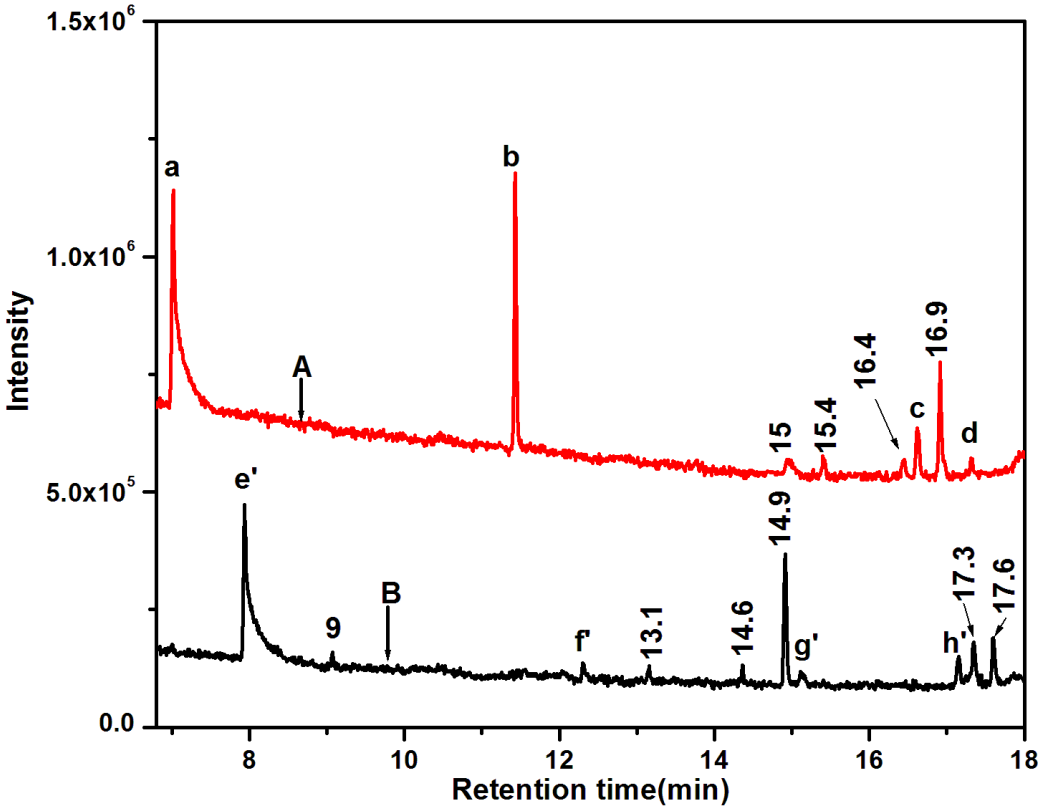

Fig. 3.7. Total ion chromatogram of products of the reactions of A: cis-cyclooctene and B: 1,5-cyclooctadiene with O_3 (Column: CPWAX(30 m × 0.25 mm × 0.25 μm)) with temperature programming, 35-2-10-200 and flow of 1 ml min^{-1}). The confirmed products by comparison with library are- a: heptanal, b: 1,2-epoxycyclooctane, c: 9-Oxabicyclo [6.1.0] nonan-4-ol, d: heptanoic acid, e': 4-hepten-1-al, f': 1,2-epoxy-5-cyclooctene, g': 1,5-cyclooctadiene-4-one, h': 1,5-cyclooctadiene diepoxide.

3.3.2.1. Reactions of OH and Cl

The major oxidized product of the reaction of both OH and Cl with cyclooctane is cyclooctanone, as shown in Fig. 3.4 (peaks with a retention time of 15.8 min). Cyclooctanol is the second major product observed in the reaction of OH (retention time

of 18.0 min), but it is not observed in the reaction of Cl atom. The absence of cyclooctanol may be due to its further reaction with Cl atoms. A very small yield of cyclooctene (5.8 min) is observed in the reactions of both OH and Cl with cyclooctane, and a very small amount of 4-cycloocten-1-one (16.2 min) is observed in the reaction with only Cl atom.

The ion chromatograms of the products of the reactions of OH and Cl with cyclooctene are given in Fig. 3.5. The identified major products in the reaction of OH with cyclooctene are epoxycyclooctane (peak *a* at 14.7 min), cyclooctanones (peak *b* at 15.8 min), 4-cycloocten-1-one (peak *c* at 16.2 min) and 2-cyclooctene-1-one (peak *d* at 17.4 min). A very small yield of 1,5-cyclooctadiene (9 min) is also observed, though not very clear in the ion chromatogram. The peak at 9.8 min is identified as heptanal. There are two unidentified peaks, the major one at 18.3 min and the minor one at 18.6 min. Some of these products of the OH reaction are observed in the reaction of Cl atom also, namely 1,5-cyclooctadiene, epoxycyclooctane, cyclooctanone, 4-cyclooctene-1-one and 2-cyclooctene-1-one. The fragmentation pattern of the two peaks observed at 19.4 and 20.4 min (shown in the inset) could not be matched with any spectra in the literature, but analysis suggests them to be the addition products, 2-chlorocyclooctan-1-one and 2-chlorocyclooctan-1-ol.

In the case of 1,5-cyclooctadiene (Fig. 3.6), the reactions with both the OH and Cl appear to lead to a fewer number of products in the gas phase. In the reaction with OH, 1,5-cyclooctadiene-4-one (15.12 min) and 5-cyclooctene-1,2-dione (15.17 min) are the major observed products, which are very close, but with distinct mass spectra. In the reaction of Cl, 1,5-cyclooctadiene-4-one (13.9 min) is identified by comparison with its

reported MS, whereas the major product at 14.6 min is identified as 8-chlorocyclooct-5-ene-1-one by analyzing the MS fragmentation pattern (Inset). The molecular ion peak at 158 with a ratio of 3:1 for peaks at 158 and 160, typically observed for chlorocompounds, is seen along with peaks at 123(158-35(Cl)), and 130(158-28(CO)). In addition, the presence of 1,2-epoxy-5-cyclooctene is also indicated at 11.26 min.

3.3.2.2. Reactions with ozone

The ion chromatograms of the products of the reactions of ozone with cis-cyclooctene and 1,5-cyclooctadiene are shown in Fig. 3.7. Two major products, heptanal (7 min) and 1,2-epoxycyclooctane (11.4 min), are observed in the case of cis-cyclooctene, along with minor peaks at 15.0, 15.4, 16.4, and 17.3 min and two more significant peaks at 16.6 and 16.9 min. Among these minor peaks, the products at 16.6 and 17.3 min are identified as 9-oxabicyclo [6.1.0] nonan-4-ol and heptanoic acid, respectively. In the case of the reaction of cyclooctadiene with ozone, the major product is identified as 4-hepten-1-al (7.9 min). 1,2-epoxy-5-cyclooctene (12.3 min),1,5-cyclooctadiene-4-one (15.1 min) and 1,5-cyclooctadiene diepoxide (17.1 min) are identified among the minor products.

The yield of CO_2 during the reaction of ozone with 1,5-cyclooctadiene is estimated in 4 separate experiments, with different extent of the reaction, and the average yield is determined to be 34.5 ± 5 %.

3.4. Discussion

3.4.1. Rate coefficients

There are two reports on the rate coefficients of the reaction of Cl atom with cyclooctane at 298 K. The present measured value of $(4.48 \pm 0.37) \times 10^{-10}$ $cm^3molecule^-$

$^{1}s^{-1}$ is more than 50% higher than that reported by Aranda et al. [55] determined using an absolute method ((2.63 ± 0.54) × 10^{-10} $cm^{3}molecule^{-1}s^{-1}$), but agrees well with that reported by Aschmann and Atkinson [56] ((4.57 ± 0.15) × 10^{-10} $cm^{3}molecule^{-1}s^{-1}$), which was determined by a relative rate method with n-butane as a reference compound. There are no reported rate coefficients for the reaction of Cl with cis-cyclooctene. The only reported rate coefficient in the case of 1,5-cyclooctadiene is from our group, but the present value (5.15 ± 0.74) × 10^{-10} $cm^{3}molecule^{-1}s^{-1}$ is found to be lower than the earlier value (6.90 ± 1.33) × 10^{-10} [13]. The present value of the rate coefficient is more accurate since there was an issue of the sample contamination in the earlier measurement. The rate coefficients obtained using n-hexane and n-pentane as reference compounds are found to agree well. Considering that the baseline is cleaner and peaks are better resolved in the present case with capillary columns, the experiments with 1,4-cyclohexadiene are also repeated. It can be observed that the rate coefficients of reactions with Cl atoms are very high, and only marginally increase with unsaturation. This is very similar to our earlier observation in the case of cyclohexane, cyclohexene and 1,4-cyclohexadiene [13]. The reason could be that the Cl atom reactions occur at almost the gas collision limit for even saturated molecules, and hence the additional reaction channel with unsaturation can't further increase the rate coefficients.

The reaction of OH with cyclooctane is well studied, and the present experimental value (shown in Table 3.2) is in good agreement with the reported rate coefficients. The errors reported by Donahue et al. [50] and Aschmann et al. [52] are smaller as compared to the present ones because they have not included the errors in the rate coefficients of the

reference compounds. The value of $k_{OH,}$ determined for cyclooctene, also matches well with the only reported value by Aschmann et al. [47]. There are no previous reports on the reaction of OH with 1,5-cyclooctadiene. The two rate coefficients determined here, using two different reference compounds, are in good agreement with each other. The rate coefficients predicted by the frequently used structure-activity relationship [60,61] are (6.50×10^{-11}) and (1.19×10^{-10}) $cm^3molecule^{-1}s^{-1}$ for cis-cyclooctene and 1,5-cyclooctadiene with OH, respectively. These are reasonably in good agreement with the experimental values, the one for cis-cyclooctene being marginally higher. As expected, the rate coefficients increase with increasing unsaturation, becoming about 8 times with two double bonds. This increase is qualitatively similar to that observed in six-membered cyclic compounds, cyclohexane (($6.97 \pm 0.14) \times 10^{-12}$ $cm^3molecule^{-1}s^{-1}$) [62] and 1,4-cyclohexadiene (($9.48 \pm 0.39) \times 10^{-11}$ $cm^3molecule^{-1}s^{-1}$) [63].

There are three previous reports on the rate coefficient of the reaction of ozone with cis-cyclooctene, of which the latest one by Stewart et al. [59] is almost 20% higher than the previously reported values [31,54], as shown in Table 3.3. The present value matches well with the previously reported values. In the case of 1,5-cyclooctadiene, the value of k_{O3} determined using the two different reference molecules differ considerably as shown in Table 3.3, but the average value agrees well with the only reported value [31]. The k_{O3} value of 1,5-cyclooctadiene is found to be lower than that of cis-cyclooctene. Similarly, the reported k_{O3} value of 1,4-cyclohexadiene is also found to be lower than that of cyclohexene [64]. However, when the two double bonds are conjugated, as in 1,3-

cyclohexadiene, the rate coefficient of reaction with O_3 is reported to be almost 50 times higher than that of unconjugated one.

3.4.2. Products

Products of the reaction of OH with cyclooctane have already been studied in the atmospheric condition, in the presence of NO, along with other cycloalkanes [52], where the presence of the product cyclic hydroxyketone (28% yield) established the occurrence of isomerisation of cyclic alkoxy radicals. In n-alkanes both in presence and absence of NO, it is reported that hydroxycarbonyls, the isomerisation products of alkoxy radicals, are also formed. However, in the absence of NO, the yield is almost an order of magnitude lower [65]. A similar result is expected in the present case also, where NO is absent. Thus the major part of the peroxy radicals is expected to give ketone and alcohol, by disproportionation reaction along with hydroperoxides [65], and a smaller percentage gives an alkoxy radical. This alkoxy radical is further converted to cyclooctanone and the isomerisation to cyclic hydroxyl ketone and dissociation products (Scheme 3.1).

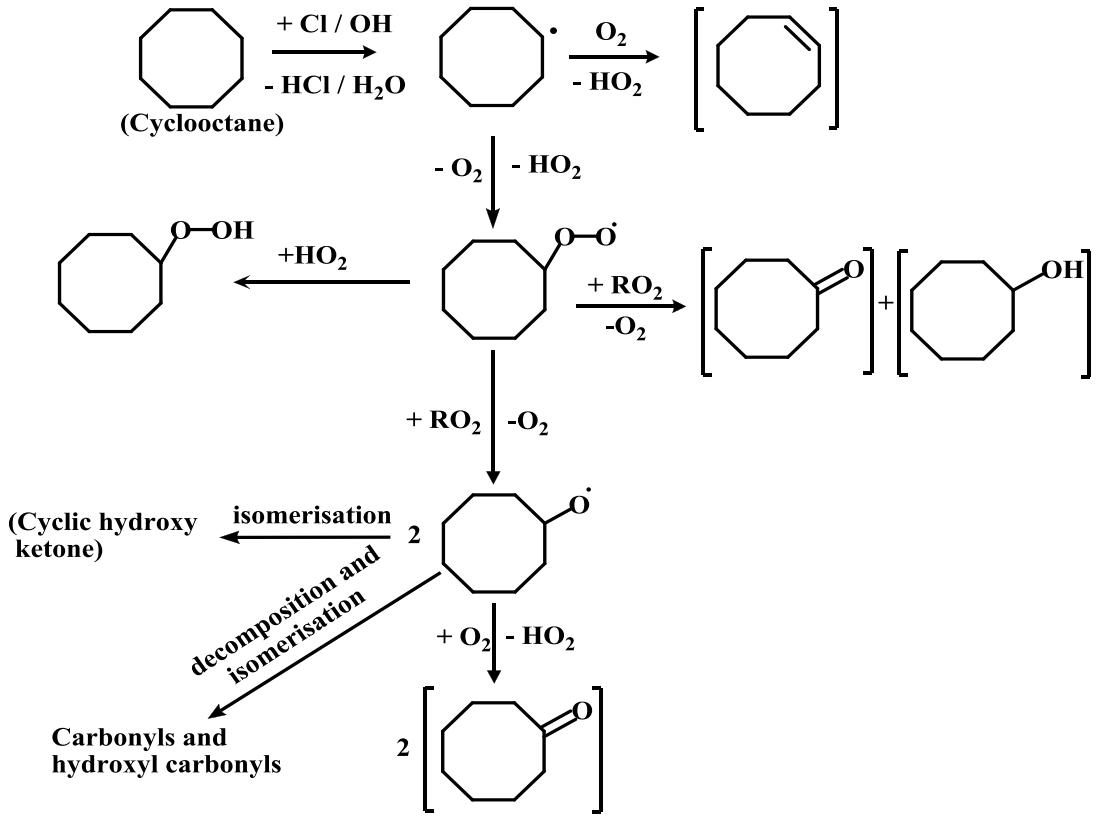

Scheme 3.1: Major reactions during the Cl / OH initiated oxidation of cyclooctane. The products observed here are marked in square brackets.

The lower vapour pressure of cyclooctanol and higher rate coefficient of its reaction with OH (secondary reactions) may be responsible for the lower gas-phase yield of cyclooctanol as compared to cyclooctanone. The additional pathway of cyclooctanone formation via alkoxy radical also may contribute to this. The fact that the products of isomerisation and dissociation of alkoxy radicals could not be observed here is not surprising as these could be observed only with derivatization [52]. It is difficult to detect hydroperoxides also by GC-MS because these are thermally labile. A negligibly small

amount of 4-cycloocten-1-one could have formed as a secondary product of cyclooctene oxidation.

The major reactions of OH and Cl with cis-cyclooctene are summarized in Scheme 3.2. The OH radical reacts mainly by addition with unsaturated molecules, as the rate coefficient of abstraction of H atom is almost two orders of magnitude lower [60]. However, in the case of Cl atom the rate coefficient of abstraction is only about an order of magnitude lower than that of addition, and hence not negligible, and reaction proceeds by both addition and H atom abstraction [13,66]. Aschmann et al. [47] have estimated the abstraction by OH to be 15% in cis-cyclooctene, based on the predicted rate coefficients of the H atom abstraction [61], but almost 50% of reaction with Cl atom is expected to proceed through abstraction reaction, based on the estimated rate coefficients of addition and H atom abstraction from allylic hydrogen atoms by Cl atoms [66]. Thus, some products, formed via abstraction of H atom, are expected to be common in the reactions of OH and Cl with cis-cyclooctene and 1,5-cyclooctadiene. Based on the radical stability, H abstraction from carbon atom at the allyl position is expected to be more, and it is supported recently by Jenkin et al. [48] who have also calculated higher substituent factors (F(X)) for H abstraction reaction of OH adjacent to C=C. Earlier, in the case of 1-alkenes, we have observed alkenols and alkenones, resulting from the abstraction of H atom at all carbon atoms, the one farthest from the double bond being the major one [46]. The product formed by H atom abstraction at allyl carbon was observed, but in spite of higher stability of the allyl radical, that was not the dominant product. It is also possible that the radical formed at allyl position undergoes dissociation, as aldehydes lower by 3 carbon atoms were observed in 1-alkenes. In the present study, both 4-cyclooctene-1-one

and 2-cyclooctene-1-one, which have distinct mass spectra, are observed in the reactions of both OH and Cl with cyclooctene (Fig. 3.5), with the yield of the former being about 3 times that of the latter. This suggests that the abstraction of H atom at the 4^{th} carbon atom from unsaturation dominates, even though the abstraction from 2^{nd} carbon gives a more stabilized allyl radical, as mentioned earlier. The third expected isomer 3-cyclooctene-1 could not be observed in our experiments. Although the mass spectra of 3-cyclooctene-1 are not available, its fragmentation pattern is expected to be different, as in the other two isomers. Thus, the product distribution suggests that the H atom abstraction takes place more efficiently from the carbon atom farthest away from the unsaturation centre. However, it cannot be concluded unambiguously, since secondary reactions (such as dissociation, ring-opening, etc.) involving the radical formed at allyl position can alter the relative yields of the products. In the case of reaction with OH, the ratio of products with the keto group at C4 to C2 appears to be higher. This is not surprising because OH is known to be more selective than the Cl atom. 1,5-cyclooctadiene, observed as a minor product, is another H atom abstraction product (Scheme 3.2A).

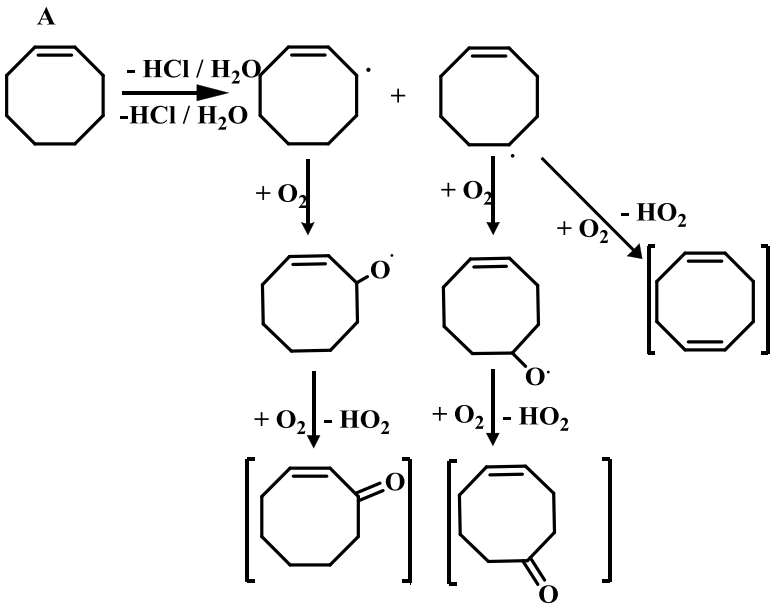
A
- HCl / H2O
-HCl / H2O
+
+ O2
+ O2
- HO2
+ O2
+ O2
- HO2
+ O2
- HO2

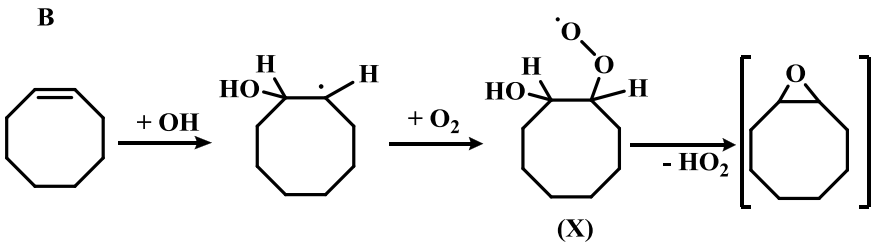
B
+ OH
+ O2
- HO2
(X)

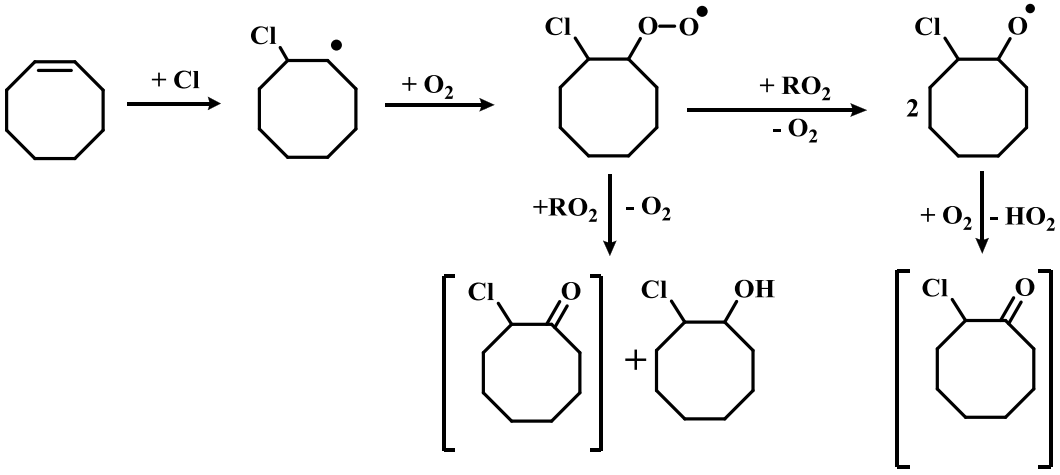
C
+ Cl
+ O2
+ RO2
- O2
2
+RO2
- O2
+ O2
- HO2
+

D

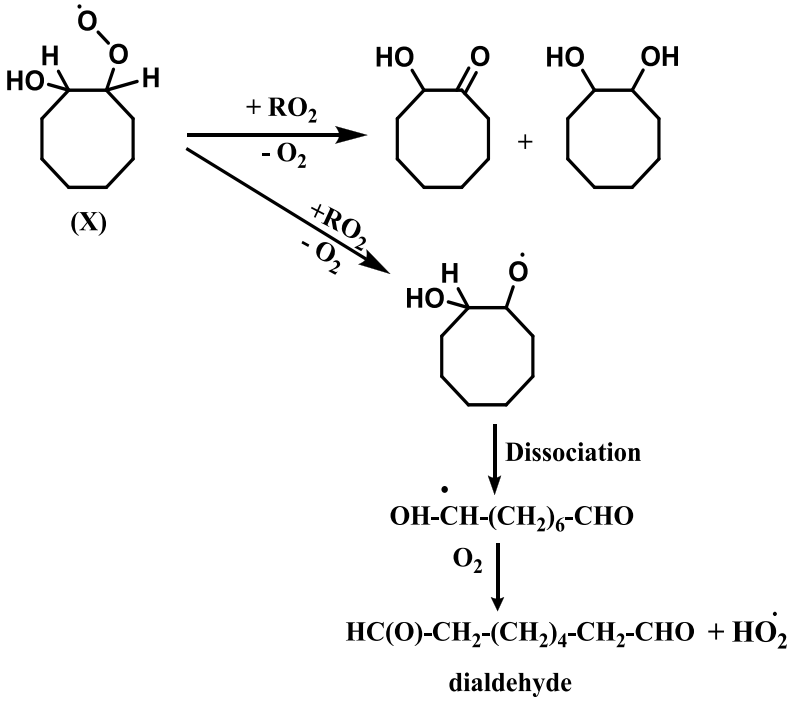

Scheme 3.2: Major reaction pathways during the Cl/OH initiated oxidation of cis-cyclooctene. The products observed in the present studies are marked separately.

The major gaseous product observed in the case of addition reaction of Cl with cis-cyclooctene is 2-chlorocyclooctan-1-one as shown in Scheme 3.2C, which also explains the presence of 2-chlorocyclooctan-1-ol in low yield (20.4 min, Fig. 3.5). In the case of OH reaction, in addition to the products common with Cl reaction, heptanal (9.8 min) and two unknown products at 18.3 and 18.6 min are observed, which could be the addition products. Although the mechanism of heptanal formation in the reaction of O_3 with cis cyclooctene is understood (discussed later), there exists an ambiguity in the formation of heptanal in the case of the reaction of OH with cis cyclooctene. Formation of an aldehyde with one carbon less is not reported earlier in the room temperature

oxidation of cyclopentene / cyclohexene [67] and that of cyclooctene [47]. However, in a recent report on the OH initiated oxidation of cyclic alkene at temperatures around 500 K, such products are reported along with formaldehyde [68]. It is not clear whether such a reaction is responsible for heptanal formation in the present case. The detailed investigation on the reaction of OH with cycloalkenes in the presence of NO reports dicarbonyls, formed by the dissociation of the cyclic hydroxyl peroxy radicals, to be the major addition product [47], apart from the cyclic hydroxynitrate formed by the reaction of the initial radical with NO. Thus, 1,8-octadienal is the expected major product of the reaction of OH with cyclooctene, written as dialdehyde in Scheme 3.2D. However, as in the case of hydroxycarbonyls, derivatization to oximes is needed for observing these products by GC-FID. In the earlier study with 1-methyl-1-cyclohexene [67,69] the corresponding dicarbonyl was observed by GC-FID, but the quantitative analysis underestimated its yield. It was concluded that dicarbonyls are probably not eluted efficiently from these columns, and may be the reason for not observing these major addition products expected from the OH reaction. The MS of the products at 18.3 and 18.6 min (Fig. 3.5), which are likely to be formed via addition reaction, are examined thoroughly. The mass spectrum at 18.3 min does not have any aldehyde related peaks. The observation of epoxy cyclooctane in both OH and Cl reactions is surprising. Meloni et al. [67], while studying oxidation of cyclic alkenes by using photoionization mass spectrometry, suggested epoxy compound as a likely product in their low-temperature oxidation, which could not be experimentally observed due to the high ionization energy. The suggested mechanism [67] is via the addition of OH and peroxidation followed by elimination of HO_2, which may occur in the case of cyclooctene also, as shown in

Scheme 3.2B. It is not clear whether the presence of a significant yield of epoxide in the Cl atom reaction demands another pathway via abstraction reaction. It is also possible that the epoxide is a secondary oxidized product.

In the case of 1,5-cyclooctadiene, the number of gas-phase products and their yields are much lower than those of cyclooctane and cyclooctene (Fig. 3.6). The probable reactions are summarized in Scheme 3.3.

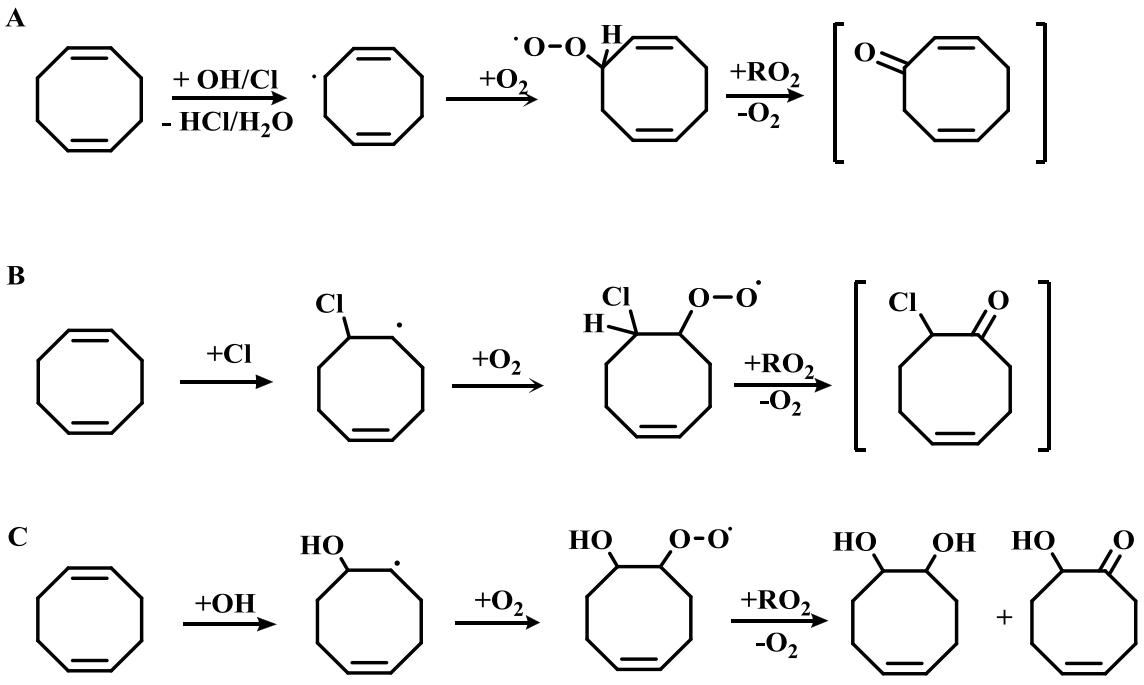

Scheme 3.3: Major reaction pathways in the Cl/OH initiated oxidation of 1,5-cyclooctadiene. The products observed in the present studies are marked in square brackets.

The common product in the reaction of OH and Cl is only 1,5-cyclooctadien-4-one, which is the expected product of H atom abstraction (Scheme 3.3A). The reaction of

OH with 1,4-cyclohexadiene has been studied earlier [67], but there is no such report on cyclooctadienes. Based on the estimated rate coefficients of addition and abstraction [61], the possibility of direct H atom abstraction in the reaction of OH is about 3.6% in 1,5-cyclooctadiene, whereas it is negligibly small in 1,4-cyclohexadiene (0.1%). In the case of the reaction of Cl, the possibility of H atom abstraction is about 27% in 1,4-cyclooctadiene [66]. Although the formation of unsaturated products and other products is shown together as an abstraction pathway in scheme 3A, it may involve the addition-elimination pathway as well, especially in the case of reactions with OH. In the case of 1,4-cyclohexadiene, photoionisation experiments suggested two isomers of cyclohexadienols, cyclohexen-3-one and ring opened linear hexadienals as products [67] of reaction with OH. Cyclohexadienols are considered to be formed by the addition of OH followed by H atom elimination. In the present study with 1,5-cyclooctadiene, equivalent unsaturated products observed in the gas phase are dienones, not dienols. In the case of reaction with Cl, where the product yield is higher, there is an indication of the presence of epoxy cyclooctene at a retention time of 11.26 min (Fig. 3.6). The major addition product of reaction with Cl is 8-chlorocyclooct-5-ene-1-one, (Scheme 3.3B) with minor unidentified products at 15 and 17 min (Fig. 3.6). The radical formed after addition of OH is expected to give hydroxyketone and diol as shown in Scheme 3.3C. 5-cyclooctene-1,2-dione may be formed as a secondary product from these molecules. Like in the case of cis-cyclooctene, it is possible that most of the hydroxycarbonyls and dials that could have formed, may not be observable in our study without derivatization.

The reaction of ozone with unsaturated cyclic molecules is well studied. Ozone adds across the carbon-carbon double of an alkene to form an ozonide (1,2,4-trioxolane),

which decomposes to produce a carbonyl compound (RR'CO) and a carbonyloxide intermediate (known as a Criegee intermediate). Schematically this is shown in Scheme 3.4.

In general, for the reaction of ozone with unsaturated cyclic molecules, the yield of secondary organic aerosol (SOA) is found to increase with an increasing number of carbon atoms [49]. Prominent products in the SOA are expected to be large dicarboxylic acids or hydroxylated dicarboxylic acids, which are formed by secondary oxidation of aldehydes. The expected major products of the reaction of ozone with cis-cyclooctene and 1,5-cyclooctadiene in the gas phase [70] are aldehydes with one carbon atom less, and dialdehydes with all the 8 carbon atoms, but there is no experimental confirmation. The present study confirms that aldehydes, less by one carbon atom, are formed not only in the cyclic alkenes (heptanal, scheme 3.4 and Fig.3.7), but also in the cyclic diene (4-hepten-1-al, Fig. 3.7).

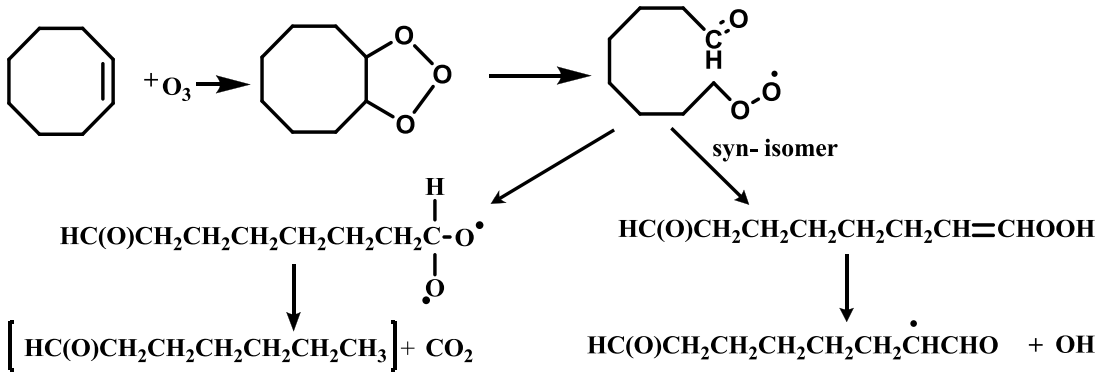

Scheme 3.4: Major reaction pathways in the O_3 initiated oxidation of cis-cyclooctene.

The reaction mechanism involves the formation of primary ozonide, which is converted to a Criegee intermediate, as shown in Scheme 3.4, and dissociates or reacts by

different pathways as shown in the Scheme. This mechanism of heptanal formation is similar to pentanal formation from the reaction of O_3 with cyclohexene [71]. As mentioned earlier in the case of the reaction of OH, the dialdehyde is not observed probably due to the limitation of GC-MS without derivatization. CO_2 is a major product estimated to be 30% in cycloheptene [72]. We have not come across a measurement of yield of CO_2 in the reaction of ozone with cyclic dienes. The observed CO_2 yield of 34% supports the mechanism and suggests the relative importance of the reaction pathways to be very similar to that of the corresponding monoalkenes. Ozonolysis of cyclooctene is also reported to give the OH radical (36%) [73], as shown in the Scheme. A similar yield of OH can be expected in cyclooctene also. Multifunctional hydroxyl carboxyl compounds and carboxylic acids, which are the other expected products of the reaction of ozone, may not be observed in the gas phase [71,72]. The mechanism of the reactions of ozone with cyclic alkenes is given in detail [70,71] and presented in short in Scheme 3.4. Most of the other products observed here appear to be secondary products or products of the reaction of OH with cis-cyclooctene / 1,5-cyclooctadiene.

3.4.3. Atmospheric implications

Based on the rate coefficients determined in the present studies at 298 K, and assuming that the values are not very different from that at 277 K, the tropospheric lifetimes due to each oxidant can be estimated so that the relative importance of various pathways can be compared. The ambient concentration of Cl is 1×10^3 molecules cm^{-3} [74], which is too low and does not influence the degradation of CyOs molecules. So the reaction with Cl is considered to be effective only in the conditions of the marine

boundary layer (MBL). The rate coefficients and tropospheric lifetimes of straight-chain hydrocarbons, n-octane and 1-octene are also included in Table 3.4 for a comparison. From Table 3.4, it can be seen that the reaction of Cl becomes very important in the conditions of MBL for cyclooctane as in the case of n-octane.

Table 3.4: Tropospheric lifetimes (τ) calculated for CyOs with respect to reactions with different tropospheric oxidants. The concentrations used for Cl_{MBL} [15] (under marine boundary layer conditions), OH and O_3 [75] are 1.3×10^5, 2×10^6 and 7×10^{11} molecules cm^{-3}, respectively. All the rate coefficients are in the unit of $cm^3 molecule^{-1} s^{-1}$. The rate coefficients for CyOs are from the present work. For the calculation of net tropospheric lifetime (τ_{net}) in ambient air, reaction with Cl atom is not considered.

Compound	$k_{OH}\times$ 10^{11}	τ_{OH} (h)	$k_{O3}\times$ 10^{17}	τ_{O3} (h)	$\boldsymbol{\tau_{net}}$ **ambient air (h)**	$k_{Cl}\times$ 10^{10}	$\tau_{Cl\text{-}MBL}$ (h)	$\boldsymbol{\tau_{net}}$ **MBL (h)**
cyclooctane	1.4	9.9			9.9	4.5	4.7	3.2
cis-cyclooctene	5.1	2.8	41.1	1.0	0.7	4.7	4.5	0.6
1,5-cyclooctadiene	11.1	1.3	14.4	2.8	0.9	5.2	4.1	0.7
n-octane	0.8[a]	17.2			17.2	3.2[b]	6.7	4.8
1-octene	4.1[c]	3.4	1.3[d]	31.7	3.1	5.5[e]	4.0	1.7

a: [62]; b:[76]; c: [77]; d: [78]; e: [46]

The tropospheric lifetime of cis-cyclooctene is not reduced significantly, as in the case of 1-octene in the MBL. Although the reactions with both OH and ozone are important in cis-cyclooctene and 1,5-cyclooctadiene, the reaction with OH (ozone) dominates in the latter (former). The reactions of both Cl and OH are important in the degradation of cyclooctane in the MBL, and these reactions give almost the same gas-phase products. The importance of relative degradation is based on the assumption that the concentrations of the oxidative species remain constant at different times and locations. However, in practice, there are atmospherically-relevant ranges of concentrations, and different initiation reactions may dominate at different times and locations. In addition, a high concentration of emitted organics would substantially suppress [Cl], because it is not regenerated from the subsequent chemistry.

Even though OH is a major contributor, and the Cl atom does not contribute to the degradation of cis-cyclooctene and 1,5-cyclooctadiene, some of the observed unsaturated products of their reactions with Cl are also observed in the reactions with OH. So it is important to understand the mechanism of the formation of these products in detail.

3.5. Conclusions

The rate coefficients of reactions of major atmospheric oxidants, OH, ozone and Cl with cyclooctane, cis-cyclooctene and 1,5-cyclooctadiene are measured at room temperature (298 K). The experimental rate coefficients of reactions of Cl with cis-cyclooctene and that of OH with 1,5-cyclooctadiene are being reported for the first time. All the other values are in good agreement with the earlier reported values. The reported rate coefficients values indicate that the reaction with Cl atom contributes more than that with OH to the atmospheric degradation of cyclooctane in the conditions of the marine

boundary layer. In cis-cyclooctene and 1,5-cyclooctadiene, the reactions with both OH and ozone are relevant channels of degradation, the ozone channel being more effective in the former and the OH channel in the latter. Although all the stable products in the reaction of Cl as well as OH, with cis-cyclooctene and 1,5-cyclooctadiene, could not be identified, those observed in the gas phase show the presence of unsaturated cyclic ketones among other products. This result is similar to our earlier observation in the case of 1-alkenes, and emphasizes the importance of H atom abstraction, though the major channel of reaction is addition. Among the abstraction products, the one with oxidation at a carbon centre farthest away from the double bond is found to dominate as compared to that at an allyl position, very similar to what was observed in 1-alkenes. Surprisingly, similar products are observed in the reaction with OH also, which could be formed by addition elimination reaction, because direct H atom abstraction is expected to be negligible in the reaction of OH with these molecules, especially 1,5-cyclooctadiene. More gas phase and particulate products, especially the carboxyl products, need to be identified and quantified using derivatization. In addition, the probable influence of surfaces, humidity etc. on the product distribution needs to be investigated for a complete picture on atmospheric implications of the studied hydrocarbons.

Chapter-4

Reactivity Study of 1-Chlorocyclopentene with Tropospheric Oxidants

4.1. Introduction

Organic compounds, particularly halogenated hydrocarbons, play a critical role in the chemistry of the troposphere. Chlorohydrocarbons, like many other volatile organic compounds (VOCs), are released into the atmosphere from biogenic and anthropogenic sources and undergo reactions with highly reactive species, such as OH radicals, O_3, NO_3 (in the nighttime), etc. Chloro compounds are used as intermediates in the synthesis of a vast variety of drugs [79,80] and in the preparation of synthetically important organometallic reagents, like Grignard reagents and Reformatksy adducts. They are also used as solvents and in cleaning applications, such as degreasing and dry-cleaning. It is well established that oxidation reactions of unsaturated hydrocarbons with the above oxidative species play a major role in the tropospheric photochemistry and generation of aerosols [81,82]. Previous studies have shown that, for many organic molecules, reactions with Cl atoms are also important in the troposphere, due to higher rate coefficients of their reactions [57]. The reactions of Cl atoms with VOCs are suggested to play an important role in the atmospheric chemistry of the remote marine boundary layer [15], as well as the polluted urban areas with significant anthropogenic emission of Cl_2 [83]. A recent field study suggests that the role of the reactions of Cl atoms in polluted non-coastal areas may be more significant than what was thought earlier [84]. Hence, there is considerable interest in measuring the rate coefficients of the reactions of different VOCs, including unsaturated molecules, with Cl atoms in addition to OH and O_3 [8]. Recently,

the rate coefficients of the reactions of Cl atoms with cyclic alkenes, namely, cyclopentene, cyclohexene and cycloheptene, were measured in our laboratory and observed an increase in the rate coefficient with the number of carbon atoms in the ring [85]. This was attributed to the increase in the number of abstractable hydrogen atoms. In our earlier experiments of cyclic alkenes and cyclic-dienes, it was observed that the rate coefficients in the presence of air were marginally higher than N_2, indicating OH generation in the presence of air [13,85]. But in the case of acyclic alkenes, this effect was not observed [46].

In the present study, the reactions of 1-chlorocyclopentene with Cl, OH, and O_3 at 298 K and 1 atmosphere pressure are investigated, using the relative rate method, to further understand the effect of heteroatom (chlorine) and air on the reactivity. Not much work is reported on the reaction of 1-chlorocyclopentene with the atmospheric oxidants. The only report available is the determination of the rate coefficient for its reaction with O_3 [86]. In addition to the rate coefficients (k_{Cl}, k_{OH}, and k_{O3}), the stable products formed in the above reactions are characterized using Gas Chromatography-Mass Spectrometry (GC-MS) technique. Further, the temperature dependent rate coefficients for the reaction of 1-chlorocyclopentene with OH radical are also measured experimentally over the temperature range of 262 to 335 K and at the total pressure of 30 Torr using LP-LIF technique, to obtain the activation energy and the Arrhenius frequency factor. Along with these experimental studies, preliminary theoretical calculations are also carried out to understand the reaction mechanism of H atom abstraction and addition of Cl atom to the double bond. The tropospheric lifetime, and the global warming potential (GWP), and ozone depletion potential (ODP) for 1-chlorocyclopentene are estimated. An attempt is

also made to understand the reactivity trend due to presence of heteroatom (chlorine) with 1-cyclopentene and similar cyclic molecules.

4.2. Experimental

4.2.1. Relative rate coefficient measurement using GC technique

The relative rate coefficient measurement for the reactions of 1-chlorocyclopentene with tropospheric oxidants is described in detail in chapter two. A Quartz reaction chamber (3 L volume), fitted with vacuum stopcocks and a sealed port, is used to carry out the reactions. The experiments are performed at room temperature (298 $\pm$ 2 K). The OH radicals and Cl atoms are generated *in situ* by photolysis of H_2O_2 and oxalyl chloride $(COCl)_2$, respectively, by a UV lamp (Rayonett) at 254 nm. The reaction with O_3 is carried out using O_3/O_2 mixture stored in a glass bulb, and it is added intermittently using a syringe. The reaction mixture, consisting of 1-chlorocyclopentene (100-200 ppm), reference compound (50-100 ppm) and oxalyl chloride (typically ~ 400 ppm), is prepared in the reaction chamber, using a vacuum manifold, and the total pressure is maintained at (800 $\pm$ 3) Torr by adding N_2 /air (buffer gas). In case of the reaction of 1-chlorocyclopentene with O_3, OH is also generated [35,87], and hence, cyclohexane (~20000 ppm) is also filled in the reaction chamber to scavenge OH. The pressure is measured, using a capacitance manometer (Pfeiffer Vacuum). Before the photolysis, the prepared reaction mixture is allowed to get equilibrated by keeping it for 60 - 80 min for uniform distribution, and the same is confirmed by the reproducibility of the gas chromatogram. The stability of the reaction mixture with respect to the wall losses and dark reactions is checked for about 7 hours, which is more than the total duration of a

relative rate measurement. Non-interference of any reaction product of 1-chlorocyclopentene and that of reference with oxidant in the GC analysis is also checked independently. For the kinetic measurement, the prepared reaction mixture is photolyzed for a period of 5 - 6 minutes, in steps of about 1 min, and after each photolysis step, the decrease in the concentration of 1-chlorocyclopentene (CCP) and the reference molecule (R) are determined, using Gas Chromatograph (Shimadzu GC 2014, 5% SE 30 column, flame ionization detector). Using the relative rate method, assuming that both the molecules react only with oxidants, the kinetic data are obtained by plotting the fractional loss of 1-chlorocyclopentene and R, according to relative rate equation (4.3),

$$CCP + X\ (Cl/OH/O_3) \rightarrow \text{Products} \qquad (k_{ccp}) \qquad (4.1)$$

$$\text{Reference} + X\ (Cl/OH/O_3) \rightarrow \text{Products} \qquad (k_R) \qquad (4.2)$$

$$\ln\left(\frac{[CCP]_{t0}}{[CCP]_t}\right) = \left(\frac{k_{CCP}}{k_R}\right)\ln\left(\frac{[R]_{t0}}{[R]_t}\right) \qquad (4.3)$$

where, $[R]_{to}$ and $[CCP]_{to}$ are the concentrations of R and CCP, respectively, at time t_0, $[R]_t$ and $[CCP]_t$ are the corresponding concentrations at time t, and k_{CCP} and k_R are the rate coefficients of their reactions with oxidant (X). The linearity of the plot and zero intercept ensure the absence of complications due to any secondary reaction. In the present study, butane, cyclopentene and 1-butene, for which the rate coefficients are well reported, are found to be suitable reference compounds based on the similarity of the rate coefficients and the minimum GC interference.

1-chlorocyclopentene (97%), cyclopentene (>95%) and cyclohexane (97%) are from Sigma Aldrich, whereas H_2O_2 (50 wt %), butane (>99%) and 1-butene (>99%) are

used from Matheson. All the reagents are subjected to freeze-pump-thaw cycles, before use. Nitrogen gas (99.9 % purity), from INOX Air Products Ltd, Mumbai, India, and zero grade air from Chemtron Science Laboratories, Mumbai, India are used.

4.2.2. Absolute rate coefficient measurement using LP-LIF technique

The rate coefficient for the reaction of 1-chlorocyclopentene with OH is measured using LP-LIF technique. This method is based on the measurement of the rate of OH decay in the absence and presence of a known excess concentration of 1-chlorocyclopentene. The hydroxyl radicals are generated *in situ* by photolysis of H_2O_2 at 248 nm using KrF excimer laser, and are monitored by collecting the resulting fluorescence after exciting the $P_1(2)$ line in the (0,0) band of the ($A^2\Sigma$, $v'=0$) ← ($X^2\Pi$, $v''=0$) transition at 308 nm using a tunable dye laser. The experimental details of the LP-LIF set-up are given in Chapter 2. Briefly, the temporal profile of OH concentration is followed by varying the time delay between the pump and the probe laser pulses from 10 μs to 10 ms, in steps of a few microseconds, with the help of a delay generator.

In the initial blank experiments, known flow rates of H_2O_2 seeded in N_2, and N_2 buffer are flowed using MFC into the reaction cell through, the premix chamber, without 1-chlorocyclopentene and the OH decay kinetic is measured, in the pump-probe experiments. Subsequently, the flow rate of buffer gas N_2 is reduced by the desired quantity and the same quantity of 1-chlorocyclopentene sample prepared in N_2 flow into the reaction cell. In the cell, the H_2O_2 concentration is kept constant by maintaining a fixed flow of N_2 through H_2O_2 bubbler. The total pressure in the reaction cell is also maintained constant (~ 30 Torr) by keeping the sum of the flow of 1-chlorocyclopentene

in N_2 and N_2 buffer gas constant. The H_2O_2 number density in the reaction cell is ~1×10^{14} molecules cm^{-3}. Using the laser fluence and the absorption cross-section of H_2O_2, the OH radical concentration in the cell is calculated to be 10^{10} to 10^{12} molecules cm^{-3}. A pseudo-first order condition is maintained with [CCP]>>[OH] and the number density of 1-chlorocyclopentene in the reaction volume is calculated from the flow rate and the total pressure in the cell for each experiment. It is re-confirmed by analysis of outlet of the reaction cell by FTIR spectrometer.

The pseudo-first order rate coefficient values are measured experimentally over the temperature range of 262 to 335 K for the different number density of 1-chlorocyclopentene for determining bimolecular rate coefficient at various temperatures.

4.2.3. IR absorption cross section and GWP calculation

The IR absorption spectra of 1-chlorocyclopentene are measured by using an FTIR spectrometer with a spectral resolution of 0.1 cm^{-1}, employing a liquid-nitrogen-cooled wide range MCT detector. A known pressure of 1-chlorocyclopentene is taken in the cell and the total pressure is made up to 760 Torr with nitrogen as a buffer gas. Absorption spectra of 1-chlorocyclopentene are recorded at different pressures in the linear absorption region, and are converted into absorption cross-sections on the Y-axis employing the relation,

$$\sigma(\nu) = \frac{\ln(10)\times A_{CCP}(\nu)}{[CCP]\times l} \qquad (4.4)$$

where σ (ν) is the absorption cross-section at wavenumber ν, in units of cm^2 $molecule^{-1}$; A_{CCP} (ν) is the absorbance of 1-chlorocyclopentene at wavenumber ν, [CCP] is the molecular concentration in molecules cm^{-3} of 1-chlorocyclopentene, and l is the optical

path length (28 cm). From the above data of absorption cross-sections, the integrated absorption cross-sections at 1 cm^{-1} band interval are calculated and assigned to the centre of each band. Thus, all the absorption spectra obtained at various pressures of a compound maintaining the total pressure of ~760 Torr are converted into absorption cross-section spectra, and the mean value of integrated cross-section at 1 cm^{-1} band interval is obtained in a wavelength range of 400-2500 cm^{-1}. These values are employed for the radiative efficiency calculation, using a modified Pinnock curve [36] incorporating the Oslo Line-By-Line model, the latter takes into account atmospheres representing the tropics and extra-tropics.

4.2.4. Stable products analysis

The products of the reaction of 1-chlorocyclopentene with Cl/OH/O_3, formed in the presence of air at atmospheric pressure, are characterized by a GC-MS, using HT8 column (30m × 0.25mm × 0.25μm) and CP WAX 52CB (30m × 0.25 mm × 0.25 μm) columns, independently. The observed spectral features of the products are compared with the reported mass spectra for identification.

4.3. Results

4.3.1. Determination of the rate coefficients of 1-chlorocyclopentene

Experiments are carried out ensuring the criteria required for employing the relative rate method for determination of the rate coefficients of the reaction are met [85]. To rule out any decrease in concentration due to direct photolysis of 1-chlorocyclopentene and reference (R) molecules, the photolysis experiments are carried out in the prepared sample of these compounds in N_2, at 760 Torr total pressure for about

8 minutes, in steps of 1 min, as in the actual measurements. There is no decrease in the concentration of 1-chlorocyclopentene, butane, cyclopentene and 1-butene, in the above experiments, which confirmed the absence of any significant loss due to direct photolysis. Reactions of butane, cyclopentene and 1-butene and the 1-chlorocyclopentene with $Cl/OH/O_3$ are also individually monitored, using GC, to see if any product build-up occurs which interferes with the analysis.

4.3.1.1. Reaction with Cl

The experimental results, the fractional loss of 1-chlorocyclopentene versus the fractional loss of the reference molecules (1-butene, cyclopentene, and n-butane) due to their reactions with Cl atoms, are shown in Fig. 4.1, in N_2 as well as in an air environment. The plots correspond to Eqn. (4.3).

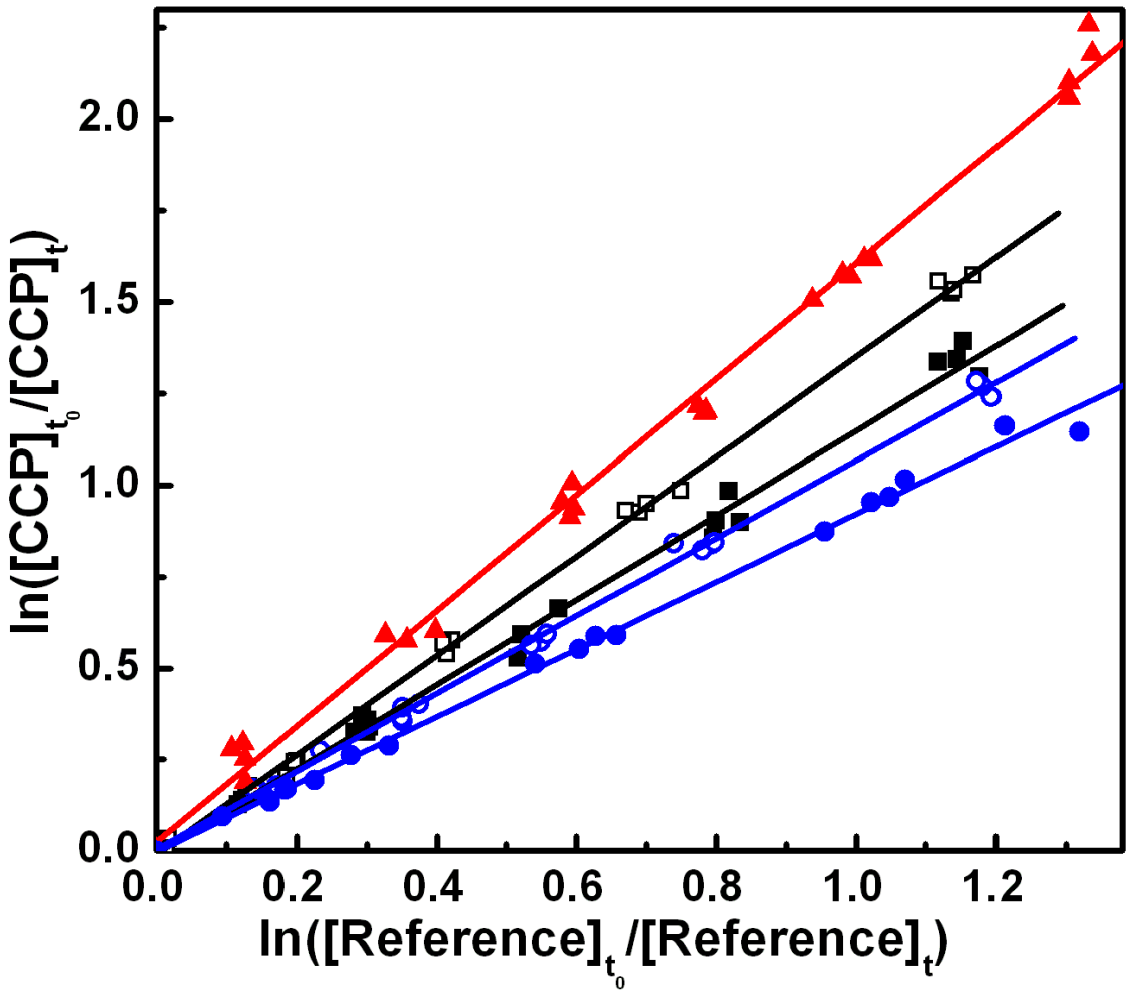

Fig. 4.1. The plots of the fractional decrease in the concentration of 1-chlorocyclopentene against that of a reference compound due to their reaction with Cl atoms. Reference compounds are butane (■), cyclopentene (●) and butane (▲), in N_2; and butene (□) and cyclopentene (○) in the air; total pressure: 800 Torr.

From the linear least-square fit, the slopes of the linear plots are obtained, which are the ratios of the rate coefficients of 1-chlorocyclopentene to that of the reference molecule. The experiments are repeated 3-5 times, and the slopes obtained are given in Table 4.1.

Table 4.1: Relative ratios and rate coefficients of the reactions of Cl/OH/O_3 with 1-chlorocyclopentene with different reference molecules, [1-chlorocyclopentene] = 100 - 150 ppm, [R] = 50 – 100 ppm, buffer gas - N_2 and air. Total pressure = 800 Torr for relative rate method (RRM) and 30 Torr for absolute rate method. Numbers in parentheses under the buffer gas column represent the number of times the experiments are repeated.

Oxidant	**Reference molecule**	**Buffer gas**	**Average slope**	**Rate coefficient k_{298} ($cm^3 molecule^{-1} s^{-1}$)**	**Method**
Cl	1-butene	N_2(5)	1.22 ± 0.07	(3.92 ± 0.53) × 10^{-10}	RRM
		Air (3)	1.35 ± 0.04	(4.33 ± 0.55) × 10^{-10}	
	Cyclopentene	N_2 (4)	0.99 ± 0.03	(3.36 ± 1.07) × 10^{-10}	
		Air (2)	1.06 ± 0.03	(3.59 ± 1.15) × 10^{-10}	
	n-Butane	N_2 (5)	1.59 ± 0.07	(3.26± 0.42) × 10^{-10}	
				(3.51 ± 1.26) × 10^{-10} (average)	
OH	1-butene	N_2(5)	1.86 ± 0.23	(5.77 ± 0.77) × 10^{-11}	RRM
	Cyclopentene	N_2(5)	0.92 ± 0.10	(6.17 ± 0.74) × 10^{-11}	
				(5.97 ± 1.08) × 10^{-11} (average)	
		N_2 (3)		**(**5.76 ± 0.55**)** × **10^{-11}**	ABSOLUTE
O_3	1-butene	N_2(5)	1.56 ± 0.14	**(1.50 ± 0.19)** × **10^{-17}**	RRM

				$(1.50 \pm 0.10) \times 10^{-17}$ **[86]**	

To see the effect of O_2 on the rate coefficients, the experiments are also carried out in the presence of air, taking 1-butene and cyclopentene as reference compounds; the typical plots are shown in Fig. 4.1. Results show a small increase of about 9% in the average slope in the presence of air (Table 4.1), suggesting some additional reactions in this condition as observed in cyclic-dienes [13], and cyclic alkenes [85]. But this effect of enhanced rate coefficient in air was not observed in case of straight chain 1-alkenes [46]. The rate coefficients for the reaction of Cl atom at 298 K with reference molecules 1-butene, n-butane, and cyclopentene used here are $(3.21 \pm 0.41) \times 10^{-10}$, $(2.05 \pm 0.25) \times 10^{-10}$ [13] and $(3.39 \pm 1.08) \times 10^{-10}$ [85] cm^3 $molecule^{-1}$ s^{-1}, respectively. The given values of average slopes are calculated from a number of measurements, the error in the average slope is calculated by error propagation formula taking individual error in the slope value for five experiments. Using the calculated slope values, the rate coefficient for the reaction of 1-chlorocyclopentene with Cl in N_2 is $(3.92 \pm 0.53) \times 10^{-10}$, $(3.36 \pm 1.07) \times 10^{-10}$ and $(3.26 \pm 0.42) \times 10^{-10}$ cm^3 $molecule^{-1}$ s^{-1} using 1-butene, cyclopentene and butane as reference molecules, respectively, with quoted error, including the error in the reported rate coefficient of the reference molecule reaction. Thus, the average rate coefficients of 1-chlorocyclopentene with Cl in N_2 and air atmosphere are respectively $(3.51 \pm 1.26) \times 10^{-10}$ and $(3.96 \pm 1.27) \times 10^{-10}$ cm^3 $molecule^{-1}$ s^{-1}, the latter being about 13% greater.

4.3.1.2. Reaction with OH

In case of 1-chlorocyclopentene reactions with the OH radicals, the latter are generated by photolysis of H_2O_2 at 254 nm. The plots of fractional decrease in the

concentration of 1-chlorocyclopentene versus that of reference molecules are shown in Fig. 4.2.

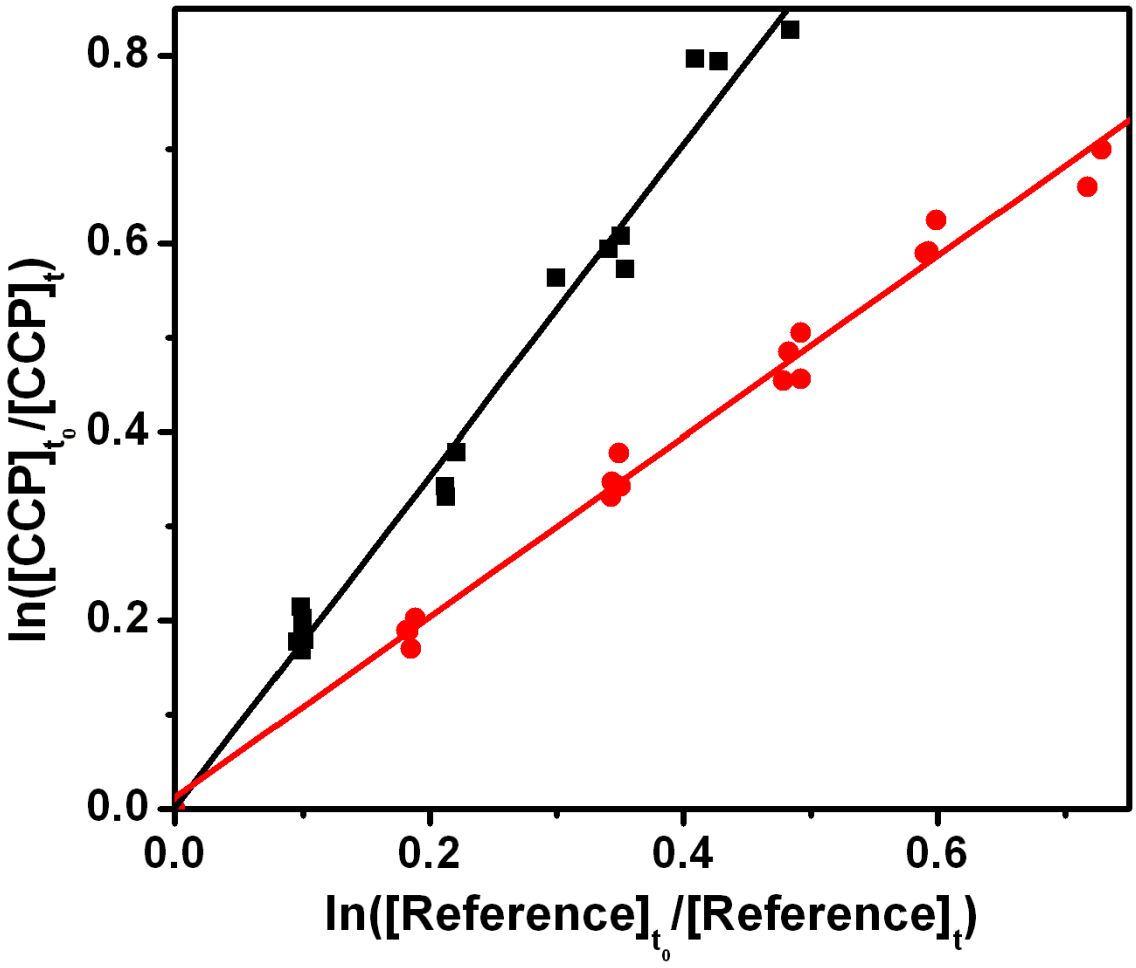

Fig. 4.2. The figure shows plots of the fractional decrease in the concentration of 1-chlorocyclopentene versus that of the reference compound due to reaction with OH; the reference compounds used are butane (■) and cyclopentene (●) in N_2, total pressure 800 Torr.

The rate coefficients for the reactions of OH at 298 K with reference compounds, 1-butene and cyclopentene, used here are $(3.15 \pm 0.57) \times 10^{-11}$ and $(6.70 \pm 1.34) \times 10^{-11}$ [88] molecule^{-1} cm^3 s^{-1}, respectively. The measured rate coefficient for the reaction of 1-

chlorocyclopentene with OH is (5.77 ± 0.77) × 10^{-11} and (6.17 ± 0.74) × 10^{-11} cm^3 $molecule^{-1}$ s^{-1} using 1-butene and cyclopentene, respectively.

Rate coefficient measurement using absolute method

The temperature dependent rate coefficients for the reaction of 1-chlorocyclopentene with the OH radical are measured experimentally over the temperature range of 262 to 335 K and at the total pressure of 30 Torr using LP-LIF technique. The OH radicals are generated in the reaction cell by photolysis of H_2O_2 at 248 nm (Eqn. 4.5), using KrF laser (20 Hz) and are probed by LIF technique using a dye laser to excite the $P_1(2)$ line of the (0,0) band of the ($A^2\Sigma^+ \leftarrow X^2\Pi$) transition. The total fluorescence intensity, which is proportional to the concentration of the OH radicals, decreases with time because of its reaction with H_2O_2, 1-chlorocyclopentene, in addition to diffusion from the detection zone (Eqn. 4.6-4.8). Therefore, the time dependent decay can be represented by the rate law, given in Eqn. 4.9.

$$H_2O_2 + h\nu\ (\lambda=248\ nm) \rightarrow 2OH \qquad (4.5)$$

$$OH + H_2O_2 \rightarrow HO_2 + H_2O \qquad (k_2) \qquad (4.6)$$

$$OH \rightarrow \text{diffusion out of the detection zone} \qquad (k_3) \qquad (4.7)$$

$$OH + \text{1-chlorocyclopentene} \rightarrow \text{product} + H_2O \qquad (k) \qquad (4.8)$$

$$-d[OH]/dt = [OH]\,(k_2[H_2O_2] + k_3 + k\,[\text{1-chlorocyclopentene}]) \qquad (4.9)$$

Since, $[H_2O_2] >> [OH]$ and the diffusion rate remained almost constant during the decay of OH as the flow velocity of the reaction mixture and the total pressure of the reaction cell are kept constant, the concentration of OH radicals at any time, $[OH]_t$, is given by the first-order kinetics Eqn. 4.10,

$$-d[OH]/dt = [OH] (k' + k [1\text{-chlorocyclopentene}]) \quad (4.10)$$

where $k' = k_2[H_2O_2] + k_3$, and stands for the rate coefficient for the loss of OH radicals due to reaction with H_2O_2 molecules, diffusion from the detection zone and any other reaction, except for the reaction with the sample. Since [OH]<<[1-chlorocyclopentene], we can write the Eqn. (4.11).

$$k' + k[1\text{-chlorocyclopentene}] = k_I \quad (4.11)$$

where k_I is the pseudo-first order rate coefficient, and solving the differential Eqn. (4.10) leads to

$$[OH]_t = [OH]_0 \exp [- k_I t] \quad (4.12)$$

Thus, the pseudo-first order rate coefficient (k_I) for decay of the OH radical has the value of the bimolecular rate coefficient k embedded in it (Eqn. 4.11). The value of k_I is obtained, using Eqn. (4.12), from the linear least square fit of the fluorescence intensity in the logarithmic scale with time (shown in Fig. 4.3).

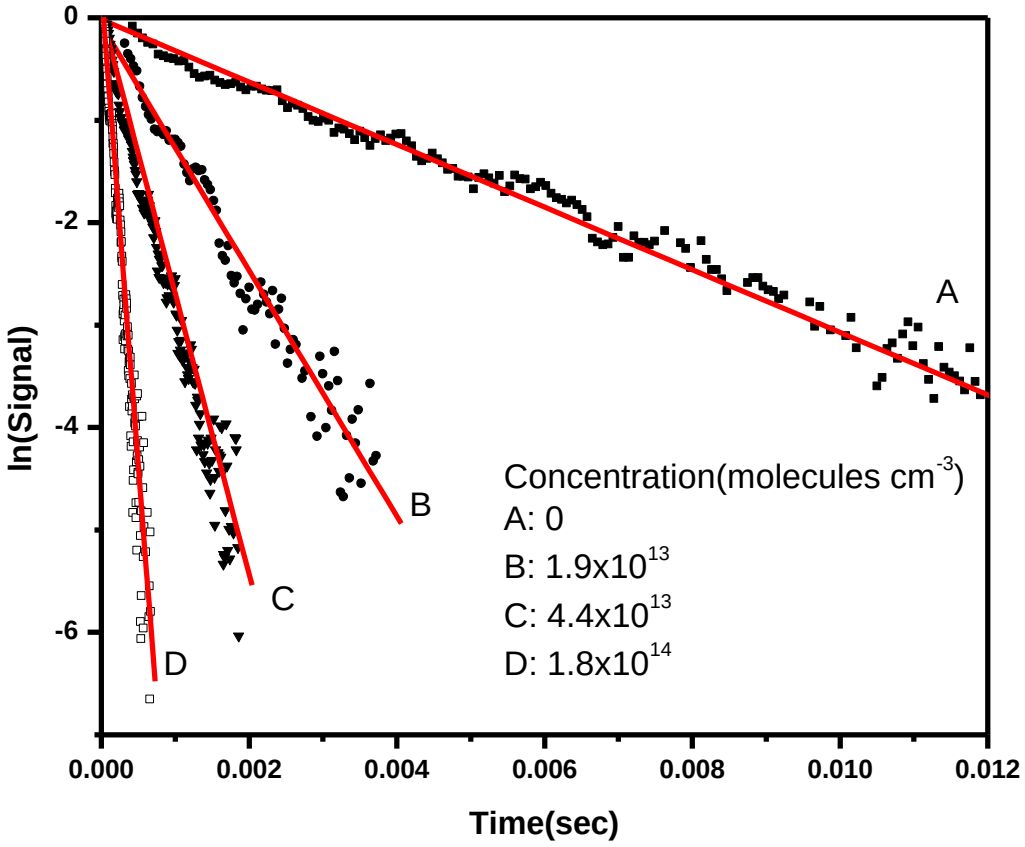

Fig. 4.3. The measured OH radical decay profiles at 298 K, with increasing concentration of CCP for various curves: A = 0; B = 1.9 × 10^{13}; C = 4.4 × 10^{13}; and D = 1.8 × 10^{14} molecules cm^{-3}.

At each concentration of 1-chlorocyclopentene, at least 3 measurements are taken for reproducibility. The exponential fitting gives quite low error (5%). The linear dependence of k_I on the concentration of 1-chlorocyclopentene, indicates that the reactions of OH + H_2O_2, OH + OH, OH + products or any other secondary reaction do not interfere with the measurements. The values of k_I, obtained at different concentrations of 1-chlorocyclopentene at a particular temperature T, are plotted against [1-

chlorocyclopentene], following Eqn. (4.11), to obtain the required value of the bimolecular rate coefficients k as shown in Fig. 4.4.

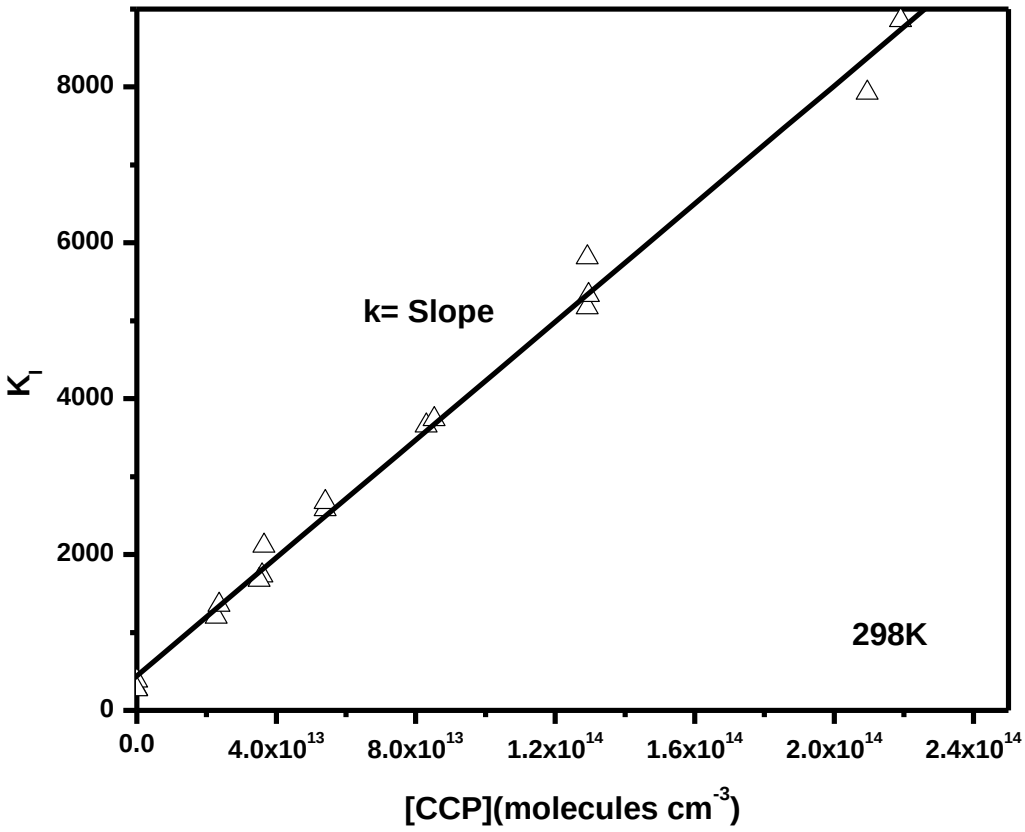

Fig. 4.4. Variation of the k_I with concentration of sample with slope corresponding to bimolecular rate coefficient.

The slope of the linear graph gives the value of k for the reaction of the OH radical with 1-chlorocyclopentene at that temperature. The measured bimolecular rate coefficient for reaction (Eqn. 4.8) at room temperature, k (298K), is $(5.76 \pm 0.55) \times 10^{-11}$ cm^3 $molecule^{-1}$ s^{-1}. Similarly, k values at different temperatures are obtained. Fig. 4.5

shows the plot of k_I against concentrations of 1-chlorocyclopentene at different temperatures, in the range of 262 to 335 K.

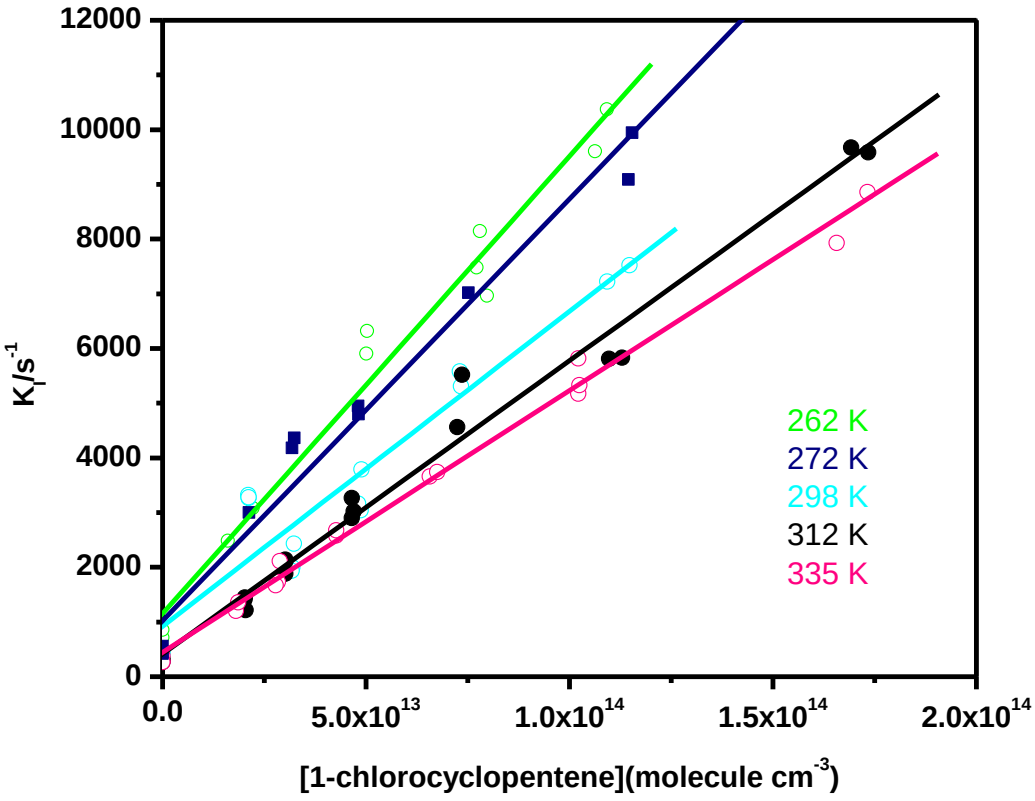

Fig. 4.5. Dependence of the pseudo-first order decay constant (k_I) on the concentration of 1-chlorocyclopentene at different temperatures. The bimolecular rate coefficient k (T) is determined from slope of the line.

The values of the bimolecular coefficient (k (T)) at different temperatures are given in Table 4.2. The quoted errors given above correspond to 2σ of the linear regression and do not include any systematic errors. Any error introduced in the measured rate coefficients from secondary reactions involving photolysis products of 1-chlorocyclopentene is insignificant as measured by Gas Chromatography. The Arrhenius

plot, where ln(k(T)) is plotted against inverse of temperature (according to Eqn. 4.13), is shown in Fig. 4.6.

$$lnk = lnA - \frac{E_a}{RT} \tag{4.13}$$

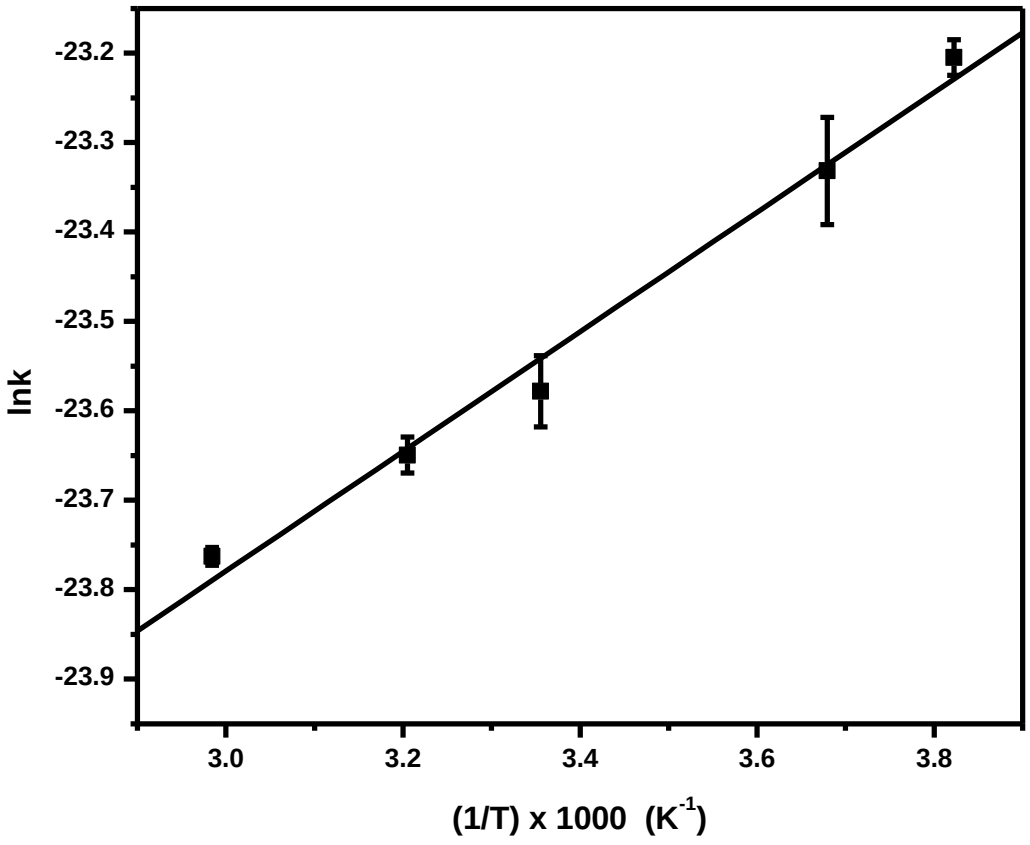

Fig. 4.6. Arrhenius plot of the average value of rate coefficient k (T) of the reaction of 1-chlorocyclopentene molecule with OH radicals.

From the temperature dependence of k (T), the activation energy is determined. The plot shows negative temperature dependence. From the linear regression of this plot, E_a/R and A-factor are found to be (669 ± 45) K and (6.32 ± 0.46) × 10^{-12} $cm^3molecule^{-1}s^-$

[1], respectively. The errors quoted here are 2 σ of the linear regression. The Arrhenius expression for the measured data is given by Eqn. (4.14).

$$k = (6.32 \pm 1.16) \times 10^{-12} \exp((669 \pm 45)/T)\ cm^3 molecules^{-1} s^{-1} \quad (4.14)$$

Table 4.2: The rate coefficient data for the reaction of the OH radicals with CCP at different temperatures at 30 Torr.

Temperature (^{0}K)	**[CCP]/10^{13} (molecules cm^{-3})**	**k/10^{-11} (cm^3 molecules^{-1} s^{-1})**
262	1.0–8.0	8.36 ± 0.43
272	2.0–17.0	7.38 ± 0.94
298	2.0–11.0	5.76 ± 0.55
312	2.0–19.0	5.36 ± 0.18
335	2.0–21.0	4.79 ± 0.09

The measured room temperature rate coefficient k_{OH} is (5.76 ± 0.55) × 10^{-11} cm^3 molecule^{-1}s^{-1}, which is in reasonably good agreement with that by the relative rate method. The observation of negative activation energy suggests the presence of a pre-reactive complex in the reaction pathway.

4.3.1.3. Reaction with O_3

In case of reaction of 1-chlorocyclopentene with O_3, the latter is added stepwise to mixtures containing 1-chlorocyclopentene, 1-butene and cyclohexane, where 1-butene is used as the reference molecule and cyclohexane with k_{OH} value ~6.97 × 10^{-12} cm^3 molecule^{-1}s^{-1} [8] maintained in excess (100 times, or greater) to scavenge any OH radicals

produced in the reaction of ozone. An electrical discharge in a flow of pure oxygen is used to generate ozone. A representative plot of the relative rate measurement is given in Fig. 4.7.

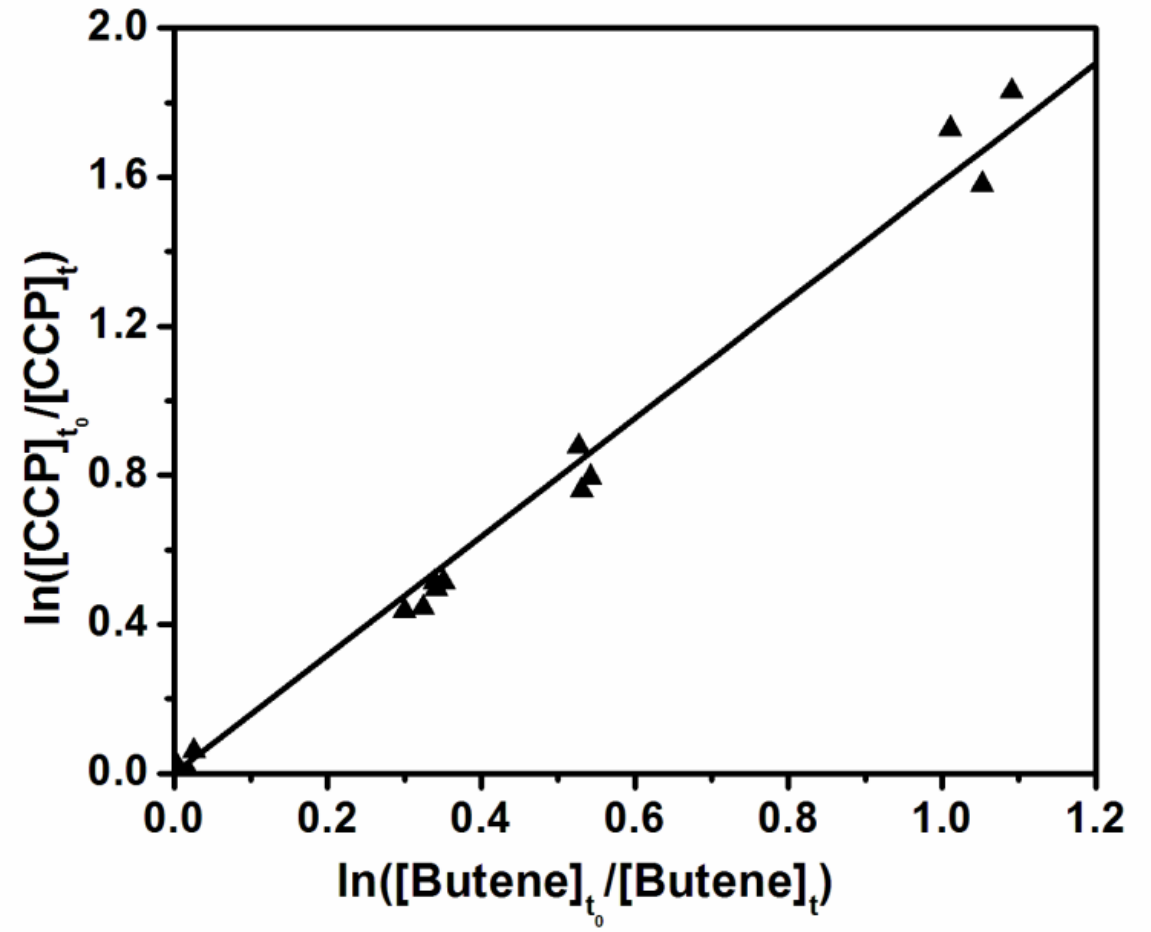

Fig. 4.7. The plot shows a fractional decrease in the concentration of 1-chlorocyclopentene with respect to that of butene in N_2 due to reaction with O_3, total pressure: 800 Torr.

The slope of the plots and the calculated values of k_{O3} are listed in Table 4.1. The IUPAC recommended k_{O3} values, $(9.60 \pm 1.76) \times 10^{-18}$ $cm^3molecule^{-1}s^{-1}$ is considered for

1-butene [89]. The measured rate coefficient for the reaction of 1-chlorocyclopentene with O_3 is $(1.5 \pm 0.19) \times 10^{-17}$ $cm^3 molecule^{-1} s^{-1}$ using 1-butene as a reference molecule.

4.3.2. Stable product analysis of oxidation

The identification of the stable products formed during Cl, OH and O_3 initiated oxidation of 1-chlorocyclopentene in atmospheric conditions is carried out using GC-MS. Different columns, HT8 column (30 m × 0.25 mm × 0.25 μm), CP WAX 52CB (30 m × 0.25 mm × 0.25 μm) and Porapak Q (1m ×1/8 in.), are used for separation of the products with appropriate temperature programming. The identified products are listed in Table 4.3.

Table 4.3: Major products of atmospheric oxidation of 1-chlorocyclopentene by Cl/OH/O_3, characterized by GC-MS. GC columns used for identification of O_3-initiated products are mentioned in the table. Other experimental conditions are given in the text.

Oxidant	**Name of the identified product (Retention time in minute)**
Cl	2-Cyclopenten-1-one (14.2) Acetic acid (15.2) Formic acid (15.7) 3-Chloro-2-cyclopenten-1-one (15.9) Chlorocyclopentanone (16.2) 1-Chloro-3-pentanone (17.1) 2-Chloro-2-cyclopenten-1-one (17.5)

	3-Chloro-3-cyclopenten-1-one (17.6)
OH	2-Chloropropenal (7.07) 2-Cyclopenten-1-one (10.45) 2-Cyclopenten-1-one, 3-chloro (13.04) 2-Chlorocyclopentanone (13.47) Butyrolactone(14.4)
O_3	**Porapak Q column** CO_2 **HT8 column** CO_2 Butanal (1.9) Methanol(2.17) Ethanol(2.62) 2-Chlorocyclopentanone (14.6) Butyrolactone (15.3) Pentanoylchloride (17.6) **CPWAX column** CO_2 2-Chlorocyclopentanone(13.5) Butyrolactone(14.4)

It is worth mentioning about Cl initiated two major products, 2-chlorocyclopentanone and 2-cyclopenten-1-one, as well as three minor products, 3-chloro-2-cyclopentene-1-one, 2-chloro-2-cyclopentene-1-one and 3-chloro-3-cyclopentene-1-one, whose formation could be easily explained theoretically. Among these three minor products (which are isomers), the first two products are produced in almost equal yield, and the third one is the least in the yield. A typical chromatogram of the products of Cl reaction is shown in Fig. 4.8.

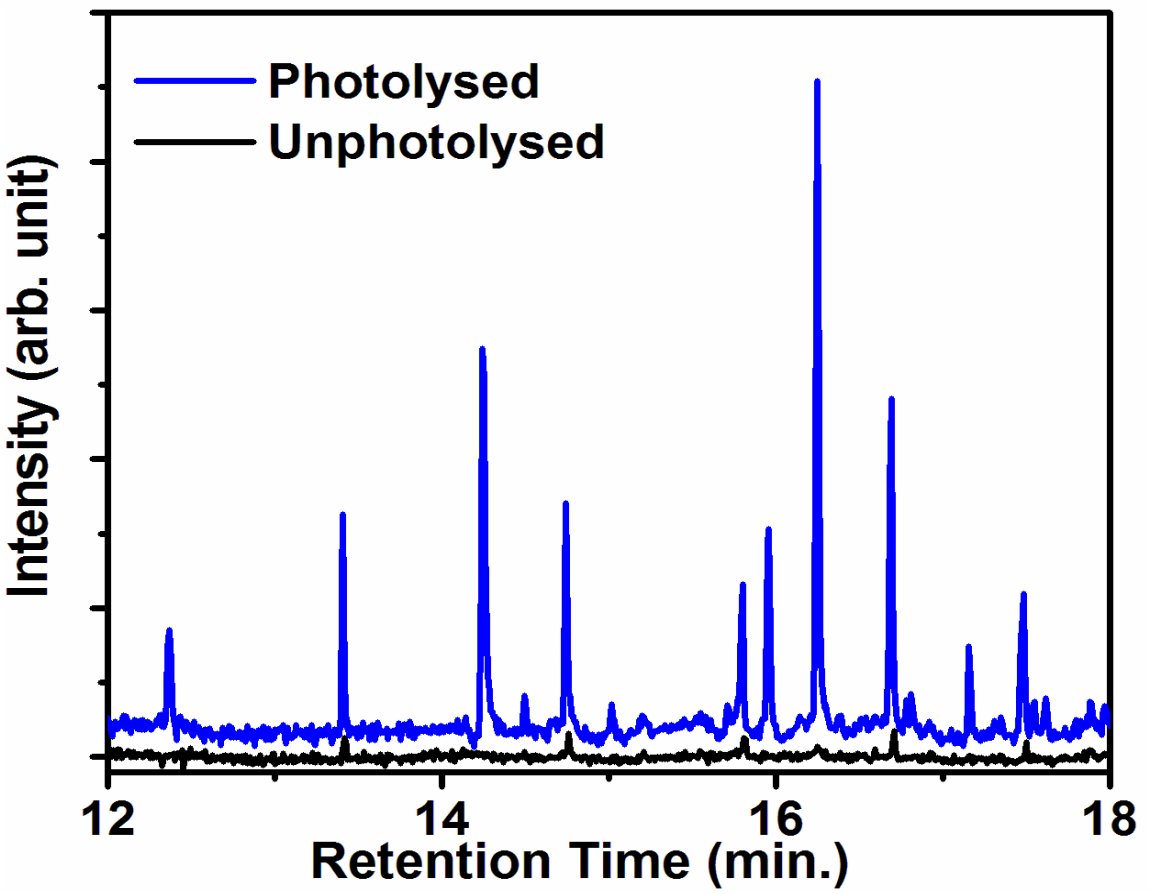

Fig. 4.8. Total ion chromatogram of the products of the reactions of 1-chlorcyclopentene with chlorine atom precursor before (that is, dark reaction with $(COCl)_2$) and after photolysis (that is, reaction with Cl atom).

The analysis of products formed in the reaction in N_2 as well as air as buffer gas, in a cell of 3 L capacity, is carried out to see the difference in yield of products in presence of these gases. Cl reacts with 1-chlorocyclopentene via addition to the C=C bond (at carbon atoms C1 and C2) and abstraction of H atoms (from three carbon atom, C3, C4 and C5). Designation of the carbon atoms of 1-chlorocyclopentene is shown in the reaction Schemes. By comparing the area of the peaks obtained by GC-MS, the addition product is found to be dominant. These results are also supported by theoretical calculations. The yields of the reaction products are not affected in the presence of O_2.

In the case of OH reaction also, similar type of addition and abstraction products are obtained as in Cl initiated oxidation of 1-chlorocyclopentene. In the OH initiated reaction also, both the major products (2-chlorocyclopentanone and 2-cyclopenten-1-one) of the Cl initiated reaction are observed, but only 3-chloro-2-cyclopentene-1-one could be observed as a minor product. In the reaction with O_3, the products due to OH reaction (2-chlorocycyclopentanone and butyrolactone) are also observed, since an OH scavenger is not added in the product analysis of the O_3 initiated reaction. The retention times are different for the same products in these three cases, because the experimental conditions of GC-MS are different.

4.3.3. Theoretical calculations

Ab initio MO calculations are performed using the Gaussian 03 [90] program to investigate the potential energy surface (PES) of the reaction of 1-chlorocyclopentene with Cl. The geometries of the ground electronic states of 1-chlorocyclopentene, the transition-state (TS) structures, and the reaction products are optimized at either the B3LYP/6-311++G(d) or B3LYP/6-311++G(d,p) level of theory. The harmonic

vibrational frequencies and the force constant are calculated to ensure the stationary points on the PESs to be true saddle points. All the TS structures calculated have only one imaginary frequency and one negative eigenvalue of the force constant matrix. The single point energies for various optimized geometries are calculated at the QCISD(T)/6-311++G(d,p) level of theory.

Since 1-chlorocyclopentene molecule has abstractable H atoms along with an unsaturation centre, Cl atom can react involving both abstraction of H atoms and addition to the C=C bond. The molecule has four different types of H atoms (located on C2, C3, C4 and C5), and hence it is worthwhile to investigate the reactivity of these H atoms towards abstraction by Cl atom. The transition state (TS) structures for abstraction of H atom of each type (shown in Fig. 4.9) are optimized, and the activation barrier for each abstraction reaction is calculated. With the optimized geometry at the lower level of HF/6-311++G(d,p) theory, the energy at the QCISD(T)/6-311++G(d,p) level predicts the activation barrier for the H atom abstraction from different carbon centres to be in the increasing order of C3, C5, C4 and C2. The order of the activation barrier for H atom abstraction from different carbon centers remains the same at relatively higher level of theory at QCISD(T)/6-311++G(d,p)//B3LYP/6-311++G(d) with energy values as -7.15, -6.50 and -3.50 kcal/mol for C3, C5 and C4, respectively (shown in Fig. 4.9). The TS structure for the H atom abstraction from C2 could not be optimized at this level of theory. Thus, our calculations suggest that H atom abstraction by Cl atom is energetically most favourable from the C3 position, followed by C5 and C4 in that order. This order of reactivity can be explained qualitatively based on stability of the TS and the radical produced after H abstraction. The radical produced after H atom abstraction from C3 will

get stabilized by both resonance effect and the inductive effect of Cl atom, and hence this abstraction is energetically most feasible. Similarly, the radical produced after H atom abstraction from C5 will get stabilized by the resonance effect, but not much by inductive effect of Cl atom. But, the radical generated after H atom abstraction from C4 is devoid of these stabilization factors. The abstraction of the H atom from C2 is the least probable, since the radical produced generates a free electron at the carbon centre (C2) that is inherently electron rich due to the C=C bond.

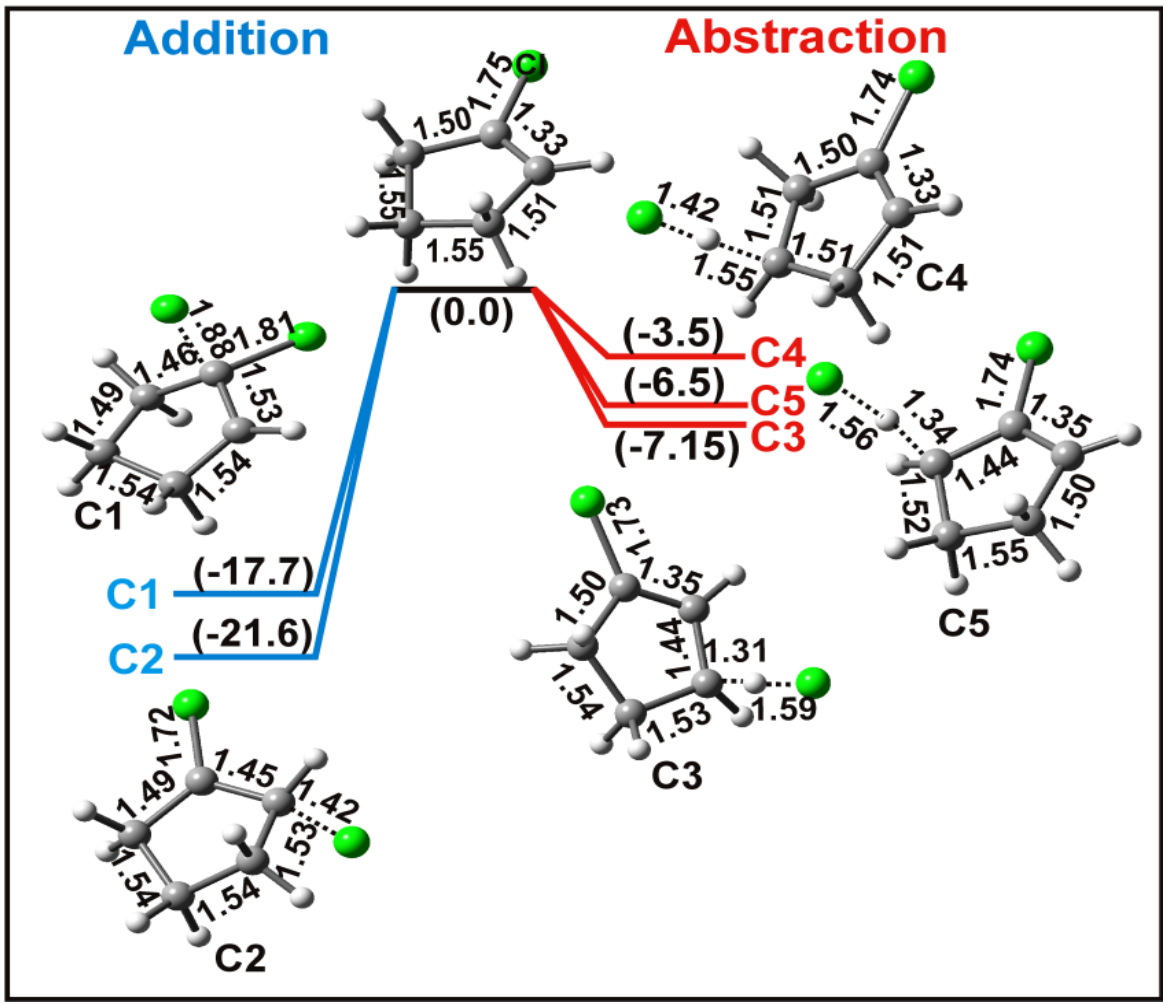

Fig. 4.9. Schematic potential energy diagram for both addition and abstraction reactions of 1-chlorocyclopentene with Cl, energies in kcal/mol and bond length in Å.

The addition reaction mechanism involves an attack of Cl atom at two carbon atoms attached by a double bond. Since these two carbon centres in 1-chlorocyclopentene are unsymmetrical in nature, there can be a preferential attack at a carbon centre. To investigate a probable preference for Cl attack, we have optimized the geometries of the radicals produced, and calculated their energies at the QCISD(T)/6-311++G(d,p)//B3LYP/6-311++G(d,p) level of theory. Our calculations predict these energies to be -21.6 and -17.7 kcal/mol for Cl atom attack on C2 and C1, respectively (shown in Fig. 4.9), implying the radical produced after Cl atom attack on C2 is more stable, and hence this addition reaction is more probable. The theoretically predicted preferential addition of Cl atom to the C=C double bond can also be explained qualitatively based on the stability of the radical produced. The radical produced by addition of Cl atom to the carbon centre C2 gets stabilized by the inductive effect of Cl atom present in the parent molecule. In the other case, the addition of Cl atom to C1 lacks such a stabilization factor.

It should be noted that the energies of the TS structures in abstraction reactions involving Cl have negative values, implying the reactions proceed via a pre-reactive complex. We expect similar reaction mechanisms for the OH radical reaction with 1-chlorocyclopentene, and the expected mechanism involving a pre-reactive complex is validated by the measured negative temperature dependence of rate coefficients.

4.4. Discussion

To the best of our knowledge, the reactions of 1-chlorocyclopentene with tropospheric oxidants (Cl and OH) are not reported. However, there is a single report

available for its reaction with O_3 [86], in which the rate coefficient is reported to be (1.50 ± 0.10) × 10^{-17} cm^3 $molecule^{-1}$ s^{-1}.

4.4.1. Reaction of 1-chlorocyclopentene with oxidants

4.4.1.1. Reaction with Cl

The average values of the rate coefficients for the Cl atom reactions from the present work are listed in Tables 4.1 and 4.4

Table 4.4: Tropospheric lifetimes calculated for 1-chlorocyclopentene with respect to reactions with different tropospheric oxidants. The concentrations used for $Cl_{Ambient}$, Cl_{MBL} (under marine boundary layer conditions), OH and O_3 are 2.5 × 10^3, 1.3 × 10^5, 2 × 10^6 and 7 × 10^{11} molecules cm^{-3} [13], respectively.

Compound	Rate coefficients (cm^3 $molecule^{-1}s^{-1}$)		
	$k_{Cl}\times10^{10}$ **(τ_{Cl})**	$k_{OH}\times10^{11}$ **(τ_{OH})**	$k_{03}\times10^{17}$ **(τ_{O3})**
1-Chlorocyclopentene	3.51 ± 1.26 **(316 hrs) Ambient** **(6 hrs) MBL**	5.97 ± 1.08 **(2hrs)**	1.50 ± 0.19 1.50 ± 0.10 [86] **(26 hrs)**
	τ_{Total}=1.85 hrs		
Cyclopentene	3.39 ± 1.08 [85]	6.7 ± 1.34 [88]	57 [8]
1-methylcyclopentene			67 [8]
cyclopentane	2.31 [91]	4.97[8]	

The measured rate coefficients have been compared with the previously reported average values for similar type of molecules (listed in Table 4.4). The rate coefficient measurements are devoid of any complications due to secondary reactions, as suggested by a linear plot obtained for reaction of Cl with 1-chlorocyclopentene (shown in Fig. 4.1), with near zero intercept. The observed average slope in the presence of air being slightly higher than that in the presence of nitrogen, suggesting some additional reactions in the former condition also, as observed in cyclic-dienes [13], and cyclic alkenes [85]. But similar effect was not observed in the reaction of straight chain 1-alkenes [46]. The formation of OH in the presence of air is a probable reason for this increase, as observed in the Cl-initiated oxidation of acetaldehyde [92,93]. Therefore, the rate coefficient measured in N_2 atmosphere should be considered as the correct rate coefficient for the reaction of 1-chlorocyclopentene with Cl atom.

The presence of chlorine in 1-chlorocyclopentene does not affect much its reactivity with Cl when compared with our earlier work on cyclopentene [85]. The rate coefficient of the Cl reaction with 1-chlorocyclopentene ($(3.51 \pm 1.26) \times 10^{-10}$ cm^3 $molecule^{-1}$ s^{-1}) is similar to that with cyclopentene ($(3.39 \pm 1.08) \times 10^{-10}$ cm^3 $molecule^{-1}$ s^{-1}) [85], but greater than that with cyclopentane ($(2.31 \pm 0.20) \times 10^{-10}$ cm^3 $molecule^{-1}$ s^{-1}) [91]. The greater rate coefficient of 1-chlorocyclopentene than cyclopentane is understandable, since the latter lacks an unsaturation centre, and hence it is devoid of any contribution from the addition reaction. In general, the rate coefficients for reactions of Cl atoms with alkanes are always greater than those of the corresponding chloroalkanes, since only abstraction reactions are involved [94]. However, it's difficult to understand

the reactivity of 1-chlorocyclopentene (or, in general a chlorine substituted VOC having both olefinic double bond and abstractable H atoms) with respect to cyclopentene (corresponding unsubstituted VOC), because of involvement of several factors.

4.4.1.2. Reaction with OH

The room temperature rate coefficient of the reaction of 1-chlorocyclopentene with OH is measured with both the relative rate method and the absolute method; the average values of the rate coefficients are listed in Table 4.4. Results indicate a reasonably good agreement between the two values (within the experimental error) obtained by these methods. Also, the rate coefficient of the OH reaction is found to be an order of magnitude lower than that of the Cl atom reaction. In addition, the temperature dependent rate coefficients for the reaction of 1-chlorocyclopentene with the OH radical are measured experimentally over the temperature range of 262 to 335 K and at 30 Torr using LP-LIF technique, and the values are given in Table 4.2. The Arrhenius expression for the measured data is given by the expression, $k = (6.32 \pm 1.16) \times 10^{-12} \exp((669 \pm 45)/T)$ $cm^3molecule^{-1}s^{-1}$, and the negative temperature dependence is observed. This negative activation energy suggests the involvement of a pre-reactive complex in the reaction. Like in the Cl reaction, in case of the OH reaction also, the presence of chlorine in 1-chlorocyclopentene does not affect its reactivity when compared with cyclopentene [88]. Like the rate coefficients for reactions of alkanes with Cl atoms, that with OH radicals are also always higher than those of the corresponding chloroalkanes [94]. Similarly, the trend of reactivity is difficult to explain for a VOC undergoing both addition and abstraction reactions with OH radicals. However, based on increasing kinetic

database of organic compounds for the gas phase reactions, a structure-activity relationship is established and the rate coefficients with OH radicals are calculated based on a group additive method [95,96]. Based on this method, the rate coefficient of 1-chlorocyclopentene with OH reaction is estimated (neglecting the ring strain) to be 2.15×10^{-11} cm^3 $molecule^{-1}$ s^{-1}, which is lower in comparison to the measured value of $(5.97 \pm 1.08) \times 10^{-11}$ cm^3 $molecule^{-1}$ s^{-1}. Thus, the group additive method can predict the rate coefficient reasonably well, but more experimental data are required to increase the accuracy.

4.4.1.3. Reaction with O_3

The average value of the rate coefficient for the O_3 reaction is listed in Table 4.4, along with the previously reported average values for 1-chlorocyclopentene and similar type of molecules. There is an excellent agreement between the present value and the reported value [86]. Due to presence of Cl in chlorocyclopentene, its reactivity with O_3 has decreased drastically, when compared with cyclopentene and 1-methylcyclopentene [8].

4.4.1.4. Comparison of rate coefficients

The rate coefficient of 1-chlorocyclopentene with Cl is an order of magnitude greater than that with OH, and the latter is greater than that with O_3 by six orders of magnitude. Thus, the reaction with Cl and OH are the most important degradation pathways for 1-chlorocyclopentene. Our earlier work [85] suggests that the mechanism of the reactions of Cl and OH with 1-chlorocyclopentene should be similar. To confirm this

prediction, the rate coefficients of reactions of OH and Cl atoms with unsaturated molecules, [13,85,97,98] are plotted in Fig. 4.10.

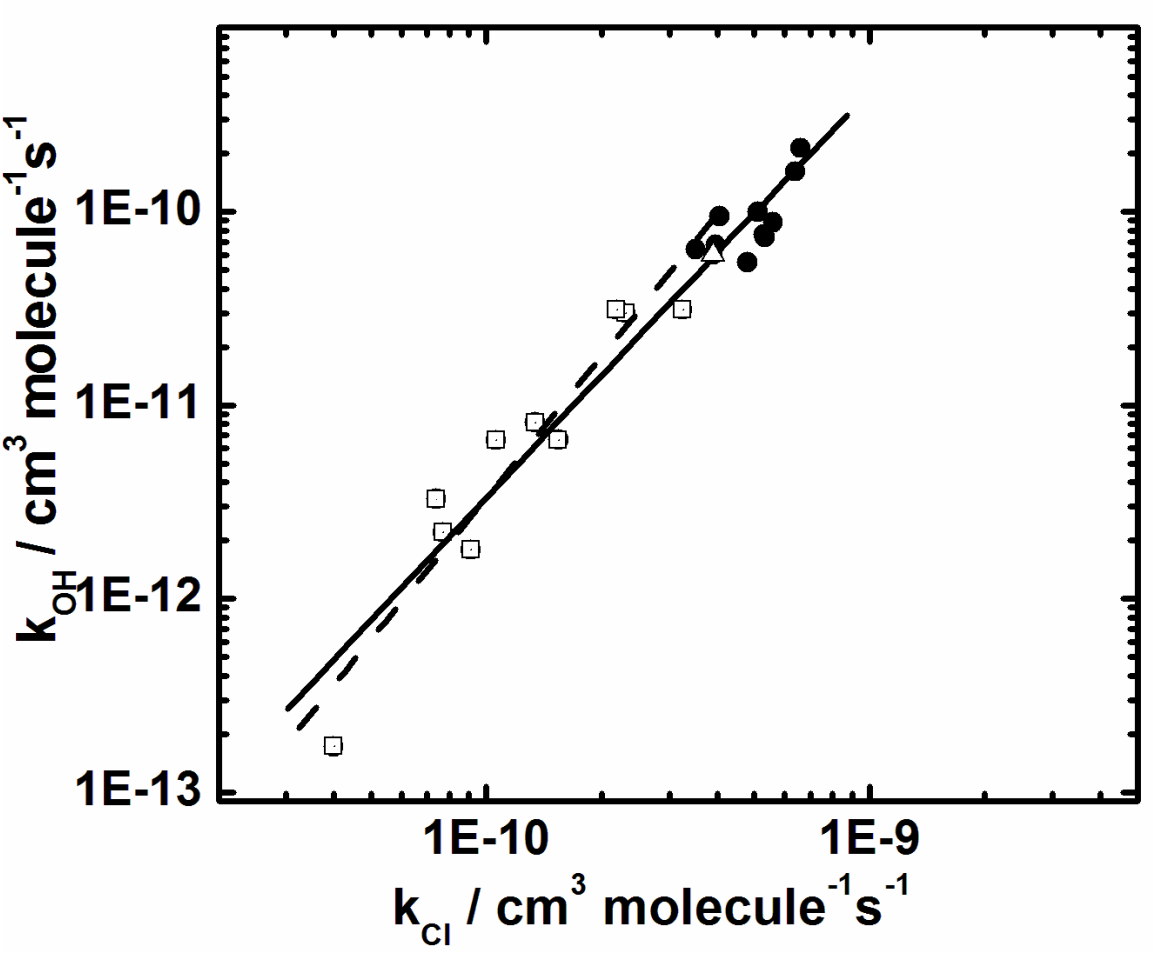

Fig. 4.10. Correlation plots between the rate coefficients for the reactions of Cl and OH radicals with unsaturated hydrocarbons only (dashed line) and with inclusion of unsaturated cycloalkenes as well (solid line). The rate coefficients of hydrocarbons (C_2H_4, C_2H_3Cl, 1,1-$C_2H_2Cl_2$, cis-$C_2H_2Cl_2$, trans-$C_2H_2Cl_2$, C_2Cl_4, C_3H_6, 1-C_4H_8, and 1-C_5H_{10}) are taken from reference [97] and depicted as open square. The data for unsaturated cycloalkenes (cyclopentene, cyclohexene, cycloheptene, 1,4-cyclohexadiene, 3-carene, α-pinenes, β-pinene, limonene, isoprene, and myrcene) are taken from references

[13,85,98] and shown as solid circles. Data of 1-chlorocyclopentene from the present work is shown as triangle **(Δ).**

An approximate linear correlation has been observed between the rate coefficients of reactions with OH and Cl atoms. Such a linear correlation indicates similarity between the mechanisms of the reactions of the OH radical and Cl atom with these hydrocarbons. Since the unsaturated molecules involve both addition and abstraction reactions, the parameters are different for the saturated molecules. It is observed that the linearity in the case of unsaturated molecules holds good within the error limits, even after the inclusion of the 1-chlorocyclopentene. The correlation obtained for unsaturated molecules considered in references [13,85,97,98] yields a straight line, with a correlation coefficient of 0.97.

$$\log k_{OH} = (2.1 \pm 0.1) \log k_{Cl} + (9.6 \pm 1.2) \qquad (4.15)$$

4.4.1.5. Reaction mechanism

Our theoretical calculations predict that 1-chlorocyclopentene react with the oxidant Cl, involving both the abstraction and addition reaction mechanisms. Energies involved in abstraction of different H atoms present in the molecule are different. Using this preferential abstraction of H atom by Cl, formation of one major product 2-cyclopenten-1-one can be explained (shown in Scheme 4.1).

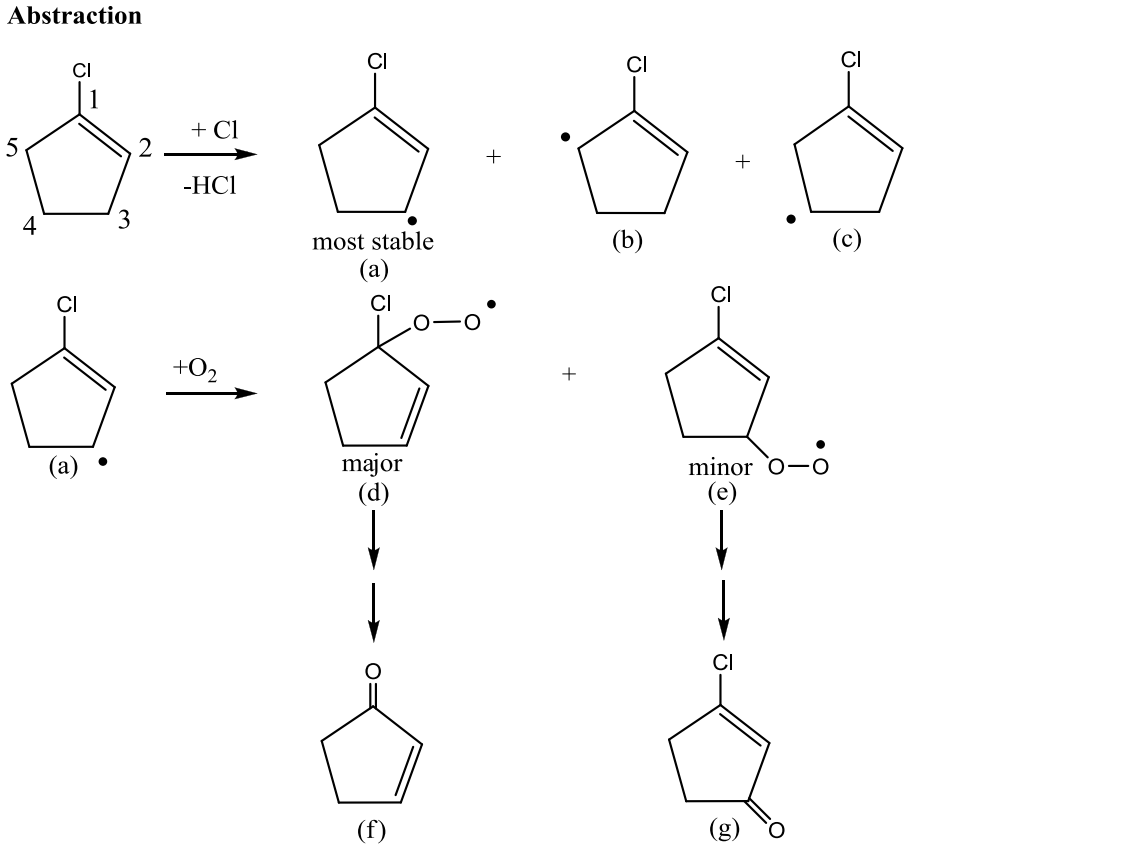

Scheme 4.1: Schematics of the proposed reactions (abstraction and addition mechanisms), leading to some of the major products observed in the present study, during the Cl and OH initiated oxidation of 1-chlorocyclopentene in NOx-free air.

Among the four possible chlorocyclopentenyl radicals formed after abstraction of H atoms from chlorocyclopentene (the least stable radical is not shown), the most stable

radical (a) can undergo secondary reaction with O_2, producing alkylperoxy radicals (d) and (e) as major and minor products, respectively. The reaction of an alkyl radical (R) with O_2, and subsequent reactions of alkylperoxy radicals (RO_2) are well documented in literature [99] to produce keto compounds through alkoxy radicals (RO). Thus, the alkoxyradicals (d) and (e) can lead to the final stable products 2-cyclopentene-1-one (f) and 3-chloro-2-cyclopenten-1-one (g), respectively. These products 2-cyclopentene-1-one (f) and 3-chloro-2-cyclopenten-1-one (g) have been observed as a major and a minor product, respectively, in GC-MS analysis at retention time of 14.2 and 17.5 minutes. The less stable chlorocyclopentenyl radical (b) can also undergo similar secondary reactions with O_2 to produce the final product 2-chloro-2-cyclopenten-1-one, an isomer of the product (g). This minor product is also observed in the chromatogram at ~17.5 minutes. The yields of these two isomers are observed to be comparable. Similar to chlorocyclopentenyl radical (b), the radical (c) can also undergo similar secondary reactions with O_2 to produce 3-chloro-3-cyclopenten-1-one, another isomer of the product (g). The product yield of this isomer is observed to be the least among all these three isomers. The probable assignment of this minor product 3-chloro-3-cyclopenten-1-one is based on theoretical predictions.

Similar to the preferential abstraction reaction, our calculations predict that the Cl atom adds preferentially to the C atom (C2, not linked to Cl) of the C=C(Cl) bond of 1-chlorocyclopentene in the addition reaction (depicted in Scheme 4.1). The 1,2-dichlorocyclopentyl radical produced undergoes similar sequence of reaction with O_2, as in the abstraction reaction, to yield the stable product 2-chlorocyclopentanone. This

product is observed in the highest yield in the chromatogram at the retention time of 16.2 minutes.

The reactions of 1-chlorocyclopentene with OH is expected to be similar to Cl, involving both abstraction and addition mechanisms, giving some common products, as explained earlier. In addition to these stable products, produced involving both abstraction and addition reactions, wherein the ring of 1-chlorocyclopentene is unaffected, other observed products, such as 2-chloropropenal and butyrolactone (shown in Table 4.2), suggest that the ring opening, and the ring opening followed by recyclization also take place. The O_3 initiated products, leading to formation of particularly CO_2, methanol and ethanol, suggest that extensive degradation of 1-chlorocyclopentene takes place in comparison to the Cl and OH initiated reactions. Ozone can react with 1-chlorocyclopentene leading to the ring opening via a Criegee intermediate, which can undergo further degradation to produce several products. Unlike the Cl and OH initiated products, most of the observed stable products in O_3 reaction originate from this intermediate.

4.4.2. Atmospheric implications

We estimated atmospheric lifetimes, and the global warming potential and ozone depletion potential of 1-chlorocyclopentene to understand its atmospheric implication.

4.4.2.1. Atmospheric lifetimes

The room temperature rate coefficients of 1-chlorocyclopentene with OH, Cl and O_3 are determined in the present work. These values are used to estimate average tropospheric lifetime with individual oxidants, τ_{Ox}, using their average tropospheric

concentration [Ox], τ_{Ox},$= \frac{1}{k_{Ox}[Ox]}$ (given in Table 4.3). The overall tropospheric lifetime (τ_{total}) in the day time can be estimated using Eqn. (4.16).

$$\tau_{\text{total}} = \left[\sum_{Ox} \frac{1}{\tau_{Ox}} \right]^{-1} \tag{4.16}$$

Table 4.4 shows that the major sink for 1-chlorocyclopentene in the day time is the reaction with the OH radical. The contribution of Cl atom reaction in the degradation of 1-chlorocyclopentene under ambient condition is negligible. However, in the marine boundary layer (MBL) conditions, where the Cl atom concentration is 50 times greater than that in the ambient condition, reaction of 1-chlorocyclopentene with Cl is found to be significant to reduce the lifetime to 6 hrs from about 316 hrs. Thus in MBL the reactions with Cl atoms also, in addition to OH, start contributing to the degradation of 1-chlorocyclopentene.

4.4.2.2. Global warming and ozone depletion potential

The IR absorption spectra for different concentrations of 1-chlorocyclopentene are measured in the linear absorbance range (shown in Fig. 4.11). A plot of absorption cross section over the wavenumber range of 500-2500 cm^{-1} is displayed in Fig. 4.12.

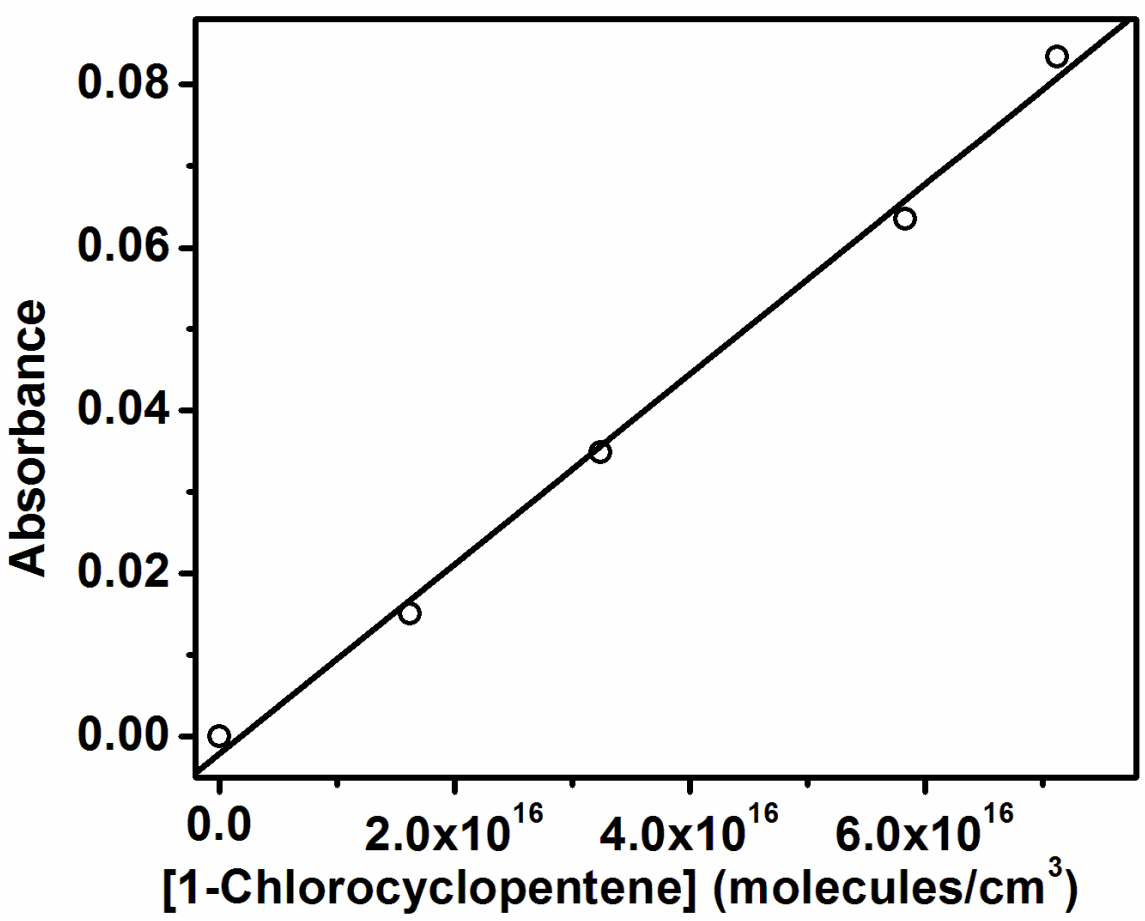

Fig. 4.11. A plot of absorbance for the vibrational band at 808.3 cm^{-1} of 1-chlorocyclopentene against its concentrations.

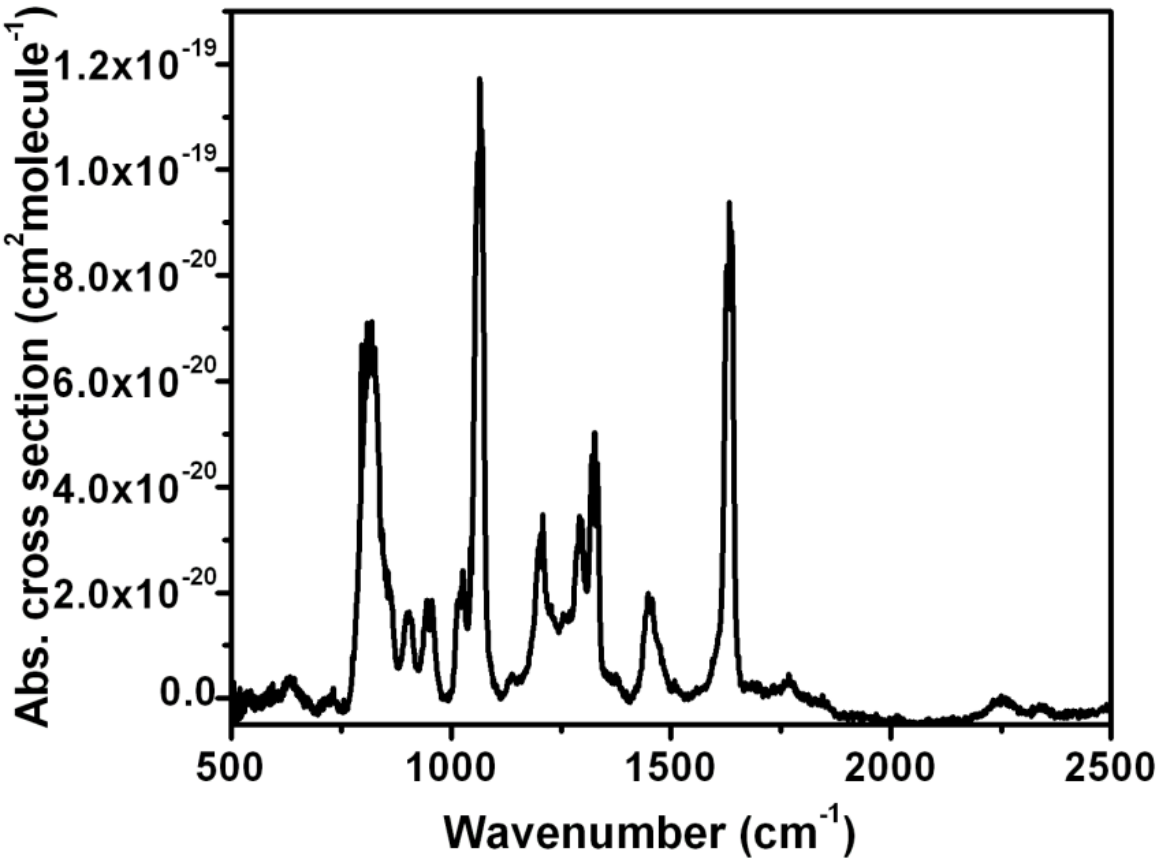

Fig. 4.12. The plot depicts absorption spectra for 0.5 Torr of 1-chlorocyclopentene in the wavenumber range of 500-2500 cm^{-1} at 298 K.

Using the IR spectrum, the radiative efficiency for 1-chlorocyclopentene is estimated, employing the method explained by Hodenbrog et al. [100], to be 22.4 $mWm^{-2}ppb^{-1}$. The estimated radiative efficiency and the global lifetime of 1-chlorocyclopentene are used to estimate its halocarbon global warming potential (HGWP) relative to CFC-11($CFCl_3$), using a semi-empirical equation (4.17)[38].

$$HGWP_{CCP} = \frac{\tau_{CCP}}{\tau_{CFCl_3}} \text{ x } \frac{M_{CFCl_3}}{M_{CCP}} \text{ x } \frac{RE_{CCP}}{RE_{CFCl_3}} \frac{\left(1\text{-}\exp^{-t/\tau_{CCP}}\right)}{\left(1\text{-}\exp^{-t/\tau_{CFCl_3}}\right)} \qquad (4.17)$$

where, τ_x, M_x, RE_x (x=CCP or $CFCl_3$) and t denote the global atmospheric lifetimes, the molecular weight, radiative efficiency and time horizon, respectively. The HGWP value of CCP (1-chlorocyclopentene) is calculated to be 1.56×10^{-6} and 0.63×10^{-6} for a time horizon of 20 and 100 years, respectively. Using the HGWP value, the global warming potential (GWP) of 1-chlorocyclopentene, relative to CO_2, can be estimated by multiplying its HGWP value with the GWP value of $CFCl_3$. Taking the GWP values of $CFCl_3$ on a time horizon of 20 and 100 years as 6730 and 4750 [39] respectively, that of 1-chlorocyclopentene are calculated to be 0.01 and 0.003 for a time horizon of 20 and 100 years. It is clear from the low GWP values that 1-chlorocyclopentene will not contribute to the radiative forcing of climate change.

Since the molecule 1-chlorocyclopentene has a chlorine atom, it can possibly contribute to stratospheric ozone depletion. Similar to GWP, its ozone depletion potential (ODP) can also be estimated, using a semi-empirical equation (4.18) [38],

$$ODP_{CCP} = \frac{\tau_{CCP}}{\tau_{CFCl_3}} \text{x} \frac{M_{CFCl_3}}{M_{CCP}} \text{x} \frac{n}{3} \qquad (4.18)$$

where, τ_x and M_x, have usual meaning as in Eqn. (4.17), n is the number of chlorine atoms in CCP (that is 1), and the number 3 refers to the three chlorine atoms in $CFCl_3$. Using the value of τ_{CFCl3} as 45 years [39], the ODP value of CCP (1-chlorocyclopentene) is calculated to be 2.1×10^{-6}. This low value of ODP suggests that 1-chlorocyclopentene will have a negligible effect on the stratospheric ozone depletion.

4.5. Conclusions

The average rate coefficients of reactions of 1-chlorocyclopentene with atmospheric oxidants Cl, OH and O_3 are measured at room temperature to be (3.51 ± 1.26) × 10^{-10}, (5.97 ± 1.08) × 10^{-11} and (1.50 ± 0.19) × 10^{-17} cm^3 $molecule^{-1}$ s^{-1} respectively in N_2 atmosphere, using a relative rate method. The temperature dependent rate coefficients for the reaction of 1-chlorocyclopentene with OH radical are measured experimentally, using LP-LIF method, over the temperature range of 262 to 335 K and at the total pressure of 30 Torr. The Arrhenius expression for the measured data is given by the expression, k = (6.32 ± 1.16) × 10^{-12} exp ((669 ± 45)/T) $cm^3 molecules^{-1} s^{-1}$, and the negative temperature dependence is observed. This negative activation energy suggests the involvement of a pre-reactive complex in the reaction. The rate coefficients with Cl in the presence of O_2 are greater than that in N_2. The major degradation pathway of 1-chlorocyclopentene is its reaction with OH radicals. However, its reaction with Cl atoms also becomes important under marine boundary layer conditions. The impact of 1-chlorocyclopentene on atmosphere is local since its tropospheric lifetime is less than 2 hours. Global warming potential of 1-chlorocyclopentene is negligible (0.01 and 0.003 for 20 and 100 years time horizon, respectively), and therefore, it can be concluded that 1-chlorocyclopentene will not contribute substantially in the global warming. The ODP value is also quite low (2.1 × 10^{-6}), suggesting that 1-chlorocyclopentene will have a negligible effect on the stratospheric ozone depletion. But the identified stable products can be responsible for formation of photochemical smog and aerosol generation [92].

The oxidants react with 1-chlorocyclopentene involving both the addition and abstraction pathways, the former mechanism being predominant. Our molecular orbital

calculations suggest that the addition reaction mechanism of the Cl atom to 1-chlorocyclopentene involves its preferential addition to the carbon atom of the C=C unsaturated centre, which is not having the Cl atom attached to it. For H atom abstraction reaction by Cl atom, the allylic H atoms of 1-chlorocyclopentene are preferentially abstracted. It's remarkable to note that the energies of the TS structures in abstraction reactions is negative, implying the reaction proceeds via a pre-reactive complex. Thus, both the experimental and theoretical calculations suggest that the mechanisms of reactions of both OH and Cl with 1-chlorocyclopentene are similar.

Chapter-5

Reactions of Lactones with Tropospheric Oxidants: A Kinetics and Products Study

5.1. Introduction

In recent years there has been considerable focus on biofuels for sustainable development, especially in the development of second generation biofuels, that can be generated from non-edible biomass such as cellulose, lignin etc., so that food production is not affected [101]. Many of these consist of oxygenates, cyclic ethers, esters etc., which can be used as solvents or converted to fuels and other carbon-based chemicals efficiently [102-104]. Thus, preparation and applications of cyclic esters or lactones such as 5-methyldihydrofuran-2(3H)-one, commonly known as gamma-valerolactone (GVL) have received substantial attention. Recently, conversion of paper waste to GVL and its use as an illuminating fuel with reduced VOC (volatile organic compound) emission has been reported [105]. Effects of GVL blending on the engine performance, combustion characteristics and exhaust emissions have been studied and found to be encouraging, with a reduced concentration of CO, smoke and unburnt fuel in the exhaust [106]. In this context, pyrolysis of GVL at high temperature relevant to diesel engine has been reported [107,108]. GVL is also identified as a product of low temperature combustion of ketones, which are prototypes of biofuels [109]. GVL may enter the atmosphere during the applications discussed above and also from its recommended use as a green solvent. GVL and other related cyclic esters (furanones) were identified as secondary products of

oxidation of cyclic ethers [110] and 1-alkenes [46] under laboratory conditions and could be formed in the atmospheric conditions also. Hence, oxidation pathways of these cyclic esters in the atmosphere are relevant and important, however, the available information is limited. Although physical removal processes such as partitioning to particle and aqueous phases may take place, reactions with OH is also expected to contribute significantly to the degradation of these molecules. Chlorine atom is another important oxidant in the troposphere, whose concentration varies in the range of 10^2 to 10^5 atoms cm^{-3}, the higher values pertaining to the conditions of marine boundary layer and polluted urban atmosphere [15,16,84]. The reaction with Cl atom was found to be an effective pathway for initiating the degradation of alkenes [46] and cyclic ethers [27] in the conditions of high Cl atom concentration and could be important in cyclic esters also. In addition to Cl atoms, Br atoms are also generated in the marine boundary layer and, despite its smaller concentration as compared to that of Cl atom, it is known to play a very important role [111]. However, the reactions of Br with most of the VOCs being very slow, do not contribute to their degradation in the troposphere [111,112]. Other oxidants, ozone and NO_3 are not considered to be important in the tropospheric degradation of the saturated esters as their reactions are also very slow [113]. Recently, Barnes et al. [114] have reported the experimental rate coefficients of reactions of OH with GVL, and few other cyclic esters, β and γ- butyrolactones and δ-valerolactone (BBL, GBL and DVL), with varying ring sizes. This study also includes computational studies on GVL and alpha-methyl gamma-butyrolactone (AMGBL), which differs from GVL only in the position of an exocyclic methyl group. In the case of GVL, where there is a previous report available

[115], a discrepancy is observed in the value of the rate coefficient of its reaction with OH. However, there is no information on the reaction of Cl with these molecules and also on the final products of the tropospheric oxidation, which decides the overall tropospheric impact. In view of the reports that GVL gives less volatile products upon combustion, it is interesting to know the products of the atmospheric oxidation of GVL and other similar molecules. The reactions of primary radicals from oxygenates may lead to more volatile products via dissociation, or oxidation products containing alcohol / keto groups that have more potential for aerosol generation. The present study was initiated with the aim of understanding the reactions of atmospheric oxidants with GVL and AMGBL, which have similar ring size but differ in the position of methyl substitution as shown below.

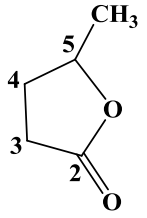

GVL

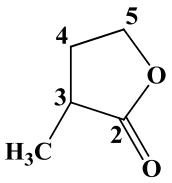

AMGBL

The rate coefficients of the reactions with both OH (k_{OH}) and Cl atom (k_{Cl}) and their major reaction products are determined and compared, to understand the effect of the structure on these reactions, if any.

5.2. Experimental

The rate coefficients are determined using the relative rate method, where the rate of decrease in the concentration of the lactones (L) due to their reactions with the atmospheric oxidant, X, is compared to that of a reference molecule (R) with known rate coefficient.

$$L + X \rightarrow \text{products} \qquad (k_L) \tag{5.1}$$

$$R + X \rightarrow \text{products} \qquad (k_R) \tag{5.2}$$

Assuming the above reactions to be the only reactions that take place, the fractional losses of L and R are related by the standard expression,

$$\ln\left[\frac{[L]_{t_0}}{[L]_t}\right] = \left[\frac{k_L}{k_R}\right] \ln\left[\frac{[R]_{t_0}}{[R]_t}\right] \tag{5.3}$$

where $[L]_{t0}$, $[L]_t$, $[R]_{t0}$ and $[R]_t$ are respective concentrations at time 0 and t, k_L and k_R are the rate coefficients for reactions 5.1 and 5.2, respectively. Thus, the slope of the linear plot of logarithms of the ratios of fractional changes in the concentration of L versus R at specific time t gives k_L/k_R.

All the experiments are performed at (298 ± 2) K. The details of the experimental setup and the procedure for determining the rate coefficients and products of the reaction of Cl atoms and OH radicals are described in chapter two. The Cl atoms are generated in situ by photolysis of $(COCl)_2$ or Cl_2 at 254 nm or 350 nm respectively, and the OH radicals are produced by photolysis of O_3-H_2O mixture at 254 nm, using monochromatic UV lamps. Dark reaction with ozone is found to be negligible. Ozone is generated as O_3/O_2 mixture (< 2%) using an ozonizer. Concentration of $(COCl)_2/Cl_2$ was in the range of 5 - 7 × 10^{15} molecules cm^{-3}. The pressure of O_3/O_2 mixture and water vapor in the reaction mixture was 4.5 - 5.5 and 1.3 kPa, respectively.

The reactions are carried out in Quartz reactors of volume of about 3L, or in a Pyrex reactor, if Cl_2 was the source of Cl atoms, maintaining a total pressure of 106.7 kPa (800 Torr), very close to the atmospheric pressure (101.3 kPa), with nitrogen as the buffer

gas. The concentration of both L and R are in the range of $1.5 – 2.7 \times 10^{15}$ molecules cm^{-3} and their depletion are followed, after photolysis for a fixed time (1- 2 min.), using a Gas Chromatograph (Shimadzu GC-2010) with a flame ionization detector. The fused silica capillary column HT8 (25m × 0.22mm × 0.25μm) is employed for separation, with suitable temperature programming. The samples are taken manually, injected using a gas tight syringe of 500 μl for kinetics (SGE-500FGT) experiments. The reaction mixture is allowed to reach equilibrium before and after each photolysis, which is confirmed by the reproducibility of the concentration measured during the consecutive sampling. The reference molecule R is selected based on the similarity of the rate coefficients (the ratio of the rate coefficients not exceeding 5) and the least interference during the Gas Chromatography analysis, either from the molecule or from the products of their reactions with the oxidants, which are individually monitored. The total photolysis time is about 5 – 8 min, leading to a maximum depletion of 30 - 40 %.

The products analysis studies are carried out with zero grade air as the buffer gas. GC-MS (QP2010, Shimadzu) is used for detection and characterization of the stable products. The quantitative comparison of products is carried out using FID, by comparing the areas of the corresponding peaks in GVL and AMGBL, after normalizing for the depletion of the parent molecules. Carbon dioxide (CO_2) is quantitatively estimated by GC-FID, equipped with a methaniser (Shimadzu MTN-1), using CO_2 standards from Sigma.

GVL (99%) and AMGBL (98%) from Sigma-Aldrich are used for the experiments. Liquid samples are stored in evacuated glass vessels and subjected to freeze-pump-thaw cycles prior to use.

5.3. Results

Vapor pressures of both GVL and AMGBL are low, being less than 65 Pa at 25°C. Samples are prepared by injecting liquid directly to the evacuated cells. The cells are passivated for sufficient time to take care of wall losses and the concentrations of the molecules monitored using GC are found to be remaining constant for more than 6 hrs, confirming complete passivation. The possibility of dark reaction is tested by keeping the mixture of lactone, reference molecule and the radical precursors for about 6 hrs and is found to be negligible. Photolyses of the sample as well as the reference molecules are carried out separately in the absence of the radical precursor, and was found to remain constant within error limits, ruling out the possibility of desorption during photolysis and self-photolysis. The reactions of the lactones and the reference molecules are also studied separately to confirm the absence of any overlapping product build-up, which may interfere with the determination of peak areas. Ethane, propane and butane are the reference molecules that could be employed which meet all the above criteria. The typical plots of the relative decrease of the concentrations of lactones and the reference molecules due to reactions with Cl and OH are given in Fig. 5.1 A and 5.1B, respectively. The average values of the rate coefficients obtained with different reference molecules for GVL and AMGBL are summarized in Table 5.1, along with the reported rate coefficient of OH reaction with GVL. The error in the values of the rate coefficient is calculated by

combining the experimental errors in the average slope values and the reported error in the values of k_R statistically.

The reaction of ozone with these molecules is found to be too slow, as mentioned in the experimental section.

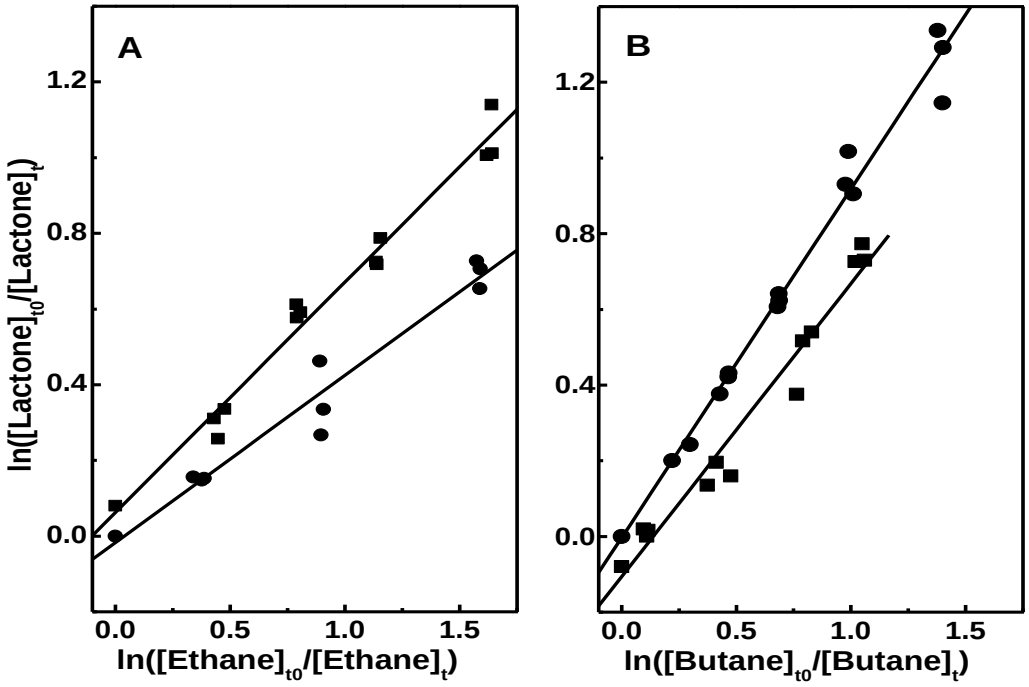

Fig. 5.1. Typical plot of the fractional decrease in the concentration of GVL (●) and AMGBL (■) at 298 ± 2 K in N_2 buffer, total pressure 800 Torr. A: Due to Cl atom reaction and B: Due to OH reaction with ethane and butane as reference molecules.

Table 5.1**:** The relative rate ratios and the rate coefficients calculated at room temperature for GVL and AMGBL with different reference molecules, along with the experimental values available in literature. The rate coefficients of reference molecules used are given

in the column Reference. The rate coefficient values determined in the present work are marked in bold. Number of experiments in each case is given in parenthesis.

Sample	**Oxidant**	**Reference**[(a)]	**Avg. slope**	**Rate coefficient** k_{298} **(cm^{3}molecule^{-1}s^{-1})**
GVL	OH	Butane (5) $(2.35 \pm 0.33) \times 10^{-12}$	0.83 ± 0.22	**$(1.95 \pm 0.58) \times 10^{-12}$**
	OH			$(1.17 \pm 0.11) \times 10^{-12}$ Ref. [115]
	OH			$(2.81 \pm 0.34) \times 10^{-12}$ Ref. [114]
	Cl	Ethane (4) $(5.8 \pm 0.67) \times 10^{-11}$	0.39 ± 0.08	**$(2.26 \pm 0.53) \times 10^{-11}$**
AMGBL	OH	Propane (3) $(1.13 \pm 0.2) \times 10^{-12}$	1.65 ± 0.24	**$(1.86 \pm 0.43) \times 10^{-12}$**
		Butane (3) $(2.35 \pm 0.33) \times 10^{-12}$	0.75 ± 0.04	**$(1.76 \pm 0.26) \times 10^{-12}$**
	Average = $(1.81 \pm 0.43) \times 10^{-12}$			
	Cl	Ethane (2) $(5.80 \pm 0.67) \times 10^{-11}$	0.60 ± 0.02	**$(3.48 \pm 0.42) \times 10^{-11}$**
		Propane (4) $(1.4 \pm 0.20) \times 10^{-10}$	0.24 ± 0.05	**$(3.36 \pm 0.85) \times 10^{-11}$**

	Average = (3.42 ± 0.63) × 10^{-11}

[(a)]The rate coefficient values are from ref. [58]

5.3.1. Products of the reactions of OH and Cl

The ion chromatograms obtained with Innovax (A for GVL and B for AMGBL) and GSBP8 columns (A' and B' for GVL and AMGBL respectively) are shown in Fig. 5.2. In the case of GVL, in both OH and Cl reactions, only one product is observed under the present conditions. By comparing the observed mass spectrum with the literature data [116] it is identified as acetic acid. In the case of AMGBL, in addition to acetic acid, three peaks are observed, of which the major one is identified as a diketone, 3,4-dihydro-3-methyl-2,5-furandione, based on the comparison of the observed (b) and reported (b') mass spectra, as shown in Fig. 5.2. The peaks marked as c, d and e could not be assigned unambiguously, but the mass spectra of c and d are shown in inset of Fig. 5.2. In all our earlier studies on cyclic and acyclic hydrocarbons and ethers [27,46], alcohols have been observed as oxidation products along with the corresponding ketones. Hence it is possible that the peak c corresponds to 2-hydroxy-4-methyl-2(2H) furanone, which gives a very small peak at 116 (molecular peak) and a peak due to the loss of water molecule (not visible in the mass spectrum). The peak e can be assigned to a chlorine containing secondary product, based on the typical isotope ratio and peaks due to removal of Cl (-35). By changing the conditions such as increasing the voltage applied to MS, two more minor products could be detected, namely ring opened product, 2-hydroxypropionic acid in the case of AMGBL and succinic anhydride, cyclic oxidation product after the elimination of CH_3 group, in the case of GVL. Absence of acetaldehyde, formaldehyde,

ethane, propene, ethanol, acetone etc. is further confirmed by injecting the standard samples.

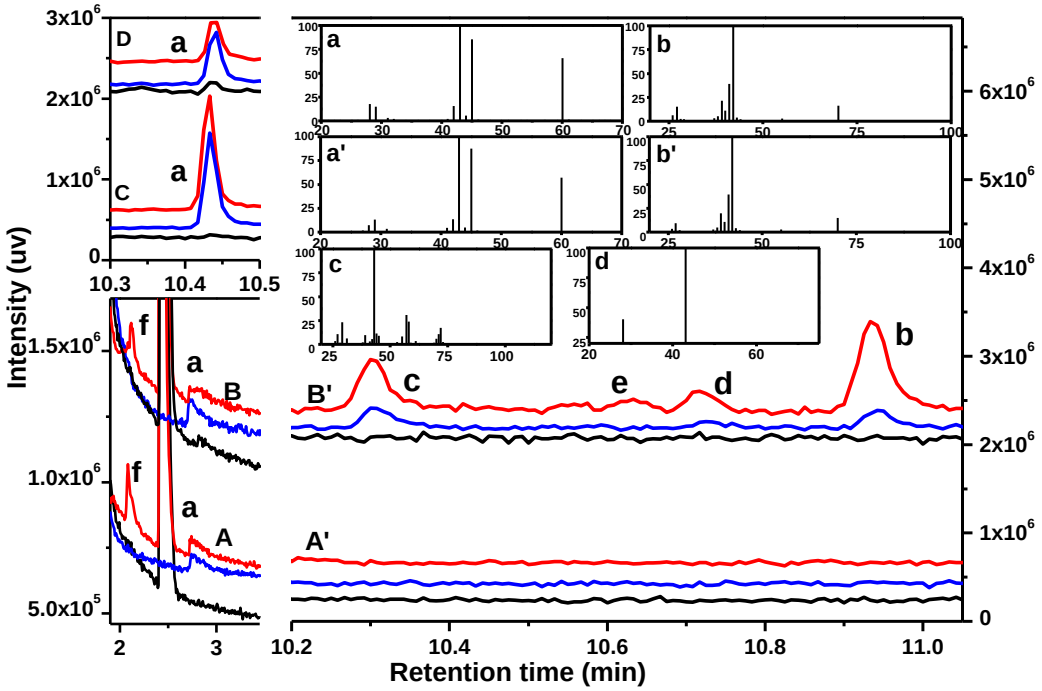

Fig. 5.2. The total ion chromatograms of the products of Cl (red) and OH (blue) initiated oxidation of GVL (A, A') and AMGBL (B, B') using GSBP8 column, and (C, D) using innowax column, along with blank run (black). Peaks a: acetic acid, b: 3,4-dihydro-3-methyl-2,5-furandione, c, d and e: unknown, f: acetylchloride. Inset: The mass spectra of the acetic acid (a-target and a'-library) and 3,4-dihydro-3-methyl-2,5-furandione (b-target and b'-library), unidentified products (c and d -target).

Based on the area in the chromatogram, the yield of acetic acid appears to be lower in the case of AMGBL as compared to GVL. However, the high uncertainty in the areas in the ion chromatograms in MS (about 25% in the case of AMGBL) makes a quantitative comparison difficult. Hence, the experiments are repeated using Flame

Ionisation Detecor (FID) to get a better quantitative comparison, using GSBP8 column, as shown in Fig. 5.3. The pattern is slightly different from the ion chromatogram, with a difference in the retention times due to the change in the carrier gas and the absence of oxalyl chloride peak at about 2.5 min. The response to the chlorinated product e is more than that of d, which is almost absent. This suggests product d to be a molecule with small number of C-H bonds. The yields of major products, acetic acid (a) as well as furandione (b) are linear with the amount of GVL / AMGBL consumed. The relative yield of acetic acid is followed for the reactions of OH and Cl with both the lactones. The experiments are conducted by keeping the extent of the reaction equal i.e., the same quantity of lactone has been reacted with OH / Cl, for both GVL and AMGBL, so that comparison of the yield is meaningful. As can be seen from Fig. 5.3, the yield of acetic acid is more in GVL, and after normalizing for the small difference in the extent of reaction of GVL and AMGBL, it is found to be about 5 times the yield in AMGBL for the reaction with Cl. The equivalent ratio in the case of reaction with OH is 2.3.

The product CO_2 formed by reaction with Cl (precursor Cl_2) is quantified in GVL and AMGBL and is found to be similar in both, about 50% of the depletion of the parent molecules.

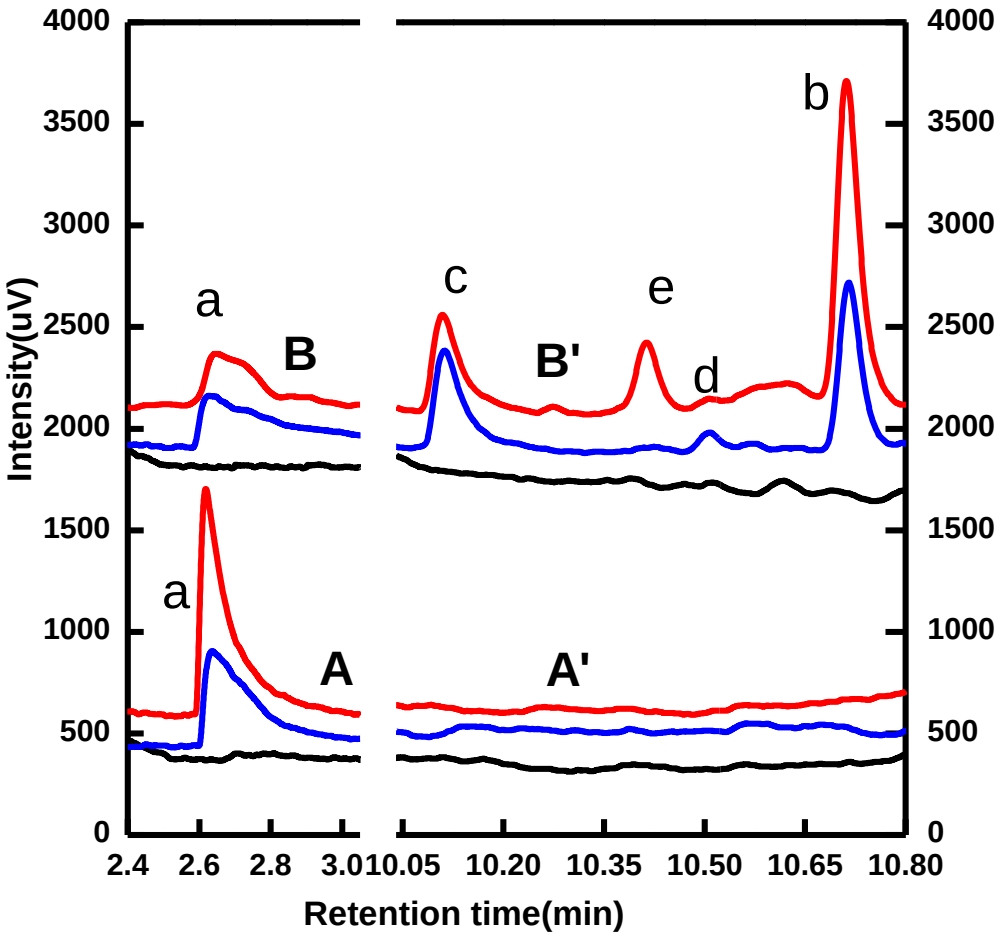

Fig. 5.3. The gas chromatograms (using FID) of the products of Cl (red) and OH (blue) initiated oxidation of GVL (A, A') and AMGBL (B, B') using GSBP8 column. Peaks a: acetic acid, b: 3,4-dihydro-3-methyl-2,5-furandione, c, d and e: unknown.

5.4. Discussion

5.4.1. Rate coefficients and products

The current experimental value of the rate coefficient of the reaction of OH with GVL is marginally lower than that reported by Barnes et al. [114] but higher than the one reported by Dóbé et al. [115]. Barnes et al. have used a relative rate method with FTIR

detection, using ethene as a standard, whereas Dóbé et al. [115] have used discharge flow and pulsed photolysis-resonance fluorescence as the method to determine the rate coefficients. The lower value reported by them is likely due to low-pressure conditions of the experiment. If the latest IUPAC recommendation for the rate coefficient of the OH reaction with the reference molecule ethene is used, the value reported by Barnes et al. is 2.61×10^{-12} $cm^3molecule^{-1}s^{-1}$, which is close to the present determination, on considering the error limits.

Barnes et al. have theoretically computed the rate coefficients of the reactions of GVL and AMGBL with OH, which were found to be 3.01×10^{-12} and 1.36×10^{-12} $cm^3molecule^{-1}s^{-1}$, respectively, for these two molecules with similar ring size [114]. These values are weighted averages of the rate coefficients computed for the two conformers, with the methyl group axial and equatorial to the plane of the ring. The current experimental value of the rate coefficient in the case of AMGBL is close to its theoretically computed value, whereas that of GVL with OH shows marginal differences. The chemistry of GVL and AMGBL following the H atom abstraction by OH/Cl is very different as indicated from the observed products. While the formation of acetic acid as the only major product indicates ring opening as the prominent reaction of GVL, and the ring oxidation is the major reaction of AMGBL. The yield of acetic acid after normalizing for the extent of reaction, and hence the contribution of the ring opening in AMGBL is only about 20% of that in GVL in Cl reaction. The equivalent value in the case of OH reaction is about 50%. The possible origin of this different behavior is contemplated below, based on the reported theoretical computations results [114].

There are different types of H atoms that can be abstracted in both the molecules, attached to different carbon atoms, numbered as shown in the structures in the Introduction Section. The *ab initio* calculations at M06-2X/6-311++G(d,p) level show the H abstracted radical at C5 (ΔH = -22.0 kcal mol^{-1}) and the radicals at C3 (ΔH = -22.3 kcal mol^{-1}) are energetically comparable in GVL. In AMGBL, the lowest energy radical is the radical at C3, (ΔH = -27.1 kcal mol^{-1}) whereas ΔH of formation of other radicals vary from -18.5 to -20.3 kcal mol^{-1}. These results are comparable to those obtained by Barnes et al., [114]. Based on the radical stability, the reaction at C3 and C5 are expected to be dominating in GVL and that at C3 in AMGBL. The bond dissociation energies of the C-H bond, calculated at CBS-QB3 level in GVL are also found to be the lowest 95.6 and 96 kcal mol^{-1} at C3 and C5, respectively [107]. However, a closer look at the computed rate coefficients of reaction of OH at each carbon atom based on TST [114] suggests that the abstraction from C5 is the only important channel in GVL, whereas abstraction from C3 as well as C5 is important in AMGBL, mainly due to low lying transition states. The computed rate coefficients for H abstraction from C5 are 3.22×10^{-12} and 0.94×10^{-12} $cm^3molecule^{-1}s^{-1}$ in the equatorial and the axial conformers of GVL, respectively, with the corresponding total rate coefficients being 3.63×10^{-12} and 1.29×10^{-12} $cm^3molecule^{-1}s^{-1}$. Thus, almost 90% of the reaction in the case of equatorial conformer and 72% in the axial conformer proceed through abstraction of H atom attached to the C5 carbon, where methyl group is also attached, leading to a weighted average of 85% for abstraction from C5 carbon in GVL. This is expected as the tertiary C-H bond dissociation energies are lower than the secondary C-H bond dissociation energies [117]. The presence of methyl

group is specifically known to decrease the bond dissociation energy of the C-H bond on the ring carbon atom in methyl furanones [118]. However, in the case of AMGBL, abstraction of H atom at C5, the carbon next to O atom is also found to be significant, along with abstraction from C3, where the methyl group is attached. In the equatorial conformer (about 70% of total) the reaction at C3 is 54% and at C5 is 33%, the rate coefficients being 1.74×10^{-12} and 1.04×10^{-12} $cm^3molecule^{-1}s^{-1}$, along with a small contribution from methyl H atoms ($k = 0.33 \times 10^{-12}$ $cm^3molecule^{-1}s^{-1}$). In the case of axial conformer, the contribution is 33% at C3 and 54% at C5, the corresponding rate coefficients being 0.44×10^{-12} and 0.73×10^{-12} $cm^3molecule^{-1}s^{-1}$. Thus, 49 % of H atom abstraction is only expected at C3 and 36 % at C5, based on the theoretical estimations. The observed product distribution in the present study, where a single product and thus a single channel dominates, matches well with the prediction based on the rate coefficients of individual channels of reaction of OH with GVL. This suggests the reactions to be kinetically controlled. The weakening due to the presence of methyl group as well as the presence of neighboring O atom together act on the H atom at C5 position, leading to the dominance of its abstraction. On the other hand, presence of at least two different types of products and computed rate coefficients both suggest two channels to dominate in AMGBL.

The rate coefficients of reaction of OH and the relative reactivity at different carbon atoms discussed above, based on the computational results, are found to agree well with the predictions from the Structure Activity Relationship (SAR) developed by Kwok and Atkinson (1995) [61]. The total rate coefficient estimated using SAR by considering $–CH_2-$, not $-CH_2C(O)-$ as the neighbouring group of C4 is 4×10^{-12}

$cm^3molecule^{-1}s^{-1}$ for GVL, very close to the theoretical estimation of Barnes et al. (3×10^{-12} $cm^3molecule^{-1}s^{-1}$). The SAR also predicts abstraction from C5 to be the most important channel with about 20% contribution from C4. The contribution from C4 (48%) is predicted to be more than that from C5 (41%) by SAR if $-CH_2C(O)-$, not $-CH_2-$ is considered as the neighbouring group of C4. However, activation due to the presence of carbonyl group appears to be not important in cyclic ketones as earlier observed by Dagaut et al. [119] in the case of cyclobutanone and cyclopentanone. Similar SAR prediction of the total rate coefficient of AMGBL is 3.78×10^{-12} $cm^3molecule^{-1}s^{-1}$, whereas the computed value is 2.76×10^{-12} $cm^3molecule^{-1}s^{-1}$. The SAR predicts almost similar reactivity for C3 (34%), C4 (27%) and C5 (36%) in AMGBL, but the computation shows abstraction from C3 and C5 to be dominant with about 10 % contribution from the methyl group.

Based on the above discussion, the major channels of reactions of OH with GVL and AMGBL and the primary products are identified as shown in Scheme 5.1. The dehydrogenation of the radical at C3 gives angelica lactone, which is found to be a very minor product in GVL. Hence, the major channel of further reactions of C3 radical can be considered to be dissociation leading to acetic acid. In general, possibility of dissociation is also known to be more in branched radicals. The calculations suggest the formation of tertiary radical and hence the possibility of ring opening to be about 1.7 times more in GVL than that in AMGBL if all these tertiary radicals lead to ring opening and formation of acetic acid, which is close to the observed ratio of 2.3.

Although the rate coefficients of the reactions of Cl with GVL and AMGBL are not theoretically estimated, the behavior is expected to be very similar to that of the reaction

of OH radical. The product distribution, i.e., the absence of ring oxidized products in Cl reaction with GVL implies that the reaction follows the same pathway as OH, abstraction of H atom from C5 (tertiary carbon) being the preferred channel in the reaction of Cl with GVL also. Preferential abstraction of hydrogen atom from C5 by H atom and methyl radical has been reported during the pyrolysis of GVL at high temperatures relevant to combustion [108]. In this work, the authors have carried out theoretical and experimental study on further dissociation of the primary radical products of H atom abstraction reactions at high temperature, and identified all the pathways of consumption of GVL, which are mainly unimolecular dissociation reactions. They noted the possibility of formation of carboxylic acids, mainly pentenoic acid, in the exhaust of an engine upon combustion of GVL, which calls for further investigations to understand the impact of GVL combustion on the air quality. The present results show the formation of acids, i.e., acetic acid, upon tropospheric oxidation. However, unlike the pyrolysis conditions, the present experiments at ambient temperature are in the presence of oxygen. Hence direct dissociation of the primary product radicals may be negligible and they are likely to react with the excess of oxygen, yielding peroxy radicals, or an alkene by removal of HO_2.

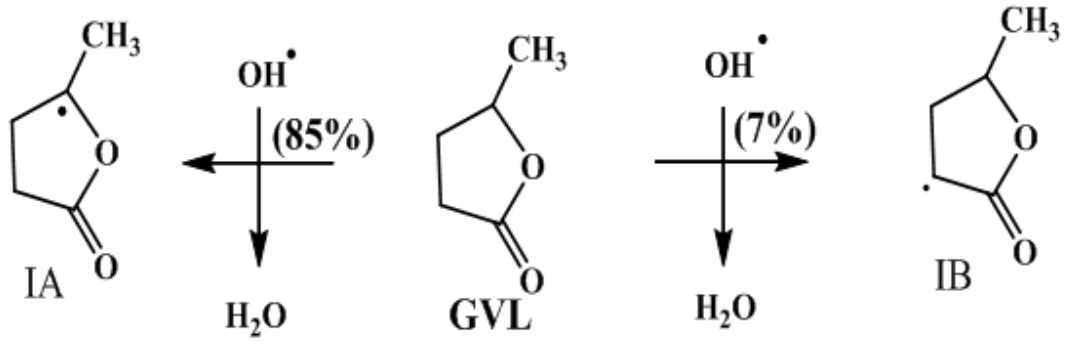

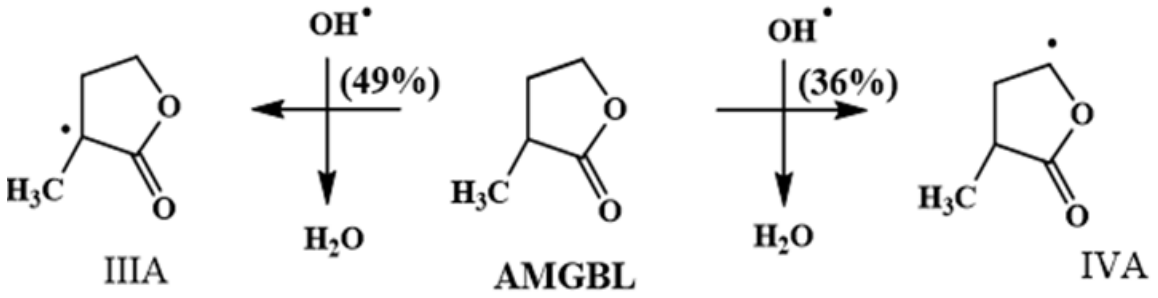

Scheme 5.1: Schematics of the prominent primary channels of reaction of OH with GVL and AMGBL.

In the atmospheric conditions, the peroxy radicals are converted to alkoxy radicals by their reaction with NO. In the absence of NO, as in the present experimental conditions, bimolecular reaction of peroxy radicals can generate two alkoxy radicals or a pair of alcohol and carboxy compound or their reaction with HO_2 radical can lead to the formation of hydroperoxide [1]. The alkoxy radicals are further converted to the corresponding ketones in the presence of oxygen. Although the alkoxy radical of equivalent hydrocarbon, cyclopentoxy radical, is known to undergo ring opening [120], the present results show ring oxidation to be the major reaction of the alkoxy radical at C5 position in AMGBL. Similar ring oxidation is reported in the case of cyclic ether, tetrahydropyran (THP), where Cl / OH initiated oxidation is dominated by abstraction of α-H atom and the peroxy radical generated is reported to give tetrahydropyranone, tetrahydropyranol, unsaturated dihydropyran etc. as the major products [110]. Ring retaining oxidation products have been reported in the case of low temperature (400 – 700 K) oxidation of the 5-membred cyclic ether, tetrahydrofuran (THF) also, along with ring

opened products [121]. A scheme showing the reactions of AMGBL leading to the formation of 3,4-dihydro-3-methyl-2,5-furandione is given below as IVD in Scheme 5.2.

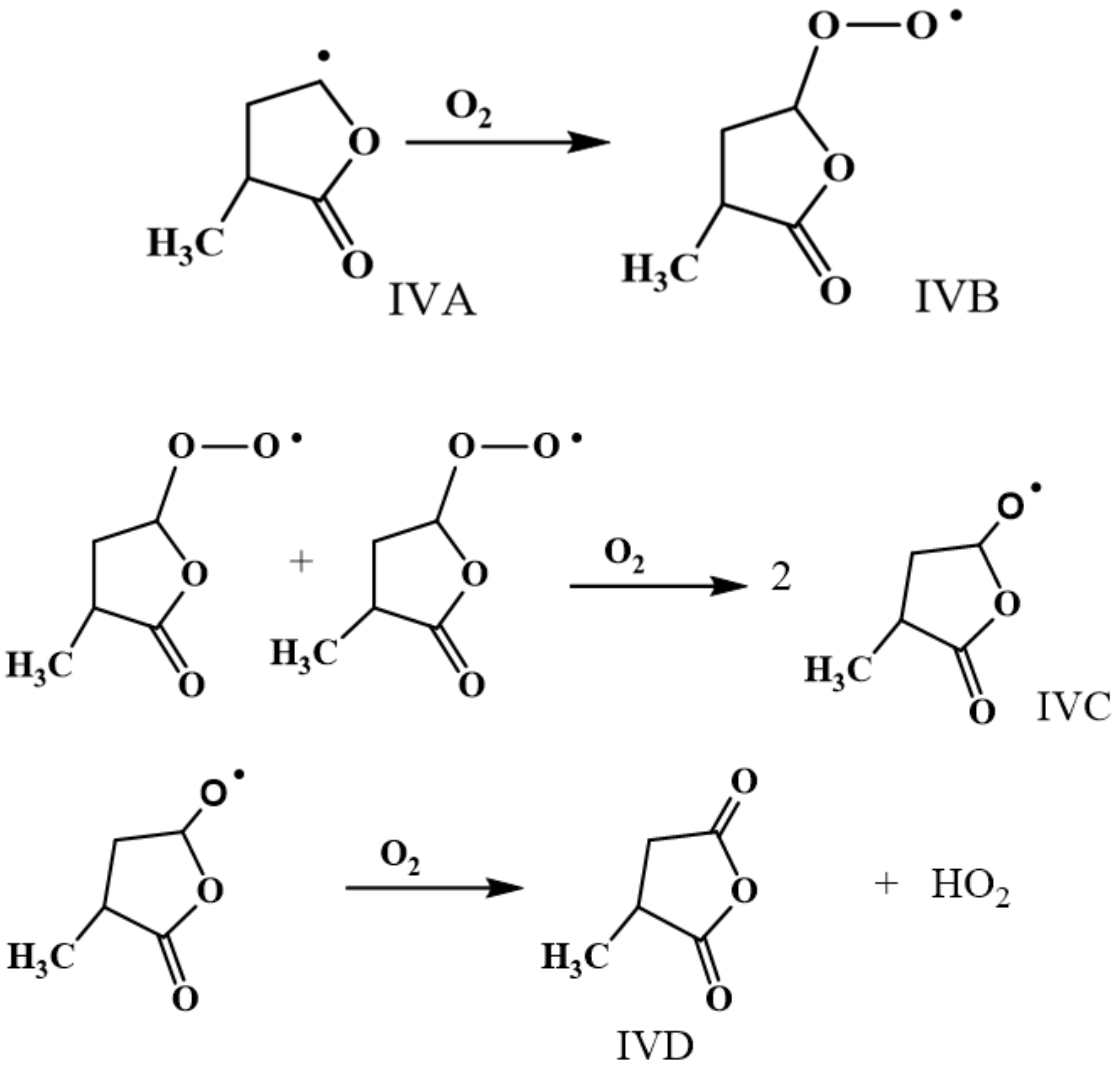

Scheme 5.2: Schematics of the reactions of C5 radicals in AMGBL leading to 3,4-dihydro-3-methyl-2,5-furandione (IVD).

The formation of acetic acid, confirmed by MS as well as FTIR, and the absence of cyclic ketone as a major product in GVL imply the ring opening to be the most dominant pathway of C5 radicals in GVL and C3 radicals in AMGBL. It is difficult to

assign all the reactions leading to acetic acid at this stage. During pyrolysis of GVL, acetic acid is found to be an important product, which is formed via isomerisation to pentenoic acid, followed by dissociation [107]. Under ambient conditions, these reactions are not likely to take place. The ring opened products in tetrahydropyran (THP) under similar conditions have been identified as propyl formate and butyl formate [110]. Similar ring opening reactions of alkoxy radicals IC and III C, formed via peroxy radicals of IA and IIIA can take place as depicted in Scheme 5.3. The GC-MS analysis does not show any product directly related to these structures, ID and IIID (Scheme 5.3), probably indicating further fragmentation of these radicals. Hence, it is proposed that under the present experimental conditions further oxidation and fragmentation of these radicals take place, leading to acetic acid and other unidentified products. Further experiments with higher sensitivity and resolution may be required for identifying the other products. In any case the present results confirm the occurrence of ring opening reactions in GVL as the dominant pathway and both ring opening and ring oxidation reactions in AMGBL. The observation of succinic anhydride in GVL as very minor product implies that a minor pathway of the C-CH_3 bond dissociation and ketone formation may be occurring at C5 position in GVL also.

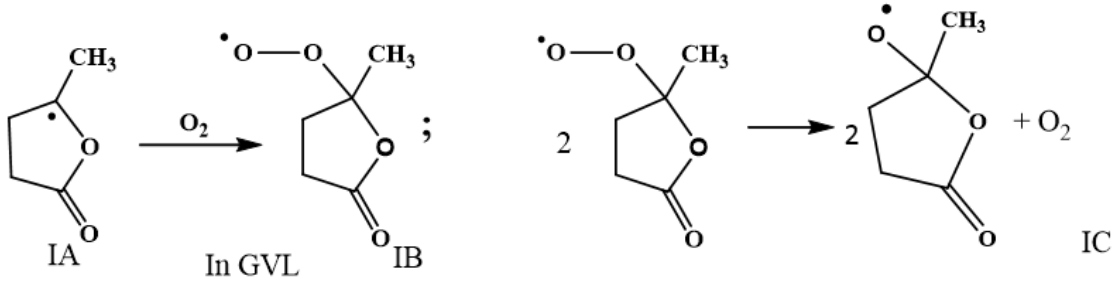

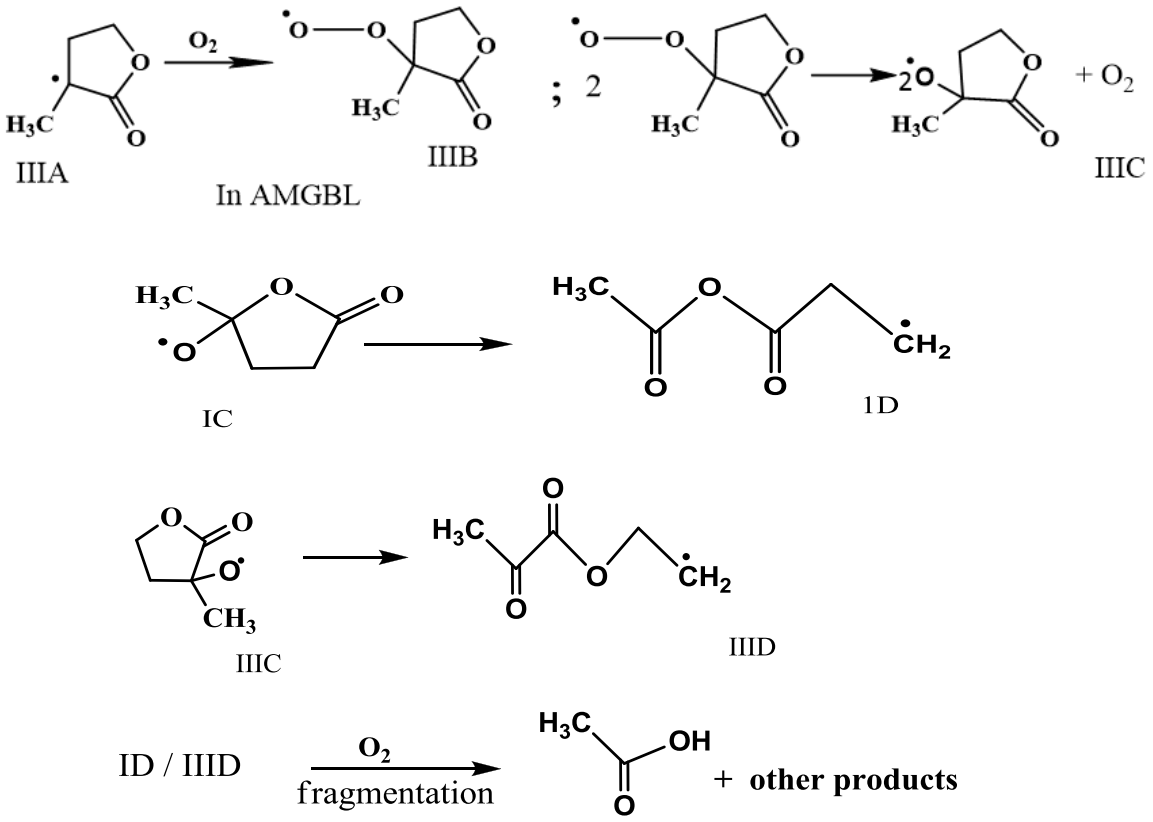

Scheme 5.3: Schematics showing the proposed reactions of secondary radicals in GVL and AMGBL, yielding acetic acid.

By increasing the voltage for GC-MS, only one additional molecule, succinic anhydride, a cyclic diketone without the methyl group, is observed as a minor product in GVL. This could arise from a minor channel of IA by elimination of CH_3 group and ring oxidation as shown in Scheme 5.1.

While the yields of acetic acid support higher possibility of ring opening in the case of GVL, the yields of CO_2 are found to be comparable in both the molecules. This could imply that the channel leading to CO_2 is an independent channel from any of the radicals present. Direct dissociation of the radicals may also be responsible for this. It is

also possible that under the present experimental conditions the products formed at various stages undergo further reactions with oxidizing radicals and get degraded to CO_2.

5.4.2. Atmospheric implications

These lactones are soluble in water and may be distributed in the particle phase as well as in solution phase, from where these can get thermally desorbed continuously. The tropospheric lifetimes of such VOCs vary from 1 day to 10 days depending on the lifetime with respect to precipitation. Meanwhile, oxidation by radicals as described above also takes place in the gas phase, contributing towards the degradation of these molecules in the troposphere and leading to smaller tropospheric lifetimes. All the experimental and computational results indicate that both GVL and AMGBL have similar rate coefficients for their reactions with the OH radical. The lifetimes of GVL and AMGBL, estimated considering only their reactions with OH and Cl (τ_{OH} and τ_{Cl}) based on the respective rate coefficients at 298 K (Table 5.1) are given in Table 5.2. Due to very small concentration of Cl, (1×10^3 molecules cm^{-3}) its reaction is not considered as an important degradation channel in the ambient conditions [74]. However, in the marine boundary layer conditions, with higher concentration of Cl atoms [15,16] the reaction with Cl is found to be significant enough to reduce the lifetime to almost half of that in the ambient conditions (Table 5.2).

Table 5.2: Rate coefficients and tropospheric lifetimes (τ) calculated for cyclic lactones with respect to reactions with OH and Cl. The concentrations used for Cl_{MBL} (under marine boundary layer conditions) [15,16] and ambient OH [122] are 1.3×10^5 and 2×10^6 molecules cm^{-3}, respectively. The rate coefficients are in the unit of $cm^3 molecule^{-1} s^{-1}$.

Molecule	$k_{OH} \times 10^{12}$	$k_{Cl} \times 10^{11}$	τ_{OH} (h)	$\tau_{Cl(MBl)}$ (h)	$\tau_{net(MBL)}$ (h)
GVL	**1.95 ± 0.58**	**2.26 ± 0.53**	**71.2**	**94.6**	**40.6**
AMGBL	**1.81 ± 0.43**	**3.42 ± 0.63**	**76.7**	**62.5**	**34.4**

5.5. Conclusion

The rate coefficients of reactions of OH and Cl with two lactones, gamma-valerolactone (GVL) and alpha-methyl gamma-butyrolactone (AMGBL), are determined. The results indicate that reaction with OH is the major degradation process for both, and reaction with Cl becomes significant only in the conditions of marine boundary layer (MBL). Both the molecules have comparable tropospheric lifetimes in ambient as well as MBL conditions. The oxidation products of these two molecules are found to be very different, probably leading to different tropospheric impact. In the case of GVL, a promising second generation biofuel, acetic acid is the only volatile product observed other than CO_2, whereas in AMGBL the major product is cyclic diketone with lower yield of acetic acid. This appears to be determined mainly by kinetic factors, the abstraction of H atom at the tertiary carbon being the only channel of reaction in GVL and abstraction of both the secondary and tertiary H atoms being important in AMGBL. The activation of hydrogen atom alpha to the ether linkage, boosted by the presence of methyl group appears to be responsible for the dominance of a single channel of reaction leading to fragmentation of the ring. The present results support the benign nature and suitability of GVL as a potential biofuel component, acetic acid being a water soluble molecule and easily removable from the troposphere.

Chapter-6

Reactivity of Ethers with Tropospheric Oxidants: A Comparison between Acyclic and Cyclic Ethers

6.1. Introduction

The compounds with ether functional group are mainly present in the atmosphere due to anthropogenic emissions. Both the straight chain and cyclic ether are released into the atmosphere as these are widely used in various industries as solvents and reagents for chemical synthesis and as anaesthetics in surgery. Due to anaesthetic effects, ethers are also used as illicit drugs to induce sedation and euphoria. In addition, during the low-temperature oxidation of n-alkanes, a range of cyclic ethers has been detected and analysed [123]. As it is well known fact that any VOC released into atmosphere generally gets finally oxidized to CO_2, and during the oxidation pathways many side products and intermediates are formed. As discussed in Chapter 1, the effect of a molecule on environment mostly depends on its lifetime, with respect to oxidation by OH, Cl, O_3, and also on the products it forms during its degradation in the atmosphere. In our earlier study on five- and six-membered cyclic ethers, it was observed that there was no increase in the rate coefficient of Cl reaction with tetrahydropyran (THP) when compared with tetrahydrofuran (THF), in spite of presence of one additional CH_2 group in the former [27]. The same trend was also observed for the OH reaction with THP and THF, unlike in the case of linear 1-alkenes [46] wherein the reactivity was found to depend strongly on the number of CH_2 groups present in the compound. It is interesting to investigate the

effect of the ring strain and presence of substituents on the reactivity of ether. In the present work, kinetics of both the straight chain (dimethyl ether) and cyclic ethers (epichlorohydrin) are studied. Dimethyl ether (DME, CH_3-O-CH_3) is an important commercial compound and precursor in production of many methylating agents. DME is also used as a substitute for LPG (liquefied petroleum gas) and normally referred to as synthetic LPG. As the physical properties of DME and LPG are similar, the blending of DME with LPG is possible. This blending is widespread in developing countries such as India, where safer fuel for cooking and heating is obtained from portable bottle [124]. It burns without smoke and has less particulate formation, and NO_x, SO_x and CO emissions [125]. Hence, DME has the potential to be used as a fuel as an alternative to natural gas and diesel fuel. The detailed combustion study of DME done by Park et al., indicates DME as an ideal fuel replacement for diesel engines [126]. Considering all these uses, the chances of DME to escape into atmosphere are high. Among cyclic ethers, epichlorohydrin (ECH) is an important commercial chemical, and mainly used as an intermediate in the manufacture of many important compounds such as epoxy resins, glycerol, oil emulsifiers and adhesives. It is also used as a solvent for resins, paints and as a stabilizer in chlorine-containing substances such as rubber and pesticide formulations. Hence, it is present in the environment because of its application. ECH has been detected at low levels in wastewater, groundwater and ambient water samples. ECH content in food and drinking water may be as a result of migration from packaging and tubing materials. It can be emitted into atmosphere from all the above uses, as it has sufficient vapour pressure (13 mmHg at 20°C). On the basis of the experiments already carried out on animals, it is understood that ECH is carcinogenic. Moreover, ECH-air mixtures with

3.8-21% ECH by volume are explosive above 34°C and can be ignited by hot surfaces, sparks, and open flames [127]. In the present work, detailed study on degradation of DME and ECH, and characterization of products formed are carried out, the results are presented in this chapter in two parts (A and B). In addition, the reactivity of straight chain and cyclic ethers are discussed along with the effect of a substituent on the reactivity. The reactivity of ether with OH and Cl is also compared with other hydrocarbons to understand the effect of O atom as well as the ring size on the reactivity.

Part A: Kinetics of dimethyl ether (DME)

Since DME is used extensively, it is manufactured in large scale from natural gas and carbon-containing feedstocks, including coal and biomass. DME is released into the atmosphere from its production plants and various applications. It is volatile (boiling point -23°C) and exists primarily in the gas phase, when released into the atmosphere. It is one of the largest organic molecules found in the interstellar gas [128]. It is a linear saturated ether, and the major pathway of its removal from the troposphere is by reaction with the hydroxyl (OH) radicals, and the reaction is initiated by abstraction of H atom from DME (reaction 6.1).

$$CH_3OCH_3 + OH \rightarrow CH_3OCH_2 + H_2O \qquad (6.1)$$

In NO polluted atmosphere, DME forms methyl formate, water, NO_2 and some CO_2 [129]. The reaction of DME with the OH radical is well studied over a range of temperature by both relative [130-132] and absolute [131,133-141] rate methods. Recently, a detailed experimental and theoretical work was carried by Carr et al. [139] at an extended range of temperature (260-450 K) using laser flash photolysis (LFP) coupled to laser induced fluorescence (LIF) for detection of OH. The rate coefficient measured

showed a curvature in the Arrhenius plot over the tropospheric temperature range. They have also studied isotope effect by investigating the reaction of the OH radical with deuterated DME and the experimentally measured bimolecular rate coefficient k was complemented with theoretically calculated k. Bänsch et al. [141] also reported a similar type of detailed experimental and theoretical work on reaction of the OH radical with DME in temperature range of 292-650 K and at very high pressure range of 6-21 bar. Shannon et al. [140] carried out experiments using the same technique at lower temperature range of 63-148 K. The rate coefficient shows marked inverse temperature dependence at low range and a significant curvature in the Arrhenius plot. The rate coefficient also showed the pressure dependence at low temperatures. They also found a decrease in the rate coefficient in the presence of O_2, due to recycling of OH from the reaction of CH_3OCH_2 with O_2.

In the present work, the absolute rate coefficients for the reaction of DME with the OH radical are measured using laser photolysis-laser induced fluorescence (LP-LIF) technique, in the temperature range of 257 to 333 K. The stable products formed in above reactions are characterized using gas chromatography-mass spectrometry (GC-MS) technique. Along with these experimental studies, theoretical calculations are also carried out to understand the reaction mechanism of H atom abstraction. The tropospheric lifetime and the global warming potential (GWP) for DME are estimated.

Part B: Kinetics of epichlorohydrin (ECH) 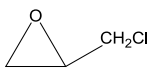

Due to the presence of both a chlorine atom and an epoxide ring in the ECH molecule (also known as chloromethyloxirane, C_3H_5ClO), it is widely used as a chemical intermediate in a variety of chemical reactions and also added as a stabilizer to prevent

oxidation of compounds. Not much work is reported on the reaction of ECH with tropospheric oxidants. To best of our knowledge, only two reports are available for the determination of rate coefficient of its reaction with the OH radical [142,150]. Orkin et al. [142] have studied this compound in the temperature range of 230−370 K using flash photolysis resonance-fluorescence technique. Edney et al. [150] have measured the room temperature (296 K) rate coefficient for this reaction using a relative rate method taking butane as a reference. The room temperature rate coefficient for the reaction of ECH with OH reported in the above two studies differ significantly.

Presently, the room temperature rate coefficients (k_{Cl} and k_{OH}) for the reaction of ECH with OH and Cl are measured by a relative rate method (using Gas chromatography technique) and also by an absolute method, the OH radical reaction using LP-LIF technique. The tropospheric lifetime and the ozone depletion potential (ODP) for ECH are estimated. An attempt is also made to understand the reactivity trend, due to presence of heteroatom (chlorine) in ECH, with propylene oxide, and other similar cyclic molecules studied earlier in our laboratory [26,27] in order to see the effect of the ring strain.

6.2. Experimental

6.2.1. Rate coefficient measurement using absolute method by LP-LIF technique

An absolute method is used for the rate coefficient measurement of the reaction of dimethyl ether (DME) and epichlorohydrin (ECH) with the OH radical. The methodology and experimental conditions are described in Chapter 2.

The DME / ECH sample diluted by N_2 gas is prepared in a passivated stainless steel (SS) container. The exact concentration of the DME/ECH in the SS container is

measured before and after the experiment from the calibration curve prepared using the FTIR spectrophotometer. The stability of the gas mixture is monitored over the time period of two weeks by comparing the FTIR spectra. The mass flow controllers (MFCs) are used to regulate the ratios of the different chemical components, the DME / ECH in N_2 gas, the precursor for the OH radicals and buffer gas (N_2). A constant flow of 7 (4) SCCM N_2 gas is bubbled through 30% (50%) (by weight) H_2O_2 solution in case of DME and ECH, in all the experiments, and subsequently it was passed through a trap prior to the premix chamber to arrest any H_2O_2/H_2O droplets from entering the reaction cell. The H_2O_2, DME/ ECH sample and buffer gas, N_2 are mixed in the premix chamber, and flowed into the reaction cell. In the beginning of the measurement H_2O_2 seeded in N_2, and N_2 buffer gas are flown through the reaction cell, without the DME/ECH (blank experiment), until a reproducible initial signal intensity and its decay kinetics are obtained. In the cell, the H_2O_2 concentration is kept constant by maintaining a fixed flow of N_2 through H_2O_2 bubbler. The total pressure in the reaction cell is maintained constant by keeping sum of the flow of DME / ECH in N_2 and N_2 buffer gas constant. The flow velocity of the experimental mixture is kept enough ~12 cm/sec to make sure that a fresh gas mixture is seen by each photolysis laser pulse, at 20 Hz repetition. All the kinetic measurements are performed at a total pressure of ~30(DME) / 15 (ECH) Torr. The number density of the H_2O_2 molecule inside the reaction cell is ~$1x10^{14}$ molecules cm^{-3}. From the laser fluence used for the experiments and the absorption cross section of H_2O_2, the OH radicals concentration in the cell is estimated to be 10^{10} to 10^{12} molecules cm^{-3}. A pseudo-first-order condition is maintained with [DME]>>[OH] and the number density of DME/ ECH in the reaction volume is calculated from the flow rates and the total pressure

in the cell for each experiment. The rate coefficient values are determined in the temperature range of 257–333 K for the reaction of OH with DME but in case of ECH, only room temperature rate coefficient is measured for this reaction. A reaction of DME with the OH radical is also carried out in the presence of oxygen at room temperature, by employing a buffer gas containing oxygen to nitrogen ratio of 20:80.

6.2.2. Rate coefficient measurement using relative rate method

The same experimental conditions and methodology is used as described in Chapter 2. The reaction mixture consisted of EPC (100 – 150 ppm), reference molecule (50 – 150 ppm), and $(COCl)_2$/(O_3-H_2O mixture) (400-500 ppm) along with buffer gas (N_2 / air). In situ photolyses of $(COCl)_2$ and (O_3-H_2O) mixture at 254 nm are used to generate Cl atoms and OH radicals, respectively. The total pressure is maintained at 800 ± 3 Torr. Either packed (stainless steel) or capillary (fused silica) carbowax columns are employed for the separation with suitable conditions of temperature and flow. 1,2-Dichloroethane and ethane are chosen as reference molecules, after satisfying the conditions as described in Chapter 2.

The gases O_2 (UHP, 99.9%), N_2 (UHP, 99.9%), 1,2-dichloroethane (99.5%) and ethane (>99 %) are used as supplied. CH_3OCH_3 (Aldrich, ≥99.9%), C_3H_5OCl (97 %) and H_2O_2 (30 / 50wt %) are stored in evacuated glass vessels, and these are subjected to freeze-pump-thaw cycles to remove trapped air and highly volatile impurities.

6.2.3. IR absorption cross section and GWP calculation

The IR absorption spectra of DME are recorded with a spectrophotometer (Bruker FT-IR, IFS 66v/s FTS system) with a spectral resolution of 1.0 cm^{-1} and 0.1 cm^{-1}, employing a liquid-nitrogen-cooled wide range MCT detector. A metallic absorption cell

(path length 28 cm) attached with KBr windows is used. The position of the cell in the spectrophotometer is optimized such that the baseline shift is the minimum. All spectra are recorded at 298 K temperature.

A known pressure of DME is taken in the cell and total pressure is made up to 760 Torr with nitrogen as a buffer gas. Absorption spectra of DME are recorded at different DME pressures in the linear absorption region, and are converted into absorption cross sections on Y-axis employing the relation (Eqn. 6.2),

$$\sigma(\nu) = \frac{\ln(10) \times A_{DME}(\nu)}{[DME] \times l} \qquad (6.2)$$

where $\sigma(\nu)$ is the absorption cross-section in units of cm^2 $molecule^{-1}$ at wavenumber ν,; $A_{DME}(\nu)$ is absorbance of DME at wavenumber ν, [DME] is the concentration in molecules cm^{-3} of dimethyl ether, and l is the optical path length in cm. From the above data of absorption cross sections, the integrated absorption cross-sections at 1 cm^{-1} band interval are calculated and assigned to the centre of each band. Thus, all the absorption spectra obtained at various pressures of a compound maintaining the total pressure of ~ 760 Torr are converted into absorption cross section spectra, and the mean value of integrated cross section at $1cm^{-1}$ band interval is obtained in a wavelength range of 400-2500 cm^{-1}. These values are employed for the radiative efficiency calculation, using a modified Pinnock curve [36] incorporating the Oslo Line-By-Line model [143], the latter takes into account atmospheres representing the tropics and extra-tropics.

6.2.4. Theoretical calculations

Ab initio MO calculations are performed using the Gaussian 03 [144] program to investigate the potential energy surface (PES) of the reaction of DME with OH. The

geometries of the ground electronic states of DME, the transition-state (TS) structures, are optimized at G3 level. The harmonic vibrational frequencies and the force constants are calculated to ensure the stationary points on the PESs to be true saddle points. All TS structures calculated have only one imaginary frequency and one negative eigenvalue of the force constant matrix.

6.2.5. Stable product analysis

The stable products of the reaction of the OH radical with DME formed in the presence of benign and polluted (NO_X presence) air, at 760 Torr total pressure, are characterized by GC-MS, using BPX50 (30 m × 0.25 mm × 0.25 μm) and CP WAX 52CB (30 m × 0.25 mm × 0.25 μm) columns, independently.

6.3. Results

Part A

6.3.1. Rate coefficient measurement using absolute method

The LIF intensity from OH radicals, generated by photolysis of H_2O_2 at 248 nm, in a flowing mixture of H_2O_2, DME and N_2 (buffer gas) decreases in the detection volume with time due to consumption in the reaction with the reactant DME, H_2O_2 and diffusion out of the viewing zone of the detection system. These processes are accounted by the below mentioned equations for DME.

$$OH + CH_3OCH_3 \xrightarrow{k} CH_3OCH_2 + H_2O \quad (6.1)$$

$$OH + H_2O_2 \xrightarrow{k_1} HO_2 + H_2O \quad (6.3)$$

$$OH \xrightarrow{k_d} diffusion\ out\ of\ the\ detection\ volume \quad (6.4)$$

where k, k_1, and k_d are the rate coefficients for the first two reactions, and diffusion process, respectively. The rate of decrease in the OH concentration is given as,

$$-\frac{d(OH)}{dt} = (k[CH_3OCH_3] + k_1[H_2O_2] + k_d)[OH] \quad (6.5)$$

In all the experiments, the conditions, $k[CH_3OCH_3][OH] >> k_1[H_2O_2][OH]$, $[H_2O_2] \approx$ constant and the total pressure = constant, are maintained. $[H_2O_2]$ is nearly constant during the reaction time as $[H_2O_2] >> [OH]$, a small fraction of $[H_2O_2]$ being photolyzed by the photolysis pulse, and the diffusion rate of OH radicals is also constant as flow velocity of the reaction mixer and the total pressure in reaction cell remain constant throughout the experiment. Thus, the above equation simplifies to

$$-\frac{d(OH)}{dt} = (k[CH_3OCH_3] + k'_d)[OH] \quad (6.6)$$

where k'_d represents $k_1[H_2O_2] + k_d$. Since $[OH] << [CH_3OCH_3]$ we have $k[CH_3OCH_3] + k'_d = k'$ (pseudo-first order rate coefficient), and solving the differential equation leads to

$$[OH]_t = [OH]_0 \exp(-k't) \quad (6.7)$$

To obtain the pseudo-first order rate coefficient (k'), a weighted linear least-square fit of $\ln[(LIF)_t/(LIF)_0]$ with time is plotted as shown in Fig. 6.1.

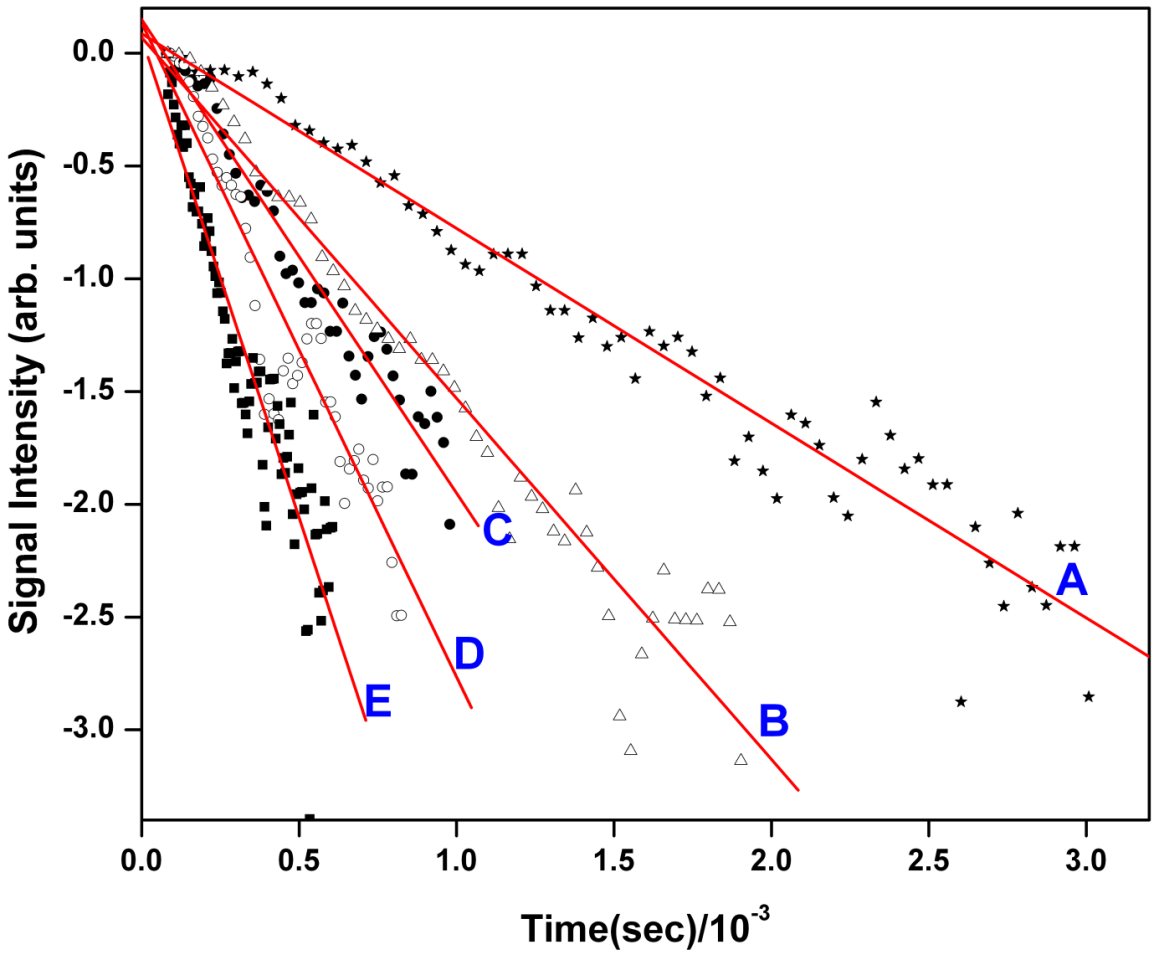

Fig. 6.1. Typical decay profiles of the OH radicals at a room temperature (297 K), with increasing concentration of DME for various plots: A = 4.6 × 10^{14}; B = 9.6 × 10^{14}; C = 1.4 × 10^{15}; D = 2.1 × 10^{15}; and E = 3.1 x 10^{15} moleculescm^{-3}. These plots fit into the first-order kinetics Eqn. (6.7), shown as solid lines.

On plotting k' versus [DME], the bimolecular rate coefficient k at room temperature (297 K) is found to be (2.7 ± 0.2) x 10^{-12} cm^3 molecule^{-1} s^{-1}. At least three measurements are taken at each concentration of [DME] to ensure consistency.

Any contribution to the measured rate coefficient from secondary reactions involving photolysis products of DME is insignificant, as DME has negligible absorption

at 248 nm. Moreover, the stable product analysis by gas chromatography, after irradiation of DME at 248 nm using KrF laser, did not show any depletion, indicating the absence of photodissociation of DME at this wavelength. The average values of the bimolecular rate coefficient ($k(T)$) measured at different temperatures and 30 Torr of pressure are given in Table 6.1. At least three measurements are taken at each temperature to get reliable data.

Table 6.1: The rate coefficient data for the reaction of OH radicals with DME at different temperatures.

Temperature (K)	**[DME]/10^{14} (molecules cm^{-3})**	**k/10^{-12} (cm^3 $molecules^{-1}$ s^{-1})**
256	3.0–30.0	2.1 ± 0.2
269	2.7–19.0	2.4 ± 0.2
280	2.3–24.0	2.5 ± 0.2
297	2.2–30.0	2.7 ± 0.2
313	2.1–22.0	2.9 ± 0.3
333	2.2–21.0	3.0 ± 0.4

The quoted errors given in the Table 6.1 correspond to 2σ of the linear regression. In addition to systematic errors, the errors in the measurements of the partial pressure of the sample and the flow rate contribute to the uncertainty in the concentration measurement, which add additional l5% error in the measured rate coefficient. The error bars are depicted in the Arrhenius plot (Fig. 6.2).

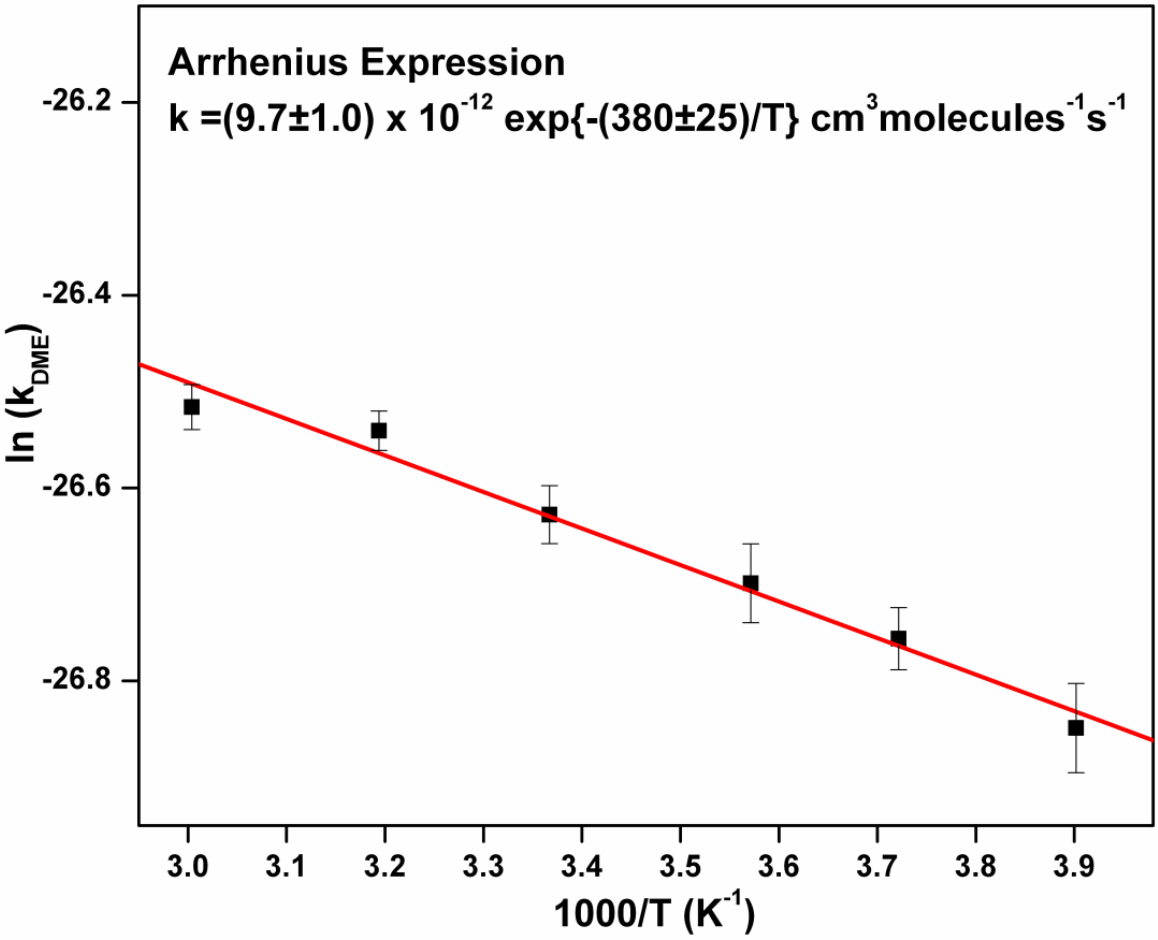

Fig. 6.2. Arrhenius plot for the reaction DME + OH, with errors corresponding to the overall uncertainty of the experimental rate measurement for k at 2σ level of confidence.

The data in the measured temperature range fit well with the Arrhenius expression given as

$$k = (9.7 \pm 1.0) \times 10^{-12} exp\{-(380 \pm 25)/T\} cm^3 molecules^{-1} s^{-1} \quad (6.8)$$

The plot is linear within the temperature range studied, and the E_a/R value estimated from the plot is 380 ± 25 K, for reaction (6.1). This corresponds to the activation energy (E_a) of ~3 kJ mol^{-1}, which is the same as reported by Carr et al. [139] over the temperature range of 260-450 K.

In order to see the effect of oxygen, the rate coefficient is also measured in the oxygen atmosphere for the OH radical reaction with DME at 298 K. However, no noticeable effect of O_2 on the rate coefficient is observed, and the rate coefficient remained the same within the experimental error. However, Shannon et al. [140] and Eskola et al. [145] observed that presence of O_2 affects the rate coefficient. Shannon et al. found a decrease in the rate coefficient in presence of O_2, and explained the effect with a proposed adduct formation between CH_3OCH_2 and O_2 at lower temperature. The difference in the effect of O_2 on the rate coefficient can be ascribed to different temperature and pressure of O_2 used in these experiments. These results indicate that in our experimental temperature range with the O_2 concentration used, the OH regeneration does not play a significant role on the rate coefficient of OH with DME.

6.3.2. Stable products analysis

The stable products for the reaction are analyzed in presence and absence of NO atmosphere, using gas chromatography coupled with mass spectrometry technique. Methyl formate is detected as one of the stable products in both the cases. This observation supports the mechanism given by other researchers [129,136,146]. The reaction pathways proposed for formation of methyl formate $CH_3OC(O)H$ in presence and absence of NO are as follows

Presence of NO:

$$CH_3OCH_3 + OH \rightarrow CH_2OCH_3 + H_2O \quad (6.1)$$

$$CH_2OCH_3 + O_2 + M \rightarrow O_2CH_2OCH_3 + M \quad (6.9)$$

$$O_2CH_2OCH_3 + NO \rightarrow OCH_2OCH_3 + NO_2 \quad (6.10)$$

$$OCH_2OCH_3 + O_2 \rightarrow HO_2 + CH_3OC(O)H \quad (6.11)$$

Absence of NO:

In the absence of NO also the reactions remain similar as in its presence, except for reaction (6.10) leading to formation of OCH_2OCH_3, which is now produced through reaction (6.12).

$$2O_2CH_2OCH_3 \rightarrow 2\ OCH_2OCH_3 + O_2 \quad (6.12)$$

The NO molecule reduces the $O_2CH_2OCH_3$ radical and gets itself oxidized to NO_2. In absence of NO, two $O_2CH_2OCH_3$ radicals interact and O_2 molecule is formed with OCH_2OCH_3 radical. Further, O_2 abstracts H atom from an α carbon of OCH_2OCH_3 radical and methyl formate is formed. From the above reaction scheme, we can expect the formation of methyl formate to be more likely in presence of NO. However, in the present studies, insignificant difference in the quantum yield of formate is observed in the experimental conditions of presence and absence of NO.

Part B

6.3.3. Rate coefficient measurements of epichlorohydrin (ECH)

$$OH/Cl + C_3H_5OCl \xrightarrow{k_{Epichlorohydrin}} Products \quad (6.13)$$

ECH + Cl

In case of the ECH reactions with Cl atom, the photolysis of $(COCl_2)_2$ at 254 nm is used to generate Cl atom. The rate coefficient for the reactions of Cl atom at 298K with the reference compound, 1,2-dichloroethane considered here is $(1.30 \pm 0.20) \times 10^{-12}$ cm^3 $molecule^{-1}s^{-1}$ [147]. The typical relative rate plot for the decay of ECH with 1,2-dichloroethane as a reference molecule is shown in Fig. 6.3, with N_2 as a buffer gas. The slopes of the linear least square fits correspond to the ratios of the rate coefficients,

$k_{ECH}/k_{1,2\text{-Dichloroethane}}$, and the average values of k_{ECH} are listed in Table 6.2. The ratio given is the average values of slopes from a number of measurements (indicated in parentheses). The method of error calculation is the same as described in Chapter 2.

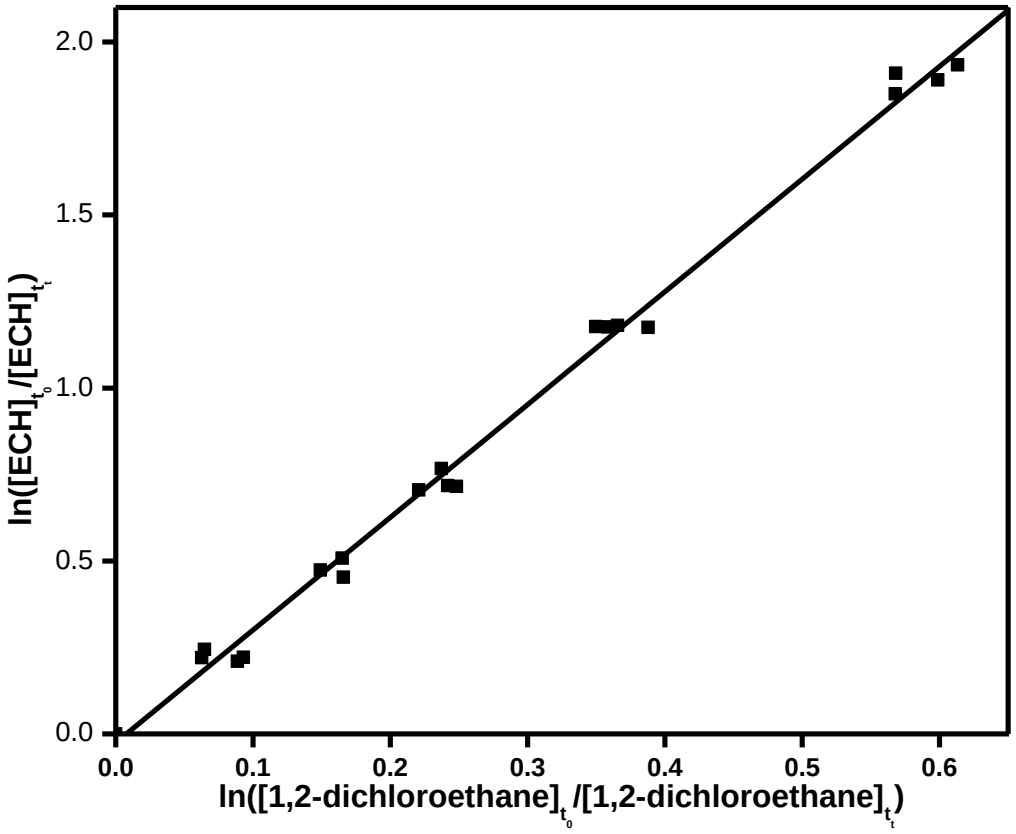

Fig. 6.3. Decays of ECH due to reaction with Cl atom, relative to 1,2-dichloroethane in 800 Torr of N_2.

ECH + OH

In case of ECH reactions with OH radicals, the photolysis of H_2O_2 at 254 nm is used to generate OH radicals. The rate coefficients for the reactions of OH at 298K with

reference compounds, 1,2-dichloroethane and ethane used here, are $(2.80 \pm 0.60) \times 10^{-13}$ [148] and $(2.40 \pm 0.33) \times 10^{-13}$ molecule^{-1} cm^3 s^{-1} [58], respectively.

Table. 6.2: Relative ratios and room temperature rate coefficients of the reactions of OH/Cl with ECH with different reference molecules, [ECH] = 100 - 150 ppm, [R] = 50 - 100 ppm, Buffer gas – (N_2 and air), Total pressure = 800 Torr. Absolute rate coefficients at room temperature for the reactions of OH with ECH at 15 Torr pressure.

Oxidant	**Reference molecule**	**Buffer gas**	**Average slope**	**Rate coefficient k_{298} ($cm^3 molecule^{-1} s^{-1}$)**	**Method**
Cl	1,2-Dichloroethane	N_2 (5)	3.25 ± 0.02	$(4.22 \pm 0.65) \times 10^{-12}$	RRM
	$(1.30 \pm 0.20) \times 10^{-12}$ [149]				
OH	Ethane $(2.40 \pm 0.33) \times 10^{13}$ [58]	N_2 (5)	1.01 ± 0.14	$(2.42 \pm 0.47) \times 10^{-13}$	RRM
	1,2-Dichloroethane $(2.80 \pm 0.60) \times 10^{-13}$ [148]	N_2 (5)	1.99 ± 0.16	$(5.57 \pm 1.27) \times 10^{-13}$	RRM
		N_2 (3)		$(3.78 \pm 0.16) \times 10^{-13}$	Absolute

The typical relative rate plots for the decay of ECH due to the reaction with OH, relative to ethane and 1,2-dichloroethane as reference molecules are shown in Fig. 6.4, with N_2 as a buffer gas. The slopes of the linear least square fits correspond to the ratios of the rate coefficients, k_{ECH}/k_{Ethane} and $k_{ECH}/k_{1,2\text{-Dichloroethane}}$, and the average calculated values of k_{ECH} with respect to both the references are listed in Table 6.2. The ratio given is average values of slopes from a number of measurements (indicated in parentheses).

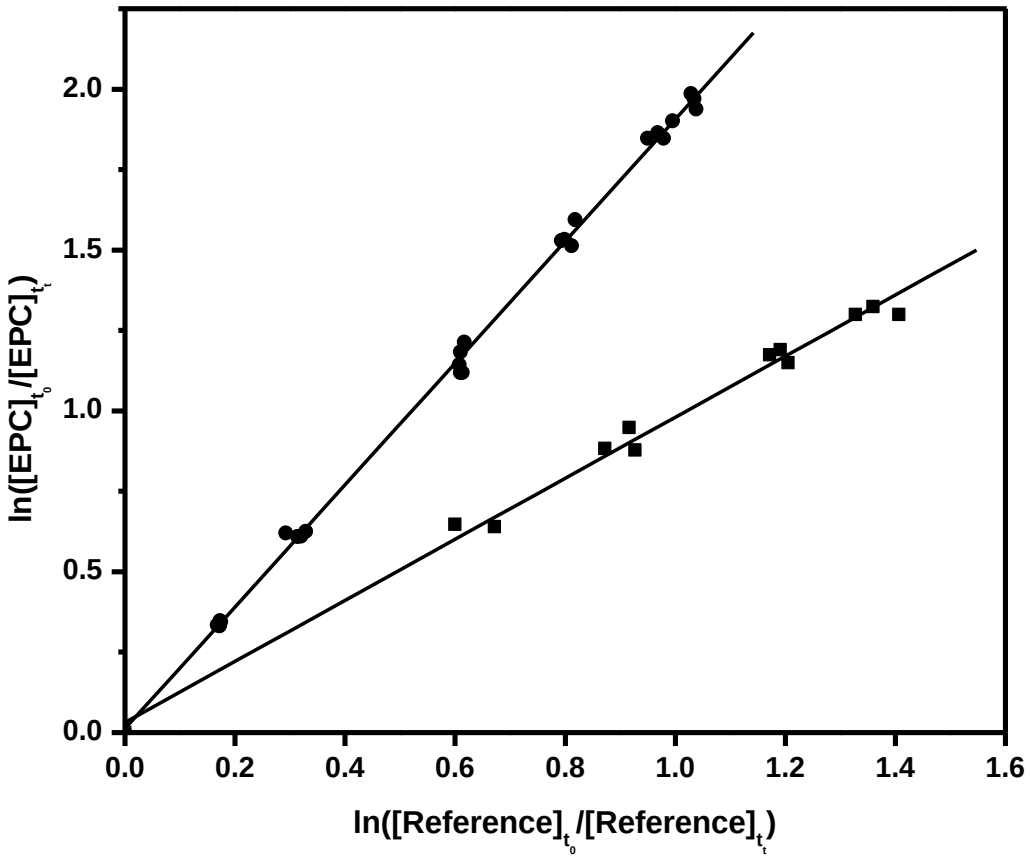

Fig. 6.4. Decays of ECH due to reaction with OH, relative to ethane (■), 1,2-dichloroethane (●) in 800 Torr of N_2.

In addition, the absolute value of the rate coefficient for the ECH reaction with the OH radical is also measured by laser photolysis-laser induced fluorescence (LP-LIF) technique at 298 K and 15 Torr total pressure. The procedure adopted for the rate coefficient measurement of ECH with OH is similar to that of DME.

$$OH + C_3H_5OCl \xrightarrow{k_{Epichlorohydrin}} Products \qquad (6.\ 13a)$$

The pseudo-first order rate coefficient, k_1 is obtained from a weighted linear least-squares fit of the logarithm of the ratio of signal intensity, $\ln[(LIF)_t/(LIF)_0]$, with time at different concentrations of ECH. A similar type of plot is obtained as in DME. Then these values of pseudo rate coefficients k_1 are plotted against the concentration of ECH, as shown in Fig. 6.5, and using the slope of the line, the bimolecular rate coefficient k_{ECH} is determined (given in Table 6.2).

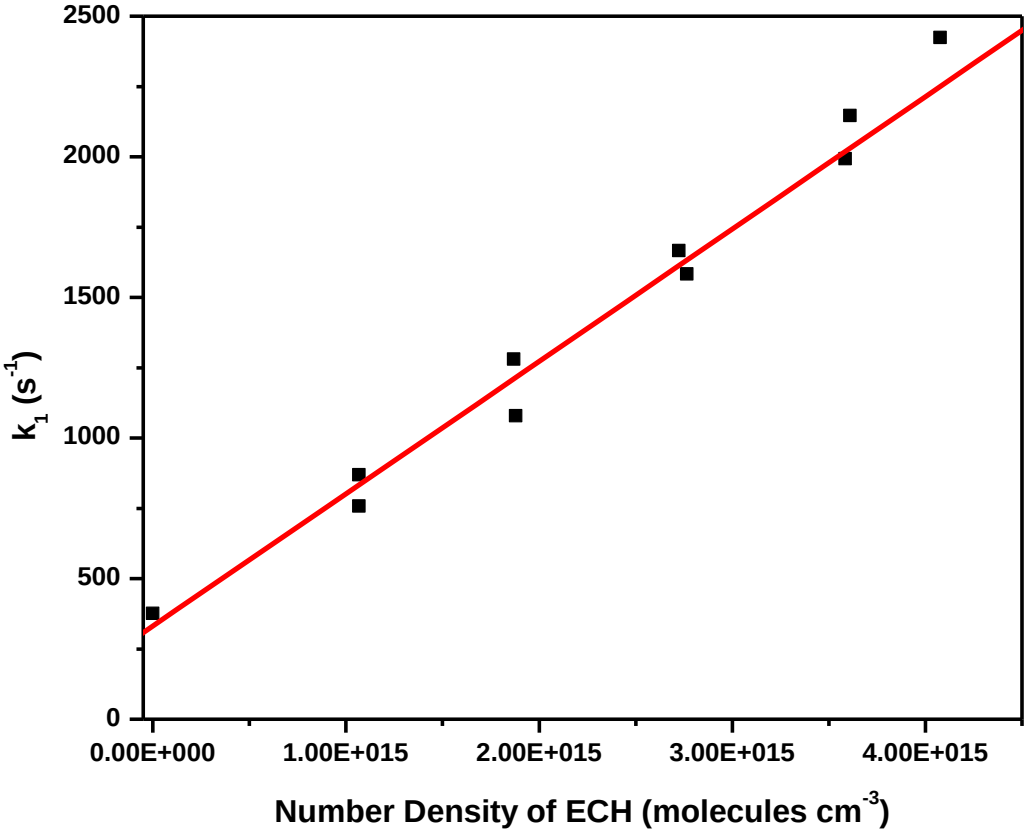

Fig. 6.5. Variation of the pseudo-first order decay coefficient with the concentration of ECH at room temperature.

6.4. Discussion

Part A: Dimethyl Ether (DME)

6.4.1. Kinetics and mechanism of the OH reaction with DME

DME belongs to the C_{2v} point group, with two equivalent C–O bonds and two distinct hydrogen environments. With geometry consideration, the hydrogen atoms in DME can be classified into two categories, which are in-plane and out-of-plane H atom. Thus, three possible H-abstraction channels for the reaction of DME with OH exist, and

these are in-plane hydrogen abstraction (through TS_1), the out-of-plane hydrogen abstraction with H atom of OH directing downwards (through TS_2) and the out-of-plane hydrogen abstraction with H atom of OH directing upwards (through TS_3). These TS structures are shown in the potential energy diagram (Fig. 6.6). The reactants form a pre-reactive complex first, and then subsequently produce reaction products through the TS structures shown in Fig. 6.6. The pre-reactive complex between OH and DME is stabilized by 22.2 kJ mol^{-1} due to hydrogen bonding between H atom of OH with the O atom of DME. This value agrees with that reported by Carr et al., [139] calculated using CCSD method, and Bänsch et al., [141] calculated using MP2, CCSD(T) and CBS-QB3 methods. The energies of 11.7 kJ mol^{-1} for TS_1, -4.3 kJ mol^{-1} for TS_2 and -2.6 kJ mol^{-1} for TS_3 are calculated with respect to the reactant molecules DME and OH. The abstraction of the in-plane hydrogen by the OH radical requires higher energy than that of both out-of-plane hydrogen atom abstractions. The TS_2 and TS_3 structures are energetically similar with a negligible energy difference of about 2 kJ mol^{-1}. The calculated energetic and the proposed reaction mechanism are similar to those reported by Carr et al. [139] and Bänsch et al. [141]. The experimental value of the activation energy for the reaction is found experimentally to be ~3 kJ mol^{-1} from the Arrhenius plot. The reaction mechanism considering pre-reactive complex is predicted to have the lowest energy barrier of 17.9 $kJmol^{-1}$, and it is slightly higher than the measured activation energy. The energy barrier calculated at the G3 level is found to be in reasonably good agreement with that at higher level of theory by Carr et al. [139] and Bänschet al. [141]. The discrepancy between the experimental and theoretical values of the barrier can be explained, since the experimental value results from the cumulative effects of all the

abstraction and addition reactions taking place in that temperature range and the theoretical calculated activation barrier corresponding to the particular channel.

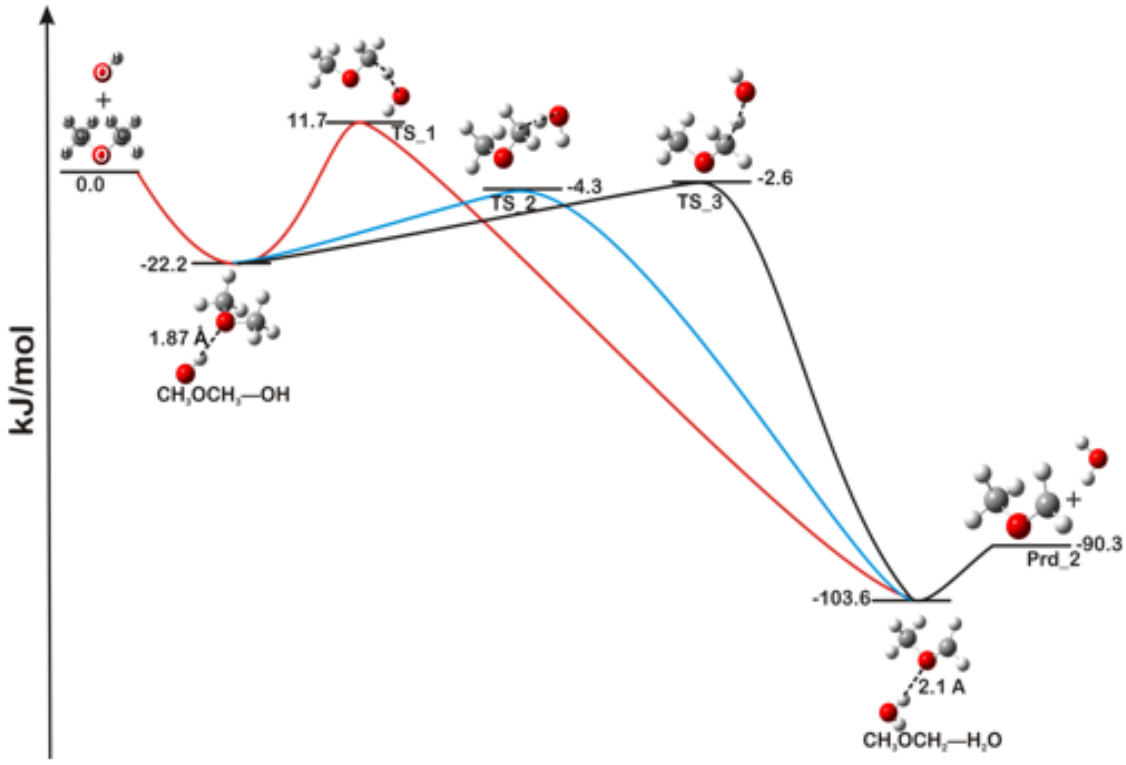

Fig. 6.6. The figure depicts a schematic energy diagram of in-plane and out-of-plane H atom abstraction reactions of DME with OH involving the pre-reactive complex formation of CH_3OCH_3–OH. Geometry optimization and single point energy calculation are at the G3 level. Energies are in kJ mol^{-1}.

All the reported rate coefficient values for the OH+DME reaction [131,133,135-137,139], and the value measured in the present work at 297 K are summarized in Table 6.3.

Table 6.3: Comparison of the rate coefficient of dimethyl ether with OH radicals from the present work with the reported literature data at 297 K.

$k/10^{-12}$ $cm^3molecule^{-1}s^{-1}$	Technique*	Reference
3.50 ± 0.35 (299K)	FP-RF	[133]
2.35 ± 0.24	PR	[131]
2.82 ± 0.07	PLP-LIF	[135]
2.95 ± 0.21	LP-LIF	[136]
2.69 ± 0.07	PLP-LIF	[137]
2.94 ± 0.12	LFP-LIF	[139]
2.68	LP-LIF	[141]
2.70 ± 0.20	LP-LIF	This work.

*FP-RF=Flash Photolysis-Resonance Fluorescence, PR=Pulse Radiolysis, PLP-LIF=Pulsed LP-LIF, LFP-LIF=Laser Flash Photolysis-LIF

Among all the reported values, the value reported by Perry et al. [133] is the highest, and that by Nelson et al. [131] is the lowest. All the rate coefficient values, measured employing LP-LIF, are similar within the experimental errors. Fig. 6.7 shows that our measured value falls within the previously reported values.

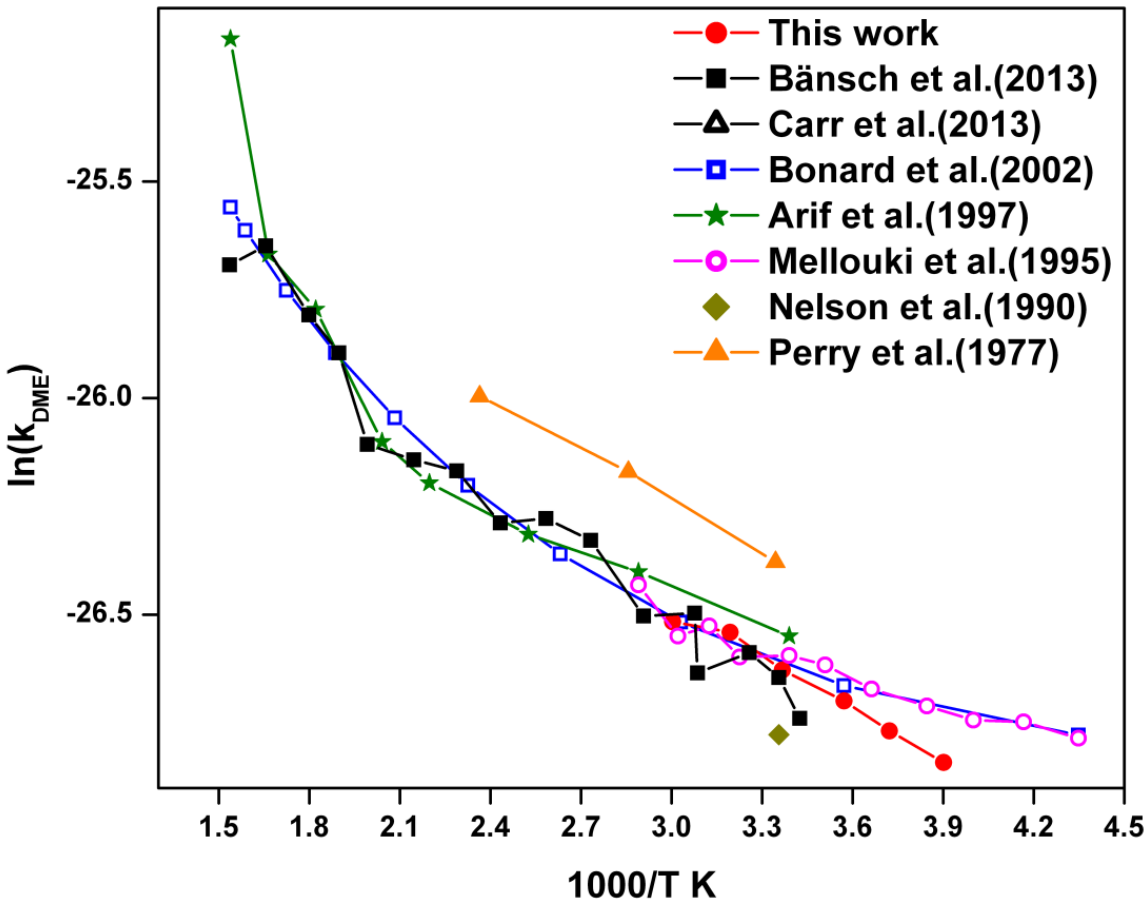

Fig. 6.7. This figure compares plots of rate coefficient (k) versus inverse of absolute temperature (T K) of the present work with literature values.

Part B: Epichlorohydrin (ECH)

6.4.2. Kinetics of ECH reactions with OH and Cl

The measured average value of the rate coefficient for the ECH reaction with Cl using 1,2-dichloroethane as a reference is $(4.22 \pm 0.65) \times 10^{-12}$ cm^3 $molecule^{-1}$ s^{-1}. Similarly, the measured average values of the rate coefficient for the ECH reaction with OH are $(2.42 \pm 0.47) \times 10^{-13}$ and $(5.57 \pm 1.27) \times 10^{-13}$ cm^3 $molecule^{-1}$ s^{-1} using ethane and 1,2 dichloroethane as the reference molecules, respectively, with quoted errors, including the errors in the reference. There is a difference between these values measured by the

relative rate method, which may be due to the error associated in references being used. In addition, the rate coefficient for the reaction of ECH with OH is also measured by absolute method using LP-LIF technique at 298 K and 15 Torr pressure, and the measured value is $(3.78 \pm 0.16) \times 10^{-13}$ $cm^3molecule^{-1}s^{-1}$. All the reported rate coefficient values for the OH + ECH reaction [142,150], along with the values measured in the present work at 298 ± 2 K are summarized in Table 6.4. The recently reported rate coefficient values of other ethers like PPO, EO, THP and THF are also listed in Table 6.4 for comparison. There is a reasonably good agreement between rate coefficients measured presently and reported by Edney et al. [150] and Orkin et al. [142]. Orkin et al. [142] have studied this reaction in the temperature range of 230−370 K, using an absolute method by flash photolysis resonance-fluorescence technique. Edney et al. [150] measured the room temperature (296 K) rate coefficient for this reaction using relative rate method, taking butane as a reference.

To understand the effects of the ring strain on kinetics of cyclic ethers with OH and Cl, we have compared the rate coefficients of cyclic ethers of different ring sizes and the values are listed in Table 6.4. It is observed that the rate coefficients of EO, PPO and THF increase in this order, but the ring strain decreases. With decreased ring strain, the rate coefficient is expected to decrease when the ring strain plays a significant role. In contrast, the rate coefficients increase with decreased ring strain. It implies that the ring strain is not an important factor to control the reactivity of these cyclic ethers. Rather, the number of abstractable H atoms, which increase with increasing ring size, governs the reactivity. In our laboratory, we had earlier studied the reactions of five- and six-

membered ethers, namely tetrahydofuran (THF) and tetrahydropyran (THP), with OH and Cl. It was observed that the measured rate coefficient of THP is the same or lower than that of THF even though there is an additional CH_2 group in THP. That may be due to higher stability of six-membered molecule (THP) than five-membered molecule (THF). Thus, with less number of abstractable H–atom available with a reactant for OH/Cl, the reactivity decreases, and the same effect is observed when cyclic and acylic ethers are compared (EO and DME). But in case of ECH and PPO, due to substitution of H atom by Cl, the reactivity in case of OH reaction is not much affected, but in case of Cl reaction it decreases by an order of magnitude. This may be due greater reactivity of Cl than OH for H atom abstraction [14,25,46].

Table 6.4: Summary of the rate coefficients of reactions of Cl and OH with ECH and DME from the present work (in bold) and other cyclic ethers from the literature at 298 ± 2 K.

Molecule	k_{OH} **($cm^3 molecule^{-1} s^{-1}$)**	k_{Cl} **($cm^3 molecule^{-1} s^{-1}$)**
DME	**2.71×10^{-12}**	1.8×10^{-10} [151]
ECH	**2.42×10^{-13} (RRM)** **5.57×10^{-13} (RRM)** **3.78×10^{-13} (absolute method)** 3.93×10^{-13} [150] 5.50×10^{-13} [142]	$(4.22 \pm 0.65) \times 10^{-12}$
PPO	3.0×10^{-13} [152]	3.0×10^{-11} [152]

EO	9.51×10^{-14} [153]	5.0×10^{-12} [154]
THF	1.92×10^{-11} [27]	2.50×10^{-10} [27]
THP	1.30×10^{-11} [27]	2.52×10^{-10} [27]

6.4.3. Atmospheric implications

The tropospheric lifetimes of majority of pollutants in the atmosphere are known to depend on their reaction rates with the tropospheric oxidants, like OH radical and Cl atom, as well as their uptake in the cloud droplets and subsequent rain out. However, under ambient condition, the atmospheric lifetimes of VOCs containing abstractable hydrogen atom mainly depend on their reactions with the OH radical. The lifetimes, τ_i of DME due to the reaction with the individual tropospheric oxidant is calculated by the below given formula.

$$\tau_{Oxidant}^{VOC} = \frac{1}{k_{Oxidant}^{VOC} \times [Oxidant]} \quad (6.14)$$

$$\tau_{OH}^{DME} = \frac{1}{k_{OH}^{DME} \times [OH]} \quad \text{and} \quad \tau_{Cl}^{DME} = \frac{1}{k_{Cl}^{DME} \times [Cl]} \quad (6.14a \text{ and } 6.14b)$$

In terms of the individual tropospheric lifetimes, the overall tropospheric lifetime, τ, is calculated using the formula

$$\tau = \left[\sum_i (\tau_i)^{-1}\right]^{-1} \quad (6.15)$$

Here, τ_{OH}^{DME} and k_{OH}^{DME} are the tropospheric lifetime and the rate coefficient of DME for removal by OH radicals, respectively, and the same notations are used for Cl atoms. The average atmospheric concentration of OH radicals, [OH], is taken as 1.0×10^6 molecules cm^{-3} [155]. The tropospheric lifetime calculated using the above equation is found to be 4.3 days (103 hrs), which matches with the reported value [156]. Also tropospheric

lifetime of DME with respect to Cl atom is calculated using the reported rate coefficient as 1.8×10^{-10} cm^3 $molecule^{-1}$ s^{-1} [151], both under the ambient condition and also in the MBL condition, taking [Cl] to be 1×10^3 and 1.3×10^5 molecules cm^{-3}, respectively. These estimated lifetimes are listed in Table 6.5, and it can be concluded from these values that DME reaction with the OH radical is the most important degradation pathway under the ambient condition, but in the MBL the Cl atom reaction is more significant removal pathway for DME. This implies that DME degrades fast in the troposphere, and its direct impact on the troposphere seems to vary from local to regional as tropospheric lifetime is less than five days. However, the GWP of any pollutant species depends upon its atmospheric lifetime and radiative forcing. The radiative forcing for DME is calculated from the IR absorption cross-sections of DME, in the tropospheric important IR wavelength region emitted by earth (discussed or calculated later in this chapter). In case of ECH also, the tropospheric lifetime is measured in a similar manner, and listed in Table 6.5. In case of ECH, the OH radical reaction is the most important degradation pathway in ambient condition between the two degradation channels, but the Cl atom reaction is equally important in MBL. Thus, the total lifetime of ECH in the MBL is reduced significantly (nearly half) in comparison to that in the ambient condition. Similarly, for five and six-membered ethers (THF and THP) also, the OH radical reaction is the most important degradation pathway in the ambient condition, but the Cl atom reaction is more important in the MBL.

Table 6.5: Tropospheric lifetimes (τ) calculated for DME and ECH with respect to reactions with Cl atoms and OH radicals. The recently reported value of rate coefficient

for the reaction of Cl with DME is taken from Jenkin et al. [151]. The concentrations used for $Cl_{Ambient}$, Cl_{MBL}, OH and O_3 are 1×10^3, 1.3×10^5 , 1×10^6 and 7×10^{11} molecules cm^{-3}, respectively (details are given in chapter two)

Molecule	k_{OH}	τ_{OH} (h) (days)	k_{Cl}	$\tau_{Cl\text{-}Amb}$ (h) (days)	$\tau_{Cl\text{-}MBL}$ (h) (days)	τ_{net} (h) (days)	$\tau_{net(MBL)}$ (h) (days)
DME	2.71×10^{-12}	103 (4.3)	1.80×10^{-10}	1543 (64)	12 (0.5)	96 (4) days	11 (0.46) day
ECH	2.42×10^{-13}*	1148 (48)	2.59×10^{-12}	107250 (4469)	825 (34)	1136 (47)	480 20

* This value of k measured by relative rate using ethane as a reference is used for lifetime calulations; τ_{net} is used for estimating ozone depletion potential.

6.4.4. GWP measurement

The IR spectra for various concentrations of DME are recorded, Fig. 6.8, is the plot of integrated IR absorbance versus the concentrations of DME.

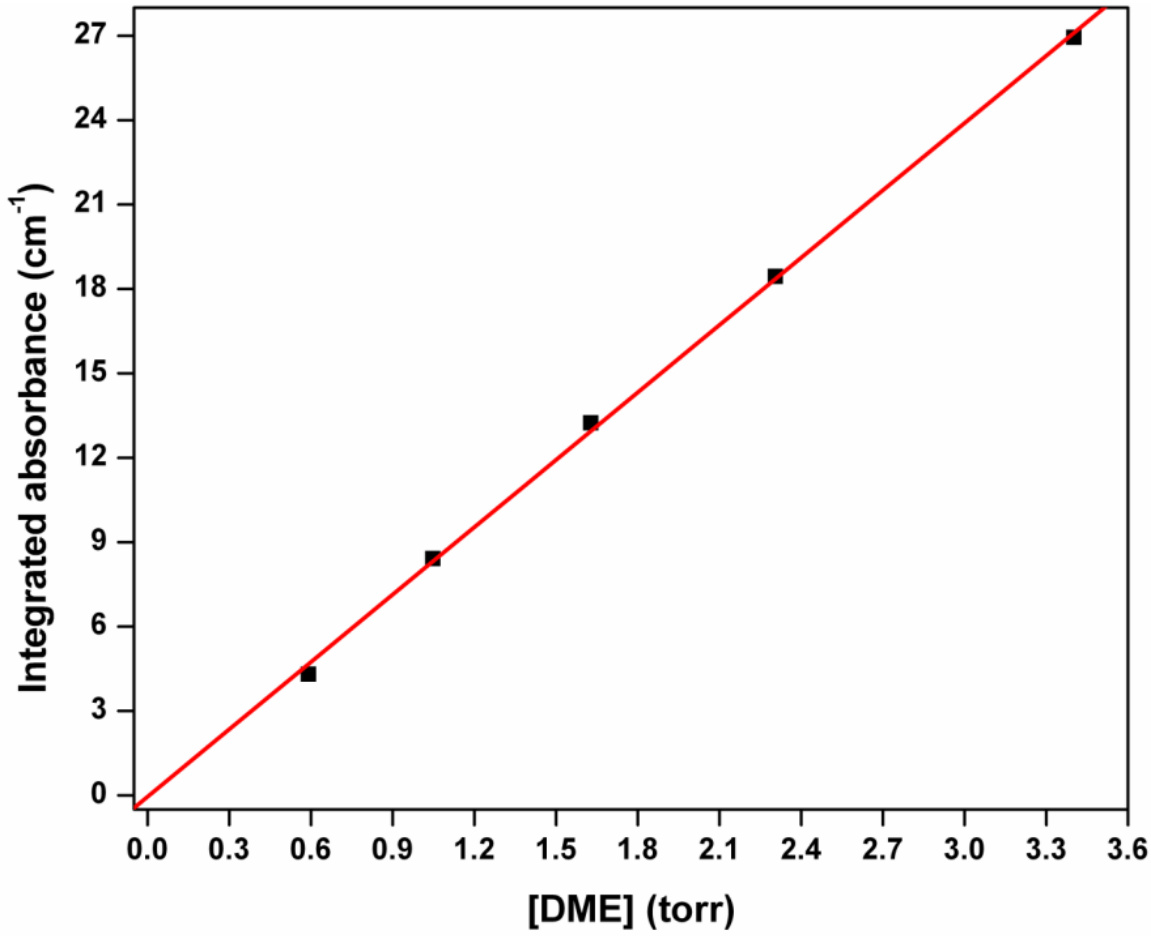

Fig. 6.8. Plot of integrated absorbance in the wavelength range of 1000-1300 cm^{-1} versus DME concentration, at total pressure of 760 Torr, maintained by N_2 buffer gas.

The plot of absorption cross section over the wave number range of 550 to 2500 cm^{-1} is displayed in Fig. 6.9.

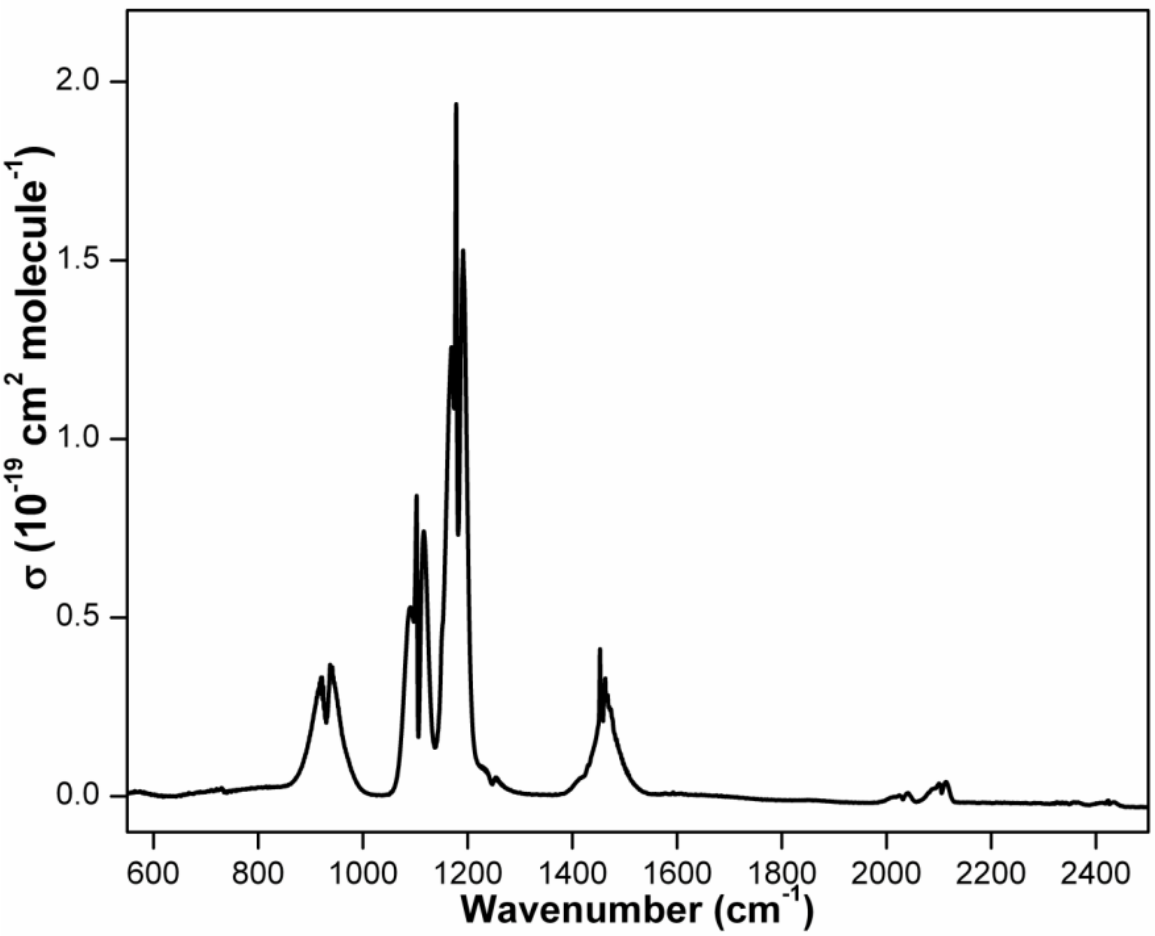

Fig. 6.9. Absorption cross-section plot of DME in the wavelength range of 550-2500 cm^{-1} at 298 K, integrated for 1 cm^{-1} interval.

The radiative efficiency is estimated from IR spectrum using the method explained by Hodenbrog et al. [157]. The radiative forcing for DME is estimated to be 0.03 $Wm^{-2}ppb^{-1}$. The Global warming potential (GWP) for DME is estimated with respect to CO_2 using the expression given by Hodnebrog et al.

$$(GWP)_x(TH) = \frac{\int_0^{TH} a_x[x(t)dt]}{\int_0^{TH} a_r[r(t)dt]} \quad (6.16)$$

It can be estimated for any chosen time-period by combining radiative forcing efficiency with atmospheric lifetime [36]. The GWP in 100 years time horizon for DME

is estimated to be 0.06. This shows that DME doesn't impose radiative burden on the atmosphere.

6.4.5. Ozone depletion potential

The ozone depletion potential (ODP) of a chemical compound refers to the relative amount of degradation it can cause to the ozone layer, in comparison to trichlorofluoromethane (R-11 or CFC-11) whose ODP is fixed at 1.0.

Since the molecule ECH has a chlorine atom, it can possibly contribute to stratospheric ozone depletion. The ODP value is calculated, using a semi-empirical Eqn. 6.17 [38],

$$\mathrm{ODP_{CCP}} = \frac{\tau_{\mathrm{ECH}}}{\tau_{\mathrm{CFCl_3}}} \mathrm{x} \frac{\mathrm{M_{CFCl_3}}}{\mathrm{M_{ECH}}} \mathrm{x} \frac{\mathrm{n}}{3} \qquad (6.17)$$

where τ_x , M_x, (x=ECH or $CFCl_3$) denote the global atmospheric lifetimes, the molecular weight (M_{CFCl3} =137.36 and M_{ECH} = 92.52 g/mol), n is the number of chlorine atoms in ECH (that is 1), and the number 3 refers to the three chlorine atoms in $CFCl_3$. Using the value of τ_{ECH} as 1136 hrs and τ_{CFCl3} as 45 years [39], the ODP value of ECH is calculated to be 4.28×10^{-3}. This low value of ODP suggests that ECH will have a negligible effect on the stratospheric ozone depletion.

6.5. Conclusions

In this chapter for part A, we report the rate coefficient for the reaction of the OH radical with dimethyl ether (DME) as a function of temperature in the range of 257 to 333 K. The Arrhenius expression for the reaction of DME with OH showed a very weak temperature dependence and represented by the expression,

$$k(T) = (9.7 \pm 1.0) \times 10^{-12} exp\{-(380 \pm 25)/T\} cm^3 molecules^{-1} s^{-1}$$

Methyl formate is observed as a major stable product, in the reaction carried out at atmospheric pressure with synthetic air as buffer gas, both in the presence and absence of NO. The rate coefficient is almost unaffected in presence of O_2 at low concentration. Theoretical calculations of structures and energies suggest that the reaction of OH with DME proceeds with formation of a hydrogen-bonded complex, in which OH is the H donor.

Considering average tropospheric OH radical concentration of 1.0×10^6 molecules cm^{-3}, the average tropospheric lifetime of the DME with respect to removal by the OH radicals is estimated to be 4.3 days, and the GWP, in 100 years time horizon, is found to be 0.06. Therefore, it can be concluded that DME will not contribute substantially to the global warming on its usage as a substitute for domestic fuel and diesel. In part B, the room temperature rate coefficients of ECH with Cl atoms and OH radicals are reported. The major degradation pathway of both DME and ECH is their reaction with the OH radicals. However, their reaction with Cl atoms also becomes important under the marine boundary layer conditions. The impact of DME and ECH on atmosphere may vary from local to regional, since its tropospheric lifetime is in days. The reactivity of acyclic ether is more compared to cyclic ethers that may be due to availability of less number of abstractable H-atom. The ODP value of ECH is also quite low (4.28×10^{-3}), suggesting that it will have a negligible effect on the stratospheric ozone depletion.

Homi Bhabha National Institute

SYNOPSIS OF Ph. D. THESIS

1. **Name of the Student:** Asmita Sharma
2. **Name of the Constituent Institution:** RPCD, Bhabha Atomic Research Centre
3. **Enrolment No. :** CHEM01201404007
4. **Title of the Thesis:** Kinetic studies of gas phase reactions of volatile organic compounds (VOCs) relevant in atmospheric chemistry
5. **Board of Studies:** Chemical Sciences, HBNI

SYNOPSIS

Advances in technology and with increasing demand by human being, the burden on atmosphere is increasing due to emission of chemical compounds, particularly volatile organic compounds (VOCs), from various anthropogenic (chemical industries, vehicular exhaust, etc.) and natural sources (forest fire), which may have detrimental effect on the air quality and global climate change [1]. Therefore, it is very important to investigate the impact of any compound on the atmosphere before being used at an industrial level. Depending on nature and reactivity, the lifetimes of different classes of VOC are different. Hence, the impact can be very different from local (aerosol generation, ozone generation in the troposphere) to regional (acid rain, the formation of photochemical smog) to global (global warming potential, ozone depletion in the stratosphere). For example, chlorofluorocarbons (CFCs) are not reactive in the troposphere and have long tropospheric lifetimes. Therefore, CFCs enter into the stratosphere and take part in ozone depletion, whereas highly reactive unsaturated

hydrocarbons lead to local ozone generation in the troposphere. Under different atmospheric conditions, trace species can undergo different reactions e.g., oxides of nitrogen lead to ozone generation in the troposphere, whereas they are responsible for ozone depletion in the stratosphere. For modelling the atmospheric changes, such as the global climate change, air quality deterioration and stratospheric ozone depletion revival, the understanding of the processes that the molecules undergo is necessary.

Lifetime of a molecule (VOC) released into the troposphere, is mainly dependent on the three degradation processes i.e. 1) Photodissociation by solar light available in the troposphere, 2) Dissolution in aqueous media that depends upon Henry's law constant and 3) Reaction with oxidative species (Cl, OH, NO_x, O_3 etc.) which depends upon reactivity of a VOC with respective oxidants and concentrations of different oxidants [2]. Combining all these processes, the residence time of any VOC in the troposphere is defined as an atmospheric lifetime (τ), given by

$$\tau = \frac{1}{\int \sigma_M(\lambda) I(\lambda) dI + k_{dissolution} + \sum_i k_i [X_i]}$$

where k_i is the rate coefficient for the reaction with oxidative species i, with the atmospheric concentration of X_i. Since most of the VOCs absorb only in the ultraviolet region and have very low solubility in water, their atmospheric lifetimes are decided by the rate coefficients of their reactions with the major tropospheric oxidative species such as OH, NO_3, O_3, Cl etc.[3]. Among these, OH radicals are the most effective oxidant in the troposphere in the daytime. Nighttime oxidation is dominated by reactions with NO_3. In the case of unsaturated molecules, reaction with ozone is also important. The reactions of some VOCs with Cl atoms are significant in the remote marine boundary layer (MBL) as well as the polluted urban areas.

In this regard, an effort has been made to understand the kinetics and the degradation mechanism in the troposphere of some selected class of VOCs. The selected VOCs are (a) saturated and unsaturated cyclic hydrocarbon (containing eight carbon atoms) to understand any change in reactivity with unsaturation and to compare its reactivity with saturated and unsaturated acyclic hydrocarbon, (b) unsaturated cyclic halogenated hydrocarbon (1-cholorocyclopentene) for comparison of its reactivity with cyclopentene and substituted cyclopentene to understand the effect of substituent Cl on the reactivity, (c) esters (gamma-valerolactone, GVL and alpha-methyl gamma-butyrolactone, AMGBL) to study the effect of ring O atom on the reactivity, (d) ethers (dimethyl ether and epichlorohydrin) to compare the reactivity of cyclic and acyclic ethers and also to investigate the effect of heteroatom (chlorine) on the reactivity. These VOCs are anthropogenic pollutants, released from industries where they are used in the synthesis of important drugs, combustion of fossil fuels or they are present in the atmosphere due to oxidation of other pollutants. The reactions of these pollutants play a major role in the tropospheric photochemistry. The rate coefficients of reactions of these molecules with Cl, OH, and O_3 at room temperature (298 K) are determined (k_{Cl}, k_{OH}, and k_{O3}) using relative rate method using Gas Chromatography (GC) coupled with Flame Ionization Detector (FID) technique, which are essential for assessing their environmental impact. These measured values of the rate coefficients with OH, Ozone and Cl are compared to understand relative importance (contribution) of their reactivity or degradation channels with these oxidants, and also with respect to that of analogous molecules in order to understand the reactivity pattern. In addition, for evaluation of the activation energy (E_a), temperature dependent rate coefficient for the reaction of some VOCs with the OH radical is also measured using an absolute method of Laser Photolysis-Laser Induced fluorescence (LP-LIF). The

reasonably well-established structure activity relations (SARs) are also applied in some cases to calculate rate coefficients to compare with the measured values. The rate coefficients are then used to calculate lifetimes of these VOCs to predict their impact on the atmosphere, which are further cross checked for certain VOCs studied by calculating their global warming and ozone depletion potentials.

In order to see the total impact of VOCs, their major degradation products are identified using GC and GC-MS techniques. Experimental results are corroborated with theoretical calculations to understand the reaction mechanism.

The thesis has been organized into seven chapters.

Chapter 1: Introduction

In this chapter, the relevance of gas phase kinetic studies is discussed for understanding the consequences of presence of VOCs in the troposphere. It highlights the reactions responsible for the generation of the most common tropospheric oxidants, such as OH, O_3 and Cl, which play a dominant role in the removal of VOCs from the troposphere. This chapter also provides a brief description of the methods (relative rate and absolute method) used for kinetics measurements. A brief review of the ab initio theoretical methods for calculating the potential energy surface (PES) of a reaction is also provided. The last part of the chapter describes the scope of the present work, a brief outline of the work and the summary of the results.

Chapter 2: Experimental methods

In this chapter, experimental methods and techniques, which have been employed for rate coefficient and concentration measurements, are described. It includes a detailed description of absolute and relative rate methods for rate coefficient measurements, by using Laser Photolysis-Laser Induced fluorescence (LP-LIF) and Gas

Chromatography (GC) coupled with Flame Ionization Detector (FID), respectively. It also describes techniques like Gas Chromatography-Mass Spectrometer (GC-MS) used for product characterization, and Fourier Transform Infra-Red Spectrometer (FTIR) used for concentration measurement of VOCs. It also covers theoretical methodology used for characterization of transition states to understand the reaction mechanism.

Chapter 3: Tropospheric oxidation of cyclic hydrocarbons with eight carbon atoms

In this chapter, the reactions of cyclic hydrocarbons with tropospheric oxidants are investigated**.** They are significant constituents of ambient air as they are important classes of VOCs released into the troposphere from various sources, such as automobile exhausts, gasoline vaporization, forest fire, rubber abrasion, etc. [4]. Also, many such hydrocarbons are released from industry, where they are already in use as solvents, precursors etc. The atmospheric oxidation of these hydrocarbons leads to the gas phase as well as particulate products. It was observed that the rate coefficients of the reactions with Cl atoms do not increase much with an increase in unsaturation. Also, the major products in our studies, mentioned above, indicate a significant contribution of H atom abstraction in the case of the reaction of Cl, the maximum abstraction being from the carbon atom away from unsaturation. In the present study, we have extended our investigations to the reactions of eight membered cyclic hydrocarbons (CyOs), cyclooctane, cis-cyclooctene and 1,5-cyclooctadiene with tropospheric oxidants to understand the effect of unsaturation on the rate coefficients and occurrence of H atom abstraction in these cyclic molecules. The stable products formed during these reactions are also identified by GC-MS to understand the reaction

mechanism. The reactivities of these CyOs are compared with 1-alkenes for reactions of both Cl atom and OH. In addition, the measured rate coefficients are compared to know the relative importance of these three oxidants in the degradation of these CyOs. The rate coefficients of reaction of Cl (k_{Cl}) atom at 298 K are determined as (4.5± 0.4), (4.7 ± 0.4) and (5.2 ± 0.7) × 10^{-10} $cm^3molecule^{-1}s^{-1}$ for cyclooctane, cis-cyclooctene and 1,5-cyclooctadiene, respectively. The corresponding values of rate coefficients of reactions with OH (k_{OH}) at 298 K are (1.4 ± 0.2), (5.1 ± 1) and (11.1 ± 2) × 10^{-11} $cm^3molecule^{-1}s^{-1}$ for cyclooctane, cis-cyclooctene and 1,5-cyclooctadiene, respectively, and the values of k_{O3} at 298 K are (4.1 ± 0.8) and (1.4 ± 0.2) × 10^{-16} $cm^3molecule^{-1}s^{-1}$ for cis-cyclooctene and 1,5-cyclooctadiene, respectively. The results suggest that Cl atom is more effective in the atmospheric degradation of cyclooctane than OH, in the conditions of the marine boundary layer. Reactions with both OH and ozone contribute to the degradation of cis-cyclooctene and 1,5-cyclooctadiene, the ozone reaction being more effective in the former and the OH reaction in the latter. Analysis of the stable products suggests that the addition of Cl atom, and not the H atom abstraction by Cl, is dominant in the unsaturated molecules. Unsaturated ketones and alcohols are identified as products in the reactions of OH and Cl with cis-cyclooctene and 1,5-cyclooctadiene in the gas phase, emphasizing the importance of H atom abstraction / addition-elimination channels in these unsaturated molecules. Based on the identified products, the reaction mechanisms for these reactions are proposed.

Chapter 4: Reactivity study of 1-cholorocyclopentene with tropospheric oxidants

In this chapter the reactions of unsaturated cyclic halogenated hydrocarbon (1-cholorocyclopentene) with OH, Cl and O_3 are investigated, and compared with that of cyclopentene and substituted cyclopentene to understand the effect of substituent Cl

on the reactivity. Chlorocompounds, in general, are quite useful, since these are used as intermediates in the synthesis of a vast variety of drugs and in the preparation of synthetically important organometallic reagents. They are also used as solvents and in cleaning applications, such as degreasing and dry-cleaning [5]. In this chapter reactions of 1-chlorocyclopentene with Cl, OH, and O_3 at 298 K and 1- atmosphere pressure are investigated, using the relative rate method. In addition to the rate coefficients (k_{Cl}, k_{OH}, and k_{O3}), the stable products formed in the above reactions are characterized using GC-MS technique. Further, the temperature dependent rate coefficients for the reaction of 1-chlorocyclopentene with OH radical are also measured experimentally over the temperature range of 262 to 335 K and the total pressure of 30 Torr using LP-LIF technique, to obtain the Arrhenius parameters. Along with these experimental studies, theoretical calculations are also carried out to understand the reaction mechanism of H atom abstraction by Cl atom and its addition to the double bond. The tropospheric lifetime and the global warming potential (GWP) for 1-chlorocyclopentene are estimated. An attempt is also made to understand the effect of a heteroatom (chlorine) on reactivity by comparing the kinetics result with 1-cyclopentene and similar cyclic molecules.

The measured average rate coefficient values of k_{Cl}, k_{OH} and k_{O3} (in cm^3 $molecule^{-1}$ s^{-1}) are $(3.51 \pm 1.26) \times 10^{-10}$, $(5.97 \pm 1.08) \times 10^{-11}$ and $(1.50 \pm 0.19) \times 10^{-17}$, respectively. The abstraction and addition products are identified as the stable products formed during the reaction of Cl, OH and O_3 initiated oxidation of the 1-chlorocyclopentene in presence of air, and among them. the latter is found to be the major products. Molecular orbital calculations support the experimental results, and the abstraction of the allylic hydrogen atoms is predicted to be the major abstraction

channel. Calculations predict the preferential addition of chlorine atom to the carbon atom of the unsaturation center not having Cl attached to it. The rate coefficients of 1-chlorocyclopentene are compared with that of cyclopentene and substituted cyclopentene to understand the effect of substituent Cl on the reactivity. The measured rate coefficients have been used to calculate the tropospheric lifetime of the compound to be 316, 2 and 26 hrs for Cl, OH and O_3, respectively, which indicates that the major degradation pathway of 1-chlorocyclopentene is its reaction with OH. Atmospheric impact of these molecules is local as tropospheric lifetime (τ) < 2 hours. The global warming potentials (GWP) for 20 and 100 years time horizon were calculated to be 0.01 and 0.003, respectively. Ozone depletion potential (ODP) value of 1-chlorocyclopentene is calculated to be 2.1×10^{-6}. These low values of GWP and ODP suggest that 1-chlorocyclopentene will have a negligible effect on global warming and stratospheric ozone depletion. From the temperature dependence of k (T), the Arrhenius parameters E_a/R and A-factor are found to be 669 ± 45 K and (0.95 ± 0.06) × 10^{-12} $cm^3 molecule^{-1} s^{-1}$, respectively.

Chapter 5: Reactions of lactones with tropospheric oxidants: A kinetics and products study

Recently, preparation and applications of cyclic esters or lactones, such as gamma-valerolactone (GVL), have received substantial attention due to conversion of paper waste to GVL and its use as an illuminating fuel with reduced VOCs emission [6]. In this chapter, the reactions of esters (gamma-valerolactone, GVL and alpha-methyl gamma-butyrolactone, AMGBL) with OH and Cl are investigated to understand the effect of the ring O atom on the reactivity. These two molecules have similar ring size

but differ in the position of methyl substitution. So, their reactivities are compared to understand the effect of the structure on these reactions.

The measured rate coefficients of the reactions of GVL (k_{OH} = (1.95 ± 0.58) × 10^{-12}; k_{Cl} = (2.26 ± 0.53) × 10^{-11} $cm^3molecule^{-1}s^{-1}$) and AMGBL (k_{OH} = (1.81 ± 0.43) × 10^{-12}; k_{Cl} = (3.42 ± 0.63) × 10^{-11} $cm^3molecule^{-1}s^{-1}$) at 298 K imply that the reaction with OH is the dominant reaction in the ambient conditions, and the reaction with Cl atom becomes relevant under marine boundary layer (MBL) conditions. Also, it is observed that the reactivity is not affected by a difference in the position of the methyl group. The tropospheric lifetimes of GVL and AMGBL are comparable, 71.2 and 76.7 hrs, respectively, and suggest that these molecules will have a local impact on the atmosphere. However, the products of the reactions are found to be different. This suggests that the impact in terms of aerosol generation in the troposphere may be different for GVL and AMGBL.

Chapter 6: Reactivity study of ethers with tropospheric oxidants

The compounds with ether functional group are mainly present in the atmosphere due to anthropogenic emissions [7]. In this chapter, the reactions of straight chain and cyclic ethers (dimethyl ether and epichlorohydrin) with OH and Cl are presented in two parts: Part A for dimethyl ether and Part B for epichlorohydrin. Their reactivities are compared with that of cyclic and acyclic ethers, and change in the reactivity due to the presence of heteroatom (chlorine) is also investigated. In addition, the reactivity of ether with OH and Cl is also compared with other hydrocarbons to understand the effect of the O atom.

Part A: Dimethyl ether

In this part, the rate coefficients for the reaction of the OH radical with dimethyl ether as a function of temperature in the range of 257 to 333 K are

presented, and the Arrhenius parameters are calculated. The Arrhenius expression showed a very weak temperature dependence and represented by the expression,

$$k = (9.7 \pm 1.0) \times 10^{-12} \exp(380 \pm 25/T)\ cm^3 molecule^{-1} s^{-1}$$

The average tropospheric lifetime of the dimethyl ether with respect to removal by OH radicals is estimated to be 4.7 days and the GWP in 100 years time horizon is found to be 0.06. Therefore, it can be concluded that DME will impose a local effect on the atmosphere and not contribute substantially in Global Warming. Among stable products, methyl formate is observed as a major product.

Part B: Epichlorohydrin

The measured rate coefficients at 298 K for reaction of epichlorohydrin with OH and Cl are as follows: $k_{OH} = (2.51 \pm 0.26) \times 10^{-13}$ by RRM and $(3.78 \pm 0.16) \times 10^{-13}$ by absolute method, $k_{Cl} = (2.59 \pm 0.46) \times 10^{-12}$ $cm^3 molecule^{-1} s^{-1}$. When the reactivity of cyclic (ethylene oxide) and acylic (DME) ethers are compared, the latter is found to be more reactive. Due to the presence of heteroatom in epichlorohydrin, the reactivity in case of OH reaction is not much affected, but in case of Cl reaction it decreases by an order of magnitude when compared with propylene oxide. The measured lifetime of ECH indicates that it will have a local impact on the atmosphere.

Chapter 7: Conclusions and future work

This chapter contains the conclusion of the work carried out as a part of the PhD thesis and also future works which will substantiate the present research work.

References

1. R. Atkinson, *Atmos. Environ.* 41 (2007) S200 – S240.
2. Introduction Atmospheric Chemistry, P. V. Hobbes, Cambridge University Press, 2000.
3. R. Atkinson and J. Arey, *Chem. Rev.*, 103 (2003) 4605-4638.
4. Asmita Sharma, Mohini Walavalkar, Awadhesh Kumar, S. Dhanya, Prakash D. Naik, Atmos. Environ., 213, (2019), 433-443.
5. Asmita Sharma, Mohini P. Walavalkar, Ankur Saha, Monali Kawade, Awadhesh Kumar, Prakash D. Naik, Atmos. Environ., 2019,199, 274–283.
6. M. P. Walavalkar, A. Sharma, S. Dhanya, P.D. Naik, Atmospheric Environment, 2017,161, 18-26.
7. Monali Kawade, Asmita Sharma, D. Srinivas, Ankur Saha, Hari P. Upadhyaya, Awadhesh Kumar, Prakash D. Naik, Chemic. Phys. Lett., 2018, 706 558–563

Publications in Refereed Journal:

Published

1. Reactions of lactones with tropospheric oxidants: A kinetics and products study.
   M.P. Walavalkar, A. Sharma, S. Dhanya, P.D. Naik, Atmos. Environ., 2017,161, 18-26.
2. Rate coefficients of hydroxyl radical reaction with dimethyl ether over a temperature range of 257–333 K.
   Monali Kawade, Asmita Sharma, D. Srinivas, Ankur Saha, Hari P. Upadhyaya, Awadhesh Kumar, Prakash D. Naik, Chem. Phys. Lett., 2018, 706 558–563
3. Rate coefficients of reactions of 1-chlorocyclopentene with tropospheric oxidants at 298 K.
   Asmita Sharma, Mohini P. Walavalkar, Ankur Saha, Monali Kawade, Awadhesh Kumar, Prakash D. Naik, Atmos. Environ., 2019,199, 274–283.

4. Reactions of tropospheric oxidants- Cl, OH and O_3 with cyclic hydrocarbons with eight carbon atoms at 298 K.

Asmita Sharma, Mohini Walavalkar, Awadhesh Kumar, S. Dhanya, Prakash D. Naik. Atmos. Environ., 213, (2019), 433-443.

Other Publications:

Conference/Symposium

1. Effect of unsaturation on the tropospheric degradation pathways of cyclic hydrocarbons–A comparison of six-and eight-membered molecules. A. Sharma, M. P. Walavalkar, H. D. Alwe, S. Dhanya and P. D. Naik Proc. TSRP, 6 – 9th January 2014, BARC, Mumbai.
2. Tropospheric oxidation of unsaturated cyclic ethers – contribution towards regeneration of OH radicals. H. D. Alwe, A. Sharma, M. P. Walavalkar, S. Dhanya and P. D. Naik. Proc. TSRP-2014, 6 – 9th January 2014, BARC, Mumbai.
3. Rate coefficients of reactions of tropospheric oxidants with triple bonded alcohols. M. P. Walavalkar, H. D. Alwe, A. Sharma, S. Dhanya and P. D. Naik. Proc. TSRP, 6 – 9th January 2014, BARC, Mumbai.
4. Direct observation of OH formation during Cl atom initiated oxidation of hydrocarbons. H. D. Alwe, A. Sharma, M. P. Walavalkar, S. Dhanya, A. Saha, S. Sengupta and P. D. Naik. Proc. 13th DAE-BRNS Biennial TSRP, January 5 – 9, 2016, BARC, Mumbai
5. Rate coefficients of reactions of 1-chlorocyclopentene with tropospheric oxidants. A. Sharma, M. P. Walavalkar, A. Kumar and P. D. Naik, Proc. TSRP-APSRC 2018, BARC Mumbai.
6. Kinetic studies of gas phase reactions of cyclic eight membered hydrocarbons M. P. Walavalkar, Asmita Sharma, Awadhesh Kumar and P. D. Naik. Proc. TSRP-APSRC 2018, BARC Mumbai.
7. Assessment of environmental impact of 1-chlorocyclopentene in terms of tropospheric lifetime, global warming and ozone depletion potentials. A. Sharma, M. P. Walavalkar, A. Kumar and P. D. Naik. Proc. NSE – 20, 13-15th December, 2018, IIT Gandhinagar, Gujarat.

8. Kinetics of gas phase reaction of hydroxyl radical with 1-chlorocyclopentene over a temperature range of 258-335 using LP-LIF technique. Anmol Virmani, A. Sharma, M.P. Walavalkar, A. Saha, A. Kumar and P.D. Naik. Proc. NSRP, 6-9th Feb, 2019, Visva-Bharati, Santiniketan.

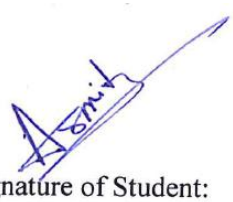

Signature of Student:

Date: 29-11-2019

Doctoral Committee:

S. No.	Name	Designation	Signature	Date
1.	Prof. H. Pal	Chairman		29-11-2019
2.	Prof. P. D. Naik	Guide & Convener		29/11/19
3.	Prof. Awadhesh Kumar	Co-guide Member	Awadhesh Kuma	29.11.19
4.	Prof. R. K. Vatsa	Member		29/11/2019.
5.	Prof. S. K. Jha	Member	Sanjay Kumar Jha	29-11-2019

Thesis Highlight

Name of the student: ASMITA SHARMA

Name of the CI/OCC: Bhabha Atomic Research Centre, Mumbai

Enrolment no.: CHEM01201404007

Thesis title: Kinetic studies of gas phase reactions of volatile organic compounds (VOCs) relevant in atmospheric chemistry

Discipline: Chemical Sciences **Date of viva voce:** March 11, 2021

Estimation of impact of volatile organic compounds (VOCs) on atmosphere

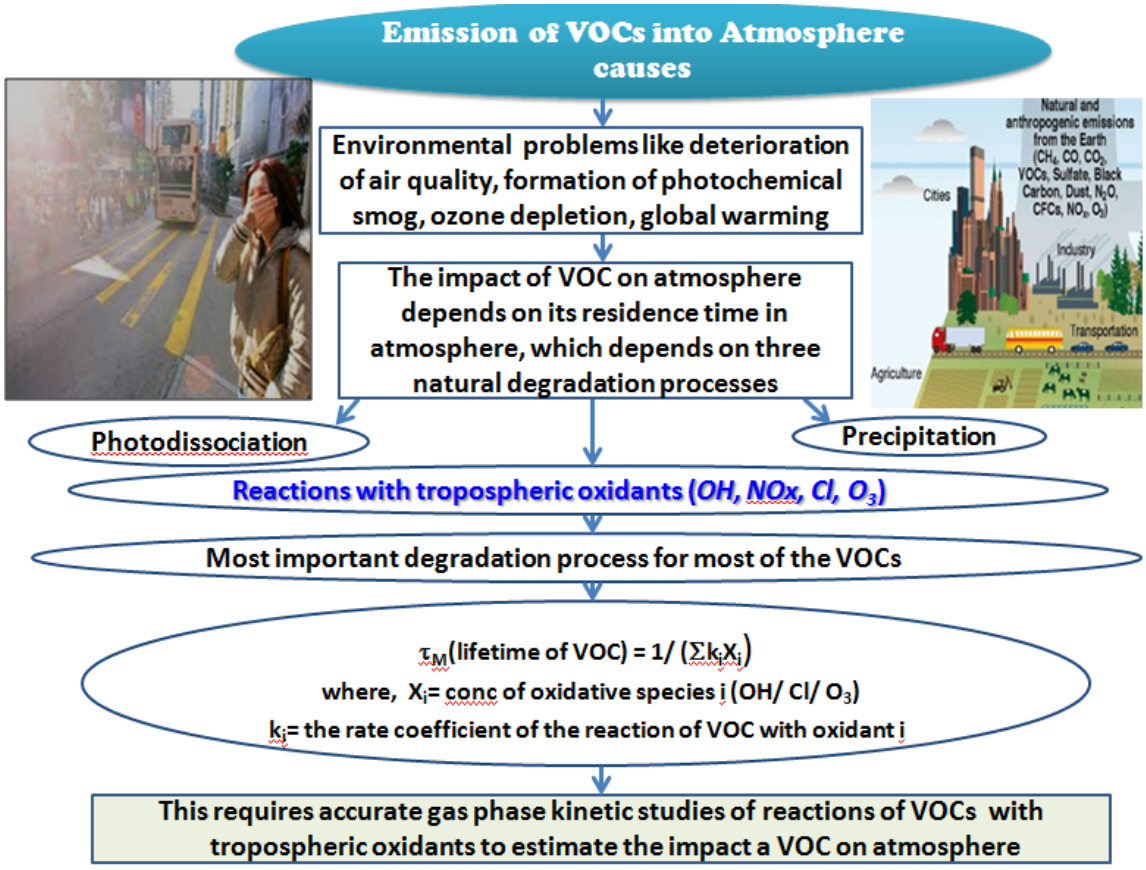

The research work was aimed at understanding the atmospheric implications of some selected VOCs (cyclooctane, cis-cyclooctene and 1,5-cyclooctadiene, and 1-chlorocyclopentene, and gamma-valerolactone and alpha-methyl gamma-butyrolactone, and dimethylether and epichlorohydrin), which are released into the atmosphere as pollutants. The gas phase reaction kinetics of these VOCs with important tropospheric oxidants (OH, Cl and O_3) have been investigated, and their stable products identified to estimate the impact of VOCs on atmosphere.

The impact of these VOCs on the atmosphere is found to be local, except for ethers wherein it extends to regional level. The major degradation pathway of these VOCs is mainly their reactions with the OH radicals, except for cyclooctene for which reaction with O_3 is major pathway of degradation. It is noted that the reactions with Cl atoms are important under the marine boundary layer conditions for all the investigated VOCs.